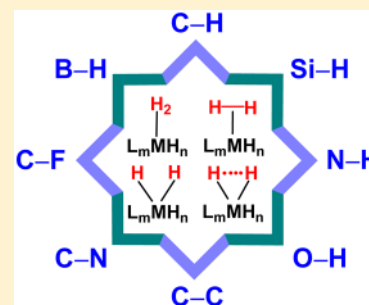


## Polyhydrides of Platinum Group Metals: Nonclassical Interactions and $\sigma$ -Bond Activation Reactions

Miguel A. Esteruelas,\* Ana M. López, and Montserrat Oliván

Departamento de Química Inorgánica, Instituto de Síntesis Química y Catálisis Homogénea (ISQCH), Centro de Innovación en Química Avanzada (ORFEO-CINQA), Universidad de Zaragoza-CSIC, 50009 Zaragoza, Spain

**ABSTRACT:** The preparation, structure, dynamic behavior in solution, and reactivity of polyhydride complexes of platinum group metals, described during the last three decades, are contextualized from both organometallic and coordination chemistry points of view. These compounds, which contain dihydrogen, elongated dihydrogen, compressed dihydride, and classical dihydride ligands promote the activation of B–H, C–H, Si–H, N–H, O–H, C–C, C–N, and C–F, among other  $\sigma$ -bonds. In this review, it is shown that, unlike other more mature areas, the chemistry of polyhydrides offers new exciting conceptual challenges and at the same time the possibility of interacting with other fields including the conversion and storage of regenerative energy, organic synthetic chemistry, drug design, and material science. This wide range of possible interactions foresees promising advances in the near future.



### CONTENTS

1. Introduction	8770	3.6.5. Si–H, Ge–H, and Sn–H Bond Activations	8807
2. Ruthenium	8772	3.6.6. N–H and O–H Bond Activations	8810
2.1. Phosphine Complexes	8772	3.6.7. Other $\sigma$ -Bond Activations	8814
2.2. Complexes with Tetrapodal and Tripodal Phosphine Ligands	8775	4. Rhodium	8816
2.3. Half Sandwich Compounds	8776	5. Iridium	8817
2.4. Complexes with Tris(pyrazoyl)borate and Related Ligands	8777	5.1. Phosphine Complexes	8817
2.5. Complexes with Pincer Ligands	8778	5.2. Complexes with Tripodal Phosphine Ligands	8821
2.6. Ruthenium-Polyhydride Complexes Involved in $\sigma$ -Bond Activation Reactions	8780	5.3. Half Sandwich Compounds	8821
2.6.1. B–H Bond Activation Reactions and Related Processes	8780	5.4. Complexes with Tris(pyrazoyl)borate and Related Ligands	8822
2.6.2. C–H Bond Activation	8782	5.5. Complexes with Pincer Ligands	8823
2.6.3. Si–H Bond Activation	8784	5.6. Iridium-Polyhydride Complexes Involved in $\sigma$ -Bond Activation Reactions	8825
2.6.4. N–H and O–H Bond Activations	8785	5.6.1. B–H Bond Activation	8825
2.6.5. Other $\sigma$ -Bond Activations	8786	5.6.2. C–H Bond Activation	8826
3. Osmium	8787	5.6.3. Si–H Bond Activation	8828
3.1. Phosphine Complexes	8787	5.6.4. O–H Bond Activation	8829
3.2. Complexes with Tetrapodal Phosphine Ligands	8792	6. Group 10	8829
3.3. Half Sandwich Compounds	8792	7. Conclusion and Outlook	8830
3.4. Complexes with Tris(pyrazoyl)borate and Related Ligands	8793	Author Information	8831
3.5. Complexes with Pincer Ligands	8794	Corresponding Author	8831
3.6. Osmium-Polyhydride Complexes Involved in $\sigma$ -Bond Activation Reactions	8796	Notes	8831
3.6.1. B–H Bond Activation Reactions	8796	Biographies	8831
3.6.2. Direct C–H Bond Activation	8798	Acknowledgments	8832
3.6.3. Chelate-Assisted C–H Bond Activation	8800	Dedication	8832
3.6.4. C–H Bond Activation of Imidazolium and Benzimidazolium Salts: Formation of NHC Complexes	8805	References	8832

**Special Issue:** Metal Hydrides

**Received:** February 4, 2016

**Published:** June 6, 2016

## 1. INTRODUCTION

Hydride is the ligand with the smallest number of valence electrons. It can only make single bonds to transition metal centers, which are among the strongest metal–ligand bonds.<sup>1</sup> Despite the strength of the M–H bonds, this ligand shows a great mobility and hydride site exchange is often observed.<sup>2</sup> On the other hand, hydride has almost no steric influence. With its uniquely small steric requirement, this ligand is ideal for achieving high coordination numbers.

A major milestone for the understanding of the chemistry of transition metal hydride complexes was the discovery that the hydrogen molecule can coordinate to a transition metal retaining almost intact the H–H bond.<sup>3–6</sup> In contrast to the M–H bond, the metal–dihydrogen interaction is weak. Metal–dihydrogen and metal–dihydride forms are both parts of the same redox equilibrium. Reducing metal centers favor the oxidized dihydride form. However, oxidizing metal centers stabilize the reduced dihydrogen. The coordination enhances the acidity of the hydrogen molecule,<sup>7,8</sup> which can undergo heterolytic cleavage<sup>9</sup> and position exchange, through proton transfer, when a hydride coligand is also present in the complex. In addition, the hydrogen atoms rapidly rotate around the metal–dihydrogen axis.

Other factors that have significantly contributed to the development of the field are the improvement of the quality of the characterization techniques, including X-ray and neutron diffractions,<sup>10</sup> and NMR spectroscopy,<sup>11–13</sup> and the availability of more sophisticated programs and more potent computers for DFT calculations,<sup>14–18</sup> which are making possible the study of real molecules. Thus, today, it is possible to have a quite exact knowledge of the coordination polyhedra of the majority of the hydride complexes and the separation between the hydrogen atoms bound to the metal center, in the solid state and in solution, and their mobility in solution.

What do we understand by polyhydride complexes? We define polyhydride complexes as compounds having enough hydrogen atoms bound to the metal center of a  $L_nM$  fragment to form at least two different types of ligands. These ligands can be classified in four types depending upon the separation between the coordinated hydrogens: (i) classical hydrides (>1.6 Å), (ii) dihydrogen (0.8–1.0 Å), (iii) elongated dihydrogen (1.0–1.3 Å), and (iv) compressed dihydrides (1.3–1.6 Å). The distinction between elongated dihydrogen and compressed dihydrides is formal, since for these species, the energy cost to move the two hydrogens atoms between 1.00 and 1.60 Å is lower than 4 kcal mol<sup>-1</sup> (i.e., the energy of the complex is practically independent of the separation between the hydrogen atoms).<sup>19</sup> The main difference between them is the activation barrier for the combined rotation of both hydrogen atoms around the M–H<sub>2</sub> axis, less than 8 kcal mol<sup>-1</sup> for the elongated dihydrogen, and between 8 and 12 kcal mol<sup>-1</sup> for the compressed dihydrides.<sup>20</sup> Nonclassical interactions are called those that occur around the metal coordination sphere, between hydrogen atoms separated by less than 1.6 Å.

A noticeable feature of polyhydride complexes is the combined movements of the hydrogen atoms bound to the metal center, in agreement with the mobility of hydride and dihydrogen ligands. These position exchanges are thermally activated and take place with activation barriers which are much lower than those involved in the movements of the rest of the ligands. Mass, geometry, rigidity, and size of the heavy coligands are factors that determine the geometry of the

polyhydride skeleton and prevent position exchanges of these groups. In addition to the thermally activated site exchanges, some polyhydrides undergo quantum exchange coupling,<sup>21</sup> which manifests in the high field region of the <sup>1</sup>H NMR spectra through large values of the observed H–H coupling constants ( $J_{\text{obs}}$ ), which increase as the temperature increases. The phenomenon involves the exchange of the hydrogen nuclei. It occurs by tunneling through a barrier between the two sides of the double-well potential,<sup>22</sup> which is even lower than those calculated for the hydrogen movements. For each temperature and a given hydrogen–hydrogen separation ( $a$ ),  $J_{\text{obs}}$  is determined by eq 1, according to a two-dimensional harmonic oscillator model.<sup>23</sup> Constant  $J_{\text{mag}}$  is the portion of  $J_{\text{obs}}$  due to the Fermi contact interaction, parameter  $\lambda$  is the hard sphere radius of the hydrides, and  $\nu$  describes the H–M–H vibrational wag mode that allows the movement along the H–H vector. They are characteristic for each compound and considered temperature invariant.

$$J_{\text{obs}} = J_{\text{mag}} + 2 \left[ \left( \frac{\nu a}{\pi \lambda \coth[h\nu/2kT]} \right) \exp \left\{ \frac{-2\pi^2 m \nu (a^2 + \lambda^2)}{h \coth[h\nu/2kT]} \right\} \right] \quad (1)$$

Saturated polyhydrides have the ability of losing molecular hydrogen to afford unsaturated species, which coordinate and subsequently activate  $\sigma$ -bonds, including B–H, C–H, Si–H, N–H, and O–H bonds, among others. In this respect, platinum group metals occupy a prominent place between the metal elements.<sup>24–29</sup> The activation of B–H bonds<sup>30,31</sup> is a reaction of great interest concerning the borylation of organic molecules<sup>32–36</sup> and the dehydrocoupling of ammonia-borane.<sup>37–39</sup> The C–H bond activation is a classical issue in organometallics because of its connection with the functionalization of nonactivated organic substrates.<sup>40–47</sup> The metal-mediated rupture of Si–H bonds is notable due to the relevance of the M–SiR<sub>3</sub> species in the hydrosilylation of unsaturated organic substrates, the direct synthesis of chlorosilanes, and SiH/OH coupling.<sup>48</sup> The N–H bond activation promoted by platinum group metals is a key step in reactions of hydroamination of unsaturated organic molecules<sup>49</sup> and for the use of ammonia in homogeneous catalysis.<sup>50</sup> The cleavage of O–H bonds is of potential relevance to metal-mediated solar-energy conversion routes.<sup>51</sup> It is expected that water splitting driven by sunlight will constitute a growing area of particular interest in the near future.<sup>52</sup>

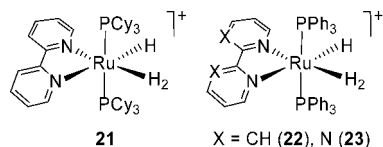
The coordination of a  $\sigma$ -E–E' bond to a transition metal involves  $\sigma$ -donation from the  $\sigma$ -orbital of the coordinated bond to empty orbitals of the metal and back bonding from the metal to the  $\sigma^*$ (EE') orbital. The activation toward homolysis or heterolysis of the coordinated bond depends on the electronic nature of the metal center. Nucleophilic metal centers enhance the back-donation, resulting in the homolytic addition of E–E' to the metal. On the other hand, electrophilic metal centers increase the  $\sigma$ -donation to the metal, promoting the heterolytic cleavage of the E–E' bond. The cation acceptor can be an external Lewis base, including the solvent of the reaction, a hydride ligand or a group in the coordination sphere of the metal with free electron pairs (Scheme 1).

A third form of cleavage is the  $\sigma$ -bond metathesis, which involves the transfer of E or E' from E' or E to another ligand R



species appear to take place.<sup>62,63</sup> The *cis* hydride-dihydrogen disposition has been stabilized by using bulky phosphines and rigid quelating N–N ligands (Chart 2).<sup>83,84</sup> These compounds,

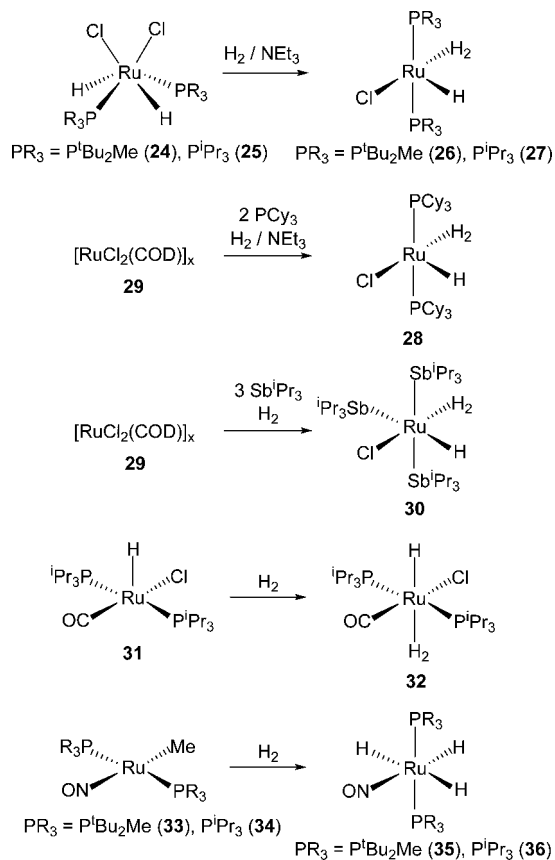
Chart 2. *cis*-Hydride-Dihydrogen Cations  $[L_nRuH(\eta^2-H_2)]^+$



$[RuH(\eta^2-H_2)(N-N)(PR_3)_2]^+$  (N–N = 2,2'-bipyridine,  $PR_3$  =  $PCy_3$  (21),  $PPh_3$  (22); N–N = bipyrimidine,  $PR_3$  =  $PPh_3$  (23)), which have been prepared by protonation of the corresponding dihydrides, exhibit very fast hydride-dihydrogen exchange ( $\Delta G^\ddagger = 2-3$  kcal mol<sup>-1</sup>), which precludes decoalescence of the high field resonance in the <sup>1</sup>H NMR spectra even at low temperatures.

Neutral five- and six-coordinate  $RuH(\eta^2-H_2)$ -complexes are also known (Scheme 2). Although the low stability of the five-

Scheme 2. Preparation of  $L_nRuH_3$  Complexes

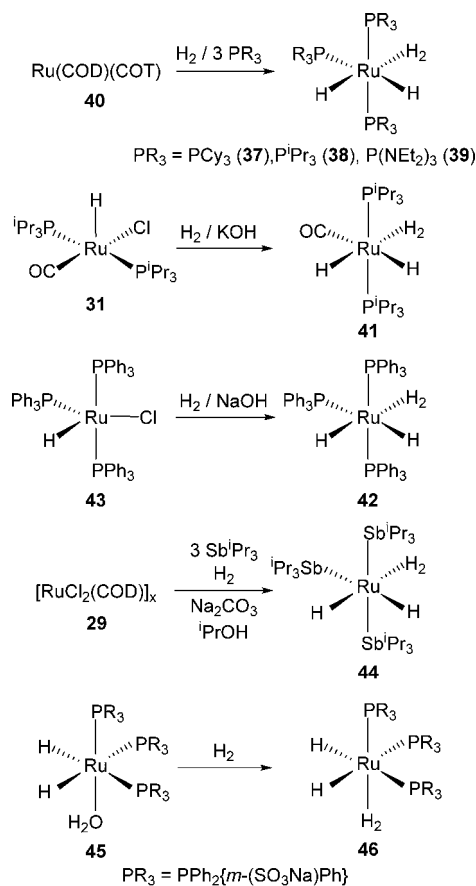


coordinate species prevents isolation, they have proved to be useful synthetic intermediates to prepare interesting five-coordinate hydride-vinylidene derivatives<sup>85,86</sup> and Grubbs-type carbene catalysts.<sup>87</sup> These intermediates have been generated through two different methods. Treatment of toluene solutions of  $RuH_2Cl_2(PR_3)_2$  ( $PR_3 = P^iBu_2Me$  (24),  $P^iPr_3$  (25)) with  $NEt_3$  under 1.5 atm of  $H_2$ , at room temperature, affords  $RuHCl(\eta^2-H_2)(PR_3)_2$  ( $PR_3 = P^iBu_2Me$  (26),  $P^iPr_3$  (27)).<sup>88</sup> The tricyclohexylphosphine counterpart  $RuHCl(\eta^2-H_2)$

$(PCy_3)_2$  (28) however has been prepared by reacting  $[RuCl_2(\eta^4-COD)]_x$  (29, COD = 1,5-cyclooctadiene),  $PCy_3$ , and  $NEt_3$  in *sec*-butyl alcohol, at 80 °C, under 1.5 atm of  $H_2$ .<sup>87</sup> By using triisopropylstibane instead of tricyclohexylphosphine, the same procedure yields the six-coordinate stibane derivative  $RuHCl(\eta^2-H_2)(Sb^iPr_3)_3$  (30).<sup>89</sup> Reaction of  $H_2$  with the coordinatively unsaturated complex  $RuHCl(CO)(P^iPr_3)_2$  (31) leads to  $RuHCl(\eta^2-H_2)(CO)(P^iPr_3)_2$  (32).<sup>90</sup> In contrast, the hydrogenolysis of the square-planar compounds  $RuMe(NO)(PR_3)_2$  ( $PR_3 = P^iBu_2Me$  (33),  $P^iPr_3$  (34)) gives the classical trihydrides  $RuH_3(NO)(PR_3)_2$  ( $PR_3 = P^iBu_2Me$  (35),  $P^iPr_3$  (36)).<sup>91</sup>

The  $RuH_4$ -complexes are dihydride-dihydrogen species,<sup>92–94</sup> which show a marked tendency to lose the dihydrogen ligand and to form dimers in the absence of coordinating molecules.<sup>95,96</sup> These compounds can be obtained according to Scheme 3. Complexes  $RuH_2(\eta^2-H_2)(PR_3)_3$  ( $PR_3 = PCy_3$

Scheme 3. Preparation of  $L_nRuH_2(\eta^2-H_2)$  Complexes

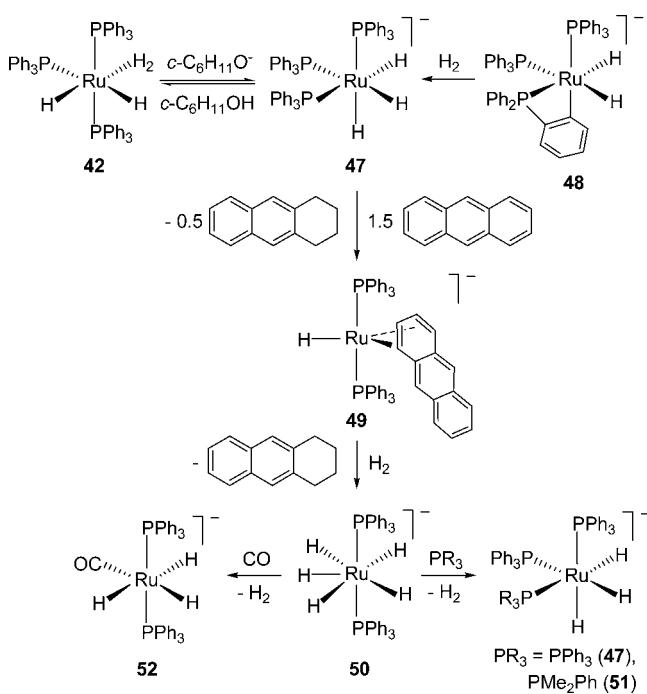


(37),  $P^iPr_3$  (38),  $P(NEt_2)_3$  (39)) have been prepared by hydrogenation of  $Ru(\eta^4-COD)(\eta^6-COT)$  (40, COT = cyclooctatetraene) in the presence of 3 equiv of phosphine.<sup>97</sup> Compounds  $RuH_2(\eta^2-H_2)(CO)(P^iPr_3)_2$  (41)<sup>90</sup> and  $RuH_2(\eta^2-H_2)(PPh_3)_3$  (42)<sup>98</sup> are usually generated by hydrogenolysis of the corresponding chloride-hydride precursors, 31 and  $RuHCl(PPh_3)_3$  (43), in the presence of a base. The stibane derivative  $RuH_2(\eta^2-H_2)(Sb^iPr_3)_3$  (44) has been synthesized through a procedure intermediate between both methods, involving the hydrogenation of the diolefin and the hydrogenolysis of the Ru–Cl bonds of the polymeric material 29 in the presence of 3 equiv of  $Sb^iPr_3$ ,  $Na_2CO_3$ , and 2-propanol as solvent.<sup>89</sup> The

replacement of the water molecule of  $\text{RuH}_2(\text{H}_2\text{O})(\text{mtppms})_3$  (**45**,  $\text{mtppms}$  = sodium 3-diphenylphosphinobenzenesulfonate) by molecular hydrogen has afforded the water-soluble dihydride-dihydrogen  $\text{RuH}_2(\eta^2\text{-H}_2)(\text{mtppms})_3$  (**46**).<sup>99</sup>

The dihydride-dihydrogen **42** is deprotonated by  $c\text{-C}_6\text{H}_{11}\text{O}^-$  to reach an equilibrium with the anionic trihydride  $[\text{RuH}_3(\text{PPh}_3)_3]^-$  (**47**) and cyclohexanol ( $K_{\text{eq}} \approx 0.13$  at ambient temperature in THF).<sup>100</sup> This anion is conveniently prepared by means of reaction of  $[\text{RuH}_2(\text{PPh}_3)_2\{\kappa^2\text{-P,C-PPh}_2(\text{C}_6\text{H}_4)\}]^-$  (**48**) with  $\text{H}_2$  (1 atm).<sup>101,102</sup> After adding a slight excess of 18-crown-6-ether to its THF solutions, single crystals of the  $[\text{K}(\text{C}_{12}\text{H}_{24}\text{O}_6)]^+$ -salt of **47** suitable for X-ray diffraction analysis were obtained. The structure revealed a *fac*-disposition of both hydride and phosphine ligands in an octahedral environment.<sup>103</sup> Complex **47** reacts with 1.5 equiv of anthracene in THF to form 0.5 equiv of 1,2,3,4-tetrahydroanthracene and  $[\text{RuH}(\text{PPh}_3)_2(\text{anthracene})]^-$  (**49**), which has been isolated as the  $\text{K}^+$ -salt. In THF, at 25 °C, anion **49** rapidly reacts with molecular hydrogen to yield the pentahydride  $[\text{RuH}_5(\text{PPh}_3)_2]^-$  (**50**), which has been also isolated as the  $\text{K}^+$ -salt, and 1 equiv of 1,2,3,4-tetrahydroanthracene. In agreement with this sequence of reactions, complexes **47**–**50** have been found to serve as catalyst precursors for the hydrogenation of anthracene with rates which ultimately level off to approximately the same value, suggesting that they give rise to a common catalytic mechanism. On the basis of NMR data, a pentagonal bipyramidal structure has been proposed for **50**. This compound is the entry to anionic trihydride derivatives. Its reactions with phosphines and CO rapidly afford  $[\text{RuH}_3(\text{PR}_3)(\text{PPh}_3)_2]^-$  ( $\text{PR}_3 = \text{PPh}_3$  (**47**),  $\text{PMe}_2\text{Ph}$  (**51**)) and  $[\text{RuH}_3(\text{CO})(\text{PPh}_3)_2]^-$  (**52**), according to Scheme 4. The triisopropylphosphine counterpart  $[\text{RuH}_3(\text{CO})(\text{P}^i\text{Pr}_3)_2]^-$  (**53**) has been generated under hydrogen, by reaction of the chloride-hydride **31** with KH in the presence of crown ethers, and isolated as the  $[\text{KQ}]^+$ -salts ( $\text{Q} = 2.2.2\text{-crypt}$ , 18-crown-6, 1-aza-18-crown-6).<sup>104</sup> On the other

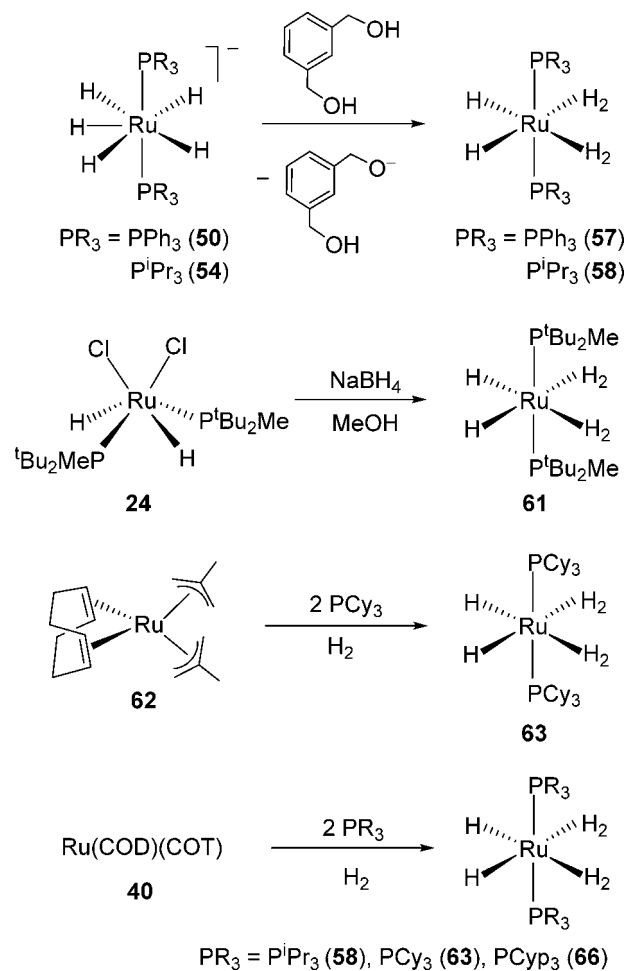
**Scheme 4. Hydrogenation of Anthracene Promoted by Ruthenium Complexes and Related Reactions**



hand, the related salts  $[\text{KQ}][\text{RuH}_3(\text{P}^i\text{Pr}_3)_2]$  (**54**) have been formed in a one-pot synthesis procedure starting from  $\text{RuCl}_3 \cdot x\text{H}_2\text{O}$ .<sup>105</sup> Treatment of  $[\text{RuCl}_2(\text{dcypb})(\text{CO})]_2$  (**55**,  $\text{dcypb} = 1,4\text{-bis}(\text{dicyclohexylphosphino})\text{butane}$ ) with 8 equiv of  $\text{K}[\text{HB}^t\text{Bu}_3]$  affords  $[\text{RuH}_3(\text{CO})(\text{dcypb})]^-$  (**56**), stabilized by interactions with a  $\text{K}^+$  counteranion and an intact  $[\text{HB}^t\text{Bu}_3]$  moiety in the third coordination sphere. Complex **56** effects reduction of benzophenone under mild conditions. It is also active for ortho functionalization of this ketone under 20 atm of ethylene.<sup>106</sup>

Pentahydrides **50** and **54** undergo protonation with 1,3-benzenedimethanol to give the dihydride-bis(dihydrogen) derivatives  $\text{RuH}_2(\eta^2\text{-H}_2)_2(\text{PR}_3)_2$  ( $\text{PR}_3 = \text{PPh}_3$  (**57**),  $\text{P}^i\text{Pr}_3$  (**58**)).<sup>107</sup> These compounds are very unstable with respect to loss of  $\text{H}_2$  and form the trihydride-bridged polyhydride dimers  $(\text{PR}_3)_2\text{HRu}(\mu\text{-H})_3\text{RuH}_2(\text{PR}_3)_2$  ( $\text{PR}_3 = \text{PPh}_3$  (**59**),  $\text{P}^i\text{Pr}_3$  (**60**)). The classical or nonclassical nature of the terminal  $\text{RuH}_2$  unit of these species is not clear and appears to depend upon the phosphine.<sup>107–109</sup> In addition to the protonation of anionic pentahydrides,  $\text{RuH}_6$ -complexes can be obtained by a variety of procedures (Scheme 5). Complex  $\text{RuH}_2(\eta^2\text{-H}_2)_2(\text{P}^t\text{Bu}_2\text{Me})_2$  (**61**) has been prepared by reaction of the dichloride-dihydride **24** with  $\text{NaBH}_4$  in the presence of methanol.<sup>86</sup> Leitner and co-workers have observed that a mixture of  $\text{Ru}(\eta^3\text{-C}_4\text{H}_7)_2(\eta^4\text{-COD})$  (**62**) and  $\text{PCy}_3$  reacts with hydrogen to give  $\text{RuH}_2(\eta^2\text{-H}_2)_2(\text{PCy}_3)_2$  (**63**) in high yield, whereas  $\text{Ru}(\eta^3\text{-C}_4\text{H}_7)_2\{\text{C}_y\text{P}(\text{CH}_2)_3\text{PCy}_2\}$  (**64**) leads to  $\{\text{C}_y\text{P}(\text{CH}_2)_3\text{PCy}_2\}\text{HRu}(\mu\text{-H})_2(\eta^2\text{-H}_2)_2(\text{C}_y\text{P}(\text{CH}_2)_3\text{PCy}_2)_2$  (**66**).

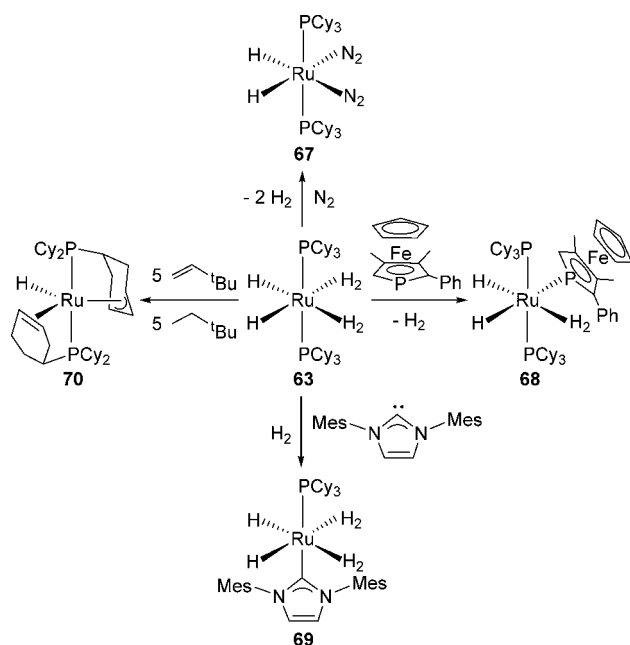
**Scheme 5. Preparation of  $\text{RuH}_2(\eta^2\text{-H}_2)_2(\text{PR}_3)_2$  Complexes**



$\text{H})_3\text{RuH}_2\{\text{Cy}_2\text{P}(\text{CH}_2)_3\text{PCy}_2\}$  (**65**) under identical conditions.<sup>110</sup> Grubbs has shown that complex **63** can be also obtained by hydrogenation (2 atm) of the polymeric material **29** in the presence of 2 equiv of  $\text{PCy}_3$  and NaOH (excess) in *sec*-butyl alcohol;<sup>111</sup> modifications to this method have been described in several patents.<sup>112,113</sup> The most general procedure to prepare this type of compounds appears to be the hydrogenation of **40** in the presence of 2 equiv of phosphine.<sup>97</sup> In this way, complex  $\text{RuH}_2(\eta^2\text{-H}_2)_2(\text{PCyp}_3)_2$  (**66**,  $\text{PCyp}_3 = \text{tricyclopentylphosphine}$ ) has been obtained, in addition to **58** and **63**. The nonclassical nature of these compounds has been corroborated through the neutron diffraction structure of **66**.<sup>114</sup> The H–H distances in the coordinated hydrogen molecules are equal [0.825(8) and 0.835(8) Å], in excellent agreement with the results from DFT calculations at the B3LYP level (0.853 Å). The Ru–( $\text{H}_2$ ) distances lie between 1.730(5) and 1.764(5) Å, whereas the Ru–H bond lengths of 1.628(4) and 1.625(4) Å are in the expected range for classical hydrides. The separation between each hydride and its *cis* dihydrogen ligand of about 2.1 Å rules out the presence of any *cis* interaction. In solution, the hydride and dihydrogen ligands of these compounds rapidly exchange their positions. Furthermore, the dihydrogen ligands exchange with uncoordinated  $\text{H}_2$  molecules. In agreement with both processes, the exposure of **63** and **66** to 3 bar of  $\text{D}_2$  over a day has afforded the respective  $\text{RuD}_2(\eta^2\text{-D}_2)_2(\text{PR}_3)_2$  ( $\text{PR}_3 = \text{PCy}_3$ ,<sup>115,116</sup>  $\text{PCyp}_3$ <sup>117</sup>).

The tricyclohexylphosphine derivative **63** is the best-studied complex of this family. Its reactivity, which was reviewed by Sabo-Etienne and Chaudret in 1998,<sup>55</sup> is dominated by substitution and hydrogen transfer reactions. Substitutions (Scheme 6) can give rise to unusual complexes as the

Scheme 6. Some Reactions of **63**



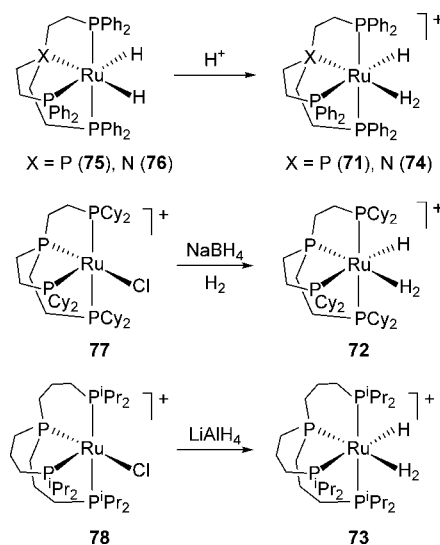
bis(dinitrogen) derivative  $\text{RuH}_2(\eta^2\text{-N}_2)_2(\text{PCy}_3)_2$  (**67**) or the mixed phosphine-phosphine' dihydride-dihydrogen compound  $\text{RuH}_2(\eta^2\text{-H}_2)(\text{PR}_3)(\text{PCy}_3)_2$  (**68**,  $\text{PR}_3 = 2\text{-phenyl-3,4-dimethylphosphaferrrocene}$ ).<sup>118</sup> In contrast to this ferrocenephosphine, the treatment of **63** with 1,3-dimesitylimidazol-2-ylidene (IMes), under hydrogen, in hydrocarbon solvents leads to the

mixed phosphine-NHC dihydride-bis(dihydrogen)  $\text{RuH}_2(\eta^2\text{-H}_2)_2(\text{IMes})(\text{PCy}_3)$  (**69**).<sup>119</sup> Rapid hydrogen transfer of up to five hydrogen molecules from **63** to unsaturated organic substrates can be achieved at room temperature to form  $\text{RuH}\{(\eta^3\text{-C}_6\text{H}_8)\text{PCy}_2\}\{(\eta^2\text{-C}_6\text{H}_9)\text{PCy}_2\}$  (**70**). The regeneration of **63** upon bubbling hydrogen into solutions of **70** confers to this compound hydrogen store character. This property makes **63** a good catalyst precursor for hydrogenation reactions, including those of arenes.<sup>120,121</sup> It is also a catalyst precursor for the dehydrogenative silylation of alkenes and the ortho alkylation of aromatic ketones.<sup>55</sup>

## 2.2. Complexes with Tetrapodal and Tripodal Phosphine Ligands

Tetrapodal tetra- and triphosphines stabilize the cationic *cis*-hydride-dihydrogen derivatives  $[\text{RuH}(\eta^2\text{-H}_2)(\text{PP}_3)]^+$  ( $\text{PP}_3 = \text{P}(\text{CH}_2\text{CH}_2\text{PPh}_2)_3$  (**71**),  $\text{P}(\text{CH}_2\text{CH}_2\text{PCy}_2)_3$  (**72**),  $\text{P}(\text{CH}_2\text{CH}_2\text{CH}_2\text{P}^i\text{Pr}_2)_3$  (**73**) and  $[\text{RuH}(\eta^2\text{-H}_2)(\text{NP}_3)]^+$  (**74**,  $\text{NP}_3 = \text{N}(\text{CH}_2\text{CH}_2\text{PPh}_2)_3$ ) related to **21–23**. Complexes **71**<sup>122,123</sup> and **74**<sup>124</sup> have been prepared by protonation of the corresponding dihydrides  $\text{RuH}_2\{\text{P}(\text{CH}_2\text{CH}_2\text{PPh}_2)_3\}$  (**75**) and  $\text{RuH}_2\{\text{N}(\text{CH}_2\text{CH}_2\text{PPh}_2)_3\}$  (**76**), whereas the treatment of tetrahydrofuran solutions of the cationic five-coordinate chloride-precursors  $[\text{RuCl}(\text{PP}_3)]^+$  ( $\text{PP}_3 = \text{P}(\text{CH}_2\text{CH}_2\text{PCy}_2)_3$  (**77**),  $\text{P}(\text{CH}_2\text{CH}_2\text{CH}_2\text{P}^i\text{Pr}_2)_3$  (**78**) with  $\text{NaBH}_4$  or  $\text{LiAlH}_4$  and subsequently with ethanol, affords **72**<sup>125</sup> and **73**<sup>126</sup> (Scheme 7).

Scheme 7. Preparation of Cationic *cis*-Hydride-Dihydrogen-Ruthenium(II) Complexes Containing Tetrapodal Phosphine Ligands

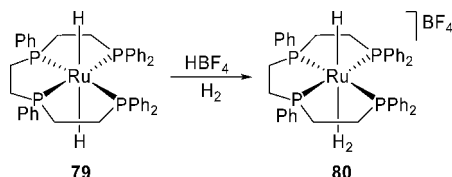


The *trans*-disposition of the dihydrogen ligand to the bridging atom of the phosphine has been confirmed by means of the X-ray diffraction structures of **73**<sup>126</sup> and **74**.<sup>124</sup> For complex **71**, a barrier to the rotation of the dihydrogen ligand ( $d_{\text{H}_2} = 0.87$  Å) of 1.36 kcal mol<sup>-1</sup> has been determined by inelastic neutron scattering.<sup>127</sup> This compound has shown to be an efficient catalyst precursor for the dimerization of terminal alkynes to *Z*-1,4-disubstituted enynes,<sup>128</sup> the hydrogenation of phenylacetylene to styrene,<sup>129</sup> and the chemoselective reduction of  $\alpha,\beta$ -unsaturated ketones to allylic alcohols via hydrogen transfer.<sup>130,131</sup>

The ligand *meso*-tetraphos-1 *S,R*- $\text{Ph}_2\text{PCH}_2\text{CH}_2\text{P}(\text{Ph})\text{CH}_2\text{CH}_2\text{P}(\text{Ph})\text{CH}_2\text{CH}_2\text{P}(\text{Ph})\text{CH}_2\text{CH}_2\text{PPh}_2$  stabilizes a *trans*-hydride-dihy-

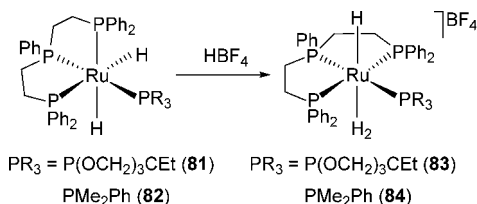
drogen counterpart,<sup>132</sup> in contrast to the phosphines shown in Scheme 7. Thus, the addition of HBF<sub>4</sub>·OEt<sub>2</sub> to diethyl ether solutions of the dihydride RuH<sub>2</sub>(*meso*-tetraphos-1) (79), under hydrogen (1 atm), leads to [RuH( $\eta^2$ -H<sub>2</sub>)(*meso*-tetraphos-1)]BF<sub>4</sub> (80), which displays a dihydrogen H–H distance of 0.89 Å according to *T*<sub>1</sub>(min) and *J*<sub>H–D</sub> values (Scheme 8). In contrast to 71–74, the position exchange between the hydride and dihydrogen ligands of 80 is slow.

Scheme 8. Protonation of 79



The protonation of the *cis*-dihydrides RuH<sub>2</sub>(P<sub>3</sub>)(PR<sub>3</sub>)(P<sub>3</sub> = PPh(CH<sub>2</sub>CH<sub>2</sub>PPh<sub>2</sub>)<sub>2</sub>; PR<sub>3</sub> = P(OCH<sub>2</sub>)<sub>3</sub>CEt (81), PMe<sub>2</sub>Ph (82)), containing tridentate and monodentate phosphines, with HBF<sub>4</sub>·OEt<sub>2</sub> gives the *trans*-hydride-dihydrogen derivatives [RuH( $\eta^2$ -H<sub>2</sub>)(P<sub>3</sub>)(PR<sub>3</sub>)]BF<sub>4</sub> (PR<sub>3</sub> = P(OCH<sub>2</sub>)<sub>3</sub>CEt (83), PMe<sub>2</sub>Ph (84)).<sup>133</sup> In the reaction, the binding mode of the triphos ligand changes from facial to meridional, which makes possible to place the  $\eta^2$ -dihydrogen molecule *trans* to the high *trans*-influence terminal hydride ligand (Scheme 9).

Scheme 9. Protonation of 81 and 82



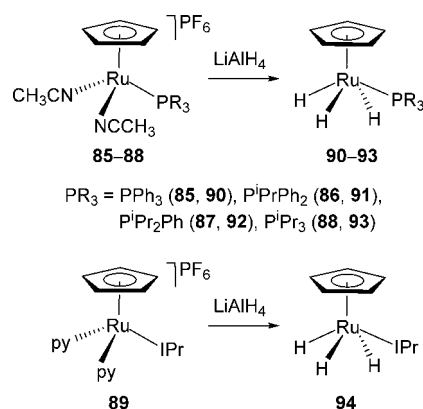
### 2.3. Half Sandwich Compounds

Most complexes of this type are cyclopentadienyl (Cp) and pentamethylcyclopentadienyl (Cp\*) trihydride derivatives. A noticeable characteristic of these species is the exceptionally large value of the H–H coupling constants of the hydride ligands, in the <sup>1</sup>H NMR spectra, which has been attributed to a quantum-mechanical exchange process,<sup>134,135</sup> although it has not been quantified on the basis of the two-dimensional harmonic oscillator model described in eq 1.

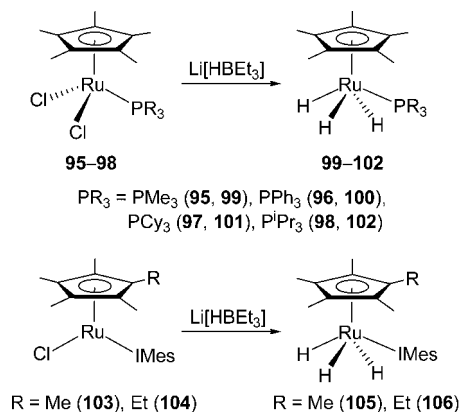
A facile general access to Cp-complexes has been reported by Nikonov and co-workers (Scheme 10). Treatment of the cationic precursors [Ru( $\eta^5$ -C<sub>5</sub>H<sub>5</sub>)(CH<sub>3</sub>CN)<sub>2</sub>(PR<sub>3</sub>)]PF<sub>6</sub> (PR<sub>3</sub> = PPh<sub>3</sub> (85), P<sup>i</sup>PrPh<sub>2</sub> (86), P<sup>i</sup>Pr<sub>2</sub>Ph (87), P<sup>i</sup>Pr<sub>3</sub> (88)) and the related NHC-supported derivative [Ru( $\eta^5$ -C<sub>5</sub>H<sub>5</sub>)(py)<sub>2</sub>(IPr)]PF<sub>6</sub> (89; py = pyridine, IPr = 1,3-bis(2,6-diisopropylphenyl)imidazol-2-ylidene) with LiAlH<sub>4</sub> in tetrahydrofuran, followed by quenching the reaction mixture with degassed water, leads to the trihydride derivatives RuH<sub>3</sub>( $\eta^5$ -C<sub>5</sub>H<sub>5</sub>)(PR<sub>3</sub>)(PR<sub>3</sub> = PPh<sub>3</sub> (90), P<sup>i</sup>PrPh<sub>2</sub> (91), P<sup>i</sup>Pr<sub>2</sub>Ph (92), P<sup>i</sup>Pr<sub>3</sub> (93))<sup>136</sup> and RuH<sub>3</sub>( $\eta^5$ -C<sub>5</sub>H<sub>5</sub>)(IPr) (94),<sup>137</sup> respectively, in good yields.

The related Cp\* complexes have been mainly prepared by three different methods, using Li[HB(Et)<sub>3</sub>], NaBH<sub>4</sub>, and H<sub>2</sub> as hydride sources.

Treatment of the ruthenium(III) precursors RuCl<sub>2</sub>( $\eta^5$ -C<sub>5</sub>Me<sub>5</sub>)(PR<sub>3</sub>) (PR<sub>3</sub> = PMe<sub>3</sub> (95), PPh<sub>3</sub> (96), PCy<sub>3</sub> (97),

Scheme 10. Preparation of RuH<sub>3</sub>( $\eta^5$ -C<sub>5</sub>H<sub>5</sub>)L Complexes Using LiAlH<sub>4</sub>

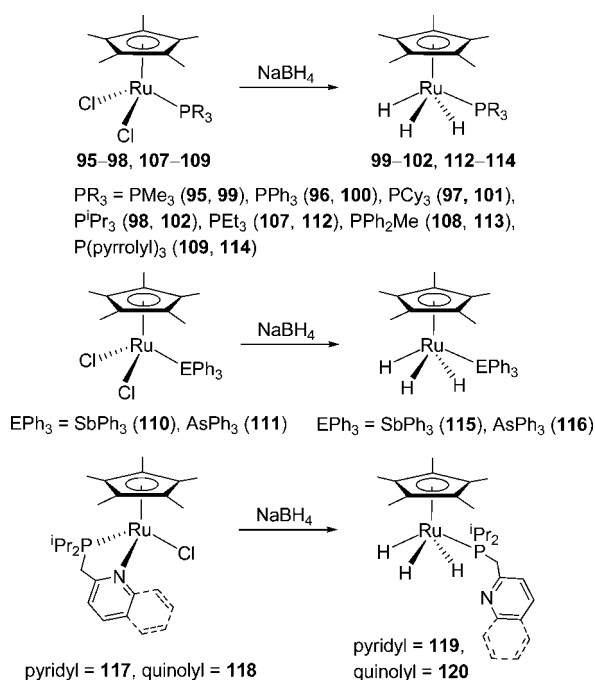
P<sup>i</sup>Pr<sub>3</sub> (98)) with 2 equiv of Li[HB(Et)<sub>3</sub>] in tetrahydrofuran directly leads to the trihydrides RuH<sub>3</sub>( $\eta^5$ -C<sub>5</sub>Me<sub>5</sub>)(PR<sub>3</sub>) (PR<sub>3</sub> = PMe<sub>3</sub> (99), PPh<sub>3</sub> (100), PCy<sub>3</sub> (101), P<sup>i</sup>Pr<sub>3</sub> (102)),<sup>138</sup> according to Scheme 11. Similarly, the addition of 2 equiv of

Scheme 11. Preparation of RuH<sub>3</sub>( $\eta^5$ -C<sub>5</sub>Me<sub>5</sub>)L Complexes by Using Li[HB(Et)<sub>3</sub>]

Li[HB(Et)<sub>3</sub>] to the ruthenium(II) NHC-precursors RuCl( $\eta^5$ -C<sub>5</sub>Me<sub>5</sub>)(IMes) (103) and RuCl( $\eta^5$ -C<sub>5</sub>Me<sub>4</sub>Et)(IMes) (104) affords RuH<sub>3</sub>( $\eta^5$ -C<sub>5</sub>Me<sub>5</sub>)(IMes) (105) and RuH<sub>3</sub>( $\eta^5$ -C<sub>5</sub>Me<sub>4</sub>Et)(IMes) (106), respectively.<sup>139</sup>

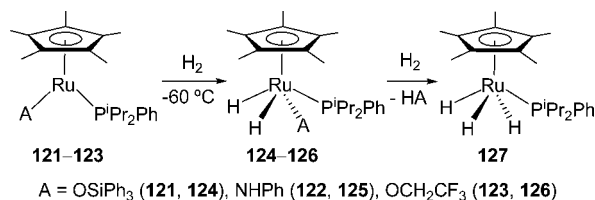
Sometimes NaBH<sub>4</sub> has been used instead of Li[HB(Et)<sub>3</sub>] (Scheme 12). Thus, reactions of NaBH<sub>4</sub> with RuCl<sub>2</sub>( $\eta^5$ -C<sub>5</sub>Me<sub>5</sub>)(PR<sub>3</sub>) (PR<sub>3</sub> = PMe<sub>3</sub> (95), PPh<sub>3</sub> (96), PCy<sub>3</sub> (97), P<sup>i</sup>Pr<sub>3</sub> (98), PEt<sub>3</sub> (107), PPh<sub>2</sub>Me (108), P(pyrrolyl)<sub>3</sub> (109)) and RuCl<sub>2</sub>( $\eta^5$ -C<sub>5</sub>Me<sub>5</sub>)(EPh<sub>3</sub>) (EPh<sub>3</sub> = SbPh<sub>3</sub> (110), AsPh<sub>3</sub> (111)) in ethanol result in the formation of the trihydrides RuH<sub>3</sub>( $\eta^5$ -C<sub>5</sub>Me<sub>5</sub>)(PR<sub>3</sub>) (PR<sub>3</sub> = PEt<sub>3</sub> (112), PPh<sub>2</sub>Me (113), P(pyrrolyl)<sub>3</sub> (114)<sup>141</sup>) and RuH<sub>3</sub>( $\eta^5$ -C<sub>5</sub>Me<sub>5</sub>)(EPh<sub>3</sub>) (EPh<sub>3</sub> = SbPh<sub>3</sub> (115), AsPh<sub>3</sub> (116)),<sup>142</sup> in addition to 99–102. In this case, the reactions take place via the tetrahydrideborate intermediates Ru( $\kappa^2$ -H<sub>2</sub>BH<sub>2</sub>)( $\eta^5$ -C<sub>5</sub>Me<sub>5</sub>)(PR<sub>3</sub>), which decompose in the alcohol. Starting from RuCl( $\eta^5$ -C<sub>5</sub>Me<sub>5</sub>)( $\kappa^2$ -P,N<sup>i</sup>-Pr<sub>2</sub>PCH<sub>2</sub>X) (X = pyridyl (117), quinolyl (118)), the same procedure gives RuH<sub>3</sub>( $\eta^5$ -C<sub>5</sub>Me<sub>5</sub>)( $\kappa^1$ -P<sup>i</sup>-Pr<sub>2</sub>PCH<sub>2</sub>X) (X = pyridyl (119), quinolyl (120)).<sup>143</sup>

Reactions of Ru(A)( $\eta^5$ -C<sub>5</sub>Me<sub>5</sub>)(P<sup>i</sup>Pr<sub>2</sub>Ph) (A = OSiPh<sub>3</sub> (121), NHPh (122), OCH<sub>2</sub>CF<sub>3</sub> (123)) with hydrogen give, at –60 °C, Ru(A)(H)<sub>2</sub>( $\eta^5$ -C<sub>5</sub>Me<sub>5</sub>)(P<sup>i</sup>Pr<sub>2</sub>Ph) (A = OSiPh<sub>3</sub> (124), NHPh (125), OCH<sub>2</sub>CF<sub>3</sub> (126)), where the two hydride

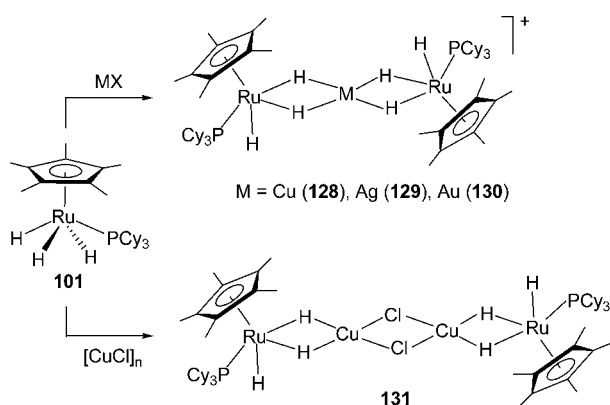
Scheme 12. Preparation of  $\text{RuH}_3(\eta^5\text{-C}_5\text{Me}_5)\text{L}$  Complexes by Using  $\text{NaBH}_4$ 

ligands are *cisoid* disposed. These molecules react with additional hydrogen to yield  $\text{RuH}_3(\eta^5\text{-C}_5\text{Me}_5)(\text{P}^i\text{Pr}_2\text{Ph})$  (127) and liberate HA (Scheme 13).<sup>144</sup>

Scheme 13. Sequential Hydrogenolysis of 121–123

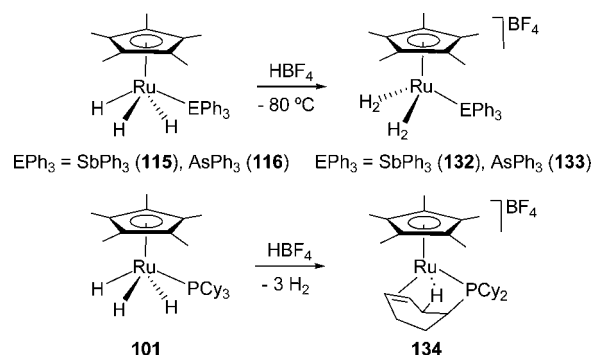


These trihydride derivatives are good Lewis bases that have been used to prepare acid–base adducts with metallic Lewis acids (Scheme 14). Addition of  $[\text{Cu}(\text{CH}_3\text{CN})_4]\text{PF}_6$ ,  $\text{AgBF}_4$ , and  $[\text{Au}(\text{THT})_2]\text{PF}_6$  (THT = tetrahydrothiophene) to tetrahydrofuran solutions of **101** leads to the heterometallic derivatives  $[\{\text{RuH}(\eta^5\text{-C}_5\text{Me}_5)(\text{PCy}_3)(\mu\text{-H})_2\}_2\text{M}]\text{A}$  ( $\text{M} = \text{Cu}$

Scheme 14. Reactions of **101** with Metallic Lewis Acids

(128),  $\text{Ag}$  (129),  $\text{Au}$  (130);  $\text{A} = \text{BF}_4$  or  $\text{PF}_6$ ),<sup>145</sup> whereas the reaction of **101** with  $[\text{CuCl}]_n$  affords  $[\{\text{RuH}(\eta^5\text{-C}_5\text{Me}_5)(\text{PCy}_3)(\mu\text{-H})_2\}_2\text{Cu}(\mu\text{-Cl})_2]$  (131),<sup>146</sup> which has been characterized by X-ray diffraction analysis. The  $\text{d}^{10}$  cation of these adducts has a significant effect on the quantum-mechanical exchange coupling of the hydride ligands, increasing the H–H coupling constant, with regard to the starting trihydride, with increasing electronegativity of the coinage metal.<sup>145</sup>

These trihydride complexes are also Brønsted bases (Scheme 15). Thus, for instance, complexes **115** and **116** are protonated

Scheme 15. Protonation of  $\text{RuH}_3(\eta^5\text{-C}_5\text{Me}_5)\text{L}$  Complexes

by  $\text{HBF}_4\cdot\text{OEt}_2$  in dichloromethane at  $-80\text{ }^\circ\text{C}$ , furnishing the cationic bis(dihydrogen) derivatives  $[\text{Ru}(\eta^5\text{-C}_5\text{Me}_5)(\eta^2\text{-H}_2)_2(\text{EPh}_3)]\text{BF}_4$  ( $\text{EPh}_3 = \text{SbPh}_3$  (132),  $\text{AsPh}_3$  (133)). These species are unstable and decompose at temperatures higher than  $0\text{ }^\circ\text{C}$ .<sup>142</sup> On the other hand, the protonation of **101** with  $\text{HBF}_4\cdot\text{OEt}_2$  produces the evolution of 3 mol of  $\text{H}_2$  and the formation of  $[\text{Ru}(\eta^5\text{-C}_5\text{Me}_5)(\text{C}_6\text{H}_5\text{PCy}_2)]\text{BF}_4$  (134), containing a cyclohexenyl group coordinated through the C–C double bond and a strong agostic interaction.<sup>146</sup>

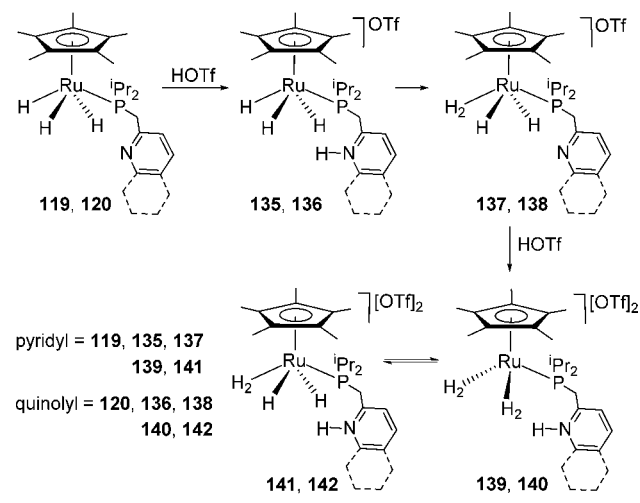
The reactions of **119** and **120** with weak Brønsted acids such as  $\text{PhCO}_2\text{H}$ , indole, and salicylic acid in benzene or toluene result in the formation of hydrogen-bonded adducts between the proton donor and the pendant pyridyl of quinolyl group. In dichloromethane, there is spectroscopic evidence for the proton transfer to a hydride to yield a dihydride-dihydrogen species. In agreement with this, the protonation with  $\text{CF}_3\text{SO}_3\text{H}$  (HOTf) initially gives  $[\text{RuH}_3(\eta^5\text{-C}_5\text{Me}_5)(\kappa^1\text{-P}^i\text{Pr}_2\text{PCH}_2\text{XH})]^+$  ( $\text{X} = \text{pyridyl}$  (135), quinolyl (136)). Then, the NH-proton is transferred to one of the hydrides. The protonation of the resulting dihydride-dihydrogen species  $[\text{RuH}_2(\eta^5\text{-C}_5\text{Me}_5)(\eta^2\text{-H}_2)(\kappa^1\text{-P}^i\text{Pr}_2\text{PCH}_2\text{X})]^+$  ( $\text{X} = \text{pyridyl}$  (137), quinolyl (138)) affords the bis(dihydrogen) derivatives  $[\text{Ru}(\eta^5\text{-C}_5\text{Me}_5)(\eta^2\text{-H}_2)_2(\kappa^1\text{-P}^i\text{Pr}_2\text{PCH}_2\text{XH})]^{2+}$  ( $\text{X} = \text{pyridyl}$  (139), quinolyl (140)), in equilibrium with the corresponding dicationic dihydride-dihydrogen tautomers  $[\text{RuH}_2(\eta^5\text{-C}_5\text{Me}_5)(\eta^2\text{-H}_2)(\kappa^1\text{-P}^i\text{Pr}_2\text{PCH}_2\text{XH})]^{2+}$  ( $\text{X} = \text{pyridyl}$  (140), quinolyl (142); Scheme 16).<sup>143</sup>

#### 2.4. Complexes with Tris(pyrazolyl)borate and Related Ligands

The tris(pyrazolyl)borate (Tp) group avoids four-legged piano stool structures, typical for Cp and Cp\* ligands, and enforces dispositions allowing N–M–N angles close to  $90^\circ$ . These structures favor the nonclassical interactions between the hydrogen atoms bound to the metal center. Thus, in contrast to Cp and Cp\*, the TpRu-polyhydride species always contain at least a dihydrogen ligand.

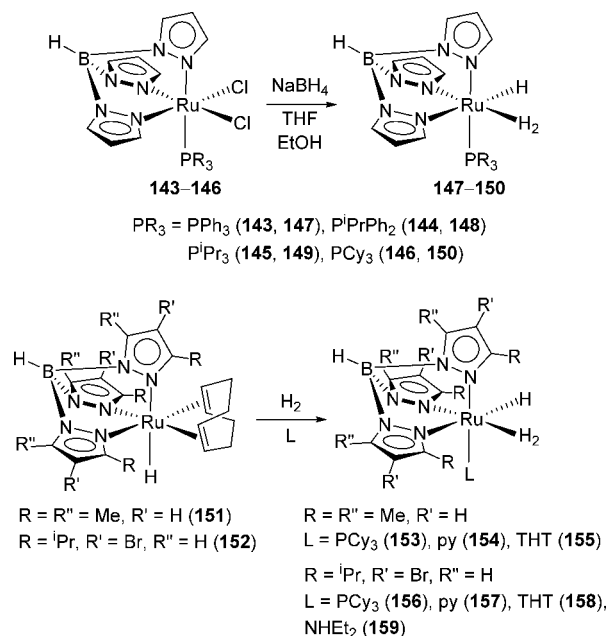


Scheme 16. Double Protonation of 119 and 120



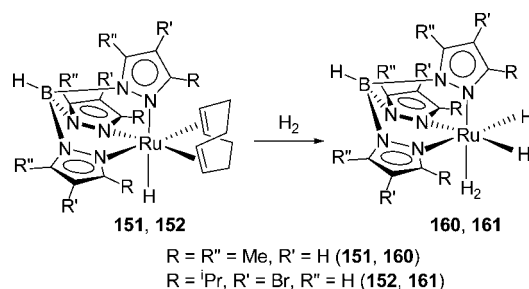
Several hydride-dihydrogen complexes have been isolated and characterized with Tp-type ligands. They have been mainly prepared through two procedures. Reduction of the ruthenium(III) precursors  $\text{RuCl}_2\text{Tp}(\text{PR}_3)$  ( $\text{PR}_3 = \text{PPh}_3$  (**143**),  $\text{P}^i\text{PrPh}_2$  (**144**),  $\text{P}^i\text{Pr}_3$  (**145**),  $\text{PCy}_3$  (**146**)) with  $\text{NaBH}_4$  in a mixture of tetrahydrofuran-ethanol affords  $\text{RuHTp}(\eta^2\text{-H}_2)(\text{PR}_3)$  ( $\text{PR}_3 = \text{PPh}_3$  (**147**),  $\text{P}^i\text{PrPh}_2$  (**148**),  $\text{P}^i\text{Pr}_3$  (**149**),  $\text{PCy}_3$  (**150**)),<sup>147</sup> whereas the hydrogenation of  $\text{RuHTp}^{\text{R}}(\eta^4\text{-COD})$  ( $\text{Tp}^{\text{R}} = \text{hydridetris}(3,5\text{-dimethylpyrazolyl})\text{borate}$  ( $\text{Tp}^{\text{Me}2}$ ; **151**),  $\text{hydridetris}(3\text{-isopropyl-4-bromopyrazolyl})\text{borate}$  ( $\text{Tp}^{\text{R}}$ ; **152**)) in the presence of a monodentate ligand leads to  $\text{RuHTp}^{\text{R}}(\eta^2\text{-H}_2)\text{L}$  ( $\text{Tp}^{\text{R}} = \text{Tp}^{\text{Me}2}$ ,  $\text{L} = \text{PCy}_3$  (**153**),  $\text{py}$  (**154**),  $\text{THT}$  (**155**);  $\text{Tp}^{\text{R}} = \text{Tp}^{\text{R}}$ ,  $\text{L} = \text{PCy}_3$  (**156**),  $\text{py}$  (**157**),  $\text{THT}$  (**158**),  $\text{NHET}_2$  (**159**)).<sup>148,149</sup> The octahedral geometry of these compounds (Scheme 17) has been confirmed by the X-ray structure of **149**.<sup>150</sup> The H–H distance of about 1.0 Å is consistent with the  $T_1(\text{min})$  values found for these species.<sup>147–153</sup>

Scheme 17. Hydride-Dihydrogen–Ruthenium(II) Complexes with Tp-Type Ligands



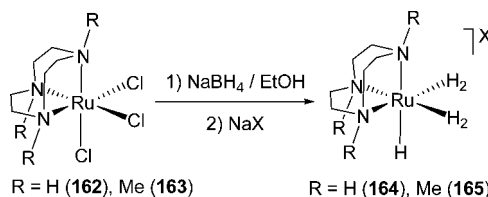
Hydrogenation of **151** and **152** in the absence of a monodentate ligand yields the hydride-bis(dihydrogen) complexes  $\text{RuHTp}^{\text{R}}(\eta^2\text{-H}_2)_2$  ( $\text{Tp}^{\text{R}} = \text{Tp}^{\text{Me}2}$  (**160**),  $\text{Tp}^{\text{R}}$  (**161**)), according to Scheme 18. These compounds have been characterized by classical analytical and spectroscopic methods, including  $T_1$  measurements and  $J_{\text{H-D}}$  coupling constants.<sup>148,149</sup>

Scheme 18. Hydride-bis(Dihydrogen)-Ruthenium(II) Complexes with Tp-Type Ligands



1,4,7-Triazacyclononane (TACN) and 1,4,7-trimethyl-1,4,7-triazacyclononane (TACN\*) are neutral Tp counterparts, which also enforce dispositions allowing N–Ru–N angles close to 90° and therefore favor nonclassical interactions. Thus, the treatment of  $\text{RuCl}_3(\text{TACN})$  (**162**) and  $\text{RuCl}_3(\text{TACN}^*)$  (**163**) with  $\text{NaBH}_4$  in ethanol leads to the respective cationic hydride-bis(dihydrogen) derivatives  $[\text{RuH}(\eta^2\text{-H}_2)_2(\text{TACN})]^+$  (**164**) and  $[\text{RuH}(\eta^2\text{-H}_2)_2(\text{TACN}^*)]^+$  (**165**), after the addition of  $\text{Na}[\text{BPh}_4]$ ,  $\text{NaBF}_4$  or  $[\text{NH}_4]^+\text{PF}_6^-$  ( $\text{X}^-$  in Scheme 19). At

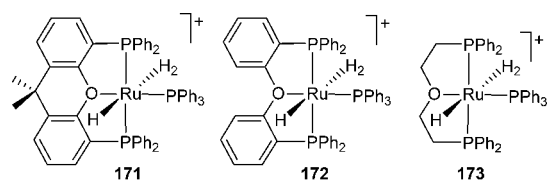
Scheme 19. Hydride-bis(Dihydrogen)-Ruthenium(II) Complexes with TACN-Type Ligands



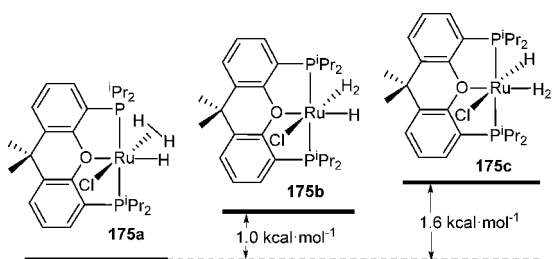
room temperature, these cations lose molecular hydrogen. Complex **164** is converted into the tetranuclear octahydride cluster compound  $[\{(\text{TACN})\text{Ru}\}_4(\mu\text{-H})_6(\mu_3\text{-H})_2]^{4+}$  (**166**), whereas the dehydrogenation of **165** affords the diruthenium-trihydride derivative  $[\{(\text{TACN}^*)\text{Ru}\}_2(\mu\text{-H})_3]^{2+}$  (**167**). Reactions of **165** with 5d-polyhydrides give rise to heterobimetallic dinuclear species.<sup>154,155</sup>

## 2.5. Complexes with Pincer Ligands

Molecular hydrogen displaces the water molecule of the POP-cations  $[\text{RuH}(\text{H}_2\text{O})(\text{POP})(\text{PPh}_3)]^+$  ( $\text{POP} = 9,9\text{-dimethyl-4,5-bis(diphenylphosphino)xanthene}$  (**168**),  $\text{bis}(2\text{-diphenylphosphino)phenyl}(\text{DPEphos})$  (**169**),  $(\text{Ph}_2\text{PCH}_2\text{CH}_2)_2\text{O}$  (**170**)) to give the respective *trans*-hydride-dihydrogen derivatives  $[\text{RuH}(\eta^2\text{-H}_2)(\text{POP})(\text{PPh}_3)]^+$  ( $\text{POP} = \text{xantphos}$  (**171**),  $\text{DPEphos}$  (**172**),  $(\text{Ph}_2\text{PCH}_2\text{CH}_2)_2\text{O}$  (**173**)). The *trans*-disposition of the hydride and dihydrogen ligands (Chart 3), which agrees well with the low thermal stability of these compounds, is strongly supported by the presence of two high field resonances in the  $^1\text{H}$  NMR spectra of the complexes. The values of  $T_1(\text{min})$  of the dihydrogen signal and  $J_{\text{H-D}}$  coupling constants are consistent with dihydrogen H–H distances of about 0.9 Å.<sup>156</sup>

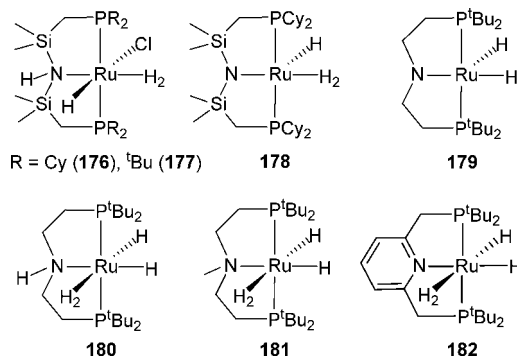
**Chart 3. *trans*-Hydride-Dihydrogen Derivatives [RuH( $\eta^2$ -H<sub>2</sub>)(POP)(PPh<sub>3</sub>)<sup>+</sup>**

Molecular hydrogen also displaces the dimethyl sulfoxide ligand of the neutral complex RuHCl{xant(P<sup>i</sup>Pr<sub>2</sub>)<sub>2</sub>}(κ<sup>1</sup>-S-DMSO) (**174**, xant(P<sup>i</sup>Pr<sub>2</sub>)<sub>2</sub> = 9,9-dimethyl-4,5-bis-(diisopropylphosphino)xanthene) to afford RuHCl( $\eta^2$ -H<sub>2</sub>){xant(P<sup>i</sup>Pr<sub>2</sub>)<sub>2</sub>} (**175**). DFT calculations have revealed that there are three isomers with the chloride ligands *cis*-disposed to the oxygen atom of the diphosphine and the hydrogen atoms bonded to the metal center lying in the perpendicular plane to the P–Ru–P direction, which differ by 1.6 kcal mol<sup>−1</sup> ( $\Delta G$  at 1 atm and 298.15 K): the *trans*-Cl–Ru–H<sub>2</sub> derivatives **175a** and **175b** and the *trans*-O–Ru–H<sub>2</sub> species **175c** (Chart 4). The

**Chart 4. Relative Energies of RuHCl( $\eta^2$ -H<sub>2</sub>){xant(P<sup>i</sup>Pr<sub>2</sub>)<sub>2</sub>} Isomers**

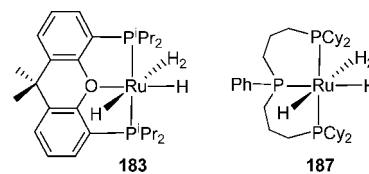
main difference between **175a** and **175b** is the separation between the atoms of the dihydrogen: 1.248 Å for the first of them and 0.907 Å for the second one. The separation in **175c** of 0.933 Å is similar to that of **175b**. The average of these distances, 1.03 Å, is consistent with the  $J_{\text{H-D}}$  value found, suggesting a fast equilibrium between the three isomers in solution. The *trans*-disposition of the  $\pi$ -donor oxygen and chlorine atoms causes the destabilization of **175**. Thus, there are also three *trans*-hydride-dihydrogen structures ( $d_{\text{H}_2} = 0.812\text{--}0.820$  Å), which lie between 8.6 and 11.0 kcal mol<sup>−1</sup> above **175a**.<sup>157</sup>

The PNP-complexes RuHCl( $\eta^2$ -H<sub>2</sub>){(R<sub>2</sub>PCH<sub>2</sub>SiMe<sub>2</sub>)<sub>2</sub>NH} (R = Cy (**176**), <sup>t</sup>Bu (**177**)) are also *cis*-hydride-dihydrogen species. The X-ray structure of **177** has revealed that the dihydrogen ligand occupies the position *trans* to the NH group, in the solid state. Lithium 2,2,6,6-tetramethylpiperidine and Me<sub>3</sub>SiCH<sub>2</sub>Li remove HCl from **176** to afford the five-coordinate amido derivative RuH( $\eta^2$ -H<sub>2</sub>){(Cy<sub>2</sub>PCH<sub>2</sub>SiMe<sub>2</sub>)<sub>2</sub>N} (**178**). DFT calculations suggest an square pyramidal geometry for this compound with the hydride in the apex and the dihydrogen, *trans* to the N atom, in the base (Chart 5).<sup>158</sup> The related compound RuH( $\eta^2$ -H<sub>2</sub>){(<sup>t</sup>Bu<sub>2</sub>PCH<sub>2</sub>CH<sub>2</sub>)<sub>2</sub>NH} (**179**), containing CH<sub>2</sub> instead of SiMe<sub>2</sub>, has been generated by hydrogenation of **62** in the presence of (<sup>t</sup>Bu<sub>2</sub>PCH<sub>2</sub>CH<sub>2</sub>)<sub>2</sub>NH. Under hydrogen atmosphere, complex **179** is in equilibrium with the dihydride-dihydrogen RuH<sub>2</sub>( $\eta^2$ -H<sub>2</sub>){(<sup>t</sup>Bu<sub>2</sub>PCH<sub>2</sub>CH<sub>2</sub>)<sub>2</sub>NH} (**180**), resulting from the addition of H<sub>2</sub> along the Ru–N bond of **179**. By using (<sup>t</sup>Bu<sub>2</sub>PCH<sub>2</sub>CH<sub>2</sub>)<sub>2</sub>NMe instead of (<sup>t</sup>Bu<sub>2</sub>PCH<sub>2</sub>CH<sub>2</sub>)<sub>2</sub>NH,

**Chart 5. PNP Ruthenium Polyhydrides**

the hydrogenation yields the dihydride-dihydrogen RuH<sub>2</sub>( $\eta^2$ -H<sub>2</sub>){(<sup>t</sup>Bu<sub>2</sub>PCH<sub>2</sub>CH<sub>2</sub>)<sub>2</sub>NMe} (**181**). Because the methyl group blocks the nitrogen position, cooperative properties acting as a proton donor or acceptor are avoided for this atom. Thus, the formation of **179** is not possible due to the absence of a neighboring proton source.<sup>159</sup> Complexes **179** and **180** catalyze the hydrogenation of aromatic and aliphatic nitriles into amines and imines.<sup>160</sup> Complex RuH<sub>2</sub>( $\eta^2$ -H<sub>2</sub>)(dtbpm) (**182**, dtbpm = 2,6-bis(di-*tert*-butylphosphino)methylpyridine), which also catalyzes the hydrogenation of nitriles to amines,<sup>161</sup> can be generated in a similar way as **181** by means of the hydrogenation of **62** in the presence of the diphosphine.<sup>162</sup>

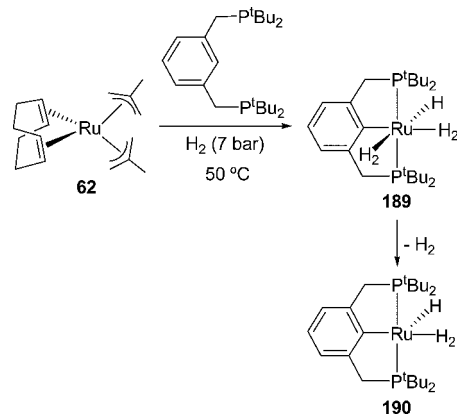
The same method has not been successful to prepare RuH<sub>2</sub>( $\eta^2$ -H<sub>2</sub>){xant(P<sup>i</sup>Pr<sub>2</sub>)<sub>2</sub>} (**183**), which is an efficient catalyst precursor for the hydrogen transfer from 2-propanol to ketones, the alkylations of nitriles and ketones with alcohols, and the regio- and stereoselective head-to-head (*Z*)-dimerization of terminal alkynes. In contrast to **62**, the hydrogenation of **40** in the presence of xant(P<sup>i</sup>Pr<sub>2</sub>)<sub>2</sub> leads to **183** in about a 40% yield. Nevertheless, the most efficient procedure to generate this compound is the decomposition of the tetrahydrideborate RuH( $\kappa^2$ -H<sub>2</sub>BH<sub>2</sub>){xant(P<sup>i</sup>Pr<sub>2</sub>)<sub>2</sub>} (**184**), which can be obtained starting from RuCl<sub>2</sub>{xant(P<sup>i</sup>Pr<sub>2</sub>)<sub>2</sub>}(κ<sup>1</sup>-S-DMSO) (**185**), via the allenylidene intermediate RuCl<sub>2</sub>(=C=C=CPh<sub>2</sub>){xant(P<sup>i</sup>Pr<sub>2</sub>)<sub>2</sub>} (**186**). DFT calculations suggest that the *trans*-disposition of the coordinated hydrogen molecule to one of the hydride ligands is favored with regard to the  $\pi$ -donor atom.<sup>157</sup> A related PPP-complex, RuH<sub>2</sub>( $\eta^2$ -H<sub>2</sub>)(Cytpp) (**187**, Cytpp = PhP(CH<sub>2</sub>CH<sub>2</sub>CH<sub>2</sub>PCy<sub>2</sub>)<sub>2</sub>), has been prepared by metathesis reaction of RuCl<sub>2</sub>(Cytpp) (**188**) with NaH in tetrahydrofuran under atmospheric hydrogen pressure<sup>163</sup> (Chart 6).

**Chart 6. Dihydride-Dihydrogen Complexes with POP- and PPP-Pincer Ligands**

The direct hydrogenation route even allows preparing RuH<sub>2</sub>-species. Thus, complex **62** cleanly reacts with H<sub>2</sub> (7 bar) at 50 °C in the presence of 1,3-bis(di-*tert*-butylphosphino)-methylbenzene to give the hydride-bis(dihydrogen) derivative RuH{2,6-(CH<sub>2</sub>P<sup>t</sup>Bu<sub>2</sub>)C<sub>6</sub>H<sub>3</sub>}( $\eta^2$ -H<sub>2</sub>)<sub>2</sub> (**189**).<sup>164</sup> DFT calculations show that the arrangement of the two dihydrogen ligands in a *cis* position is clearly favored over the alternative *trans*

disposition.<sup>165</sup> Complex **189** loses molecular hydrogen to afford the five-coordinate hydride-dihydrogen  $\text{RuH}\{\eta^2\text{-}(\text{CH}_2\text{P}^i\text{Bu}_2)_2\text{C}_6\text{H}_3\}(\eta^2\text{-H}_2)$  (**190**) with the same geometry as **179** (Scheme 20).<sup>164,165</sup>

**Scheme 20. Ruthenium(II)-Polyhydrides with PCP-Pincer Ligands**

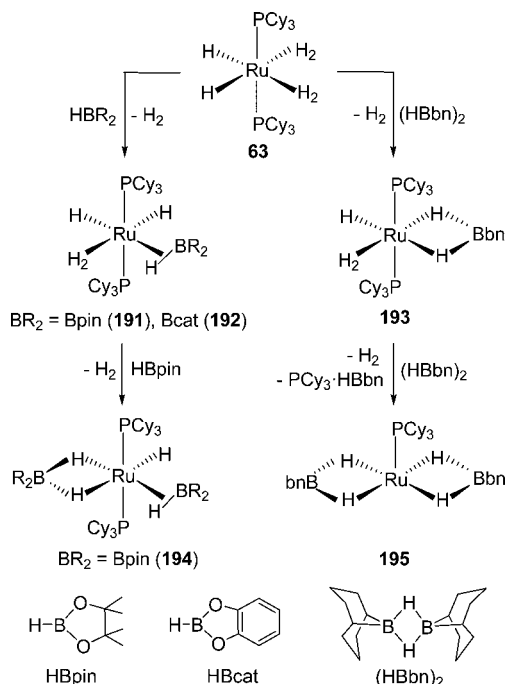


## 2.6. Ruthenium-Polyhydride Complexes Involved in $\sigma$ -Bond Activation Reactions

**2.6.1. B–H Bond Activation Reactions and Related Processes.** Boranes displace the coordinated hydrogen molecules of the dihydride-bis(dihydrogen) complex **63**. The reactions with 1 equiv of either pinacolborane (HBpin) or catecholborane (HBcat) lead to the dihydride- $\sigma$ -borane-dihydrogen derivatives  $\text{RuH}_2(\eta^2\text{-HBR}_2)(\eta^2\text{-H}_2)(\text{PCy}_3)_2$  ( $\text{BR}_2 = \text{Bpin}$  (**191**),  $\text{Bcat}$  (**192**)). In contrast to the boronate esters, the reaction with the diborane 9-borabicyclo[3.5.1]nonane ((HBbn)<sub>2</sub>), containing a more acidic boron than HBpin and HBcat, affords the hydride-dihydrideborate-dihydrogen derivative  $\text{RuH}(\kappa^2\text{-H}_2\text{Bbn})(\eta^2\text{-H}_2)(\text{PCy}_3)_2$  (**193**), as a result of the substitution of a dihydrogen ligand and the hydride stabilization of the resulting  $\sigma$ -borane intermediate.<sup>166</sup> In the presence of an excess of borane, the second coordinated hydrogen molecule is displaced. Thus, the hydride-dihydrideborate- $\sigma$ -borane complex  $\text{RuH}(\kappa^2\text{-H}_2\text{Bpin})(\eta^2\text{-HBpin})(\text{PCy}_3)_2$  (**194**)<sup>167</sup> and the bis(dihydrideborate) derivative  $\text{Ru}(\kappa^2\text{-H}_2\text{Bbn})_2(\text{PCy}_3)$  (**195**)<sup>168</sup> are formed with HBpin and (HBbn)<sub>2</sub>, respectively, under these conditions (Scheme 21). Complexes **63** and **194** catalyze HBpin-borylation of linear and cyclic alkenes with the same efficiency and selectivity. Hydroboration into the corresponding linear pinacolboronates is achieved for 1-hexene, 1-octene, styrene, and allylbenzene. However, hydroboration and dehydrogenative borylation are competitive for cyclic substrates, having the ring size a marked influence on the selectivity. Hydroboration of a C<sub>6</sub>-ring is selectively achieved, whereas allylboronate, a mixture of allylboronate and vinylboronate, and only vinylboronate are formed with C<sub>7</sub>-, C<sub>8</sub>-, and C<sub>10</sub>-rings, respectively.<sup>169</sup>

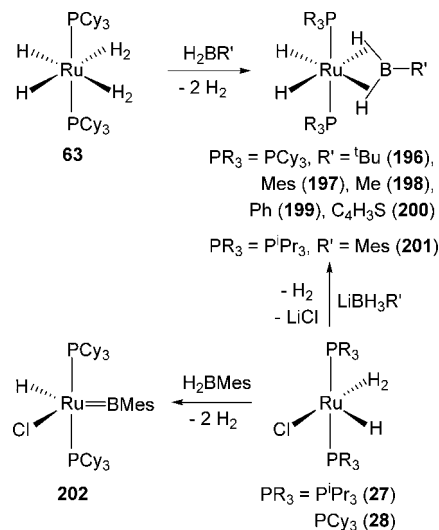
Primary alkyl- and arylboranes displace both coordinated hydrogen molecules of **63**. The reactions of the latter with *tert*-butylborane ( $\text{H}_2\text{B}^t\text{Bu}$ ) and mesitylborane ( $\text{H}_2\text{BMes}$ ) lead to the bis( $\sigma$ -borane) derivatives  $\text{RuH}_2(\eta^2, \eta^2\text{-H}_2\text{BR}')(\text{PCy}_3)_2$  ( $\text{R}' = ^t\text{Bu}$  (**196**),<sup>170</sup>  $\text{Mes}$  (**197**)<sup>171</sup>). An alternative synthesis of these compounds involves the reaction of the chloride-hydride-dihydrogen complexes **27** and **28** with the corresponding lithium trihydrideborate. In addition to **196** and **197**,

**Scheme 21. Reactions of 63 with Boranes**



complexes  $\text{RuH}_2(\eta^2, \eta^2\text{-H}_2\text{BR}')(\text{PR}_3)_2$  ( $\text{PR}_3 = \text{PCy}_3$ ,  $\text{R}' = \text{Me}$  (**198**),  $\text{Ph}$  (**199**),  $\text{C}_4\text{H}_3\text{S}$  (**200**);  $\text{PR}_3 = \text{P}^i\text{Pr}_3$ ,  $\text{R}' = \text{Mes}$  (**201**)) have been prepared by this procedure.<sup>172</sup> The reaction of **28** with mesitylborane gives the borylene  $\text{RuHCl}(\text{=BMe}_3)(\text{PCy}_3)_2$  (**202**) and  $\text{H}_2$ , as a result of the activation of both B–H bonds of the borane (Scheme 22).<sup>173</sup>

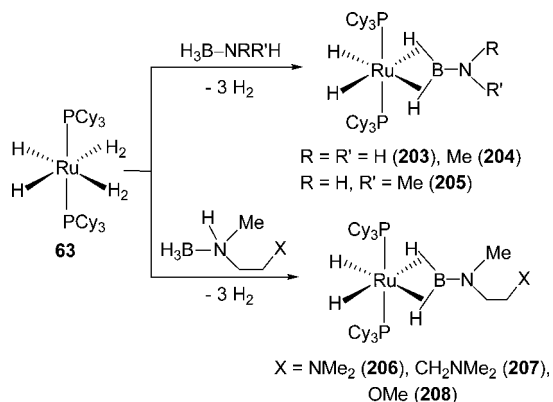
**Scheme 22. Bis( $\sigma$ -Borane) and Borylene Derivatives**



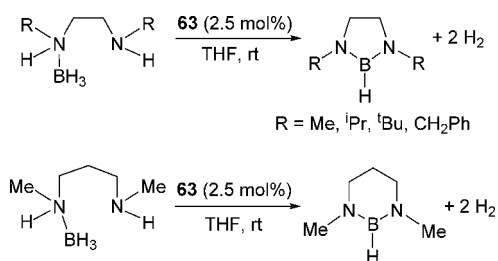
Amine-boranes ( $\text{H}_3\text{B-NH}_n\text{R}_{3-n}$ ,  $n = 1-3$ ) undergo stoichiometric dehydrogenation in the presence of **63**.<sup>174,175</sup> The resulting aminoboranes coordinate to the metal center<sup>27,176,177</sup> to form the bis( $\sigma$ -B–H) aminoborane derivatives  $\text{RuH}_2(\eta^2, \eta^2\text{-H}_2\text{BNRR}')(\text{PCy}_3)_2$  ( $\text{NRR}' = \text{NH}_2$  (**203**),  $\text{NMe}_2$  (**204**),  $\text{NHMe}$  (**205**))<sup>174,175</sup> related to **196–201**. Peripheral tertiary amine and methoxy functions in the borane are tolerated; as a consequence, complexes  $\text{RuH}_2\{\eta^2, \eta^2\text{-H}_2\text{BN}(\text{Me})\text{CH}_2\text{CH}_2\text{X}\}(\text{PCy}_3)_2$  ( $\text{X} = \text{NMe}_2$ , (**206**),

CH<sub>2</sub>NMe<sub>2</sub> (**207**), OMe (**208**)) have also been isolated and characterized (Scheme 23). However, if the peripheral function is a secondary amine, a catalytic dehydrogenative cyclization takes place to yield 1,3,2-diazaborolidines (Scheme 24).<sup>178,179</sup>

Scheme 23. Reactions of **63** with Amineboranes

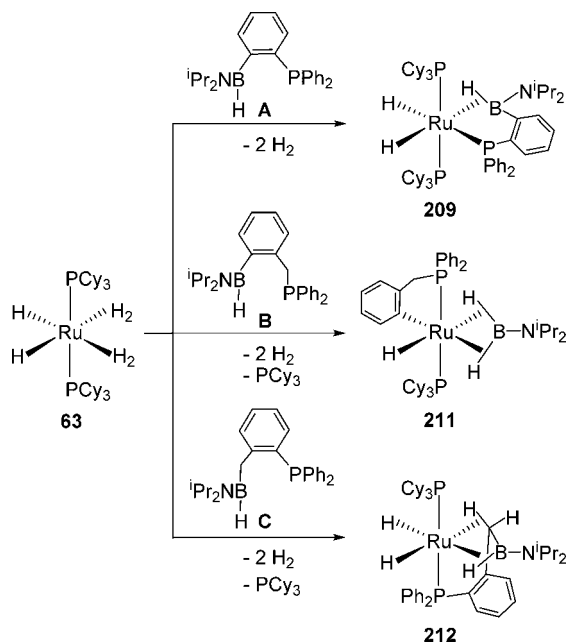


Scheme 24. Catalytic Formation of 1,3,2-Diazaborolidines Promoted by **63**



The reactions of **63** with the phosphine-aminoboranes Ph<sub>2</sub>P(CH<sub>2</sub>)<sub>n</sub>C<sub>6</sub>H<sub>4</sub>-*o*-(CH<sub>2</sub>)<sub>n</sub>BHN<sup>i</sup>Pr<sub>2</sub> (*n* = *n*' = 0 (**A**); *n* = 1, *n*' = 0 (**B**); *n* = 0, *n*' = 1 (**C**)) are of particular interest (Scheme 25). Complex **63** initially reacts with **A** to give

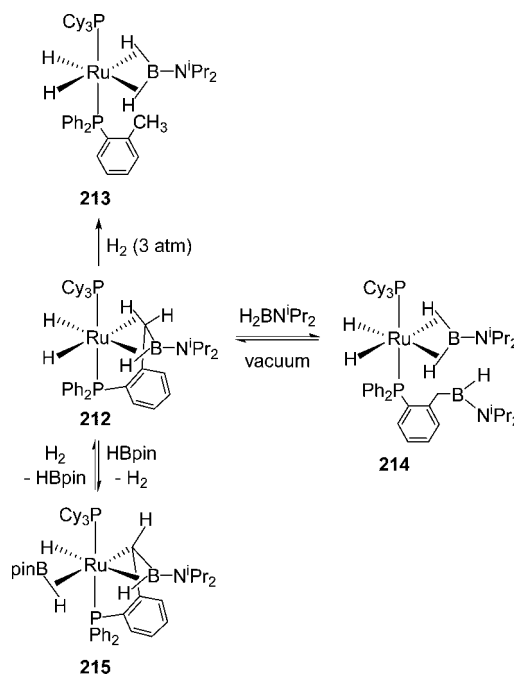
Scheme 25. Reactions of **63** with Phosphine-Aminoboranes



RuH<sub>2</sub>(PPh<sub>2</sub>C<sub>6</sub>H<sub>4</sub>-*o*-BHN<sup>i</sup>Pr<sub>2</sub>)(PCy<sub>3</sub>)<sub>2</sub> (**209**), as a result of the displacement of both dihydrogen molecules by the phosphine-aminoborane. In solution, **209** dissociates a PCy<sub>3</sub> ligand to form the unsaturated species RuH<sub>2</sub>(PPh<sub>2</sub>C<sub>6</sub>H<sub>4</sub>-*o*-BHN<sup>i</sup>Pr<sub>2</sub>)(PCy<sub>3</sub>) (**210**), with a hydride ligand trans to a vacant. In both cases, the phosphine-aminoborane acts as a bifunctional chelate ligand through the phosphine moiety and a Ru–H–B agostic interaction.<sup>180</sup> The behavior of **B**, containing a methylene linker between the phosphorus atom and the aryl bridge, is different. No agostic σ-B–H complex is formed; the reaction leads to a new bis(σ-borane)-ruthenium complex, RuH(C<sub>6</sub>H<sub>4</sub>-*o*-CH<sub>2</sub>PPh<sub>2</sub>)(η<sup>2</sup>,η<sup>2</sup>-H<sub>2</sub>BN<sup>i</sup>Pr<sub>2</sub>)(PCy<sub>3</sub>) (**211**), via B–C bond cleavage and Ru–C bond formation.<sup>181</sup> In contrast to **B**, the phosphine-aminoborane **C**, with a methylene linker between the boron atom and the aryl bridge, saturates a C-counterpart of **210**, RuH<sub>2</sub>(PPh<sub>2</sub>C<sub>6</sub>H<sub>4</sub>-*o*-CH<sub>2</sub>BHN<sup>i</sup>Pr<sub>2</sub>)(PCy<sub>3</sub>) (**212**) by means of an additional δ-agostic interaction.<sup>182</sup>

The coordination mode of **C** in **212** shows the stabilization of a 14-valence electrons fragment RuH<sub>2</sub>P<sub>2</sub> through connected σ-bonds of different polarity and allows selective B–H, C–H, and B–C bond activations as illustrated by reactions with H<sub>2</sub> and boranes (Scheme 26). Pressurization of a benzene-*d*<sub>6</sub>

Scheme 26. B–H, C–H, and B–C Bond Activation Reactions on **212**



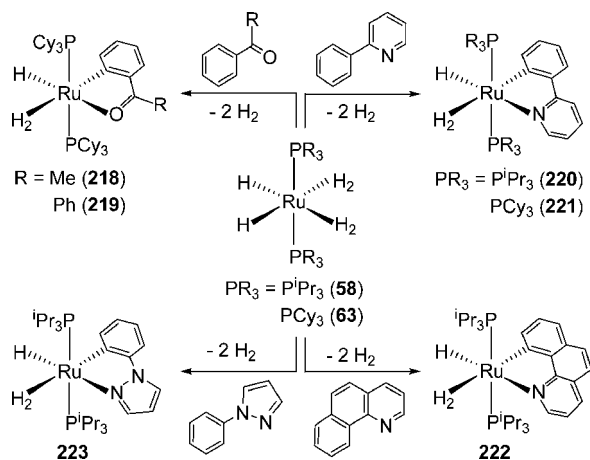
solution of **212** under 3 atm of H<sub>2</sub> leads to B–C bond cleavage of the ligand and quantitative and irreversible formation of RuH<sub>2</sub>(η<sup>2</sup>,η<sup>2</sup>-H<sub>2</sub>BN<sup>i</sup>Pr<sub>2</sub>)(PPh<sub>2</sub>C<sub>6</sub>H<sub>4</sub>-*o*-CH<sub>3</sub>)(PCy<sub>3</sub>) (**213**). Addition of diisopropylaminoborane to **212** gives rise to an equilibrium mixture between the latter and RuH<sub>2</sub>(η<sup>2</sup>,η<sup>2</sup>-H<sub>2</sub>BN<sup>i</sup>Pr<sub>2</sub>){PPh<sub>2</sub>(C<sub>6</sub>H<sub>4</sub>-*o*-CH<sub>2</sub>BHN<sup>i</sup>Pr<sub>2</sub>)}(PCy<sub>3</sub>) (**214**). Reaction of **212** with HBpin leads to the five-membered metallacycle complex RuH{PPh<sub>2</sub>(C<sub>6</sub>H<sub>4</sub>-*o*-CHBHN<sup>i</sup>Pr<sub>2</sub>)}(η<sup>2</sup>-HBpin)(PCy<sub>3</sub>) (**215**) featuring a Ru–C single bond as a result of a further activation of the agostic C–H bond and loss of H<sub>2</sub>. The reaction is reversible as shown by exposure of **215** to H<sub>2</sub>, with the bis(agostic) complex **212** and free HBpin being restored.

Complex **63** is undoubtedly the best studied from the B–H bond activation point of view. There are however a few other compounds that also promote relevant processes involving B–H cleavage, which should be mentioned. The dihydride-bis(dihydrogen) **66** catalyzes the reduction of CO<sub>2</sub> with HBpin to give formaldehyde which, under mild conditions, leads to imines by condensation with primary amines.<sup>183–185</sup> The cationic hydride-dihydrogen **74**, containing a NP<sub>3</sub>-tetrapodal polyphosphine, catalyzes the kinetically controlled dehydrogenation of ammonia-borane, with release of 2 equiv of H<sub>2</sub> per equiv of H<sub>3</sub>B–NH<sub>3</sub> and concomitant polyborazylene and cyclic polyaminoborane formation.<sup>124</sup> The dihydride-dihydrogen PNP-pincer complex **182** catalyzes the anti-Markovnikov-type addition of HBpin to terminal alkynes yielding Z-vinylboronates under mild conditions. The hydride-dihydrideborate complex RuH(κ<sup>2</sup>-H<sub>2</sub>Bpin)(dtbpm) (**216**), which was identified at the end of the reaction, is proposed as the direct precursor for the catalytic cycle involving rearrangement of coordinated alkyne to vinylidene as the key step for the apparent trans-hydroboration.<sup>186</sup>

**2.6.2. C–H Bond Activation.** The dihydride-bis(dihydrogen) **63** catalyzes the hydrogenation of benzonitrile to benzylamine, at room temperature and under mild pressure. The catalytic resting state, RuH{κ<sup>2</sup>-N,C-(NH=CHC<sub>6</sub>H<sub>4</sub>)}(η<sup>2</sup>-H<sub>2</sub>)(PCy<sub>3</sub>)<sub>2</sub> (**217**), results from the trapping of the intermediate imine by means of a chelate-assisted *ortho*-CH bond activation of the phenyl group.<sup>187</sup>

The chelate-assistance strategy is considered to be one of the most efficient ways to achieve selectivity in C–H bond activation. Complexes **58** and **63** promote the chelate assisted C–H bond activation of acetophenone, benzophenone, 2-phenylpyridine (Ph-py), benzoquinoline (Hbq), and phenylpyrazole (Ph-pz) to afford the corresponding orthometalated hydride-dihydrogen derivatives RuH{κ<sup>2</sup>-O,C-[OC(R)C<sub>6</sub>H<sub>4</sub>]}(η<sup>2</sup>-H<sub>2</sub>)(PCy<sub>3</sub>)<sub>2</sub> (R = Me (**218**), Ph (**219**)), RuH{κ<sup>2</sup>-N,C-(py-C<sub>6</sub>H<sub>4</sub>)}(η<sup>2</sup>-H<sub>2</sub>)(PR<sub>3</sub>)<sub>2</sub> (PR<sub>3</sub> = P<sup>i</sup>Pr<sub>3</sub> (**220**), PCy<sub>3</sub> (**221**)), RuH{κ<sup>2</sup>-N,C-(bq)}(η<sup>2</sup>-H<sub>2</sub>)(P<sup>i</sup>Pr<sub>3</sub>)<sub>2</sub> (**222**), and RuH{κ<sup>2</sup>-N,C-(pz-C<sub>6</sub>H<sub>4</sub>)}(η<sup>2</sup>-H<sub>2</sub>)(P<sup>i</sup>Pr<sub>3</sub>)<sub>2</sub> (**223**) (Scheme 27),<sup>188,189</sup> which are analogous to **217** and reminiscent of intermediates proposed for the insertion of olefins into aromatic C–H bonds located in the *ortho* position relative to a coordinating group, in agreement with the ability of the RuH<sub>2</sub>(η<sup>2</sup>-H<sub>2</sub>)<sub>2</sub> compounds to catalyze the *ortho* alkylation of aromatic

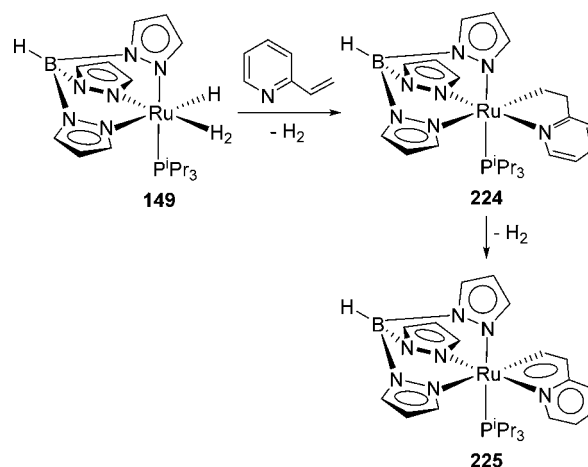
Scheme 27. Chelate-Assisted C–H Activation Reactions Promoted by **58** and **63**



ketones.<sup>55,190–192</sup> Protonation of **220** and **222** yields cationic *cis*-hydride-dihydrogen derivatives containing the heterocycle coordinated through the heteroatom and a phenyl *ortho* CH bond.<sup>193,194</sup>

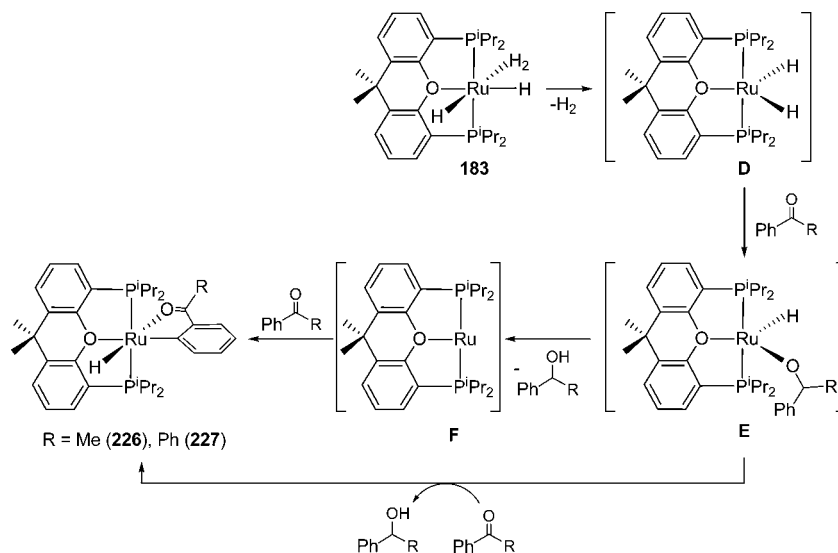
The tris(pyrazolyl)borate hydride-dihydrogen complex **149** activates 2-vinylpyridine. In toluene, the reaction initially gives the 1,2-dihydro-3-ruthenaindolizine Ru{κ<sup>2</sup>-N,C-(py-CH<sub>2</sub>CH<sub>2</sub>)}Tp(P<sup>i</sup>Pr<sub>3</sub>) (**224**), which aromatizes to afford the 3-ruthenaindolizine complex Ru{κ<sup>2</sup>-N,C-(py-CHCH)}Tp(P<sup>i</sup>Pr<sub>3</sub>) (**225**) by loss of a hydrogen molecule in the absence of any hydrogen acceptor (Scheme 28).<sup>150</sup>

Scheme 28. C–H Bond Activation of 2-Vinylpyridine Promoted by **149**

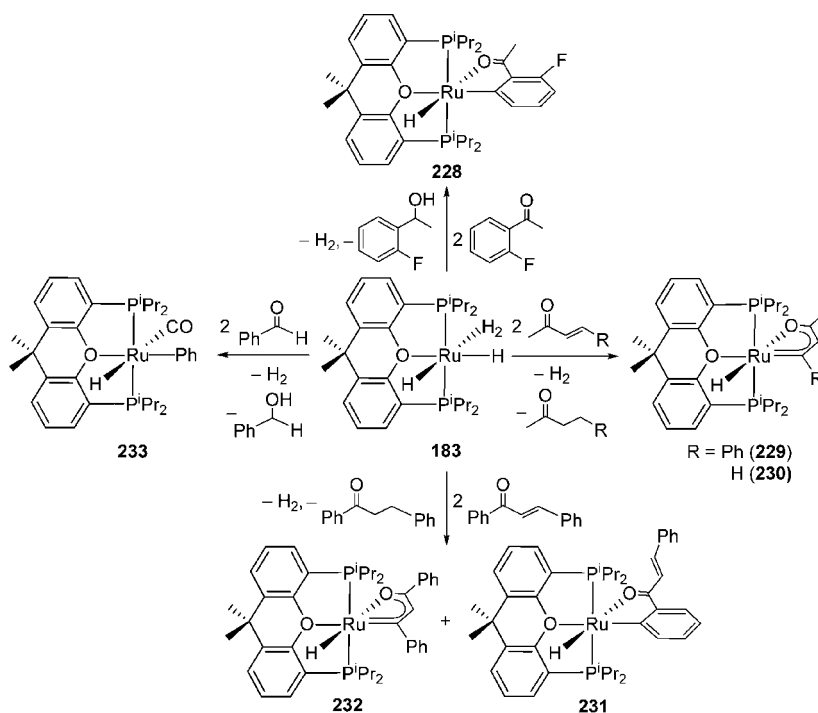


It has been demonstrated that a coordinating functional group in an organic molecule does not direct the *ortho*-CH bond activation. On the contrary, it prevents the C–H bond addition to the metal center from a kinetic point of view. However, after the C–H bond cleavage, the coordinating group acts to trap the addition product.<sup>195</sup> The POP-pincer dihydride-dihydrogen complex **183** also activates acetophenone and benzophenone. The reactions afford the ruthenaisobenzofurans RuH{κ<sup>2</sup>-O,C-[OC(R)C<sub>6</sub>H<sub>4</sub>]}{xant(P<sup>i</sup>Pr<sub>2</sub>)<sub>2</sub>} (R = Me (**226**), Ph (**227**)). Because the dihydride RuH<sub>2</sub>{xant(P<sup>i</sup>Pr<sub>2</sub>)<sub>2</sub>} (**D**) reduces ketones, 2 equiv of substrate were used. It has been proposed that this reduction occurs via the intermediate **E** shown in Scheme 29. Thus, the elimination of alcohol should lead to the 14-valence electrons ruthenium(0) derivative **F**, which could undergo the oxidative addition of the second molecule of ketone. An alternative pathway would involve the direct heterolytic C–H bond activation of the second ketone molecule promoted by **E**, using the alkoxide ligand as a base. The participation of both mechanisms is consistent with the presence of about 0.5 deuterium atoms at the hydride position of the product resulting from the reaction of **183** with perdeuterated benzophenone. Furthermore, the metalated group contains 0.6 hydrogen atoms at the *ortho*-position with regard to the metal center (meta relative to the carbonyl) and about 0.2 hydrogen atoms at the *ortho*-position with regard to the carbonyl group. This indicates that the activation of the *meta*-C–H bonds of the ketone is kinetically favored over the *ortho*-C–H bonds and proves that the *ortho*-C–H bond cleavage is not chelate directed.<sup>196</sup>

Complex **183** favors the C–H bond activation over the C–F bond cleavage. Thus, the reaction of 2-fluoroacetophenone

Scheme 29. C–H Bond Activation Reactions of Aromatic Ketones Promoted by 183.<sup>a</sup>

<sup>a</sup>Adapted from ref 196. Copyright 2015 American Chemical Society.

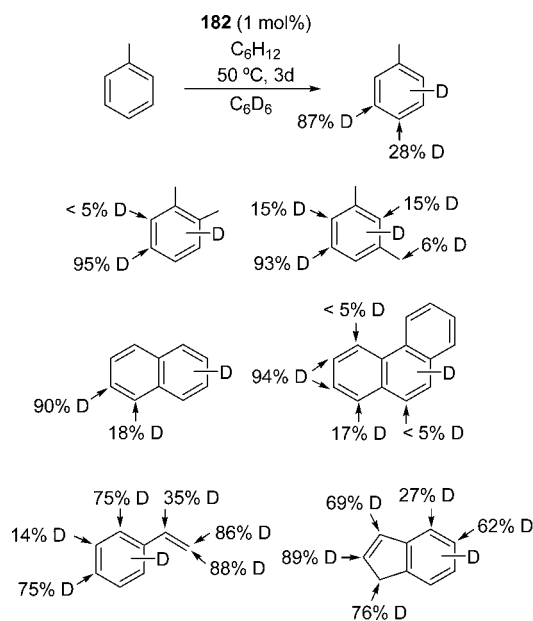
Scheme 30. C–H Bond Activation Reactions of Fluorinated Aromatic Ketones,  $\alpha,\beta$ -Unsaturated Ketones, and Benzaldehyde Promoted by 183

leads to the C–H bond activation product  $\text{RuH}\{\kappa^2\text{-O,C-}[\text{OC}(\text{Me})\text{C}_6\text{H}_3\text{F}]\}\{\text{xant}(\text{P}^i\text{Pr}_2)_2\}$  (**228**). This complex also promotes the  $\text{C}_\beta\text{-H}$  bond activation of benzylideneacetone and methyl vinyl ketone to afford the ruthenafurans  $\text{RuH}\{\kappa^2\text{-O,C-}[\text{OC}(\text{Me})\text{CHCR}]\}\{\text{xant}(\text{P}^i\text{Pr}_2)_2\}$  (R = Ph (**229**), H (**230**)). The analogous reaction with benzylideneacetophenone yields a 1:1 mixture of the corresponding products resulting from the *ortho*-CH bond,  $\text{RuH}\{\kappa^2\text{-O,C-}[\text{OC}(\text{CH}=\text{CHPh})\text{C}_6\text{H}_4]\}\{\text{xant}(\text{P}^i\text{Pr}_2)_2\}$  (**231**), and  $\text{C}_\beta\text{-H}$  bond,  $\text{RuH}\{\kappa^2\text{-O,C-}[\text{OC}(\text{Ph})\text{CHCPh}]\}\{\text{xant}(\text{P}^i\text{Pr}_2)_2\}$  (**232**), activations. In aromatic aldehydes, the OC–H bond activation is favored over the cleavage of an *ortho*-CH bond. Thus, the reaction of **183** with

benzaldehyde leads to  $\text{RuH}(\text{Ph})(\text{CO})\{\text{xant}(\text{P}^i\text{Pr}_2)_2\}$  (**233**), as a result of the phenyl deinsertion in an acyl intermediate (Scheme 30).<sup>196</sup>

The arene C–H bond activation without the need for chelate-assistance has been scarcely studied with this type of precursors. The PNP-pincer dihydride-dihydrogen complex **182** promotes the deuteration of a wide range of arenes and olefins, under mild conditions, using benzene-*d*<sub>6</sub> or D<sub>2</sub>O as a deuterium source. The incorporation provides products with site-selectivity for C–H bond cleavage that depends upon steric factors (Scheme 31). Thus, for instance, the deuterium incorporation to toluene occurs mainly at meta (87%) and

Scheme 31. Catalytic Deuteration of Arenes Promoted by 182

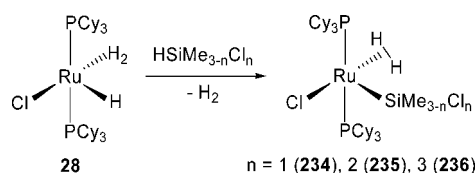


considerably less at para (28%); *ortho*-xylene undergoes deuteration almost exclusively at the  $\beta$ -positions to the methyl groups (95%); and naphthalene is preferably  $\beta$ -deuterated (90%), with a lower amount of  $\alpha$ -deuteration (18%).<sup>162,197</sup>

**2.6.3. Si–H Bond Activation.** The ruthenium-promoted Si–H bond activation reactions were reviewed by Sabo-Etienne in 2006.<sup>25</sup> A continuum exists between the two extremes, leading either to  $\eta^2$ -Si–H coordination or oxidative addition. The tendency of silicon to be hypervalent seems to favor such a continuum by creating secondary interactions, which play a significant role for the stabilization of unusual structures and intermediates in exchange processes. In order to evaluate the degree of silane activation,  $J_{Si-H}$  values, IR bands, and Si–H and Ru–Si distances would not be used alone.  $J_{Si-H}$  values should be set up to 65 Hz for a secure criterion of a  $\eta^2$ -Si–H bond. Observation of a broad and intense IR band in the range of  $1650\text{--}1800\text{ cm}^{-1}$  is also a good indication of  $\eta^2$ -coordination. Furthermore, one can consider that a Si–H distance between 1.7 and 1.8 Å is indicative of the formation of a  $\eta^2$ -silane complex, whereas separations between 1.9 and 2.4 Å are an alert of the presence of secondary interactions. The Ru–Si bond strength depends on the silicon-attached substituents, but a short bond length is a first evidence of an advanced oxidative addition process. Several interesting stoichiometric and catalytic findings involving the Si–H bond activation of, mainly, chlorosilanes have been reported since 2006. In addition, chelate-assisted Si–H bond coordination and activation have received special attention.

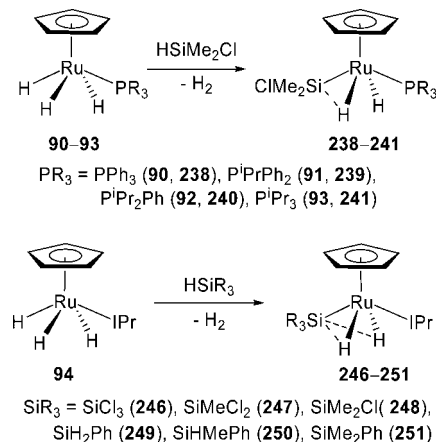
The hydride-dihydrogen complex 28 activates the Si–H bond of chlorosilanes  $HSiMe_{3-n}Cl_n$  ( $n = 1\text{--}3$ ) to form the corresponding silyl-elongated dihydrogen derivatives  $RuCl(SiMe_{3-n}Cl_n)(\eta^2-H_2)(PCy_3)_2$  ( $n = 1$  (234), 2 (235), 3 (236)). Substitution of the coordinated hydrogen molecule of 28 by the silanes to afford  $\eta^2$ -Si–H intermediates, which undergo hydride-promoted heterolytic activation, seems to be a plausible mechanism. The square pyramidal geometry proposed for these compounds, with the silyl ligand in the apex (Scheme 32), has been confirmed by means of the X-ray diffraction structure of

Scheme 32. Si–H Bond Activation Reactions of Chlorosilanes Promoted by 28



235. The  $J_{H-D}$  values reveal that the sequential replacement of methyl substituents by chlorides shortens the dihydrogen ligand, from 1.21 Å in 234 to 1.05 Å in 236. The trend, which is in agreement with an increase of the acidity of the silyl group in the same sequence, has been corroborated by DFT calculations. Complexes 235 and 236 do not react with ethylene. However, the ethylene species  $RuHCl(\eta^2-C_2H_4)(PCy_3)_2$  (237) is formed in the case of 234. The strong silyl trans influence may prevent the coordination in the vacant site of 235 and 236, whereas for 234, the interaction between the silicon atom and one hydrogen of the elongated dihydrogen seems to favor the silane elimination.<sup>198</sup> In contrast to 28, the dihydride-bis(dihydrogen) complex 63 catalyzes the silylation of ethylene with  $HSiMe_2Cl$  and  $HSiMeCl_2$ . Dehydrogenative silylation leading to the formation of vinylsilanes competes with hydrosilylation. The rate and selectivity of the reactions are influenced by the number of chloro substituents.<sup>199</sup>

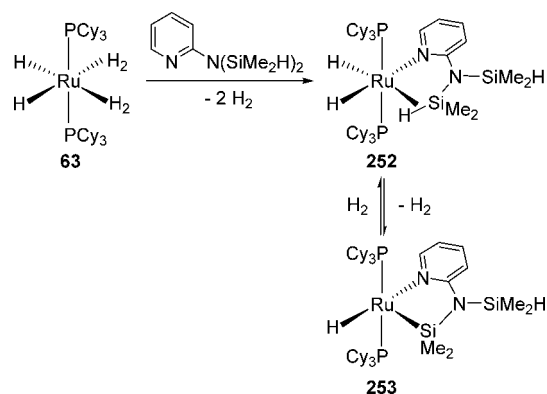
The half-sandwich trihydride complexes 90–93 also activate the Si–H bond of  $HSiMe_2Cl$ . The reactions give the dihydride-silyl derivatives  $RuH_2(SiMe_2Cl)(\eta^5-C_5H_5)(PR_3)$  ( $PR_3 = PPh_3$  (238),  $P^iPrPh_2$  (239),  $P^iPr_2Ph$  (240),  $P^iPr_3$  (241)), in good yields, and  $H_2$ . The related compounds  $RuH_2(SiMe_2Cl)(\eta^5-C_5H_5)(PR_3)$  ( $PR_3 = P^iPr_2Me$  (242),  $PMe_2Ph$  (243)) have been also prepared, starting from the corresponding chloride complexes  $RuCl(\eta^5-C_5H_5)(PR_3)_2$  ( $PR_3 = P^iPr_2Me$  (244),  $PMe_2Ph$  (245)). These ruthenium(IV) dihydride-silyl species exhibit hydride–silicon hypervalent interactions, whose strength decreases with the decreasing basicity of the phosphine coligand.<sup>200</sup> The reactions of the NHC-supported trihydride  $RuH_3(\eta^5-C_5H_5)(IPr)$  (94) with hydrosilanes  $HSiR_3$  afford the dihydride-silyl complexes  $RuH_2(SiR_3)(\eta^5-C_5H_5)(IPr)$  ( $SiR_3 = SiCl_3$  (246),  $SiMeCl_2$  (247),  $SiMe_2Cl$  (248),  $SiH_2Ph$  (249),  $SiHMePh$  (250),  $SiMe_2Ph$  (251)) with nonclassical Si··H interligand interactions (Scheme 33). The comparison of the X-

Scheme 33. Si–H Bond Activation Reactions Promoted by  $RuH_3(\eta^5-C_5H_5)L$  Complexes

ray structures of **241** and **246–251** suggests that the replacement of the phosphine by the NHC ligand in the fragment  $\text{Ru}(\eta^5\text{-C}_5\text{H}_5)(\text{P}^i\text{Pr}_3)$  results in the strengthening of the  $\text{RuH}\cdots\text{Si}$  interactions.<sup>137</sup>

The dihydride-bis(dihydrogen) complex **63** promotes pyridyl-chelate-assisted Si–H bond activation (Scheme 34).

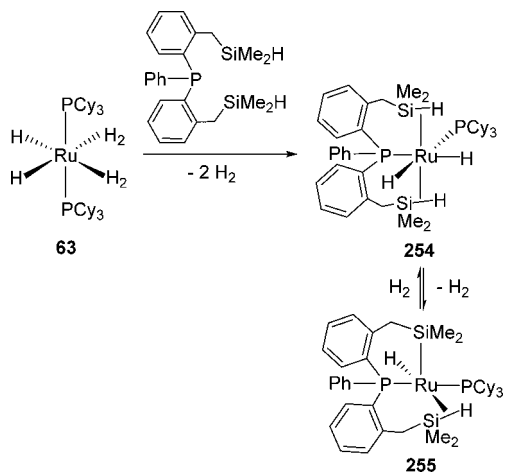
**Scheme 34. Pyridyl-Chelate-Assisted Si–H Bond Activation Promoted 63**



2-Pyridinetetramethyldisilazane displaces the coordinated hydrogen molecules of **63** to initially give  $\text{RuH}_2\{(\eta^2\text{-HSiMe}_2)\text{-N}(\kappa\text{-N-C}_5\text{H}_4\text{N})(\text{SiMe}_2\text{H})\}(\text{PCy}_3)_2$  (**252**) by means of the coordination to the ruthenium atom of the pyridyl group and one of the Si–H bonds, as demonstrated by deuterium-labeling experiments. Heating **252**, at 70 °C under vacuum for 24 h, produces the loss of  $\text{H}_2$  and the formation of the unsaturated compound  $\text{RuH}\{(\text{SiMe}_2)\text{N}(\kappa\text{-N-C}_5\text{H}_4\text{N})(\text{SiMe}_2\text{H})\}(\text{PCy}_3)_2$  (**253**), as a result of the cleavage of the coordinated Si–H bond. The reaction is fully reversible under dihydrogen atmosphere.<sup>201</sup>

The phosphinodi(benzylsilane)  $\text{PhP}(\text{C}_6\text{H}_4\text{-}o\text{-CH}_2\text{SiMe}_2\text{H})_2$ , in contrast to 2-pyridinetetramethyldisilazane, acts as a pincer-type ligand capable of adopting different coordination modes at ruthenium through different extent of Si–H bond activation (Scheme 35). This phosphine reacts with **63**, in toluene, at room temperature to give  $\text{RuH}_2\{[\eta^2\text{-}(\text{HSiMe}_2)\text{CH}_2\text{-}o\text{-C}_6\text{H}_4]_2\text{PPh}\}(\text{PCy}_3)$  (**254**), as a result of the substitution of both coordinated hydrogen molecules and one tricyclohex-

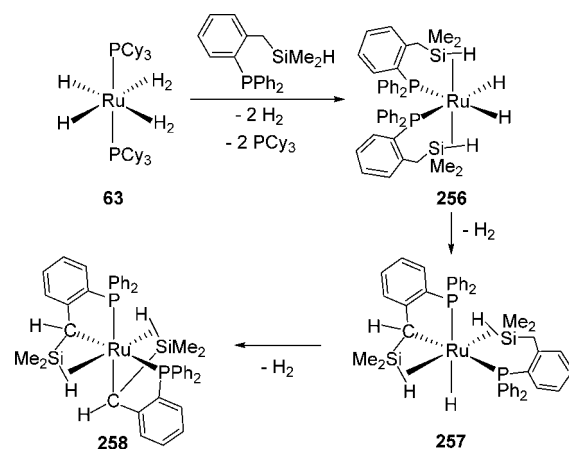
**Scheme 35. Reactions of 63 with a Phosphinodi(benzylsilane)**



ylphosphine ligand by the phosphinodi(benzylsilane), which coordinates the phosphorus atom and both Si–H bonds in a *mer* disposition. This compound, which is involved in thermal hydride-SiH exchange processes, undergoes reversible loss of molecular hydrogen leading to the unsaturated species  $\text{RuH}\{[\eta^2\text{-}(\text{HSiMe}_2)\text{CH}_2\text{-}o\text{-C}_6\text{H}_4]\text{PPh}[\text{C}_6\text{H}_4\text{-}o\text{-CH}_2\text{SiMe}_2]\}(\text{PCy}_3)$  (**255**),<sup>202</sup> most probably through a hydride-dihydrogen intermediate resulting from the hydride-promoted heterolytic cleavage of one of the coordinated Si–H bonds.

Six-membered heterometalatings as that of **255** are less stable than the five-membered ring resulting of the C–H bond activation of the methylene linker between the silane and the aromatic group. The reactions shown in Scheme 36 are a strong

**Scheme 36. Reactions of 63 with Phosphinobenzylsilanes**



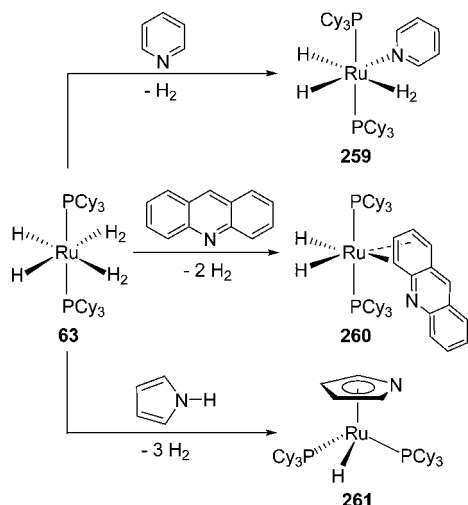
demonstration of this. Complex **63** reacts with the phosphinobenzylsilane  $\text{Ph}_2\text{P}(\text{C}_6\text{H}_4\text{-}o\text{-CH}_2\text{SiMe}_2\text{H})$  to give  $\text{RuH}_2\{[\eta^2\text{-HSiMe}_2)\text{CH}_2\text{-}o\text{-C}_6\text{H}_4]\text{PPh}_2\}_2$  (**256**), as a result of the substitution of the dihydrogen and tricyclohexylphosphine ligands by two phosphinobenzylsilanes, which act as chelating groups through the phosphorus atom and the Si–H bond. This compound loses two hydrogen molecules, as a consequence of the sequential C–H bond activation of the methylene group of the phosphine in the presence of the Si–H bonds, to yield first  $\text{RuH}\{[\text{CH}(\eta^2\text{-HSiMe}_2)\text{-}o\text{-C}_6\text{H}_4]\text{PPh}_2\}\{[\eta^2\text{-HSiMe}_2)\text{CH}_2\text{-}o\text{-C}_6\text{H}_4]\text{PPh}_2\}$  (**257**) and subsequently  $\text{Ru}\{[\text{CH}(\eta^2\text{-HSiMe}_2)\text{-}o\text{-C}_6\text{H}_4]\text{PPh}_2\}_2$  (**258**).<sup>203</sup>

The tendency shown by the  $\text{RuH}(\eta^2\text{-H-Si})$ -complexes to undergo hydride-SiH exchange processes is consistent with the reactivity discussed for **63** and its ability, and that of the related dihydride-bis(dihydrogen) **66**, for promoting the deuteration of a diverse array of silanes, including alkyl-, aryl-, alkoxy-, and chlorosilanes, siloxane and silazane, under a molecular deuterium atmosphere.<sup>204</sup>

**2.6.4. N–H and O–H Bond Activations.** The dihydride-bis(dihydrogen) complex **63** reacts with pyridine, acridine, and pyrrole to afford compounds containing the heterocycles coordinated in different modes (Scheme 37). Pyridine produces the displacement of a dihydrogen ligand and coordinates the nitrogen atom, generating the dihydride-dihydrogen  $\text{RuH}_2(\eta^2\text{-H}_2)(\text{py})(\text{PCy}_3)_2$  (**259**). In contrast to pyridine, acridine displaces both dihydrogen ligands coordinating one of the terminal aromatic rings in a  $\eta^4$ -mode to form  $\text{RuH}_2(\eta^4\text{-C}_{13}\text{H}_{19}\text{N})(\text{PCy}_3)_2$  (**260**), whereas pyrrole undergoes the activation of its N–H bond to yield the half-sandwich derivative  $\text{RuH}(\eta^5\text{-C}_4\text{H}_4\text{N})(\text{PCy}_3)_2$  (**261**).<sup>205</sup>

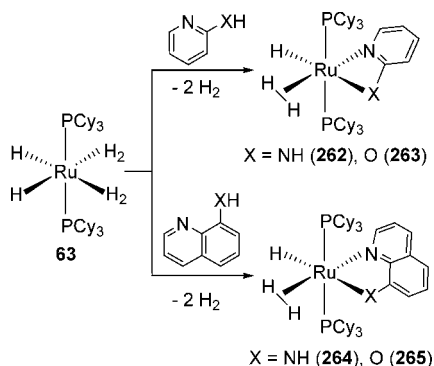


Scheme 37. Reactions of 63 with N-Heterocycles



Complex 63 also promotes the chelate-assisted cleavage of a N–H bond of 2-aminopyridine and 8-aminoquinoline and the O–H bond of 2-hydroxypyridine and 8-hydroxyquinoline (Scheme 38). These chelate-assisted activations lead to the

Scheme 38. Chelate-Assisted N–H and O–H Bond Activations Promoted by 63

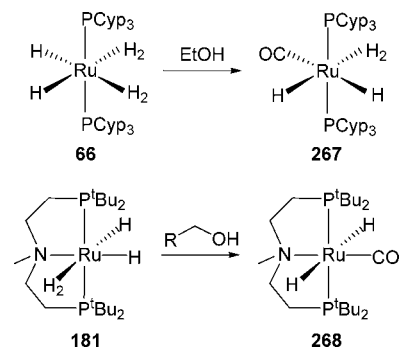


hydride-elongated dihydrogen derivatives  $\text{RuH}\{\kappa^2\text{-}N,X\text{-}(\text{py-2-X})\}(\eta^2\text{-H}_2)(\text{PCy}_3)_2$  ( $X = \text{NH}$  (262),  $\text{O}$  (263)) and  $\text{RuH}\{\kappa\text{-}N,X\text{-}(\text{quin-8-X})\}(\eta^2\text{-H}_2)(\text{PCy}_3)_2$  ( $X = \text{NH}$  (264),  $\text{O}$  (265)). The elongated character of the dihydrogen ligand of these compounds is supported by the  $J_{\text{H-D}}$  values, which allow for calculation of the separations between its hydrogen atoms of about 1.27 Å.<sup>206</sup> NMR studies on 262 and 263 have also shown that hydrogen bond donors, such as substituted phenols and hexafluoro-2-propanol, interact with the hydride ligand of the second one, whereas for 262, an equilibrium with the cation  $[\text{RuH}(\eta^2\text{-H}_2)\{\kappa\text{-}N,N\text{-}(\text{py-2-NH}_2)\}(\text{PCy}_3)_2]^+$  (266) is attained.<sup>207</sup>

The related tricyclopentylphosphine dihydride-bis-(dihydrogen) complex 66 dehydrogenates primary alcohols, which subsequently undergo decarbonylation. Thus, the carbonyl-dihydride-dihydrogen  $\text{RuH}_2(\text{CO})(\eta^2\text{-H}_2)(\text{PCyp}_3)_2$  (267) has been isolated from the reaction with ethanol.<sup>208</sup> A similar behavior has been reported for the PNP-pincer compound 181, which affords the carbonyl-dihydride  $\text{RuH}_2(\text{CO})\{(\text{t}^i\text{Bu}_2\text{PCH}_2\text{CH}_2)_2\text{NMe}\}$  (268) (Scheme 39).<sup>209</sup>

Complex 268 is an efficient catalyst precursor for the direct conversion of primary alcohols into carboxylic acids with the

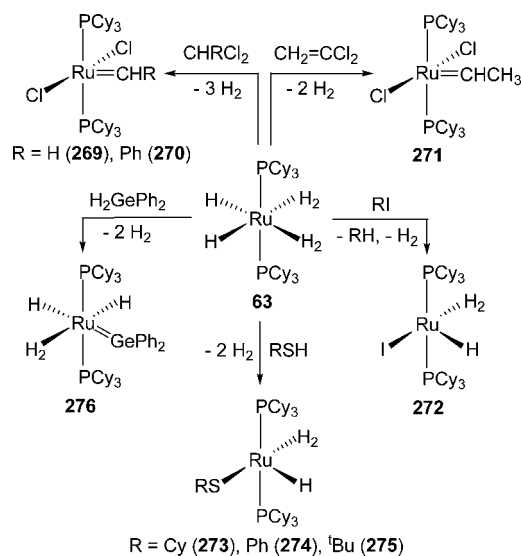
Scheme 39. Reactions of 66 and 181 with Alcohols



use of water as an oxygen source, whereas the triisopropylphosphine counterpart of 267, complex 41, catalyzes the hydrogen transfer from 2-propanol to ketones<sup>210</sup> and  $\alpha,\beta$ -unsaturated ketones.<sup>211</sup> A preferential selective reduction to saturated ketones is observed for the  $\alpha,\beta$ -unsaturated ketones case. The  $\text{Tp}^{\text{Me}_2}$ -complex 160 also shows good catalytic activity for the reduction of unsaturated ketones by dihydrogen and by hydrogen transfer from alcohols in basic media.<sup>212</sup>

**2.6.5. Other  $\sigma$ -Bond Activations.** The dihydride-bis-(dihydrogen) complex 63 is an exceptional tool to carry out the cleavage of  $\sigma$ -bonds. In addition to the previously mentioned activation reactions, it is capable of performing the activation of C–Cl, C–I, S–H, and Ge–H bonds (Scheme 40). Complex 63 serves as a formal source of the zerovalent

Scheme 40. C–Cl, C–I, S–H, and Ge–H Bond Activation Reactions Promoted by 63

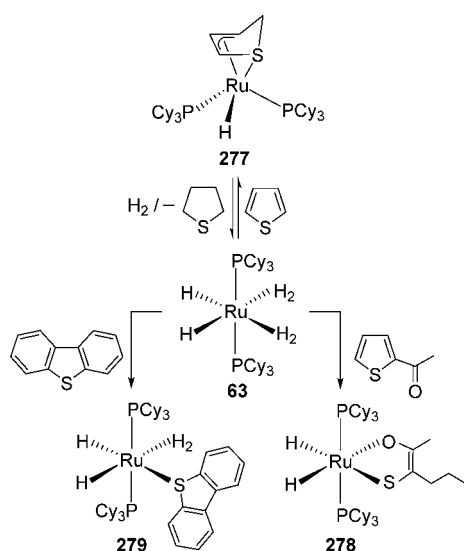


species  $\text{Ru}(\text{PCy}_3)_2$ , which undergoes the addition of both C–Cl bonds of dichloromethane to a single metal center, providing a convenient synthesis of the alkene metathesis catalyst  $\text{RuCl}_2(\text{=CH}_2)(\text{PCy}_3)_2$  (269).<sup>213</sup> The reaction with  $\text{CHPhCl}_2$  affords  $\text{RuCl}_2(\text{=CHPh})(\text{PCy}_3)_2$  (270), whereas  $\text{CH}_2=\text{CCl}_2$  gives  $\text{RuCl}_2(\text{=CHCH}_3)(\text{PCy}_3)_2$  (271) due to the hydrogenation of the C–C double bond of the presumed vinylidene, primary product, by released  $\text{H}_2$ . Hydrogenation of 269 and 270 leads to  $\text{CH}_3\text{R}$  ( $\text{R} = \text{H}$ ,  $\text{Ph}$ , respectively),  $\text{HCl}$ , and the chloride-hydride-dihydrogen 28.<sup>214</sup> The iodide counterpart  $\text{RuHI}(\eta^2\text{-H}_2)(\text{PCy}_3)_2$  (272) has been generated

through the C–I bond activation of  $\text{CH}_3\text{I}$  or  $\text{PhI}$ .<sup>215</sup> Its formation probably involves a  $\text{RuI}(\text{R})(\text{PCy}_3)_2$  intermediate, which undergoes a double hydrogenation with R–H elimination. In a consistent manner with this, Macgregor, Grushin, and co-workers have recently reported that the dihydride-dihydrogen **42** reacts with  $\text{PhX}$  ( $\text{X} = \text{I}, \text{Br}, \text{Cl}$ ) in the presence of styrene to give ethylbenzene, benzene, and the five-coordinate monohydrides  $\text{RuHX}(\text{PPh}_3)_3$ .<sup>216</sup> Similarly to  $\text{RI}$  ( $\text{R} = \text{Me}, \text{Ph}$ ), complex **63** reacts with thiols to give the thiolate derivatives  $\text{RuH}(\text{SR})(\eta^2\text{-H}_2)(\text{PCy}_3)_2$  ( $\text{R} = \text{Cy}$  (**273**),  $\text{Ph}$  (**274**),  $^t\text{Bu}$  (**275**)).<sup>217</sup> The reaction of **63** with  $\text{Ph}_2\text{GeH}_2$  yields the dihydride-dihydrogen-germylene derivative  $\text{RuH}_2(\eta^2\text{-H}_2)(=\text{GePh}_2)(\text{PCy}_3)_2$  (**276**).<sup>218</sup>

Complex **63** also has an interesting reactivity with *S*-heteroaromatic compounds (Scheme 41). Stoichiometric

**Scheme 41. Reactions of 63 with *S*-Heteroaromatic Compounds**



reaction with thiophene leads to the  $\eta^4$ -thioallyl complex  $\text{RuH}\{\kappa^4\text{-S,C,C,C-(SC}_4\text{H}_5)\}(\text{PCy}_3)_2$  (**277**). This compound easily regenerates **63** upon treatment with molecular hydrogen and, in this way, can be successfully used as a catalyst precursor in thiophene hydrogenation to 2,3,4,5-tetrahydrothiophene. The reaction of **63** with 2-acetylthiophene produces a regioselective 1,5-C–S bond splitting with formal hydrogenation of two double C–C bonds and coordination of a 2-hexen-2-olate-3-thiolate ligand in a  $\kappa^2(\text{O,S})$  mode to form  $\text{RuH}_2\{\kappa^2\text{-O,S-(C}_6\text{H}_{10}\text{OS)}\}(\text{PCy}_3)_2$  (**278**). In addition to thiophene, complex **63** is an effective catalyst precursor for the hydrogenation of 2-methylthiophene to 2-methyltetrahydrothiophene, 2-acetylthiophene to 1-(2-thienyl)ethanol, 2-thiophenecarboxaldehyde to 2-thiophenemethanol, and benzo-*[b]*thiophene to 2,3-dihydrobenzo-*[b]*thiophene. However, dibenzo-*[b,d]*thiophene is not reduced due to the formation of  $\text{RuH}_2(\eta^2\text{-H}_2)\{\kappa^1\text{-S-(C}_{12}\text{H}_8\text{S)}\}(\text{PCy}_3)_2$  (**279**).<sup>219</sup>

### 3. OSMIUM

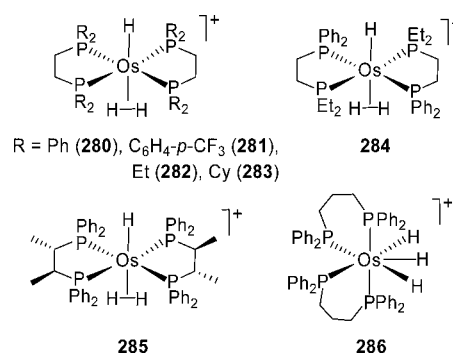
#### 3.1. Phosphine Complexes

Osmium favors classical structures with the metal in high oxidation state (4 and 6) and strong  $\text{M}(\eta^2\text{-H}_2)$  bonds because of its reducing character and marked  $\pi$ -back bonding ability. As

a consequence, osmium polyhydrides show a wider range of stoichiometries and structures than in the ruthenium case.

A variety of *trans*-hydride-elongated dihydrogen complexes  $[\text{OsH}(\eta^2\text{-H}_2)(\text{diphosphine})_2]^+$  (diphosphine =  $\text{R}_2\text{P}(\text{CH}_2)_2\text{PR}_2$ ,  $\text{R} = \text{Ph}$  (**280**),  $\text{C}_6\text{H}_4\text{-}p\text{-CF}_3$  (**281**),  $\text{Et}$  (**282**),  $\text{Cy}$  (**283**); diphosphine =  $\text{Ph}_2\text{P}(\text{CH}_2)_2\text{PEt}_2$  (**284**), (*S,S*)-chiraphos (**285**)), analogous to the ruthenium-diphosphine complexes **1–11** have been reported (Chart 7).<sup>58,59,64,65,69,220–222</sup> The separation

**Chart 7.  $[\text{OsH}(\eta^2\text{-H}_2)(\text{diphosphine})_2]^+$  and  $[\text{OsH}_3(\text{diphosphine})_2]^+$  Cations**

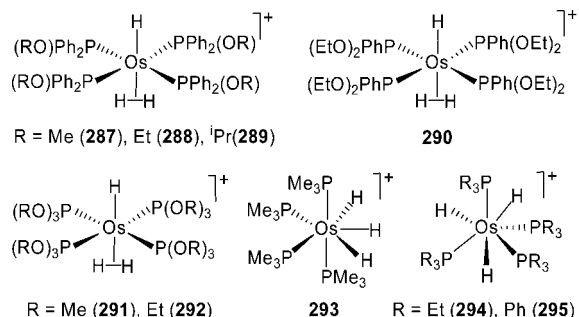


between the hydrogen atoms of the elongated dihydrogen ligand, calculated from  $J_{\text{H-D}}$  and  $T_1(\text{min})$  values, is in the range of 1.0–1.2 Å depending upon the phosphine substituents. A classical trihydride character ( $d_{\text{H-H}} = 1.6$  Å) has been proposed however for complex  $[\text{OsH}_3\{\text{Ph}_2\text{P}(\text{CH}_2)_3\text{PPh}_2\}_2]^+$  (**286**).<sup>223</sup> The comparison of spectroscopic features and some properties of these compounds with those of the triade analogous reveals several interesting trends. In accordance with the terminal hydride stretching mode  $\nu(\text{M-H})$ , the strength of the M–H bond increases in the sequence  $\text{Fe} < \text{Ru} < \text{Os}$ , as expected for isostructural species. However, indicators of dihydrogen versus dihydride character show that ruthenium is out of plane in the periodic order. Analysis of  $J_{\text{H-D}}$  and  $T_1(\text{min})$  values suggests that the overall ordering of increasing H–H distance is  $\text{Ru} \approx \text{Fe} < \text{Os}$ , whereas the lability of dihydrogen as judged by the qualitative  $\text{H}_2/\text{D}_2$  rates of exchange increases as  $\text{Os} < \text{Fe} < \text{Ru}$  (i.e., the strength of the  $\text{M}(\eta^2\text{-H}_2)$  bond increases as  $\text{Ru} < \text{Fe} < \text{Os}$ ). The hydride and dihydrogen ligands undergo thermally activated site exchange, which likely proceeds via the homolytic cleavage of the dihydrogen ligand. The  $\Delta G^\ddagger$  values for the process decrease as  $\text{Ru} > \text{Fe} > \text{Os}$  and  $\text{Ph}_2\text{P}(\text{CH}_2)_2\text{PPh}_2 > \text{Ph}_2\text{P}(\text{CH}_2)_2\text{PEt}_2$ .<sup>64</sup> Changing the metal from Ru to Os has the effect of increasing the acidity of the dihydrogen ligand even though the osmium complexes are more reducing than the ruthenium compounds. This appears to be due to a higher H–H bond dissociation energy for the ruthenium complexes.<sup>69</sup>

Complexes  $[\text{OsH}(\eta^2\text{-H}_2)\{\text{PPh}_2(\text{OR})\}_4]^+$  ( $\text{R} = \text{Me}$  (**287**),  $\text{Et}$  (**288**),  $^i\text{Pr}$  (**289**)),  $[\text{OsH}(\eta^2\text{-H}_2)\{\text{PPh}(\text{OEt})_2\}_4]^+$  (**290**), and  $[\text{OsH}(\eta^2\text{-H}_2)\{\text{P}(\text{OR})_3\}_4]^+$  ( $\text{R} = \text{Me}$  (**291**),  $\text{Et}$  (**292**)) containing four monodentate phosphonite, phosphinite, and phosphite ligands, respectively, are also *trans*-hydride-elongated dihydrogen species.<sup>75,224</sup> However, complexes  $[\text{OsH}_3(\text{PR}_3)_4]^+$  ( $\text{R} = \text{Me}$  (**293**),  $\text{Et}$  (**294**),  $\text{Ph}$  (**295**)), with basic phosphines, have been described as classical trihydride derivatives. The trimethylphosphine compound **293** seems to be a pentagonal bipyramidal trihydride in equilibrium with a hydride-capped tetrahedral structural form. Complexes **294** and **295** are

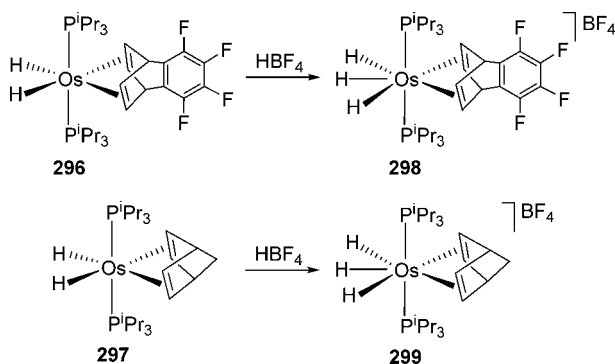
exclusively represented by the latter structural type (Chart 8).<sup>77,225–227</sup>

Chart 8.  $[\text{OsH}(\eta^2\text{-H}_2)(\text{PR}_3)_4]^+$  and  $[\text{OsH}_3(\text{PR}_3)_4]^+$  Cations



Protonation of the dihydrides  $\text{OsH}_2(\text{diolefin})(\text{P}^i\text{Pr}_3)_2$  (diolefin = tetrafluorobenzobarrelene (TFB; **296**), 2,5-norbornadiene (NBD; **297**)), containing a chelating  $\pi$ -acid and two basic monodentate ligands, with  $\text{HBF}_4 \cdot \text{OEt}_2$  leads to  $[\text{OsH}_3(\text{diolefin})(\text{P}^i\text{Pr}_3)_2]\text{BF}_4$  (diolefin = TFB (**298**), NBD (**299**)), which, in contrast to **280–285** and **287–292**, are classical trihydrides. On the basis of spectroscopic data, the pentagonal bipyramidal geometry shown in Scheme 42 has

Scheme 42. Protonation of **296** and **297**

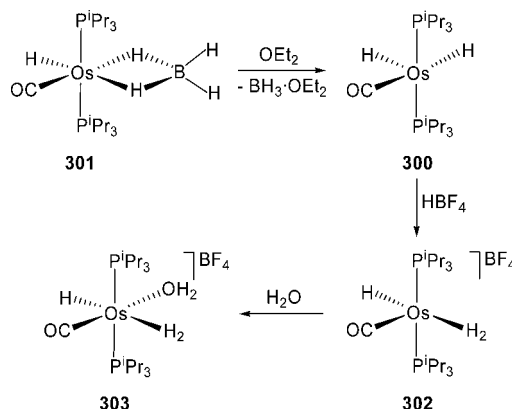


been proposed for these compounds. The hydride ligands undergo thermally activated site exchange. Furthermore, they show quantum mechanical exchange coupling. Taking  $a$  as the separation between the hydride ligands calculated from the  $T_1(\text{min})$  values, 1.7 Å for **298** and 1.8 Å for **299**, the phenomenon has been quantified by means of eq 1 and the following parameters  $J_{\text{mag}}$ ,  $\lambda$ , and  $\nu$  have been obtained: 6 Hz, 1.1 Å, and 484  $\text{cm}^{-1}$  for **298** and 10 Hz, 1.0 Å, and 496  $\text{cm}^{-1}$  for **299**.<sup>228</sup>

Most commonly  $\text{BH}_3$  is abstracted from coordinated tetrahydrideborate ligands with Lewis bases capable of forming  $\text{H}_3\text{B-L}$  adducts. This property of borane has been used to generate in situ the five-coordinate dihydride species  $\text{OsH}_2(\text{CO})(\text{P}^i\text{Pr}_3)_2$  (**300**) by means of solution of the hydride-tetrahydrideborate  $\text{OsH}(\kappa^2\text{-H}_2\text{BH}_2)(\text{CO})(\text{P}^i\text{Pr}_3)_2$  (**301**) in diethyl ether. The protonation of this dihydride with  $\text{HBF}_4 \cdot \text{OEt}_2$  gives rise to the surprising cationic five-coordinate *trans*-hydride-dihydrogen derivative  $[\text{OsH}(\eta^2\text{-H}_2)(\text{CO})(\text{P}^i\text{Pr}_3)_2]\text{BF}_4$  (**302**),<sup>229</sup> which has been a useful starting material to carry out C–C coupling reactions.<sup>230</sup> In the presence of water, it affords the six-coordinate *trans*-hydride-

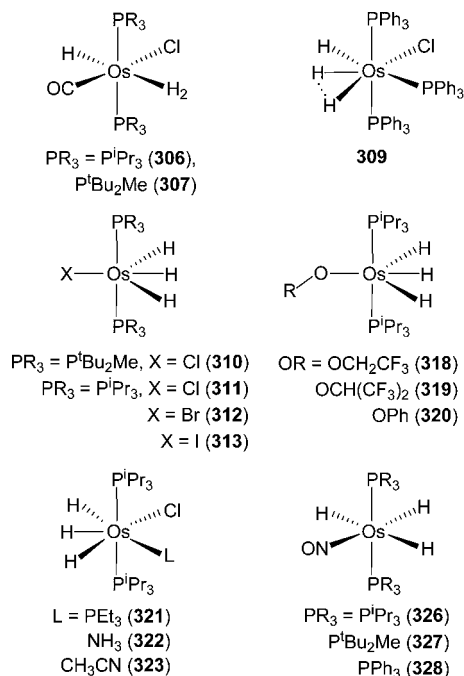
dihydrogen  $[\text{OsH}(\eta^2\text{-H}_2)(\text{CO})(\text{H}_2\text{O})(\text{P}^i\text{Pr}_3)_2]\text{BF}_4$  (**303**), with three different heavy monodentate coligands (Scheme 43).

Scheme 43. Preparation of **302**



Several types of neutral  $\text{OsH}_3$ -species have been described (Chart 9). Reactions of complexes  $\text{OsHCl}(\text{CO})(\text{PR}_3)_2$  ( $\text{PR}_3 =$

Chart 9. Several Types of Neutral  $\text{OsH}_3$ -Species



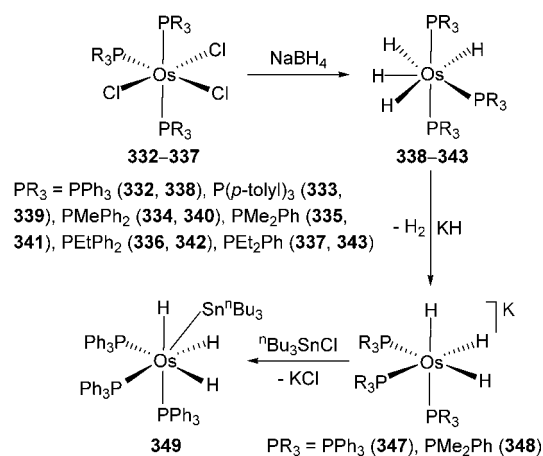
$\text{P}^i\text{Pr}_3$  (**304**),  $\text{P}^i\text{Bu}_2\text{Me}$  (**305**)) with molecular hydrogen give the *trans*-hydride-dihydrogen derivatives  $\text{OsHCl}(\eta^2\text{-H}_2)(\text{CO})(\text{PR}_3)_2$  ( $\text{PR}_3 = \text{P}^i\text{Pr}_3$  (**306**),  $\text{P}^i\text{Bu}_2\text{Me}$  (**307**)).<sup>231,232</sup> A H–H distance of 0.8 Å in the dihydrogen ligand of **306** has been determined from variable-temperature  $^1\text{H}$   $T_1$  measurements. DFT calculations have revealed the existence of a *cis*-hydride-dihydrogen isomer with a relative energy of 13.8  $\text{kcal mol}^{-1}$ .<sup>233</sup> The equilibrium between these *trans* and *cis* isomers appears to play a main role in the hydrogenation of benzylideneacetone to the saturated ketone catalyzed by the five-coordinate complexes **304** and **305**.<sup>234</sup> The five-coordinate dichloride complex  $\text{OsCl}_2(\text{PPh}_3)_3$  (**308**) also reacts with molecular hydrogen. In the presence of  $\text{NEt}_3$ , the reaction leads to the *cis*-hydride-compressed dihydride  $\text{OsHCl}(\text{H}\cdots\text{H})(\text{PPh}_3)_3$  (**309**),<sup>235</sup> which has been characterized by neutron diffraction analysis.<sup>236</sup> The

results confirm the presence of the compressed dihydride with a H...H separation of 1.48(2) Å. The molecule is substantially distorted from an ideal octahedral geometry. The hydride is located trans to a phosphine, separated by 1.67(2) Å from the compressed dihydride, which sits essentially trans to the chloride. Bulky phosphines stabilize related six-coordinate species  $\text{OsH}_3\text{X}(\text{PR}_3)_2$  ( $\text{PR}_3 = \text{P}^t\text{Bu}_2\text{Me}$ ,  $\text{X} = \text{Cl}$  (310);<sup>85</sup>  $\text{PR}_3 = \text{P}^i\text{Pr}_3$ ,  $\text{X} = \text{Cl}$  (311), Br (312), I (313)<sup>237</sup>), which have been prepared by reaction of the corresponding  $\text{OsH}_2\text{X}_2(\text{PR}_3)_2$  ( $\text{PR}_3 = \text{P}^t\text{Bu}_2\text{Me}$ ,  $\text{X} = \text{Cl}$  (314);  $\text{PR}_3 = \text{P}^i\text{Pr}_3$ ,  $\text{X} = \text{Cl}$  (315), Br (316), I (317)) complexes with molecular hydrogen in the presence of  $\text{N}(\text{Et})_3$ . These compounds are neutral species showing spectacular quantum mechanical exchange coupling, which is sensitive to halide identity.<sup>238,239</sup> Starting from 311, metathesis reactions with  $\text{TiOR}$  or  $\text{NaOPh}$  afford the alkoxide derivatives  $\text{OsH}_3(\text{OR})(\text{P}^i\text{Pr}_3)_2$  ( $\text{OR} = \text{OCH}_2\text{CF}_3$  (318),  $\text{OCH}(\text{CF}_3)_2$  (319),  $\text{OPh}$  (320)). Complex 320 has been characterized by X-ray diffraction analysis. The structure has essentially  $C_{2v}$  symmetry with *trans* phosphines and the oxygen atom of the phenoxy group, the metal center, and the hydrides lying in the plane perpendicular to the P–Os–P direction.<sup>240</sup> The H–Os–H angles ( $58.1(5)^\circ$  and  $62.1(15)^\circ$ ) markedly deviate from  $90^\circ$ . It is well-known that the octahedral geometry is not favorable for heavy metal  $d^4$  complexes, which prefer to be diamagnetic. These compounds undergo a distortion that destabilizes one orbital from the  $t_{2g}$  set and simultaneously stabilizes the occupied ones. The distortion partially cancels the electron deficiency at the metal, which receives additional electron density from the hydrides via stronger  $\sigma$ -bonds and from one lone pair of X or OR via  $\pi$ -bond. These compounds have a useful chemistry including reactions of hydroosmiation of unsaturated organic substrates,<sup>241</sup> as precursors of C–C coupling processes,<sup>242</sup> and as starting materials for the preparation of half-sandwich complexes.<sup>243</sup> The addition of Lewis bases, such as  $\text{PEt}_3$ ,  $\text{NH}_3$ , and  $\text{CH}_3\text{CN}$ , to 311 affords seven-coordinate  $\text{OsH}_3\text{Cl}(\text{L})(\text{P}^i\text{Pr}_3)_2$  ( $\text{L} = \text{PEt}_3$  (321),  $\text{NH}_3$  (322),  $\text{CH}_3\text{CN}$  (323)) species. These complexes are assigned to pentagonal bipyramidal geometry with axial phosphines and the Lewis base L *cisoid* disposed to the chloride, in the perpendicular plane along with the hydride ligands. This geometry is the most favorable thermodynamically because it minimizes steric interactions by putting bulky phosphines in *trans* positions and avoids placing hydride ligands, the strongest  $\sigma$ -donors, in *trans* or pseudo-*trans* positions, and kinetically because it places the incoming ligand in the position predicted by the LUMO of the unsaturated trihydride complex. Under excess  $\text{NH}_3$  and  $\text{CH}_3\text{CN}$ , the Lewis bases displace chloride to form the cationic compounds  $[\text{OsH}_3\text{L}_2(\text{P}^i\text{Pr}_3)_2]\text{Cl}$  ( $\text{L} = \text{NH}_3$  (324),  $\text{CH}_3\text{CN}$  (325)), related to 298 and 299, but containing two monodentate N-donor ligands instead of a diolefin. The X-ray diffraction structure of 324 confirmed the *cis*-disposition of the L ligands in these compounds ( $\text{N–Os–N} = 81.5(2)^\circ$ ).<sup>237</sup> Neutral  $d^6$  *mer*-trihydrides  $\text{OsH}_3(\text{NO})(\text{PR}_3)_2$  ( $\text{PR}_3 = \text{P}^i\text{Pr}_3$  (326),  $\text{P}^t\text{Bu}_2\text{Me}$  (327),  $\text{PPh}_3$  (328)) have been also prepared via  $\text{NaBH}_4/\text{MeOH}$  reduction of the corresponding *cis,trans*- $\text{OsH}_2\text{Cl}(\text{NO})(\text{PR}_3)_2$  ( $\text{PR}_3 = \text{P}^i\text{Pr}_3$  (329),  $\text{P}^t\text{Bu}_2\text{Me}$  (330),  $\text{PPh}_3$  (331)) compounds.<sup>91</sup>

Reaction of  $\text{OsCl}_3(\text{PR}_3)_3$  ( $\text{PR}_3 = \text{PPh}_3$  (332),  $\text{P}(p\text{-tolyl})_3$  (333),  $\text{PMePh}_2$  (334),  $\text{PMe}_2\text{Ph}$  (335),  $\text{PEtPh}_2$  (336),  $\text{PEt}_2\text{Ph}$  (337)) with  $\text{NaBH}_4$  in ethanol leads to the classical<sup>92,94,244,245</sup> tetrahydride complexes  $\text{OsH}_4(\text{PR}_3)_3$  ( $\text{PR}_3 = \text{PPh}_3$  (338),  $\text{P}(p\text{-tolyl})_3$  (339),  $\text{PMePh}_2$  (340),  $\text{PMe}_2\text{Ph}$  (341),  $\text{PEtPh}_2$  (342),  $\text{PEt}_2\text{Ph}$  (343)).<sup>246–249</sup> The structure of 341 has been

determined by neutron diffraction. The complex can be described as a distorted pentagonal bipyramid with two axial phosphines, whereas the hydrides and the other phosphine lie in the perpendicular plane to the P–Os–P direction.<sup>250</sup> The formation of these  $d^4$ -tetrahydrides probably takes place via hydride-tetrahydrideborate intermediates. In agreement with this proposal, it has been observed that complexes 304 and 305 react with  $\text{NaBH}_4$  to initially give the hydride-tetrahydrideborate intermediates 301 and  $\text{OsH}(\kappa^2\text{-H}_2\text{BH}_2)(\text{CO})(\text{P}^t\text{Bu}_2\text{Me})_2$  (344), which evolve into the dihydride-dihydrogen derivatives  $\text{OsH}_2(\eta^2\text{-H}_2)(\text{CO})(\text{PR}_3)_2$  ( $\text{PR}_3 = \text{P}^i\text{Pr}_3$  (345),  $\text{P}^t\text{Bu}_2\text{Me}$  (346)) in methanol.<sup>251,252</sup> The presence of a carbonyl group in these compounds instead of one of the phosphines of 338–343 is a determinant for the nonclassical interaction. Tetrahydrides 338 and 341 have been deprotonated with KH in tetrahydrofuran. The resulting anionic *fac*-trihydrides  $[\text{OsH}_3(\text{PR}_3)_3]^-$  ( $\text{PR}_3 = \text{PPh}_3$  (347),<sup>253</sup>  $\text{PMe}_2\text{Ph}$  (348)<sup>254</sup>) are very unstable in solution and easily revert to the starting tetrahydrides. However, they can be stabilized by addition of 18-crown-6, which forms  $[\text{K}(\text{THF})(18\text{-crown-6})][\text{OsH}_3(\text{PR}_3)_3]$ . The X-ray structure of the  $\text{PPh}_3$ -adduct has revealed cation–anion contacts achieved through three Os–H...K moieties. In the absence of stabilizer, the tetrahydrofuran solutions of 347 react with  ${}^n\text{Bu}_3\text{SnCl}$  to produce  $\text{OsH}_3(\text{Sn}^n\text{Bu}_3)(\text{PPh}_3)_3$  (349). This compound possesses a covalent Os–Sn bond in a seven-coordinate *fac*- $\text{OsH}_3(\text{PPh}_3)_3$  arrangement with the  $\text{Sn}^n\text{Bu}_3$  group capping the  $\text{OsH}_3$  face (Scheme 44).<sup>253</sup> The addition of  $(\eta^5\text{-C}_5\text{H}_5)_2\text{ZrXCl}$

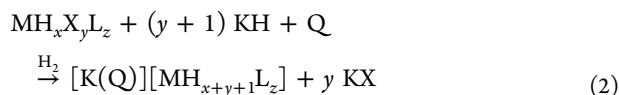
#### Scheme 44. Preparation and Deprotonation of $\text{OsH}_4(\text{PR}_3)_3$ Complexes



( $\text{X} = \text{H}, \text{Cl}$ ) to tetrahydrofuran solutions of 348 leads to the bimetallic complexes  $(\eta^5\text{-C}_5\text{H}_5)_2\text{XZr}(\mu\text{-H})_3\text{Os}(\text{PMe}_2\text{Ph})_3$  ( $\text{X} = \text{H}$  (350),  $\text{Cl}$  (351)), containing three bridging hydrides.<sup>255</sup>

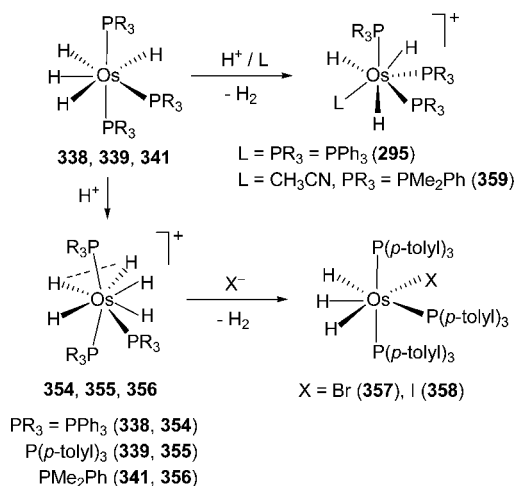
The related carbonyl complex  $[\text{OsH}_3(\text{CO})(\text{P}^i\text{Pr}_3)_2]^-$  (352) has been similarly prepared to its ruthenium counterpart 53, starting from 304, according to the reaction summarized by the general eq 2, and isolated as  $[\text{K}(\text{Q})][\text{OsH}_3(\text{CO})(\text{P}^i\text{Pr}_3)_2]$  ( $\text{Q} = 18\text{-crown-6}$ , 1-aza-18-crown-6, 2.2.2-crypt).<sup>104</sup> In agreement with eq 2, treatment of tetrahydrofuran solutions of the dihydride-dichloride 315 with excess potassium hydride, in the presence of 1 equiv of crown ether Q, and under 1 atm of  $\text{H}_2$  affords the pentahydride  $[\text{K}(\text{Q})][\text{OsH}_5(\text{P}^i\text{Pr}_3)_2]$  ( $\text{Q} = 18\text{-crown-6}$  (353a), 1-aza-18-crown-6 (353b), 1,10-diaza-18-crown-6 (353c)). The X-ray structure of 353c indicates that intermolecular short proton–hydride interactions between the hydrides of the anion and the NH moieties of the cation cause

the self-assembly of one-dimensional networks of pentagonal bipyramidal anions and cations. The X-ray structure of **353b** reveals that this salt also forms one-dimensional chains due to Os–H⋯HN and weak Os–H⋯HC interactions between the hydrides of the anion and the NH and methylene CH of the cation.<sup>105</sup>



Tetrahydrides **338**, **339**, and **341** have been protonated (Scheme 45).<sup>256</sup> The addition yields the pentahydride cations

**Scheme 45. Protonation Reactions of OsH<sub>4</sub>(PR<sub>3</sub>)<sub>3</sub> Complexes**

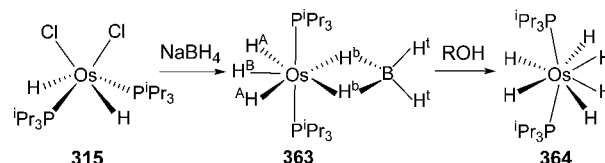


[OsH<sub>5</sub>(PR<sub>3</sub>)<sub>3</sub>]<sup>+</sup> (PR<sub>3</sub> = PPh<sub>3</sub> (**354**), P(*p*-tolyl)<sub>3</sub> (**355**), PMe<sub>2</sub>Ph (**356**)). The BF<sub>4</sub><sup>−</sup> salt of **356** has been characterized by neutron diffraction. The coordination geometry around the metal center of the cation can be rationalized as being derived from a distorted dodecahedron, which is defined by two intersecting BAAB orthogonal trapezoidal planes. One of them contains two phosphines and two hydrides and the other one a phosphine and three hydrides. The phosphines occupy the more spacious B sites of the dodecahedron. It should be also mentioned that the separation between the H<sub>B</sub> and H<sub>A</sub> hydrides in the trihydride plane is short (1.49(4) Å), and therefore, these species can be defined as trihydride-compressed dihydrides. Complex **356** catalyzes the hydrogenation of ethylene, cyclohexene, and 1,5-cyclooctadiene.<sup>257,258</sup> In the presence of bromide and iodide, complex **355** affords the neutral trihydrides OsH<sub>3</sub>X{P(*p*-tolyl)<sub>3</sub>}<sub>3</sub> (X = Br (**357**), I (**358**)),<sup>256</sup> whereas the protonations of **338** and **341** in the presence of triphenylphosphine<sup>227</sup> and acetonitrile,<sup>259</sup> respectively, give the cationic trihydrides [OsH<sub>3</sub>L(PR<sub>3</sub>)<sub>3</sub>]<sup>+</sup> (L = PR<sub>3</sub> = PPh<sub>3</sub> (**295**); L = CH<sub>3</sub>CN, PR<sub>3</sub> = PMe<sub>2</sub>Ph (**359**)).

Complexes OsH<sub>6</sub>(PR<sub>3</sub>)<sub>2</sub> (PR<sub>3</sub> = PMe<sub>2</sub>Ph (**360**), P<sup>*i*</sup>Pr<sub>2</sub>Ph (**361**), PCyp<sub>3</sub> (**362**)) with six hydrogen atoms attached to the metal center are also known. They have been generally prepared by reaction of the corresponding adducts OsCl<sub>2</sub>O<sub>2</sub>(PR<sub>3</sub>)<sub>2</sub> with LiAlH<sub>4</sub> or NaBH<sub>4</sub>.<sup>248,260</sup> In contrast to ruthenium, these compounds are classical hexahydrides. This fact has been confirmed by means of the neutron diffraction structure of **361**. The geometry of the inner coordination sphere can be rationalized as an irregular dodecahedron defined

by two orthogonal (87.5°) BAAB trapezoidal planes. One of them contains the phosphorus atoms at B sites and two hydrides at A sites, whereas the remaining hydrides lie in the other one.<sup>261</sup> Like the tetrahydrides **338**–**343**, these hexahydride derivatives are generated via tetrahydrideborate intermediates. In favor of this, it has been observed that complex **315** reacts with NaBH<sub>4</sub> to give the trihydride-tetrahydrideborate intermediate OsH<sub>3</sub>(κ<sup>2</sup>-H<sub>2</sub>BH<sub>2</sub>)(P<sup>*i*</sup>Pr<sub>3</sub>)<sub>2</sub> (**363**), which evolves into OsH<sub>6</sub>(P<sup>*i*</sup>Pr<sub>3</sub>)<sub>2</sub> (**364**) in alcohols (Scheme 46).<sup>262</sup>

**Scheme 46. Preparation of the Hexahydride 364 via the Trihydride-Tetrahydrideborate Intermediate 363**

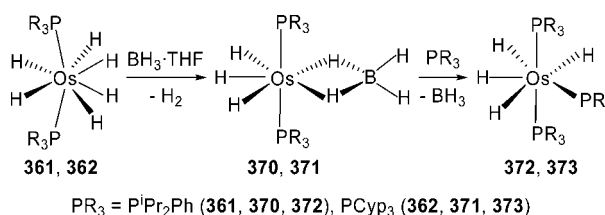


The P<sup>*t*</sup>Bu<sub>2</sub>Me-counterpart OsH<sub>6</sub>(P<sup>*t*</sup>Bu<sub>2</sub>Me)<sub>2</sub> (**365**) has been similarly prepared starting from **314** and NaBH<sub>4</sub>.<sup>263</sup> The same methodology has been used for the preparation of OsH<sub>6</sub>(P<sup>*i*</sup>Pr<sub>2</sub>R)<sub>2</sub> (R = CH<sub>2</sub>CH<sub>2</sub>OMe (**366**), CH<sub>2</sub>CO<sub>2</sub>Me (**367**), CH<sub>2</sub>CO<sub>2</sub>Et (**368**)), bearing functionalized phosphines, and the mixed phosphine derivative OsH<sub>6</sub>(P<sup>*i*</sup>Pr<sub>3</sub>)<sub>2</sub>{P(CH<sub>2</sub>CH<sub>2</sub>NMe<sub>2</sub>)<sup>*i*</sup>Pr<sub>2</sub>} (**369**).<sup>264</sup> Variable-temperature <sup>1</sup>H NMR studies and DFT calculations on **363** have revealed that this type of compounds undergo three different intramolecular rearrangements in solution. The lowest energy barrier is associated with the H<sup>A</sup>–H<sup>B</sup> hydride-exchange and goes through a dihydrogen transition state. The second lowest energy barrier corresponds to the hydride-tetrahydrideborate H<sup>A</sup>–H<sup>b</sup> exchange. In this case, the process goes through a seven-coordinate intermediate containing an η<sup>2</sup>-H–BH<sub>2</sub> ligand. The highest energy barrier is associated with the exchange between the bridging (H<sup>b</sup>) and terminal (H<sup>a</sup>) hydrogens of the tetrahydrideborate group. This rearrangement goes via a dissociative mechanism, involving a transition state with a monodentate BH<sub>4</sub> ligand.<sup>265</sup>

Borane displaces a hydrogen molecule of **361** and **362** and is added to one of the remaining hydride ligands to quantitatively form the trihydride-tetrahydrideborate derivatives OsH<sub>3</sub>(κ<sup>2</sup>-H<sub>2</sub>BH<sub>2</sub>)(PR<sub>3</sub>)<sub>2</sub> (PR<sub>3</sub> = P<sup>*i*</sup>Pr<sub>2</sub>Ph (**370**), PCyp (**371**)). These compounds react with the corresponding PR<sub>3</sub> phosphine to give the tetrahydride complexes OsH<sub>4</sub>(PR<sub>3</sub>)<sub>3</sub> (PR<sub>3</sub> = P<sup>*i*</sup>Pr<sub>2</sub>Ph (**372**), PCyp (**373**)), related to **338**–**343** (Scheme 47).<sup>266</sup>

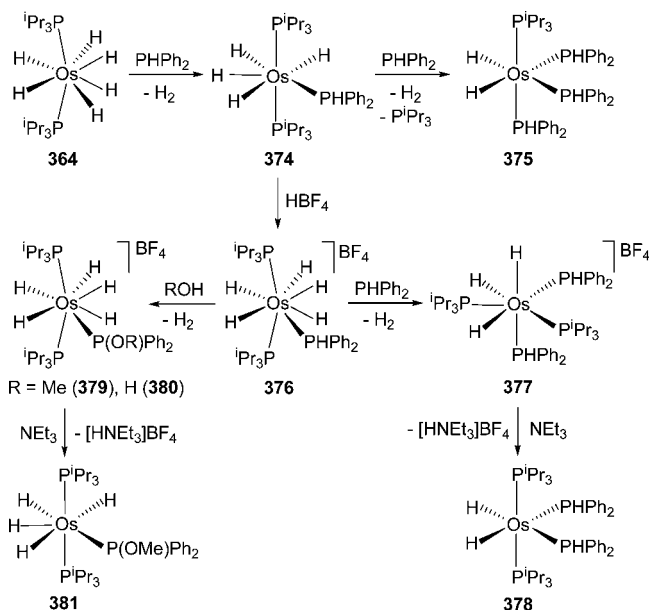
The dissociation energy of a hydrogen molecule from the hexahydride complexes OsH<sub>6</sub>(PR<sub>3</sub>)<sub>2</sub> is not too high. Thus, the triisopropylphosphine derivative **364** reacts with diphenylphosphine in toluene at 80 °C to give H<sub>2</sub> and the tetrahydride

**Scheme 47. Transformation of d<sup>2</sup>-Hexahydride into d<sup>4</sup>-Tetrahydride-Osmium Complexes via Trihydride-Tetrahydrideborate Intermediates**



$\text{OsH}_4(\text{P}^i\text{Pr}_3)_2$  (374) after 1 h. The dissociation of molecular hydrogen from complex 374 requires higher energy, which is similar to that necessary to break an Os–P bond. In contrast to 364, the reaction of 374 with diphenylphosphine needs 3 days and gives rise to  $\text{OsH}_2(\text{P}^i\text{Pr}_3)_3$  (375), as a result of the loss of one molecule of hydrogen and the replacement of one of the triisopropylphosphine ligands. The selective substitution of molecular hydrogen in 374 requires its previous acidolysis with  $\text{HBF}_4 \cdot \text{OEt}_2$  (Scheme 48), which leads

#### Scheme 48. Mixed Triisopropylphosphine-Diphenylphosphine-Osmium(II), Osmium(IV), and Osmium(VI) Complexes

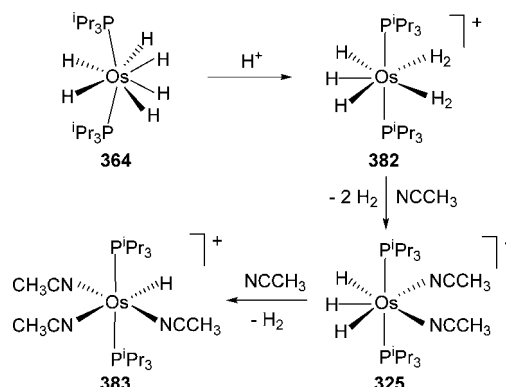


to  $[\text{OsH}_5(\text{P}^i\text{Pr}_3)_2]\text{BF}_4$  (376). In contrast to 374, the addition of diphenylphosphine to 376 produces the selective substitution of  $\text{H}_2$  to form  $[\text{OsH}_3(\text{P}^i\text{Pr}_3)_2]\text{BF}_4$  (377), which by deprotonation with  $\text{NEt}_3$  affords  $\text{OsH}_2(\text{P}^i\text{Pr}_3)_2$  (378). Complex 376 also reacts with methanol and water to give  $[\text{OsH}_5\{\text{P}(\text{OMe})\text{Ph}_2\}]\text{BF}_4$  (379) and  $[\text{OsH}_5\{\text{P}(\text{OH})\text{Ph}_2\}]\text{BF}_4$  (380), respectively. The deprotonation of 379 with  $\text{NEt}_3$  leads to  $\text{OsH}_4\{\text{P}(\text{OMe})\text{Ph}_2\}(\text{P}^i\text{Pr}_3)_2$  (381).<sup>267</sup>

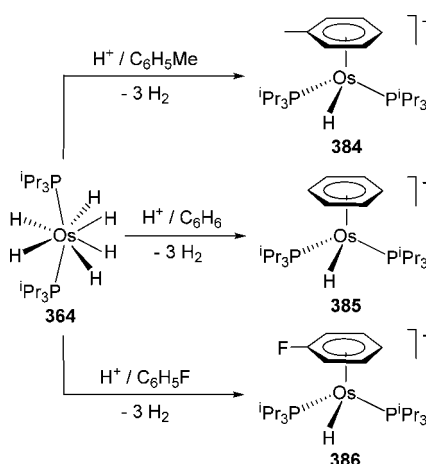
The acidolysis of 364 with  $\text{HBF}_4 \cdot \text{OEt}_2$  in diethyl ether produces the instantaneous precipitation of the trihydride-bis(dihydrogen) derivative  $[\text{OsH}_3(\eta^2\text{-H}_2)_2(\text{P}^i\text{Pr}_3)_2]\text{BF}_4$  (382), a rare case of  $\text{OsH}_7$ -species. In acetonitrile, complex 382 undergoes loss of the coordinated hydrogen molecules, which are replaced by solvent molecules to give the trihydride-bis(solvento) cation 325. Further reaction with acetonitrile leads to the monohydride  $[\text{OsH}(\text{CH}_3\text{CN})_3(\text{P}^i\text{Pr}_3)_2]\text{BF}_4$  (383) and  $\text{H}_2$  (Scheme 49).<sup>268</sup>

Complex 383 is the result of the trapping of the 12-valence electrons monohydride cation  $[\text{OsH}(\text{P}^i\text{Pr}_3)_2]^+$  by the acetonitrile solvent. This “functional equivalent” can be also trapped by aromatic solvents such as toluene, benzene, or fluorobenzene (Scheme 50). Thus, the addition of 1.5 equiv of  $\text{HBF}_4 \cdot \text{OEt}_2$  to the solutions of 364 in these aromatic solvents leads to the half-sandwich compounds  $[\text{OsH}(\eta^6\text{-arene})(\text{P}^i\text{Pr}_3)_2]\text{BF}_4$  (arene =  $\text{C}_6\text{H}_5\text{Me}$  (384),  $\text{C}_6\text{H}_6$  (385),  $\text{C}_6\text{H}_5\text{F}$  (386)), as a result of initial protonation of the hexahydride, the subsequent release of

#### Scheme 49. Acidolysis of 364 in Acetonitrile



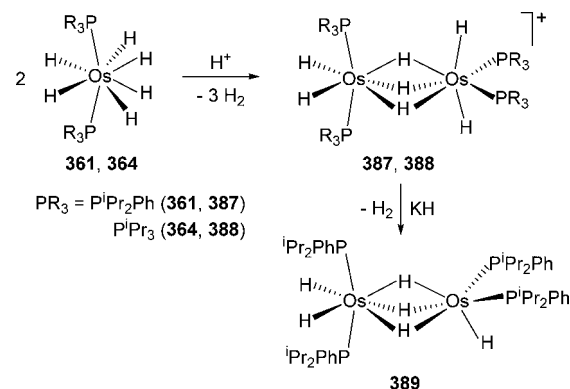
#### Scheme 50. Acidolysis of 364 in Aromatic Solvents



three hydrogen molecules from the intermediate 382, and the arene coordination to the 12-valence electrons monohydride.<sup>269</sup>

This type of monohydride cations can also be trapped by the own hexahydrides (Scheme 51). Thus, the protonation of 361

#### Scheme 51. Transformation of Hexahydride-Osmium Complexes into Dimer Species

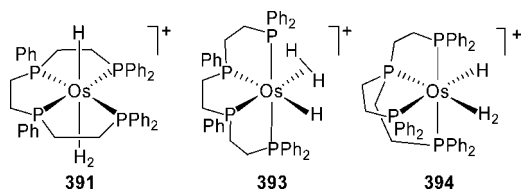


and 364 with 0.5 equiv of acid yields the heptahydride dimers  $[\{\text{OsH}_2(\text{PR}_3)_2\}_2(\mu\text{-H})_3]^+$  ( $\text{PR}_3 = \text{P}^i\text{Pr}_2\text{Ph}$  (387),<sup>270</sup>  $\text{P}^i\text{Pr}_3$  (388)<sup>269</sup>). Deprotonation of 387 with potassium hydride gives the neutral hexahydride dimer  $(\text{P}^i\text{Pr}_2\text{Ph})_2\text{H}_2\text{Os}(\mu\text{-H})_3\text{OsH}(\text{P}^i\text{Pr}_2\text{Ph})_2$  (389).

### 3.2. Complexes with Tetrapodal Phosphine Ligands

Polyhydrides stabilized with ligands of this type are rare in the osmium chemistry (Chart 10). The abstraction of the chloride

Chart 10. Complexes with Tetrapodal Phosphine Ligands

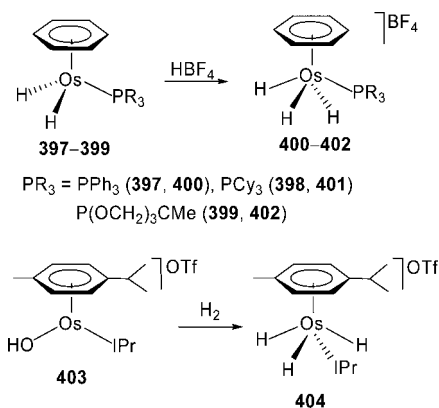


ligand of *trans*-OsHCl(*meso*-tetraphos-1) (390) with NaBPh<sub>4</sub> under hydrogen atmosphere yields the *trans*-hydride-dihydrogen [OsH(η<sup>2</sup>-H<sub>2</sub>)(*meso*-tetraphos-1)]BPh<sub>4</sub> (391; *d*<sub>H-H</sub> = 0.95–0.99 Å),<sup>132</sup> whereas the protonation of *cis*-α-OsH<sub>2</sub>(*rac*-tetraphos-1) (392) with HBF<sub>4</sub>·OEt<sub>2</sub> leads to the *cis*-hydride-elongated dihydrogen [OsH(η<sup>2</sup>-H<sub>2</sub>)(*rac*-tetraphos-1)]BF<sub>4</sub> (393; *d*<sub>H-H</sub> = 1.25–1.6 Å).<sup>271</sup> The related *cis*-hydride-dihydrogen [OsH(η<sup>2</sup>-H<sub>2</sub>){P(CH<sub>2</sub>CH<sub>2</sub>PPh<sub>2</sub>)<sub>3</sub>}]BPh<sub>4</sub> (394; *d*<sub>H-H</sub> ≈ 0.95 Å) has been prepared by displacement of the coordinated nitrogen molecule of [OsH(η<sup>2</sup>-N<sub>2</sub>){P(CH<sub>2</sub>CH<sub>2</sub>PPh<sub>2</sub>)<sub>3</sub>}]BPh<sub>4</sub> (395) by H<sub>2</sub> or by protonation of the dihydride OsH<sub>2</sub>{P(CH<sub>2</sub>CH<sub>2</sub>PPh<sub>2</sub>)<sub>3</sub>} (396) with HOTf and subsequent addition of NaBPh<sub>4</sub>. The mutually *trans*-disposition of the hydride and a terminal phosphorus atom in 394 has been established by X-ray diffraction analysis.<sup>272</sup>

### 3.3. Half Sandwich Compounds

Complexes of this type include a few cationic trihydride compounds containing arene ligands (Scheme 52). Protonation

Scheme 52. Preparation of [OsH<sub>3</sub>(η<sup>6</sup>-arene)L]<sup>+</sup> Cations

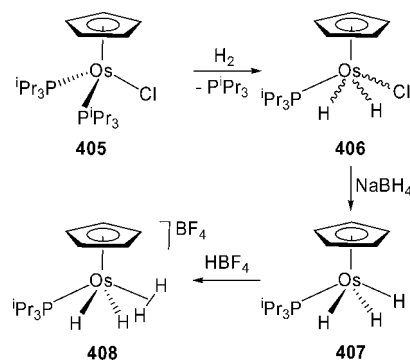


of the dihydride complexes OsH<sub>2</sub>(η<sup>6</sup>-C<sub>6</sub>H<sub>6</sub>)(PR<sub>3</sub>) (PR<sub>3</sub> = PPh<sub>3</sub> (397), PCy<sub>3</sub> (398), P(OCH<sub>2</sub>)<sub>3</sub>CMe (399)) with HBF<sub>4</sub>·OEt<sub>2</sub> in dichloromethane leads to [OsH<sub>3</sub>(η<sup>6</sup>-C<sub>6</sub>H<sub>6</sub>)(PR<sub>3</sub>)]BF<sub>4</sub> (PR<sub>3</sub> = PPh<sub>3</sub> (400), PCy<sub>3</sub> (401), P(OCH<sub>2</sub>)<sub>3</sub>CMe (402)),<sup>273</sup> whereas the hydrogenation of the cationic 16-valence electrons hydroxo [Os(OH)(η<sup>6</sup>-*p*-cymene)(IPr)]OTf (403) affords the NHC-derivative [OsH<sub>3</sub>(η<sup>6</sup>-*p*-cymene)(IPr)]OTf (404).<sup>274</sup> The hydride ligands of these compounds undergo quantum mechanical exchange coupling with temperature-dependent values of *J*<sub>obs</sub> between 70 and 370 Hz in the temperature range of 213–173 K.

One of the phosphine ligands of the Cp-complex OsCl(η<sup>5</sup>-C<sub>5</sub>H<sub>5</sub>)(P<sup>i</sup>Pr<sub>3</sub>)<sub>2</sub> (405) can be displaced by molecular hydrogen to give OsH<sub>2</sub>Cl(η<sup>5</sup>-C<sub>5</sub>H<sub>5</sub>)(P<sup>i</sup>Pr<sub>3</sub>) (406), which is isolated as a

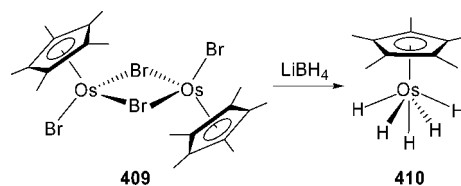
mixture of isomers *transoid*- and *cisoid*-dihydride. The reaction of the mixture with NaBH<sub>4</sub> and methanol leads to the neutral trihydride OsH<sub>3</sub>(η<sup>5</sup>-C<sub>5</sub>H<sub>5</sub>)(P<sup>i</sup>Pr<sub>3</sub>) (407). Although the *cisoid* hydride ligands of this compound are involved in a thermally activated site exchange process, in contrast to 400–402 and 404, they do not undergo quantum mechanical exchange coupling.<sup>275</sup> The addition of HBF<sub>4</sub>·OEt<sub>2</sub> to diethyl ether solutions of 407 produces the precipitation of the dihydride-elongated dihydrogen derivative [OsH<sub>2</sub>(η<sup>5</sup>-C<sub>5</sub>H<sub>5</sub>)(η<sup>2</sup>-H<sub>2</sub>)(P<sup>i</sup>Pr<sub>3</sub>)]BF<sub>4</sub> (408), for which a separation between the hydrogen atoms of the elongated dihydrogen ligand of about 1.1 Å has been calculated from the *J*<sub>H-D</sub> value (Scheme 53).<sup>276</sup>

Scheme 53. Cyclopentadienyl-Osmium Complexes



Girolami reported in 1994 the preparation of the osmium(III) dimer Os<sub>2</sub>Br<sub>4</sub>(η<sup>5</sup>-C<sub>5</sub>Me<sub>5</sub>)<sub>2</sub> (409) in high yield,<sup>277</sup> which has been the entry to an interesting osmium-polyhydride chemistry. This dimer reacts with LiBH<sub>4</sub> in tetrahydrofuran to give the osmium(VI) pentahydride OsH<sub>5</sub>(η<sup>5</sup>-C<sub>5</sub>Me<sub>5</sub>) (410) in 85% yield (Scheme 54).<sup>278</sup> Complex 410 adopts a pseudo-C<sub>4v</sub>

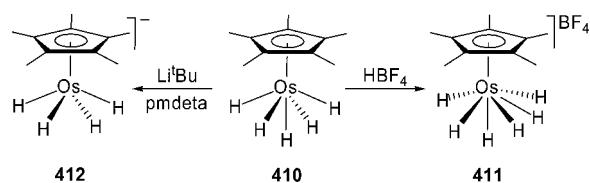
Scheme 54. Preparation of the Half-Sandwich Pentahydride 410



geometry with one axial and four equatorial hydride ligands.<sup>279</sup> A pseudo second-order Jahn–Teller distortion of this *pseudo*-octahedral geometry, where the equatorial hydride ligands bend away from the Cp\*<sup>\*</sup>-ring at a large angle, explains the diamagnetic nature of this *d*<sup>2</sup> species.<sup>280</sup>

Complex 410 reacts with strong Brønsted acids and bases (Scheme 55). The addition of HBF<sub>4</sub>·OEt<sub>2</sub> to diethyl ether solutions of the pentahydride leads to the hexahydride

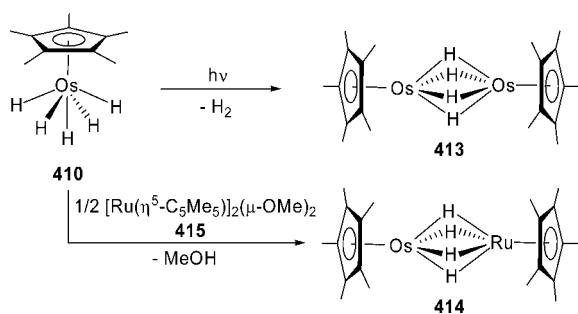
Scheme 55. Protonation and Deprotonation Reactions of 410



$[\text{OsH}_6(\eta^5\text{-C}_5\text{Me}_5)]\text{BF}_4$  (**411**). It is a classical polyhydride, which adopts a *pseudo*-pentagonal bipyramidal geometry with one axial and five equatorial hydride ligands. Treatment of **410** with *tert*-butyllithium in pentane in the presence of  $N,N,N',N'',N'''$ -pentamethyldiethylenediamine (pmdeta) produces its deprotonation and the formation of the salt  $[\text{Li}(\text{pmdeta})][\text{OsH}_4(\eta^5\text{-C}_5\text{Me}_5)]$  (**412**). The osmium(IV) tetrahydride anion adopts a four-legged piano-stool structure.<sup>281</sup>

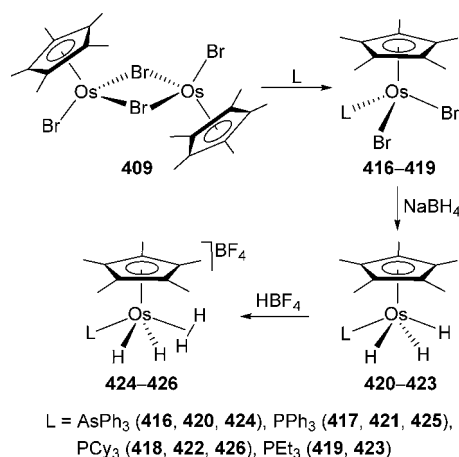
The pentahydride complex **410** loses molecular hydrogen under photolysis in benzene to give the tetrahydride dimer  $[\text{Os}(\eta^5\text{-C}_5\text{Me}_5)]_2(\mu\text{-H})_4$  (**413**).<sup>277,281</sup> The heterobimetallic osmium–ruthenium counterpart  $(\eta^5\text{-C}_5\text{Me}_5)\text{Os}(\mu\text{-H})_4\text{Ru}(\eta^5\text{-C}_5\text{Me}_5)$  (**414**) has been prepared by reaction of the ruthenium dimer  $[\text{Ru}(\eta^5\text{-C}_5\text{Me}_5)]_2(\mu\text{-OMe})_2$  (**415**) with **410** (Scheme 56).<sup>278</sup>

**Scheme 56.** Pentahydride **410** as Starting Material of Homo- and Heterometallic Compounds



Addition of Lewis bases to **409** in ethanol affords the mononuclear osmium(III) complexes  $\text{OsBr}_2(\eta^5\text{-C}_5\text{Me}_5)\text{L}$  ( $\text{L} = \text{AsPh}_3$  (**416**),  $\text{PPh}_3$  (**417**),  $\text{PCy}_3$  (**418**),  $\text{PET}_3$  (**419**)).<sup>282</sup> These paramagnetic compounds react with  $\text{NaBH}_4$  in ethanol to give the osmium(IV)-trihydrides  $\text{OsH}_3(\eta^5\text{-C}_5\text{Me}_5)\text{L}$  ( $\text{L} = \text{AsPh}_3$  (**420**),  $\text{PPh}_3$  (**421**),  $\text{PCy}_3$  (**422**),  $\text{PET}_3$  (**423**)), which are  $\text{Cp}^*$ -counterparts of **407**. Like the latter, these compounds show no evidence of quantum mechanical exchange coupling. Protonation of **420**–**422** with  $\text{HBF}_4\cdot\text{OEt}_2$  in diethyl ether leads to the precipitation of the respective dihydride-elongated dihydrogen derivatives  $[\text{OsH}_2(\eta^5\text{-C}_5\text{Me}_5)(\eta^2\text{-H}_2)\text{L}]\text{BF}_4$  ( $\text{L} = \text{AsPh}_3$  (**424**),  $\text{PPh}_3$  (**425**),  $\text{PCy}_3$  (**426**)), related to the  $\text{Cp}^*$ -compound **408** (Scheme 57).<sup>283,284</sup> These compounds have

**Scheme 57.** Preparation of  $\text{OsH}_3(\eta^5\text{-C}_5\text{Me}_5)\text{L}$  and  $[\text{OsH}_2(\eta^5\text{-C}_5\text{Me}_5)(\eta^2\text{-H}_2)\text{L}]^+$  Complexes

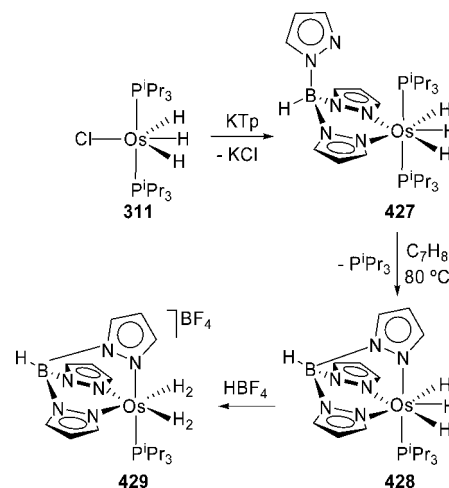


been characterized by single-crystal neutron diffraction. The coordination around the metal center can be described as four-legged piano-stool geometries in which the L ligand is transoid to the elongated dihydrogen ligand. For **424** and **425**, the coordinated hydrogen molecule is oriented with its H–H vector nearly parallel to the Os– $\text{Cp}^*$  direction, while in **426**, the elongated dihydrogen ligand is perpendicular. Not only the orientation of the elongated dihydrogen ligand but also the H–H bond length depends upon L. The H–H distance is 1.08(1) and 1.01(1) Å for **424** and **425**, respectively, but 1.31(3) Å for **426**.<sup>285</sup> In solution, the H–H distances determined from the corresponding  $T_1$  (min) and  $J_{\text{H-D}}$  values (1.15, 1.07, and 1.12 Å, respectively) are slightly shorter than in the solid state.<sup>283,284</sup>

### 3.4. Complexes with Tris(pyrazolyl)borate and Related Ligands

Tris(pyrazolyl)borate osmium complexes remain less explored than those of most *d*-block elements. As a consequence, polyhydride compounds with this type of ligands are scarce. The chloride-trihydride complex **311** reacts with  $\text{KTp}$ , in tetrahydrofuran, at room temperature to give  $\text{OsH}_3(\kappa^2\text{-Tp})(\text{P}^i\text{Pr}_3)_2$  (**427**). In toluene at 80 °C, this  $\kappa^2\text{-Tp}$  complex is transformed to the  $\kappa^3\text{-Tp}$  derivative  $\text{OsH}_3(\kappa^3\text{-Tp})(\text{P}^i\text{Pr}_3)$  (**428**), in quantitative yield after 7 h, as a result of the dissociation of one of the phosphines and the coordination of the free pyrazolyl group of **427** (Scheme 58). Protonation of

**Scheme 58.** Osmium-Tris(pyrazolyl)borate Complexes



**428** with  $\text{HBF}_4\cdot\text{OEt}_2$  in diethyl ether affords the bis-(dihydrogen) compound  $[\text{OsTp}(\eta^2\text{-H}_2)_2(\text{P}^i\text{Pr}_3)]\text{BF}_4$  (**429**).<sup>286</sup> In acetone, complex **429** releases the coordinated hydrogen molecules in a sequential manner. At room temperature, the dihydrogen solvate complex  $[\text{OsTp}(\eta^2\text{-H}_2)(\text{OCMe}_2)(\text{P}^i\text{Pr}_3)]\text{BF}_4$  (**430**) is formed, while at 56 °C the loss of both hydrogen molecules gives rise to the bis-solvento derivative  $[\text{OsTp}(\text{OCMe}_2)_2(\text{P}^i\text{Pr}_3)]\text{BF}_4$  (**431**). The bis-dihydrogen complex **429** reacts with ethylene under 2 atm to afford ethane and  $[\text{OsTp}(\text{CH}_2\text{CH}_2\text{P}^i\text{Pr}_3)(\eta^2\text{-CH}_2=\text{CH}_2)]\text{BF}_4$  (**432**), which promotes the C–H bond activation of fluorobenzene and 1,3-difluorobenzene by  $\sigma$ -bond metathesis.<sup>287</sup>

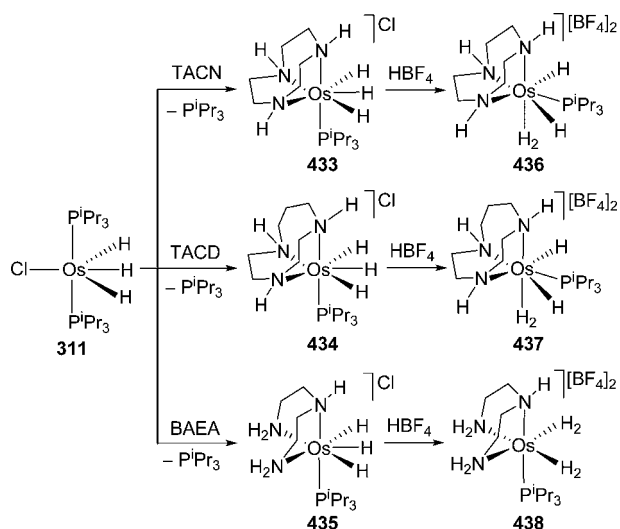
Complexes **427**–**429** have been characterized by X-ray diffraction analysis and DFT calculations. The geometry around the osmium atom of the trihydrides **427** and **428** can be rationalized as a distorted pentagonal bipyramid with the hydride ligands adopting a disposition of local  $\text{C}_{2v}$  symmetry,



separated by about 1.61 Å. The bis(dihydrogen) complex **429** adopts an octahedral geometry, where the coordinated hydrogen molecules are cis disposed with a H–H bond length of 0.906 Å. The comparison of these structures with those of their Cp-counterparts **407** and **408** reinforces the idea that Tp avoids the piano-stool structures and enforces dispositions allowing N–M–N angles close to 90°, which favor the nonclassical interactions.<sup>286</sup>

The chloride-trihydride complex **311** is also the entry to polyhydride compounds with cyclic and acyclic triamine ligands (Scheme 59). Treatment of toluene solution of **311** with

**Scheme 59.** Osmium Complexes with Cyclic and Acyclic Triamine Ligands



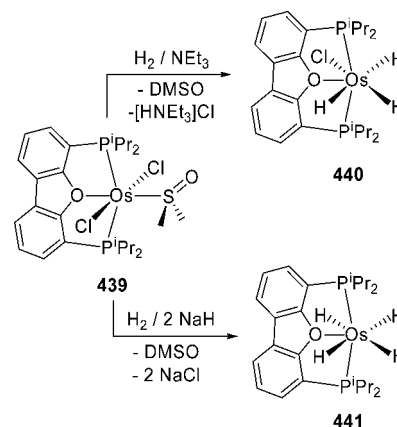
TACN, 1,4,7-triazacyclodecane (TACD), and bis(2-aminoethyl)amine (BAEA) at 60 °C affords the corresponding salts  $[\text{OsH}_3(\text{L}_3)(\text{P}^i\text{Pr}_3)]\text{Cl}$  ( $\text{L}_3 = \text{TACN}$  (**433**), TACD (**434**), BAEA (**435**)). Like their Tp-counterpart **428**, these compounds have structures that can be rationalized as pentagonal bipyramids with a nitrogen atom in the axial position and the other two lying in the equatorial plane along with the hydrides. The  $\text{N}_{\text{meridional}}-\text{Os}-\text{N}_{\text{meridional}}$  angle of the bipyramids determines the behavior of these species. As previously mentioned, the neutral Tp-complex **428**, with an angle of 83.17(12)°, reacts with  $\text{HBF}_4$  to give the monocationic bis(dihydrogen) **429**. However, the reactions of the TACN- and TACD-trihydrides **433** and **434**, which have angles close to 78°, with  $\text{HBF}_4$  lead to the dicationic dihydride-dihydrogen compounds  $[\text{OsH}_2(\eta^2-\text{H}_2)(\text{L}_3)(\text{P}^i\text{Pr}_3)][\text{BF}_4]_2$  ( $\text{L}_3 = \text{TACN}$  (**436**), TACD (**437**)), analogous to the Cp-complex **408**, but with a shorter H–H dihydrogen distance (0.87–1.03 Å). In contrast to the trihydrides containing cyclic triamines, the BAEA trihydride **435**, with an angle similar to that of the Tp-complex **428**, 82.5(3)°, reacts with  $\text{HBF}_4$  similarly to the latter to afford the dicationic bis(dihydrogen)  $[\text{Os}(\text{BAEA})(\eta^2-\text{H}_2)_2(\text{P}^i\text{Pr}_3)][\text{BF}_4]_2$  (**438**).<sup>288</sup>

The systematical comparison of the structural features of the  $\text{L}_3$ -complexes and those of the Tp- and Cp-counterparts suggests that the charge of the complexes has less influence on the interactions between the atoms of the  $\text{OsH}_n$  units than certain structural parameters.

### 3.5. Complexes with Pincer Ligands

Complex  $\text{OsCl}_2\{\text{dbf}(\text{P}^i\text{Pr}_2)_2\}(\kappa^1\text{-DMSO})$  (**439**,  $\text{dbf}(\text{P}^i\text{Pr}_2)_2 = 4,6\text{-bis}(\text{diisopropylphosphine})\text{dibenzofuran}$ ) reacts with molecular hydrogen in the presence of a Brønsted base. The products of the reaction depend upon the base (Scheme 60).

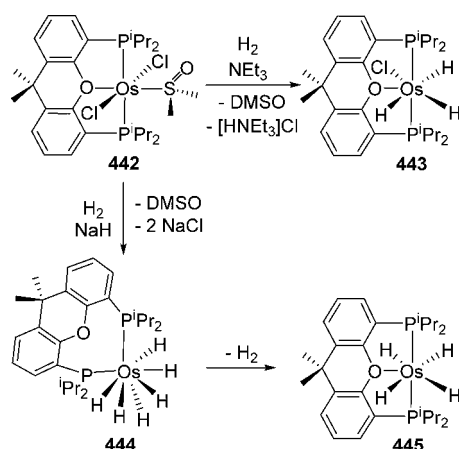
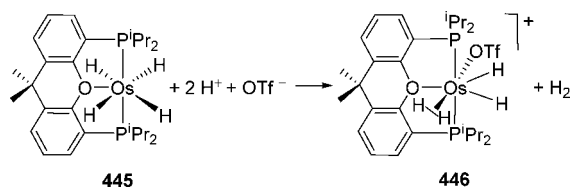
**Scheme 60.** Reactions of **439** with Molecular Hydrogen in the Presence of Bases



Triethylamine removes a chloride ligand. Thus, the reaction gives the trihydride  $\text{OsH}_3\text{Cl}\{\text{dbf}(\text{P}^i\text{Pr}_2)_2\}$  (**440**). On the other hand, NaH extracts both chloride ligands, to afford the tetrahydride  $\text{OsH}_4\{\text{dbf}(\text{P}^i\text{Pr}_2)_2\}$  (**441**). Both **440** and **441** have been characterized by X-ray diffraction analysis. The geometry around the osmium atom of **440** can be rationalized as a distorted pentagonal bipyramid, with the  $\text{P}^i\text{Pr}_2$  groups occupying axial positions and the chloride situated between the oxygen atom of the pincer and one of the hydrides. The structure of the tetrahydride **441** is as that of **440** with a hydride in the position of the chloride.<sup>289</sup>

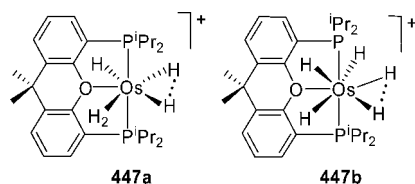
The behavior of the  $\text{xant}(\text{P}^i\text{Pr}_2)_2$ -counterpart,  $\text{OsCl}_2\{\text{xant}(\text{P}^i\text{Pr}_2)_2\}(\kappa^1\text{-DMSO})$  (**442**), is similar. In the presence of triethylamine, the reaction of **442** with molecular hydrogen leads to the trihydride  $\text{OsH}_3\text{Cl}\{\text{xant}(\text{P}^i\text{Pr}_2)_2\}$  (**443**), which has also been prepared by addition of the diphosphine to toluene solutions of **311**. Sodium hydride removes both chloride ligands, and furthermore, a hydrogen molecule displaces the oxygen atom of the diphosphine to give the hexahydride  $\text{OsH}_6\{\text{xant}(\text{P}^i\text{Pr}_2)_2\}$  (**444**), containing a  $\kappa^2$ -diphosphine. In methanol, under argon atmosphere, complex **444** slowly loses a hydrogen molecule, and the diphosphine coordinates the oxygen atom to the metal center to form the tetrahydride  $\text{OsH}_4\{\text{xant}(\text{P}^i\text{Pr}_2)_2\}$  (**445**), which can also be prepared by addition of  $\text{xant}(\text{P}^i\text{Pr}_2)_2$  to the hexahydride **364** (Scheme 61). Like in the latter, the geometry around the osmium center of **444** can be described as a distorted dodecahedron. However, in this case, the phosphorus atoms occupy a B-site at each trapezoidal plane.<sup>290</sup>

The tetrahydride **445** is a strong reductor, which is able to promote the reduction of  $\text{H}^+$  (Scheme 62), in spite of the high oxidation state of the metal center. Thus, the addition of 4 equiv of triflic acid to its dichloromethane solutions gives  $\text{H}_2$  and the dihydride-elongated dihydrogen cation  $[\text{OsH}_2(\text{OTf})(\eta^2-\text{H}_2)\{\text{xant}(\text{P}^i\text{Pr}_2)_2\}]^+$  (**446**). In agreement with the  $^1\text{H}$  NMR spectrum, the DFT-optimized structure of this species shows two groups of two equivalent hydrogen atoms, one of them in the P,H,H,P-trapezoidal plane and the other one in the

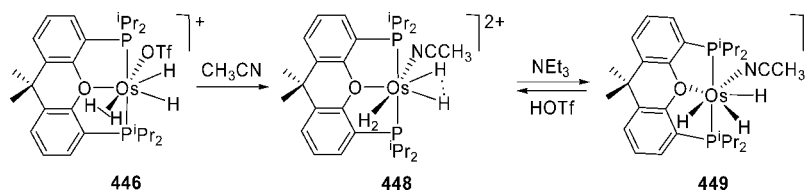
**Scheme 61. Neutral Compounds with the  $\text{xant}(\text{P}^i\text{Pr}_2)_2$  Ligand**

**Scheme 62. Reduction of  $\text{H}^+$  Promoted by 445**


O,H,H,O-trapezoidal plane. In the first plane, the hydrogen atoms are separated by 1.545 Å, whereas in the second one, the H–H distance is 1.250 Å.

The redox reaction occurs in two stages. Initially complex 445 adds a proton to afford  $[\text{OsH}_5\{\text{xant}(\text{P}^i\text{Pr}_2)_2\}]^+$  (447), which reacts with HOTf to give  $\text{H}_2$  and 446. DFT calculations reveal that 447 (Chart 11) has two tautomers very close in

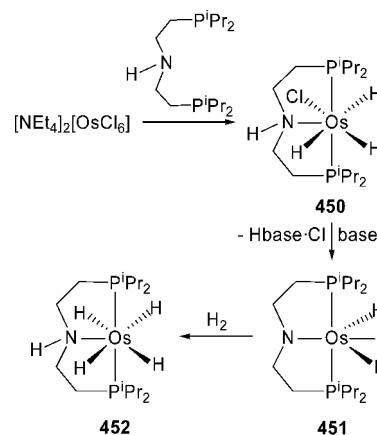
**Chart 11.  $[\text{OsH}_5\{\text{xant}(\text{P}^i\text{Pr}_2)_2\}]^+$  Species**


energy (<3 kcal mol<sup>-1</sup>): a hydride-compressed dihydride-dihydrogen (447a) and a trihydride-compressed dihydride (447b). In 447a, the dihydrogen ligand is disposed almost parallel to the P–Os–P direction with a H–H bond length of 0.87 Å, whereas the compressed dihydride (1.40 Å) lies in the perpendicular plane along with the oxygen atom of the diphosphine. In 447b, the disposition of the hydrogen atoms is the same as in 447a with the hydrogen atoms in the P,H,H,P plane separated by 1.762 Å.

**Scheme 63. Other POP-Osmium Complexes**


Acetonitrile displaces the coordinated trifluoromethanesulfonate anion of 446 to afford the dication compressed dihydride-dihydrogen  $[\text{OsH}_2(\eta^2\text{-H}_2)(\text{CH}_3\text{CN})\{\text{xant}(\text{P}^i\text{Pr}_2)_2\}]^{2+}$  (448). The dihydrogen ligand of this compound is situated in the perpendicular plane to the P–Os–P direction, with the hydrogen atoms separated by 0.898 Å, while the compressed dihydride lies in the trapezoidal plane containing the phosphorus atoms with the hydrogens separated by 1.475 Å. The treatment of 448 with NEt<sub>3</sub> causes its deprotonation and the formation of the trihydride  $[\text{OsH}_3(\text{CH}_3\text{CN})\{\text{xant}(\text{P}^i\text{Pr}_2)_2\}]^+$  (449). The reaction is reversible, the addition of HOTf to 449 regenerates 448 (Scheme 63).

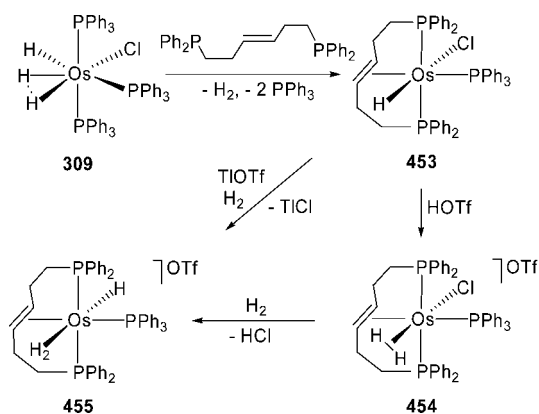
A small family of PNP complexes has been also reported. Ligand  $(^i\text{Pr}_2\text{PCH}_2\text{CH}_2)_2\text{NH}$  reacts with  $[\text{NEt}_4]_2[\text{OsCl}_6]$  in 2-propanol or 2-pentanol to give the trihydride  $\text{OsH}_3\text{Cl}\{(^i\text{Pr}_2\text{PCH}_2\text{CH}_2)_2\text{NH}\}$  (450). Upon reaction with strong bases, such as KO<sup>t</sup>Bu or  $\text{NaN}(\text{SiMe}_3)_2$ , complex 450 undergoes dehydrochlorination to give the 16-valence electrons *d*<sup>4</sup>-amido-trihydride  $\text{OsH}_3\{(^i\text{Pr}_2\text{PCH}_2\text{CH}_2)_2\text{N}\}$  (451). This diamagnetic ML<sub>6</sub> *d*<sup>4</sup>-complex has a structure similar to those of complexes  $\text{OsH}_3\text{X}(\text{PR}_3)_2$  (310–313 and 318–320) with the nitrogen atom at the X-site. Under hydrogen atmosphere, complex 451 gives the tetrahydride  $\text{OsH}_4\{(^i\text{Pr}_2\text{PCH}_2\text{CH}_2)_2\text{NH}\}$  (452), as a result of the addition of H<sub>2</sub> to the Os–N bond of 451 (Scheme 64).<sup>291</sup>

**Scheme 64. PNP-Osmium Complexes**


P(olefin)P-Pincer complexes have been reported by Lin, Lau, Jia, and co-workers. Treatment of the hydride-compressed dihydride 309 with (*E*)-Ph<sub>2</sub>P(CH<sub>2</sub>)<sub>2</sub>CH=CH(CH<sub>2</sub>)<sub>2</sub>PPh<sub>2</sub> leads to  $\text{OsHCl}(\text{PPh}_3)\{\text{Ph}_2\text{P}(\text{CH}_2)_2\text{CH}=\text{CH}(\text{CH}_2)_2\text{PPh}_2\}$  (453), which reacts with HOTf to give the elongated dihydrogen  $[\text{OsCl}(\eta^2\text{-H}_2)(\text{PPh}_3)\{\text{Ph}_2\text{P}(\text{CH}_2)_2\text{CH}=\text{CH}(\text{CH}_2)_2\text{PPh}_2\}]\text{OTf}$  (454; *d*<sub>H–H</sub> = 1.18 Å). Under molecular hydrogen atmosphere, the latter does not undergo the hydrogenation of the C–C double bond but a molecule of hydrogen chloride is removed to form the hydride-dihydrogen

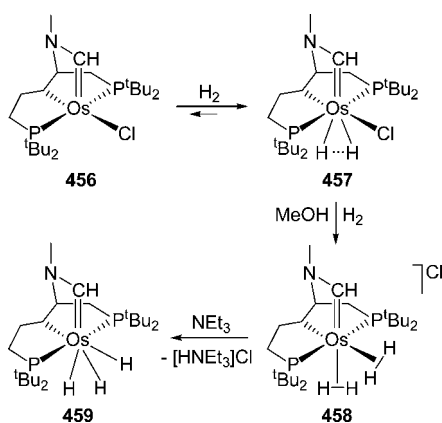
$[\text{OsH}(\eta^2\text{-H}_2)(\text{PPh}_3)\{\text{Ph}_2\text{P}(\text{CH}_2)_2\text{CH}=\text{CH}(\text{CH}_2)_2\text{PPh}_2\}]\text{OTf}$  (**455**;  $d_{\text{H}\cdots\text{H}} = 0.97 \text{ \AA}$ ), which can be directly prepared from **453**, by reaction with  $\text{TiOTf}$  under hydrogen atmosphere (Scheme 65). DFT calculations suggest that although the hydrogenation of the olefin of **454** is thermodynamically feasible, it is kinetically unfavorable.<sup>292</sup>

Scheme 65. P(olefin)P-Osmium Complexes



Gusev and co-workers have reported chiral polyhydride complexes stabilized by a  $\text{PC}(\text{sp}^3)\text{P}$ -pincer ligand with an additional Fisher-type carbene arm.<sup>293</sup> Reaction of  $[\text{OsCl}_6]^{2-}$  with the chiral ligand  $(S)\text{-}^t\text{Bu}_2\text{PCH}_2\text{CH}(\text{NMe}_2)(\text{CH}_2)_3\text{P}^t\text{Bu}_2$  affords the square-pyramidal 16-valence electrons carbene derivative  $\text{OsCl}(\text{PGP})$  (**456**,  $\text{PGP} = \kappa^4\text{-}^t\text{Bu}_2\text{PCH}_2\text{CH}\{\text{N}(\text{Me})\text{-CH}=\}\text{CH}(\text{CH}_2)_2\text{P}^t\text{Bu}_2$ ) in excellent yield. In toluene, at room temperature, under an atmosphere of hydrogen, complex **456** is in equilibrium with the chloride-compressed dihydride  $\text{OsH}_2\text{Cl}(\text{PGP})$  (**457**;  $d_{\text{H}\cdots\text{H}} = 1.40\text{--}1.43 \text{ \AA}$ ). This compound has a labile chloride ligand, which is rapidly and quantitatively displaced by  $\text{H}_2$  in methanol or in the presence of  $\text{NaBPh}_4$  in tetrahydrofuran to give the bis(elongated dihydrogen) complex  $[\text{Os}(\eta^2\text{-H}_2)_2(\text{PGP})]\text{BPh}_4$  (**458**), with two equal  $\text{H}\cdots\text{H}$  bonds of  $1.11 \text{ \AA}$ . Complex **458** can be deprotonated with  $\text{NEt}_3$  to give the trihydride  $\text{OsH}_3(\text{PGP})$  (**459**), according to Scheme 66.

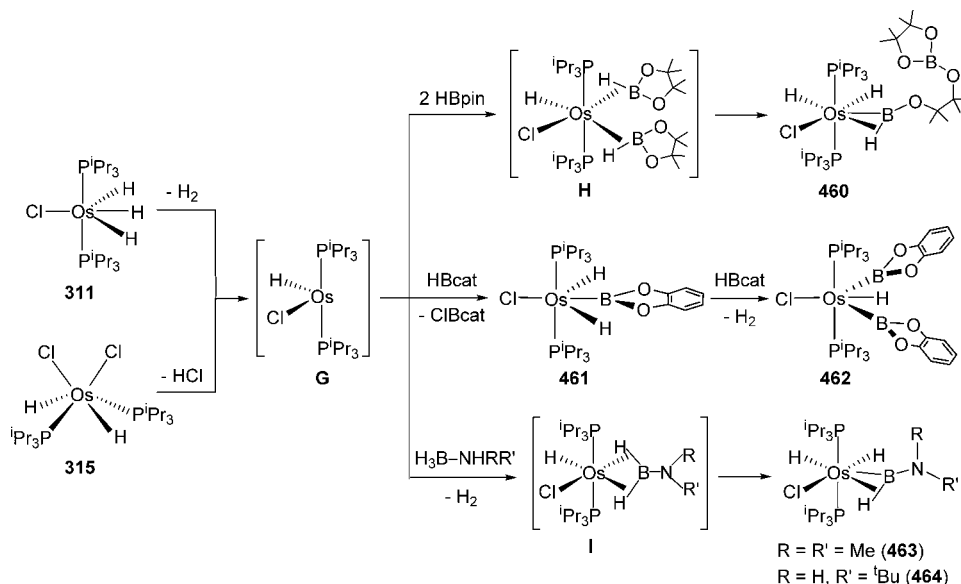
Scheme 66. Chiral Polyhydride Complexes Stabilized by a  $\text{PC}(\text{sp}^3)\text{P}$ -Pincer Ligand with an Additional Fisher-type Carbene Arm



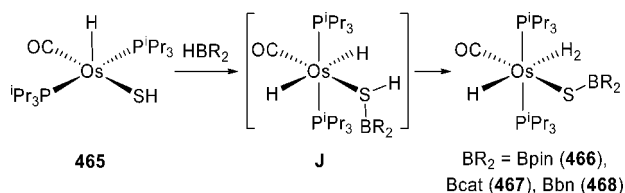
### 3.6. Osmium-Polyhydride Complexes Involved in $\sigma$ -Bond Activation Reactions

**3.6.1. B–H Bond Activation Reactions.** The previously mentioned behavior of the trihydride **311** is consistent with a marked tendency of this compound to release molecular hydrogen and to form the 14-valence electrons species  $\text{OsHCl}(\text{P}^i\text{Pr}_3)_2$  (**G**), which can also be generated from the dichloride-dihydride **315** by means of the elimination of  $\text{HCl}$ . This unsaturated species activates the B–H bond of boronic esters and amine-boranes to afford compounds with unusual bonding situations (Scheme 67). The reaction of **G** with  $\text{HBpin}$  leads to the borinium derivative  $\text{OsH}_2\text{Cl}(\eta^2\text{-HBOCMe}_2\text{CMe}_2\text{OBpin})(\text{P}^i\text{Pr}_3)_2$  (**460**).<sup>294</sup> This compound is formed via the intermediate bis( $\sigma$ -borane)  $\text{OsHCl}(\eta^2\text{-HBpin})_2(\text{P}^i\text{Pr}_3)_2$  (**H**), resulting from the coordination of two molecules of  $\text{HBpin}$  to **G**. Once coordinated, the heterolytic B–H activation of one of them, using an oxygen atom of the other one as an external base, gives **460**. In contrast to  $\text{HBpin}$ , the H–B bond of  $\text{HBcat}$  undergoes homolytic cleavage to initially afford the dihydride-boryl intermediate  $\text{OsH}_2\text{Cl}(\text{Bcat})(\text{P}^i\text{Pr}_3)_2$  (**461**), which gives the hydride-bis(boryl) derivative  $\text{OsHCl}(\text{Bcat})_2(\text{P}^i\text{Pr}_3)_2$  (**462**) and  $\text{H}_2$  by reaction with an additional molecule of  $\text{HBcat}$ . As expected for a  $\text{ML}_6 d^4$ -species, complex **462** experiences a strong distortion from the octahedral geometry, adopting a similar structure to **311** where the boryl groups occupy two equivalent sites at the perpendicular plane to the P–Os–P direction.<sup>295</sup> Amine-boranes undergo dehydrogenation in the presence of **G** to form aminoboranes. The hydride transfer from the aminoboranes to **G** yields the corresponding aminoborinium complexes  $\text{OsH}_2\text{Cl}(\eta^2\text{-HBNRR}')(\text{P}^i\text{Pr}_3)_2$  ( $\text{NRR}' = \text{NMe}_2$  (**463**),  $\text{NH}^t\text{Bu}$  (**464**)) via bis( $\sigma$ -B–H) intermediates  $\text{OsHCl}(\eta^2, \eta^2\text{-H}_2\text{BNRR}')(\text{P}^i\text{Pr}_3)_2$  (**I**).<sup>294</sup> DFT calculations suggest that the major contribution to the interaction between the metal fragment and this type of ligands is electrostatic (57%). This indicates a high degree of polarization for the osmium–boronium bond, which agrees well with the high electronegativity of the osmium atom and suggests a significant positive partial charge on the ligand. Although **463** has been described as an  $\alpha$ -agostic boryl species,<sup>177</sup> the high degree of polarization for the Os–B bond in these compounds and the calculated hybridization at the boron atom ( $\text{sp}^{1.3\text{--}1.6}$ ) is fully consistent with the boronium denomination. The orbital term of the interaction is the result of three contributions: two  $\sigma$ -interactions and a  $\pi$ -interaction. The most important  $\sigma$ -interaction involves to the boron atom and the metal center. The other one takes place between the doubly occupied  $\sigma(\text{B–H})$  bond molecular orbital and the metal fragment.<sup>296</sup>

Cooperative heterolysis of the B–H bond can be performed with a soft base coordinated to an electrophilic osmium center. When the complex also contains a hydride ligand, in addition to the B–H heterolysis, the heterolytic H–H formation is also feasible (Scheme 68). The five-coordinate hydride-hydrogensulfide complex  $\text{OsH}(\text{SH})(\text{CO})(\text{P}^i\text{Pr}_3)_2$  (**465**) reacts with  $\text{HBpin}$ ,  $\text{HBcat}$ , and  $(\text{HBbn})_2$  to give the hydride-dihydrogen-borylthiolate compounds  $\text{OsH}(\text{SBR}_2)(\eta^2\text{-H}_2)(\text{CO})(\text{P}^i\text{Pr}_3)_2$  ( $\text{BR}_2 = \text{Bpin}$  (**466**),  $\text{Bcat}$  (**467**),  $\text{Bbn}$  (**468**)) as a result of the B–H heterolysis and a proton transfer from the sulfur atom to the metal center. DFT calculations suggest that the rupture of the B–H bond initially affords the *trans*-dihydride intermediates  $\text{OsH}_2(\text{SHBR}_2)(\text{CO})(\text{P}^i\text{Pr}_3)_2$  (**J**), which evolve into **466–468** through a  $\eta^2\text{-H–SBR}_2$  transition state. On the basis of  $T_1(\text{min})$  and  $J_{\text{H–D}}$  values, a separation between the

Scheme 67. B–H Bond Activation Reactions Promoted by the 14-Valence Electrons Species  $\text{OsHCl}(\text{P}^i\text{Pr}_3)_2$ 

Scheme 68. B–H Heterolysis and Heterolytic H–H Formation



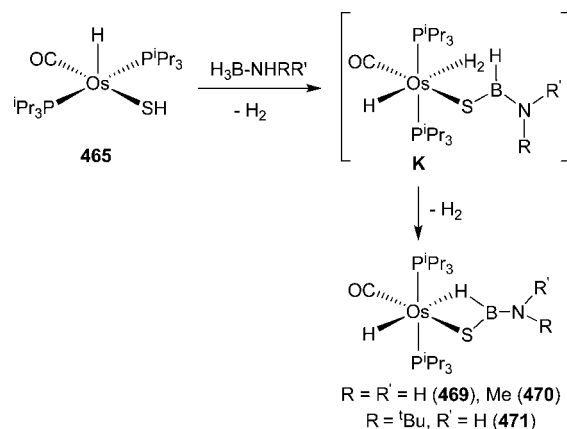
hydrogen atoms of the dihydrogen ligand of about 0.9 Å has been calculated for these compounds.<sup>297</sup>

Amine-boranes undergo catalytic dehydrogenation in the presence of the hydride-hydrogensulfide complex **465**. At low concentrations of substrate, the hydrogensulfide ligand captures the resulting aminoborane monomers, before their coupling, to initially form the hydride-dihydrogen species  $\text{OsH}(\text{SBHNRR}')(\eta^2\text{-H}_2)(\text{CO})(\text{P}^i\text{Pr}_3)_2$  (**K**), analogous to **466–468**, which release  $\text{H}_2$  to give the hydrogenaminothioborate derivatives  $\text{OsH}\{\kappa^2\text{-H}_2\text{S}[\text{HB}(\text{S})(\text{NRR}')]\}(\text{CO})(\text{P}^i\text{Pr}_3)_2$  ( $\text{NRR}' = \text{NH}_2$  (**469**),  $\text{NMe}_2$  (**470**),  $\text{NH}^t\text{Bu}$  (**471**)), according to Scheme 69.<sup>298</sup>

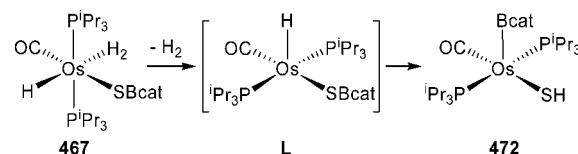
Complex **466** is stable enough to be characterized by X-ray diffraction analysis. However, the Bcat-counterpart **467** has a marked tendency to lose molecular hydrogen. The resulting hydride-borylthiolate intermediate  $\text{OsH}(\text{SBcat})(\text{CO})(\text{P}^i\text{Pr}_3)_2$  (**L**) undergoes a fast intramolecular hydride-boryl exchange process (Scheme 70). As a consequence, complex **467** rapidly evolves into the boryl-hydrogensulfide  $\text{Os}(\text{Bcat})(\text{SH})(\text{CO})(\text{P}^i\text{Pr}_3)_2$  (**472**) in toluene.<sup>297</sup> The formation of **467** via intermediate **J** and its transformation into **472** demonstrate that the hydrogensulfide group of **465** is a cooperating ligand in the heterolytic activation of the H–B bond of **HBcat** to give  $\text{H}_2$  and **472**.

The hydride-dihydrogen-borylthiolate complex **466** exchanges borylthiol by **HBpin**. The exchange process leads to the dihydride-( $\sigma$ -borane) derivative  $\text{OsH}_2(\eta^2\text{-HBpin})(\text{CO})(\text{P}^i\text{Pr}_3)_2$  (**473**). This compound and the **HBcat**-counterpart  $\text{OsH}_2(\eta^2\text{-HBcat})(\text{CO})(\text{P}^i\text{Pr}_3)_2$  (**474**) are properly prepared by coordination of the boranes to the unsaturated dihydride **300**,

Scheme 69. Amine-Borane Dehydrogenation and Capture of the Resulting Aminoborane Monomers

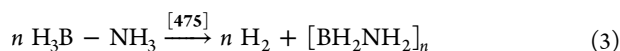
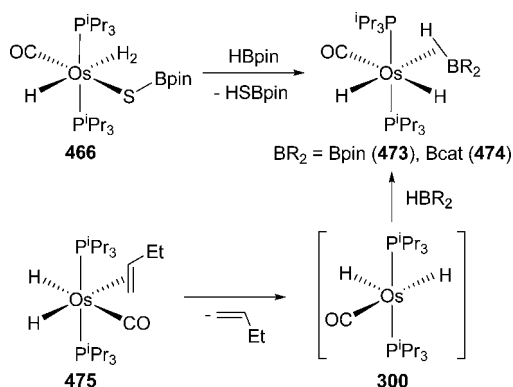


Scheme 70. Intramolecular Hydride-Boryl Exchange



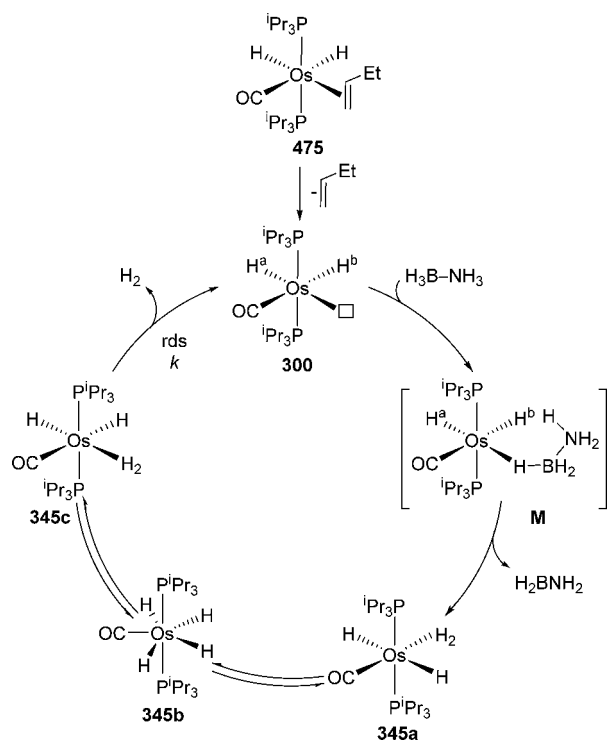
which can be generated in situ by means of the olefin dissociation from  $\text{OsH}_2(\eta^2\text{-CH}_2=\text{CHEt})(\text{CO})(\text{P}^i\text{Pr}_3)_2$  (**475** in Scheme 71). The hydrogen atoms bonded to the metal center of **473** and **474** undergo two thermally activated site-exchange processes, involving the hydride positions and that of the B–H site. The hydride–hydride site exchange, which needs an activation energy lower than the hydride-BH site exchange, appears to take place via dihydrogen species, whereas the hydride-BH site exchange seems to proceed through trihydride-boryl intermediates.<sup>299</sup>

Dihydride **300**, generated from **475** by dissociation of the olefin, promotes the release of 1 equiv of  $\text{H}_2$  from ammonia-borane and the formation of polyaminoborane (eq 3) with a catalytic rate law given by eq 4.

Scheme 71. Dihydride-( $\sigma$ -borane)-Osmium Complexes

$$d[\text{H}_2]/dt = k[475] \quad (4)$$

Scheme 72 summarizes the mechanism proposed for this process, which is strongly supported by kinetic results,

Scheme 72. Catalytic Cycle for the Dehydrogenation of Ammonia-Borane Catalyzed by 300<sup>a</sup>

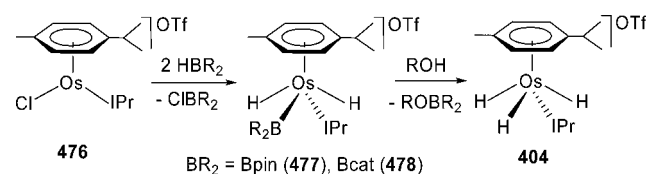
<sup>a</sup>Adapted from ref 300. Copyright 2015 American Chemical Society.

spectroscopic observations performed on the catalytic solution, and DFT calculations.<sup>300</sup> The coordination of ammonia-borane to the *cis*-dihydride 300, in a Shimoï manner, gives the intermediate OsH<sub>2</sub>(κ<sup>1</sup>-H<sub>3</sub>BNH<sub>3</sub>)(CO)(P<sup>i</sup>Pr<sub>3</sub>)<sub>2</sub> (**M**). This intermediate releases BH<sub>2</sub>NH<sub>2</sub>, which undergoes off-metal polymerization, after transferring the coordinated HB-hydrogen to the metal center and a NH-hydrogen to the hydride H<sup>b</sup>, through a concerted process. The transition state can be described as a η<sup>1</sup>-H<sup>b</sup>-H<sup>N</sup> species, where the asymmetric dihydrogen (H<sup>b</sup>-H<sup>N</sup> = 0.865 Å) is stabilized by interaction with the NH<sub>2</sub> group of the

boron ligand. The hydrogen transfer from ammonia-borane leads to the *trans*-dihydride-dihydrogen derivative 345a, which isomerizes via the tetrahydride 345b into the *cis*-dihydride isomer 345c. This transformation is barrierless. The coplanar *cis*-disposition of the dihydrogen ligand with regard to both hydrides in 345a and the protic nature of one of the hydrogen atoms of the dihydrogen ligand could also facilitate the isomerization without the participation of the tetrahydride 345b. The dissociation of H<sub>2</sub> from 345c regenerates 300.

The half-sandwich complex [OsCl(η<sup>6</sup>-*p*-cymene)(IPr)]OTf (476) also promotes the B-H bond activation of HBpin and HBCat. Treatment of this five-coordinate compound with the boranes leads to the dihydride-boryl derivatives [OsH<sub>2</sub>(BR<sub>2</sub>)(η<sup>6</sup>-*p*-cymene)(IPr)]OTf (BR<sub>2</sub> = Bpin (477), Bcat (478)) and ClBR<sub>2</sub>. In the presence of OH groups, these compounds undergo hydrolysis or alcoholysis to afford the trihydride complex 404 (Scheme 73).<sup>301</sup>

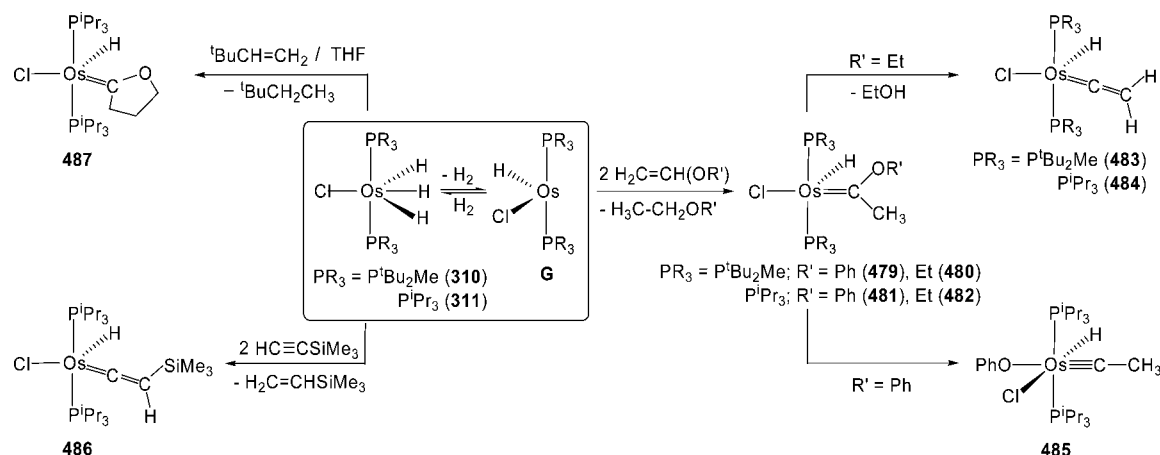
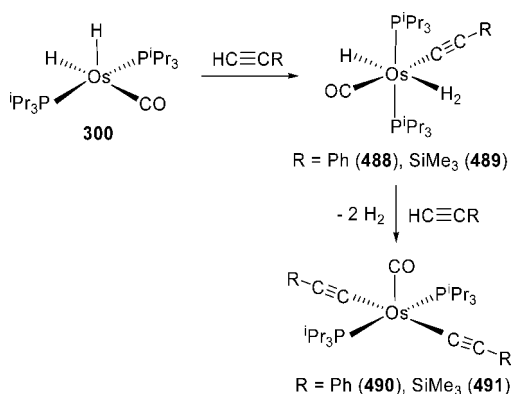
Scheme 73. Alcoholysis of Half-Sandwich Dihydride-Boryl-Osmium(IV) Complexes



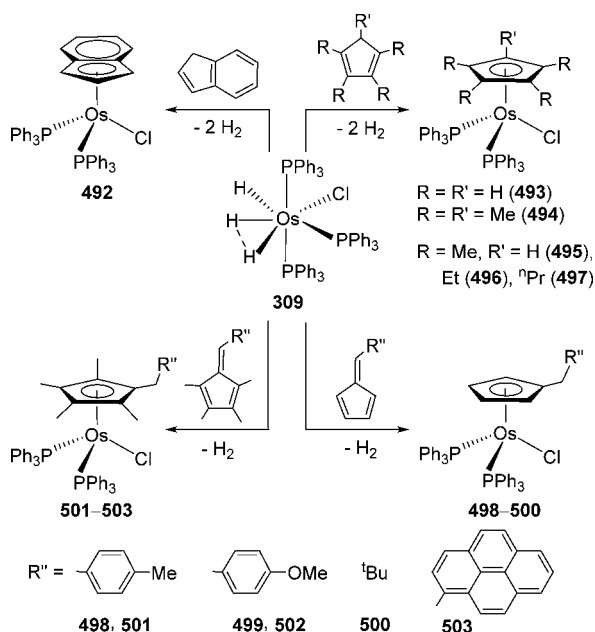
**3.6.2. Direct C-H Bond Activation.** Unsaturated G type species are also determinant in direct C-H bond activation processes promoted by trihydrides 310 and 311 (Scheme 74). For instance, these compounds react with vinyl ethers to initially form the five-coordinate hydride-carbene derivatives OsHCl{=C(OR')CH<sub>3</sub>}(PR<sub>3</sub>)<sub>2</sub> (PR<sub>3</sub> = P<sup>i</sup>Bu<sub>2</sub>Me, R' = Ph (479), Et (480); PR<sub>3</sub> = P<sup>i</sup>Pr<sub>3</sub>, R' = Ph (481), Et (482)), as a result of G-assisted olefin-carbene isomerization processes. Complexes 479–482 are unstable, even at room temperature, and evolve into the five-coordinate hydride-vinylidene or six-coordinate hydride-alkylidyne species depending upon the phosphine and OR'-substituent attached to the carbene carbon atom. Complexes 480 and 482 give ethanol and the vinylidenes OsHCl(=C=CH<sub>2</sub>)(PR<sub>3</sub>)<sub>2</sub> (PR<sub>3</sub> = P<sup>i</sup>Bu<sub>2</sub>Me (483), P<sup>i</sup>Pr<sub>3</sub> (484)), whereas complex 481 affords OsHCl(OPh)(=CCH<sub>3</sub>)(P<sup>i</sup>Pr<sub>3</sub>)<sub>2</sub> (485).<sup>302</sup> The substituted vinylidene OsHCl(=C=CHSiMe<sub>3</sub>)(P<sup>i</sup>Pr<sub>3</sub>)<sub>2</sub> (486) and CH<sub>2</sub>=CHSiMe<sub>3</sub> have been obtained by reaction of 311 and 2 equiv of the alkyne.<sup>86,88</sup> The 14-valence electrons fragment G (PR<sub>3</sub> = P<sup>i</sup>Pr<sub>3</sub>) also promotes the double dehydrogenation of the α-CH<sub>2</sub> of tetrahydrofuran to give OsHCl{=C(CH<sub>2</sub>)<sub>3</sub>O}(P<sup>i</sup>Pr<sub>3</sub>)<sub>2</sub> (487).<sup>303</sup>

In contrast to G, the five-coordinate dihydride 300, generated by dissociation of H<sub>2</sub> from the dihydride-dihydrogen 345, reacts with terminal alkynes to give the alkynyl-hydride-dihydrogen derivatives OsH(C≡CR)(η<sup>2</sup>-H<sub>2</sub>)(CO)(P<sup>i</sup>Pr<sub>3</sub>)<sub>2</sub> (R = Ph (488), SiMe<sub>3</sub> (489)).<sup>304</sup> The reactions of these compounds with a second molecule of alkyne leads to the bis(alkynyl)derivatives Os(C≡CR)<sub>2</sub>(CO)(P<sup>i</sup>Pr<sub>3</sub>)<sub>2</sub> (R = Ph (490), SiMe<sub>3</sub> (491)) and H<sub>2</sub> (Scheme 75).<sup>305</sup>

Jia and co-workers have developed two methodologies for the preparation of half-sandwich osmium complexes by using a PPh<sub>3</sub>-functionally equivalent to G (Scheme 76). The first approach involves the reactions of hydride-compressed dihydride 309 with indene and cyclopentadienes. Thus, the

Scheme 74. Direct C–H Bond Activation Reactions Promoted by 14-Valence Electrons OsHCl(PR<sub>3</sub>)<sub>2</sub> SpeciesScheme 75. Addition of Terminal Alkynes to **300**

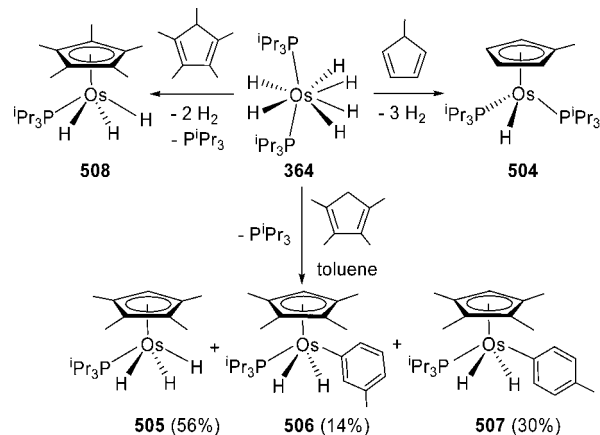
Scheme 76. Formation of Half-Sandwich Complexes by C–H Bond Activation and Insertion Reactions



treatment of **309** with this type of cyclic olefins leads to Os( $\eta^5$ -C<sub>9</sub>H<sub>7</sub>)Cl(PPh<sub>3</sub>)<sub>2</sub> (**492**), Os( $\eta^5$ -C<sub>5</sub>R<sub>5</sub>)Cl(PPh<sub>3</sub>)<sub>2</sub> (R = H (**493**), Me (**494**)), and Os( $\eta^5$ -C<sub>5</sub>Me<sub>4</sub>R')Cl(PPh<sub>3</sub>)<sub>2</sub> (R' = H (**495**), Et (**496**), <sup>n</sup>Pr (**497**)), depending upon the substrate, as a

consequence of the C(sp<sup>3</sup>)–H bond activation of the olefin and the release of two hydrogen molecules. The second approach involves the use of fulvenes. The reactions of **309** with C<sub>6</sub>-substituted fulvenes lead to Os( $\eta^5$ -C<sub>5</sub>H<sub>4</sub>CH<sub>2</sub>R'')Cl-(PPh<sub>3</sub>)<sub>2</sub> (R'' = C<sub>6</sub>H<sub>4</sub>-*p*-Me (**498**), C<sub>6</sub>H<sub>4</sub>-*p*-OMe (**499**), <sup>t</sup>Bu (**500**)) and a hydrogen molecule, whereas C<sub>6</sub>-substituted-1,2,3,4-tetramethylfulvenes give Os( $\eta^5$ -C<sub>5</sub>Me<sub>4</sub>CH<sub>2</sub>R'')Cl-(PPh<sub>3</sub>)<sub>2</sub> (R'' = C<sub>6</sub>H<sub>4</sub>-*p*-Me (**501**), C<sub>6</sub>H<sub>4</sub>-*p*-OMe (**502**), pyrenyl (**503**)) under the same conditions. The formation of **498–503** is the result of the Markovnikov insertion of the exocyclic carbon–carbon double bond of the fulvenes into the Os–H bond of **G** (PR<sub>3</sub> = PPh<sub>3</sub>).<sup>306</sup>

The hexahydride **364** is also a useful starting material to prepare half-sandwich complexes by means of C–H bond activation of cyclopentadienes, in this case hydride derivatives. The product of the reaction depends upon the substituents of the diolefin (Scheme 77). The reaction of **364** with

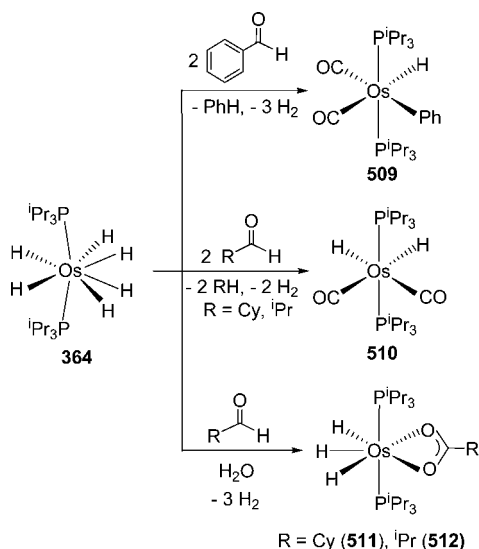
Scheme 77. C–H Bond Activation Reactions of Cyclopentadienes and Toluene Promoted by **364**

methylcyclopentadiene leads to the monohydride OsH( $\eta^5$ -C<sub>5</sub>H<sub>4</sub>Me)(P<sup>i</sup>Pr<sub>3</sub>)<sub>2</sub> (**504**). Treatment of toluene solutions of **364** with tetramethylcyclopentadiene gives a mixture of the trihydride OsH<sub>3</sub>( $\eta^5$ -C<sub>5</sub>HMe<sub>4</sub>)(P<sup>i</sup>Pr<sub>3</sub>) (**505**, 56%) and the dihydride-tolyl derivatives OsH<sub>2</sub>(*m*-tolyl)( $\eta^5$ -C<sub>5</sub>H<sub>4</sub>Me)(P<sup>i</sup>Pr<sub>3</sub>) (**506**; 14%) and OsH<sub>2</sub>(*p*-tolyl)( $\eta^5$ -C<sub>5</sub>HMe<sub>4</sub>)(P<sup>i</sup>Pr<sub>3</sub>) (**507**, 30%). However, in *n*-octane the trihydride **505** is formed in 85% yield. In contrast to tetramethylcyclopentadiene, pentam-

ethylcyclopentadiene reacts with **364** in toluene to give selectively the trihydride  $\text{OsH}_3(\eta^5\text{-C}_5\text{Me}_5)(\text{P}^i\text{Pr}_3)$  (**508**),<sup>240</sup> the  $\text{P}^i\text{Pr}_3$  counterpart of the Girolami's complexes **420–423**.

The hexahydride **364** also activates the OC–H bond of aldehydes (Scheme 78). In toluene under reflux, the reactions

**Scheme 78. C–H Bond Activation Reactions of Aldehydes Promoted by 364**

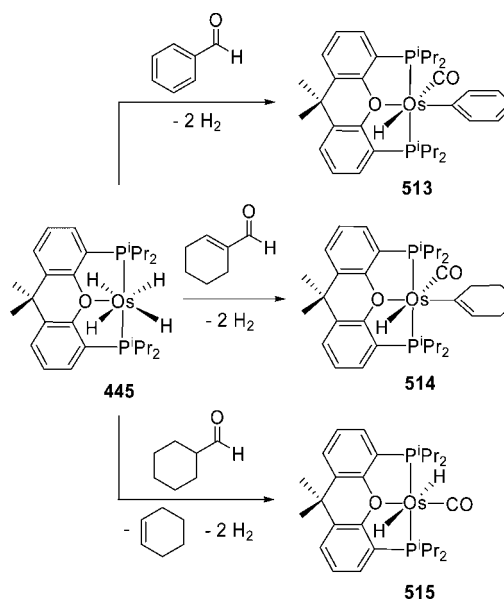


with benzaldehyde, cyclohexanecarboxaldehyde, and isobutyraldehyde lead to products resulting from OC–H bond activation and decarbonylation tandem processes. The reaction with benzaldehyde gives the hydride-phenyl-*cis*-dicarbonyl derivative  $\text{OsH}(\text{Ph})(\text{CO})_2(\text{P}^i\text{Pr}_3)_2$  (**509**) and benzene, while cyclohexanecarboxaldehyde and isobutyraldehyde yield the *cis*-dihydride-*cis*-dicarbonyl compound  $\text{OsH}_2(\text{CO})_2(\text{P}^i\text{Pr}_3)_2$  (**510**) and the corresponding alkane. In the presence of water, the reactions of **364** with cyclohexanecarboxaldehyde and isobutyraldehyde afford the carboxylate-trihydride  $\text{OsH}_3(\kappa^2\text{-O}_2\text{CR})(\text{P}^i\text{Pr}_3)_2$  ( $\text{R} = \text{Cy}$  (**511**),  $\text{R} = \text{iPr}$  (**512**)). Complexes **364**, **510**, and **511** are active catalyst precursors for classical Tishchenko dimerization of cyclohexanecarboxaldehyde. Complexes **364** and **510** are also active catalyst precursors for the classical Tishchenko dimerization of benzaldehyde and for the homo aldo-Tishchenko trimerization of isobutyraldehyde.<sup>307</sup>

The tetrahydride pincer-complex **445** also activates the OC–H bond of aldehydes. The reaction with benzaldehyde yields  $\text{OsH}(\text{Ph})(\text{CO})\{\text{xant}(\text{P}^i\text{Pr}_2)_2\}$  (**513**), a  $\text{xant}(\text{P}^i\text{Pr}_2)_2$ -counterpart of **509**. The decarbonylation of the substrate is also observed with  $\alpha,\beta$ -unsaturated aldehydes. Thus, the reaction of **445** with 1-cyclohexene-1-carboxaldehyde gives  $\text{OsH}(\text{C}_6\text{H}_9)(\text{CO})\{\text{xant}(\text{P}^i\text{Pr}_2)_2\}$  (**514**), although in this case the OC–H activation-deinsertion product is contaminated with the dihydride-carbonyl derivative  $\text{OsH}_2(\text{CO})\{\text{xant}(\text{P}^i\text{Pr}_2)_2\}$  (**515**), which is generated as a consequence of the release of 1,3-cyclohexadiene from **514**. The dehydrogenation of the substituent of the aldehyde is favored for alkyl with regard to alkenyl. Thus, complex **515** is obtained as a pure organometallic species, along with cyclohexene, from the reaction of **445** with cyclohexanecarboxaldehyde (Scheme 79).<sup>196</sup>

The hexahydride **364** reacts with pyridine, 3-methylpyridine, and 4-methylpyridine to give the classical tetrahydride derivatives  $\text{OsH}_4(\text{R-py})(\text{P}^i\text{Pr}_3)_2$  ( $\text{R-py} = \text{py}$  (**516**), 3-Mepy (**517**), 4-Mepy (**518**)). In benzene- $d_6$ , these compounds release

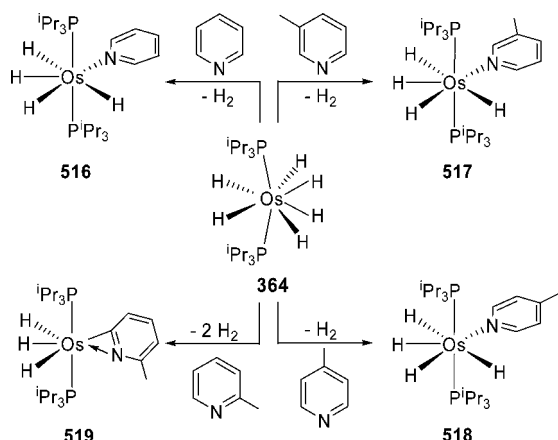
**Scheme 79. C–H Bond Activation Reactions of Aldehydes Promoted by the POP-Pincer Tetrahydride 445**



the heterocycle, and the resulting  $\text{OsH}_4(\text{P}^i\text{Pr}_3)_2$  species catalyzes the deuteration of the heterocycles by means of H/D exchanges with the solvent. The deuteration rates of the pyridinic C–H bonds depend upon their positions in the substrates. For pyridine, they increase as the C–H bonds are separated from the heteroatom. A methyl substituent has a marked negative effect on the deuteration of its adjacent C–H bonds. The kinetic analysis of the deuteration reveals that the rate-determining step for the H/D exchange is the C–H bond activation of the bond that is deuterated. DFT calculations show that this step is formed by two elemental stages: the direct coordination of the C–H bond and its subsequent rupture. Thus, the relationship between the deuteration rates of the different positions is determined by the relative stability of the  $\eta^2\text{-C-H}$  intermediates and the activation energies for the rupture of the coordinated C–H bonds. For pyridine, the stability of the  $\eta^2\text{-C-H}$  intermediates increases in the sequence positions 2,6 < position 4 < positions 3,5, while the necessary energy for the rupture of the C–H bond diminishes in the sequence positions 3,5 > positions 2,6 > position 4.<sup>308</sup> The behavior of 2-methylpyridine is significantly different to that of 3- and 4-methylpyridine (Scheme 80). The reaction of **364** with 2-methylpyridine, in contrast to 3- and 4-methylpyridine, leads to the  $\kappa^2\text{-C,N}$ -pyridyl derivative  $\text{OsH}_3\{\kappa^2\text{-C,N}(\text{NC}_5\text{H}_3\text{Me})\}(\text{P}^i\text{Pr}_3)_2$  (**519**), as a result of the activation of the C–H bond at position 6. In dichloromethane, complex **519** undergoes the selective chlorination of the hydride ligand *cisoid* disposed to the nitrogen atom to give  $\text{OsH}_2\text{Cl}\{\kappa^2\text{-C,N}(\text{NC}_5\text{H}_3\text{Me})\}(\text{P}^i\text{Pr}_3)_2$  (**520**).<sup>309</sup>

**3.6.3. Chelate-Assisted C–H Bond Activation.** The bis(phosphine)-hexahydride complex **364** as well as the half-sandwich dihydride-elongated dihydrogen derivative **408** and the tetrahydride pincer compound **445** promote the activation of  $\text{C}(\text{sp}^3)\text{-H}$  and olefinic- and aromatic- $\text{C}(\text{sp}^2)\text{-H}$  bonds of a wide range of organic molecules. The presence of a coordinating group (imine, ketone, phosphine, or *N*-heterocycle) in the substrates has allowed the stabilization of different types of hydride and polyhydride compounds, including interesting organometallic compounds, which in some cases

Scheme 80. Reactions of 364 with Pyridine and Substituted Pyridines

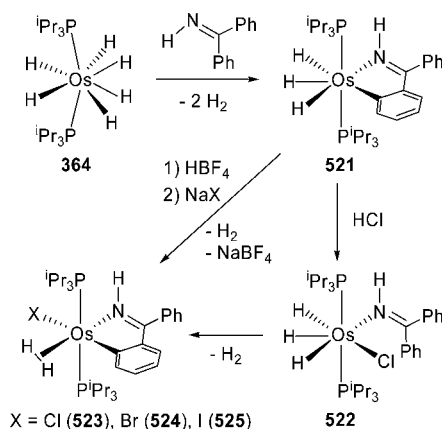


are reminiscent species of proposed intermediates of catalytic reactions relevant in organic synthesis.

The hexahydride **364** reacts with benzophenone imine to give the trihydride derivative  $\text{OsH}_3\{\kappa^2\text{-N,C-}[\text{NH}=\text{C}(\text{Ph})\text{-C}_6\text{H}_4]\}(\text{P}^i\text{Pr}_3)_2$  (**521**). The hydride ligands and the bidentate group are situated in the equatorial plane of a pentagonal-bipyramidal arrangement of ligands around the metallic center. In solution, the hydride ligands undergo two thermally activated site-exchange processes, with different activation energies. The slower process involves the hydride ligand *transoid* to the N atom and the central hydride, whereas the faster one takes place between the latter and the hydride *transoid* to the aryl ring. DFT calculations suggest that the exchanges occur via dihydrogen species, being the relative energy between them the determining factor for the difference in rates, since once the dihydrogen structure has been reached, the energies associated with their rotations are similar. Treatment of **521** with a toluene solution of HCl leads to  $\text{OsH}_3\text{Cl}(\text{NH}=\text{CPh}_2)(\text{P}^i\text{Pr}_3)_2$  (**522**), which evolves into the elongated dihydrogen ( $d_{\text{H-H}} = 1.31 \text{ \AA}$ )  $\text{OsCl}\{\kappa^2\text{-N,C-}[\text{NH}=\text{C}(\text{Ph})\text{C}_6\text{H}_4]\}(\eta^2\text{-H}_2)(\text{P}^i\text{Pr}_3)_2$  (**523**), in methanol, as a result of the release of molecular hydrogen. This compound and the related derivatives  $\text{OsX}\{\kappa^2\text{-N,C-}[\text{NH}=\text{C}(\text{Ph})\text{C}_6\text{H}_4]\}(\eta^2\text{-H}_2)(\text{P}^i\text{Pr}_3)_2$  ( $\text{X} = \text{Br}$  (**524**),  $\text{I}$  (**525**)) can also be prepared by protonation of **521** with  $\text{HBF}_4\cdot\text{OEt}_2$  in dichloromethane and subsequent treatment of the resulting solution with a methanol solution of NaX (Scheme 81).<sup>310</sup>

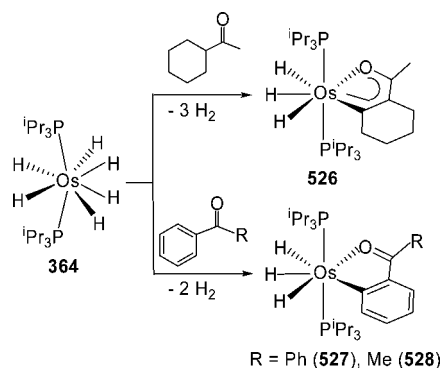
The hexahydride **364** is also able to produce a triple  $\text{C}(\text{sp}^3)\text{-H}$  bond activation in the cyclohexyl ring of cyclohexyl methyl ketone to give the trihydride-osmafuran derivative  $\text{OsH}_3\{\kappa^2\text{-O,C-}[\text{OC}(\text{Me})\text{C}_6\text{H}_8]\}(\text{P}^i\text{Pr}_3)_2$  (**526**). The reaction probably occurs in two steps; initially the activation of a  $\text{C}_\beta\text{-H}$  bond of the six-membered ring generates an  $\text{Os}\{\kappa^2\text{-O,C-}[\text{OC}(\text{Me})\text{-C}_6\text{H}_{10}]\}$  intermediate which releases molecular hydrogen to afford the osmafuran.<sup>311</sup> The aromatic character of the latter should be the driving force for the dehydrogenation, in a similar manner to the formation of the 3-ruthenaindolizine complex **225**. In solution, the hydride ligands of **526** also undergo two thermally activated site-exchange processes. However, in contrast to **521**, both processes have similar activation energies. Reactions of **364** with benzophenone and acetophenone lead to the osmaisobenzofuran derivatives  $\text{OsH}_3\{\kappa^2\text{-O,C-}[\text{OC}(\text{R})\text{-C}_6\text{H}_4]\}(\text{P}^i\text{Pr}_3)_2$  ( $\text{R} = \text{Ph}$  (**527**),  $\text{Me}$  (**528**)) as a result of the *ortho*-CH bond activation of the aromatic group of the ketones.

Scheme 81. C–H Bond Activation of Benzophenone Imine Promoted by 364 and Related Reactions



Like the hydride ligands of **521** and **526**, in solution, the hydride ligands of **527** and **528** undergo two thermally activated site-exchange processes. In these cases, the exchange of lower activation energy involves the hydride ligand disposed *cisoid* to the carbonyl ligand and the central one, which also show quantum exchange coupling (Scheme 82).<sup>312</sup>

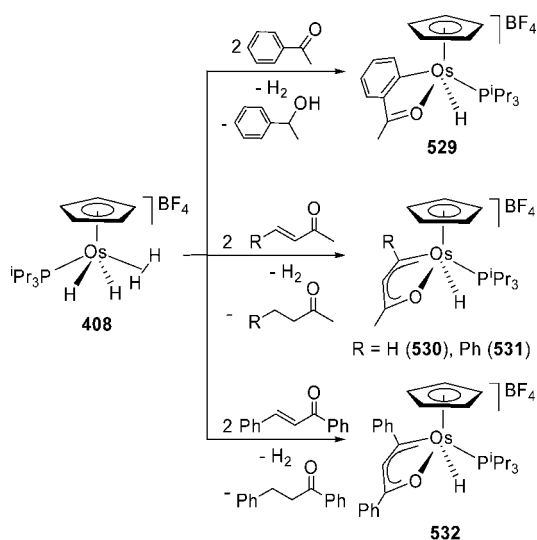
Scheme 82. C–H Bond Activation of Cyclohexyl Methyl Ketone and Aromatic Ketones Promoted by 364



The half-sandwich dihydride-elongated dihydrogen **408** reacts with acetophenone and  $\alpha,\beta$ -unsaturated ketones to give the osmaisobenzofuran complex  $[\text{OsH}(\eta^5\text{-C}_5\text{H}_5)\{\kappa^2\text{-O,C-}[\text{OC}(\text{Me})\text{C}_6\text{H}_4]\}(\text{P}^i\text{Pr}_3)]\text{BF}_4$  (**529**) and the osmafuran derivatives  $[\text{OsH}(\eta^5\text{-C}_5\text{H}_5)\{\kappa^2\text{-O,C-}[\text{OC}(\text{Me})\text{CHC}(\text{R})]\}(\text{P}^i\text{Pr}_3)]\text{BF}_4$  ( $\text{R} = \text{H}$  (**530**),  $\text{Ph}$  (**531**)), respectively. Complex **408** favors the vinylic C–H bond activation with regard to the aromatic C–H bond cleavage in substrates with both types of bonds. Thus, the reaction with benzylideneacetophenone exclusively gives the osmafuran  $[\text{OsH}(\eta^5\text{-C}_5\text{H}_5)\{\kappa^2\text{-O,C-}[\text{OC}(\text{Ph})\text{CHC}(\text{Ph})]\}(\text{P}^i\text{Pr}_3)]\text{BF}_4$  (**532**). These reactions generate molecular hydrogen and 1-phenylethanol or saturated ketones as side products (Scheme 83). This is consistent with a three step process involving the displacement of the coordinated hydrogen molecule by the substrates, their subsequent hydrogenation, and finally the C–H bond addition to the  $[\text{Os}(\eta^5\text{-C}_5\text{H}_5)(\text{P}^i\text{Pr}_3)]^+$  metal fragment.<sup>276</sup>

The dehydrogenation of the metallic center is also a determinant in the reactions of **408** with alkynes. In acetone, this compound reacts with 1-phenyl-1-propyne and 2-butyne to give  $\gamma$ -( $\eta^3$ -allyl)- $\alpha$ -alkenylphosphine derivatives  $[\text{OsH}(\eta^5\text{-$



Scheme 83. C–H Bond Activation Reactions of Aromatic and  $\alpha,\beta$ -Unsaturated Ketones Promoted by 408

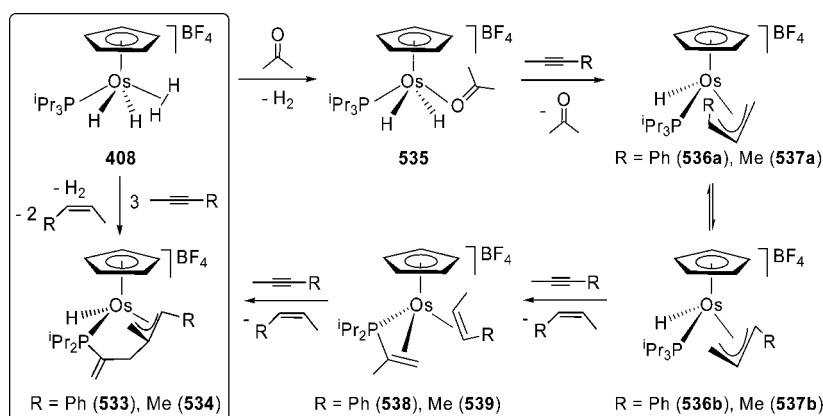
$C_5H_5\{\kappa^4-P,C,C,C-CH_2C[CH_2C(=CH_2)P^iPr_2]CHR\}BF_4$  ( $R = Ph$  (533),  $Me$  (534)), in addition to molecular hydrogen and 2 equiv of the corresponding olefin (Scheme 84). The formation of 533 and 534 takes place by means of a one-pot tandem process of four reactions, including two C–H bond activations of an isopropyl substituent of the phosphine. In acetone, complex 408 dissociates the dihydrogen ligand and coordinates the solvent to afford  $[OsH_2(\eta^5-C_5H_5)(OCMe_2)(P^iPr_3)]BF_4$  (535), which reacts with a molecule of alkyne to form  $[OsH(\eta^5-C_5H_5)(\eta^3-CH_2CHCHR)(P^iPr_3)]BF_4$  ( $R = Ph$  (536),  $Me$  (537)). The reactions of 536 and 537 with a second molecule of alkyne lead to the corresponding *Z*-olefins and  $[Os(\eta^5-C_5H_5)\{\eta^2-(Z)-CH(CH_3)=CHR\}\{\kappa^3-P,C,C-C[CH_2=C(CH_3)]P^iPr_2\}BF_4$  ( $R = Ph$  (538),  $Me$  (539)). A third alkyne molecule displaces the olefin of these compounds and couples with the isopropenyl group of the phosphine to give 533 and 534.<sup>313</sup> In contrast to 1-phenyl-1-propyne and 2-butyne, the reaction of 408 with phenylacetylene leads to the allenylcarbene derivative  $[OsH(\eta^5-C_5H_5)\{\eta^2-C(Ph)(\eta^2-CH=C=CHPh)\}(P^iPr_3)]BF_4$  (540).<sup>314</sup>

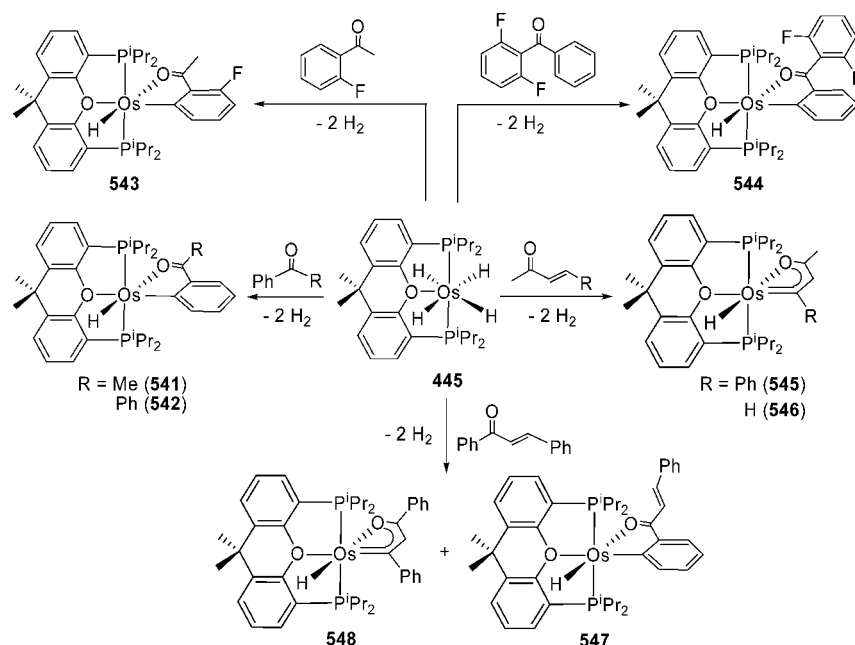
The metallic center of the tetrahydride pincer compound 445 does not necessitate that it undergoes a complete dehydrogenation for promoting the C–H bond activation of aromatic and  $\alpha,\beta$ -unsaturated ketones. Thus, its reactions do

not need the presence of additional sacrificial substrate, in contrast to its ruthenium counterpart 183 and the half-sandwich derivative 408. Treatment of toluene solutions of 445 with 1 equiv of acetophenone and benzophenone under reflux leads to the osmaisobenzofuran pincer derivatives  $OsH\{\kappa^2-O,C-[OC(R)C_6H_4]\}\{xant(P^iPr_2)_2\}$  ( $R = Me$  (541),  $Ph$  (542)). Isotopic labeling experiments, using perdeuterated benzophenone as a substrate, demonstrate that the selectivity of the *ortho*-C–H bond activation is thermodynamic in origin, while the activation of the C–H bonds at meta and para positions are kinetically preferred. Furthermore, they suggest that the C–H bond activation takes place on an unsaturated  $OsH_4$ -species containing a bidentate phosphine. Thus, a heterolytic C–H bond cleavage using a hydride as internal base could generate trihydride intermediates related to 527 and 528, with a bidentate diphosphine, which would evolve into 541 and 542 by means of the release of  $H_2$  and the coordination of the phosphine oxygen atom, in a similar manner to the transformation of the hexahydride 444 into 445. This precursor favors the C–H bond activation over the C–F bond cleavage in fluorinated aromatic ketones. Thus, the fluorinated osmaisobenzofurans  $OsH\{\kappa^2-O,C-[OC(Me)C_6H_3F]\}\{xant(P^iPr_2)_2\}$  (543) and  $OsH\{\kappa^2-O,C-[OC(C_6H_3F_2)C_6H_4]\}\{xant(P^iPr_2)_2\}$  (544) are obtained from the reactions with 2-fluoroacetophenone and 2,6-difluorobenzophenone, respectively. Complex 445 also activates benzylideneacetone and methyl vinyl ketone to afford the osmafurans  $OsH\{\kappa^2-O,C-[OC(Me)CHC(R)]\}\{xant(P^iPr_2)_2\}$  ( $R = Ph$  (545),  $H$  (546)). In contrast to the half-sandwich complex 408, the reaction of 445 with benzylideneacetophenone yields a mixture of  $OsH\{\kappa^2-O,C-[OC(CH=CHPh)C_6H_4]\}\{xant(P^iPr_2)_2\}$  (547) and  $OsH\{\kappa^2-O,C-[OC(Ph)CHC(Ph)]\}\{xant(P^iPr_2)_2\}$  (548) in a 2:1 molar ratio (Scheme 85).<sup>196</sup>

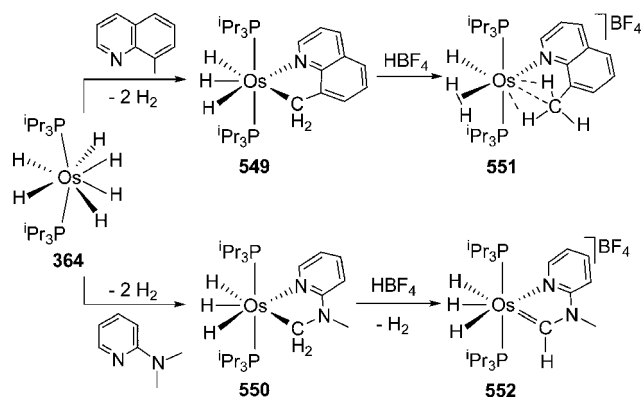
The hexahydride 364 reacts with 8-methylquinoline and 2-(dimethylamino)pyridine to give  $OsH_3\{\kappa^2-N,C-(quin-8-CH_2)\}\{P^iPr_3\}_2$  (549) and  $OsH_3\{\kappa^2-N,C-[py-2-N(Me)CH_2]\}\{P^iPr_3\}_2$  (550), respectively, as a result of the release of two hydrogen molecules and the *N*-heterocyclic-assisted  $C(sp^3)$ -H bond activation of a methyl group of the organic substrates. Treatment of the quinolyl derivative 549 with  $HBF_4 \cdot OEt_2$  affords the hydride-elongated dihydrogen complex  $[OsH(\eta^2-H_2)(quin-8-CH_3)(P^iPr_3)_2]BF_4$  (551), with the methyl substituent of the quinolyl group coordinated in a  $\eta^3-H_2C$  fashion and a separation between the hydrogen atoms of the elongated dihydrogen ligand of about 1.2 Å. The reaction of the pyridyl

Scheme 84. Reactions of 408 with Internal Alkynes



Scheme 85. C–H Bond Activation Reactions of Aromatic, Fluorinated Aromatic, and  $\alpha,\beta$ -Unsaturated Ketones Promoted by 445

derivative **550** with  $\text{HBF}_4 \cdot \text{OEt}_2$  leads to the cyclic carbene compound  $[\text{OsH}_3\{\kappa^2\text{-C}, \text{N}[\text{=CHN}(\text{Me})\text{-}2\text{-py}]\}(\text{P}^i\text{Pr}_3)_2]\text{BF}_4$  (**552**), as a result of the release of a hydrogen molecule and a  $\text{C}(\text{sp}^3)\text{-H}$  bond activation of the methylene group (Scheme 86). In these systems, the activation energy for the rupture of a

Scheme 86. Chelate-Assisted  $\text{C}(\text{sp}^3)\text{-H}$  Bond Activation Reactions Promoted by 364

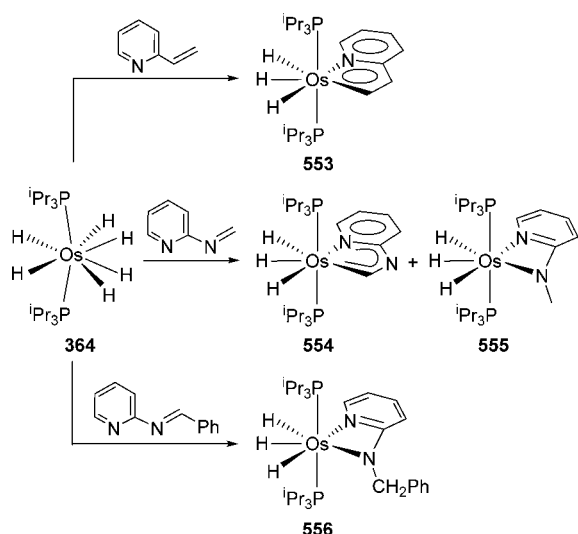
coordinated  $\text{C}(\text{sp}^3)\text{-H}$  bond appears to be similar to that for the cleavage of a coordinated  $\text{H-H}$  bond. Consequently, exchange processes between the hydrogen atoms bound to the metal center and a methyl group of the substrates occur in a competitive manner. The activation energies for the position exchanges between the hydrogen atoms attached to the metal center are not too sensitive to the coordination assistant. However, hydrogen exchanges between hydride and elongated dihydrogen ligands and the  $\text{C}(\text{sp}^3)\text{-H}$  bond of the substituent of the heterocycle show a noticeable dependence, since the coordination assistant seems to carry out a fine-tuning of the stabilities and activation energies involving the osmium-methyl unit. With regard to the quinolyl group, the 2-aminopyridine assistant provides lower activation energies for the  $\text{C}(\text{sp}^3)\text{-H}$

bond rupture and higher stabilities of the resulting alkyl derivative. Furthermore, it facilitates a second  $\text{C}(\text{sp}^3)\text{-H}$  bond activation.<sup>315</sup>

The formation of **552** reveals that the pyridyl group is an efficient coordination assistant for the activation of methylene groups. In agreement with this, it has been observed that 2-vinylpyridine and *N*-methylene-2-pyridinamine react with the hexahydride **364** to give the osmaindolizine derivative  $\text{OsH}_3\{\kappa^2\text{-N}, \text{C}(\text{pyCHCH})\}(\text{P}^i\text{Pr}_3)_2$  (**553**) and the osmainimidazopyridine compound  $\text{OsH}_3\{\kappa^2\text{-N}, \text{C}(\text{pyNCH})\}(\text{P}^i\text{Pr}_3)_2$  (**554**), respectively, as a result of the pyridyl-assisted  $\text{C}(\text{sp}^2)\text{-H}$  bond activation of the terminal  $\text{CH}_2$  group of the substituent of the heterocyclic substrates. Complex **554** is formed along with  $\text{OsH}_3\{\kappa^2\text{-N}, \text{N}(\text{pyNCH}_3)\}(\text{P}^i\text{Pr}_3)_2$  (**555**; about 25%), resulting from the insertion of the  $\text{N-C}$  double bond of the substrate into a  $\text{Os-H}$  bond of the transitory species  $\text{OsH}_4(\text{P}^i\text{Pr}_3)_2$ . In contrast to *N*-methylene-2-pyridinamine, (*E*)-*N*-(phenylmethylene)2-pyridinamine selectively affords the insertion product  $\text{OsH}_3\{\kappa^2\text{-N}, \text{N}(\text{pyNCH}_2\text{Ph})\}(\text{P}^i\text{Pr}_3)_2$  (**556**). The role of the phenyl group seems to be double. On one hand, it increases the electrophilic character of the carbon atom of the  $\text{C-N}$  double bond, favoring the migration of the hydride ligand; on the other, its steric hindrance prevents the coordination of the  $\text{CPh}$  group to the osmium atom (Scheme 87).<sup>316</sup> The formation of the insertion products **555** and **556** is strong evidence in favor of the participation of the unsaturated species  $\text{OsH}_4(\text{P}^i\text{Pr}_3)_2$  in the  $\text{C-H}$  bond activation reactions mediated by the hexahydride **364**. The 16-valence electrons of this species are consistent with no-directed  $\text{C-H}$  bond cleavage processes. To the contrary, the heterolytic rupture of the coordinated  $\text{C-H}$  bond, using a hydride ligand, should generate the necessary coordination vacancy for the entry of the coordination assistant in order to stabilize the activation product.

The addition of  $\text{HBF}_4 \cdot \text{OEt}_2$  to dichloromethane solutions of the osmaindolizine complex **553** leads to the hydride-elongated dihydrogen  $[\text{OsH}(\eta^2\text{-H}_2)(\text{pyCH=CH}_2)(\text{P}^i\text{Pr}_3)_2]\text{BF}_4$  (**557**),

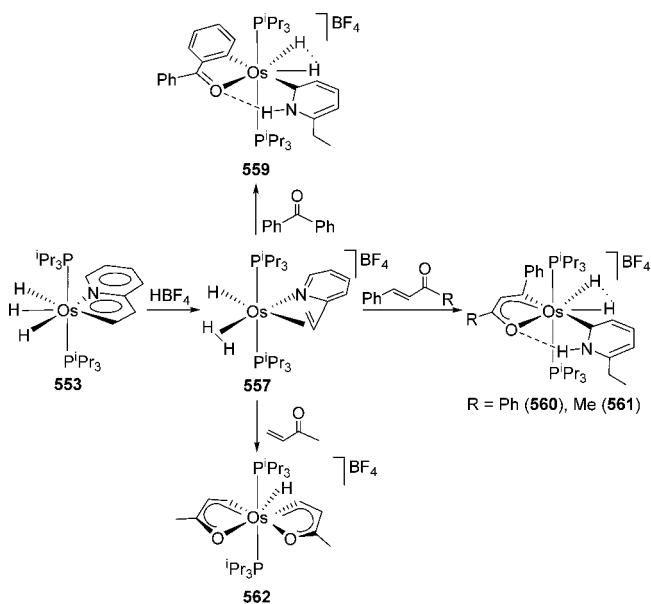
Scheme 87. Reactions of 364 with 2-Vinylpyridine and 2-Pyridinamines



which catalyzes the hydrogenation of 2-vinylpyridine to 2-ethylpyridine in dichloromethane, although its durability is low due to the formation of the chloride-elongated dihydrogen  $\text{OsCl}\{\kappa^2\text{-}N,C\text{-}(\text{pyCHCH})\}(\eta^2\text{-H}_2)(\text{P}^i\text{Pr}_3)_2$  (558). The separation between the hydrogen atoms of the elongated dihydrogen ligand is similar in both compounds, about 1.32 Å. Treatment at 50 °C of 557 with benzophenone in the absence of the solvent gives  $[\text{OsH}_2\{\kappa^2\text{-}O,C\text{-}[\text{OC}(\text{Ph})\text{C}_6\text{H}_4]\}\{\kappa^1\text{-}C\text{-}(\text{HNC}_5\text{H}_3\text{Et})\}(\text{P}^i\text{Pr}_3)_2]\text{BF}_4$  (559), as a consequence of a one-pot process of three reactions: (i) hydrogenation of the vinyl substituent of the pyridine by means of the transfer of the elongated dihydrogen from the metal center to the C–C double bond; (ii) *ortho*-C–H bond activation of the ketone by the resulting monohydride; and (iii) C,N-1,2-H rearrangement of 2-ethylpyridine.<sup>317</sup> In the absence of solvent, 557 also reacts with benzylideneacetophenone and benzylideneacetone to give the related osmafuran-pyridylidene derivatives  $[\text{OsH}_2\{\kappa^2\text{-}O,C\text{-}[\text{OC}(\text{R})\text{CHC}(\text{Ph})]\}\{\kappa^1\text{-}C\text{-}(\text{HNC}_5\text{H}_3\text{Et})\}(\text{P}^i\text{Pr}_3)_2]\text{BF}_4$  (R = Ph (560), Me (561)). The separation between the compressed hydrides of 559–561 is about 1.4 Å. In contrast to benzylideneacetophenone and benzylideneacetone, the reaction of 557 with methyl vinyl ketone leads to  $[\text{OsH}\{\kappa^2\text{-}O,C\text{-}[\text{OC}(\text{CH}_3)\text{CHCH}]\}_2(\text{P}^i\text{Pr}_3)_2]\text{BF}_4$  (562), which can be described as two osmafurans joined by the  $[\text{OsH}(\text{P}^i\text{Pr}_3)_2]^+$  fragment (Scheme 88).<sup>318</sup>

The pyridyl group is also an efficient coordination assistant for stabilizing products resulting from the activation of *ortho*-CH bonds of aryl groups attached at positions 2 and 6 of the heterocycle (Scheme 89). Thus, 2-phenylpyridine and 2,6-diphenylpyridine react with the hexahydride 364 to form  $\text{OsH}_3\{\kappa^2\text{-}N,C\text{-}(\text{pyC}_6\text{H}_4)\}(\text{P}^i\text{Pr}_3)_2$  (563) and  $\text{OsH}_2\{\kappa^2\text{-}C,N,C\text{-}(\text{C}_6\text{H}_4\text{pyC}_6\text{H}_4)\}(\text{P}^i\text{Pr}_3)_2$  (564), respectively. The reactions with 2,2'-diphenyl-4,4'-bipyridine and 2,2',6,6'-tetraphenyl-4,4'-bipyridine lead to the respective dimers  $(\text{P}^i\text{Pr}_3)_2\text{H}_3\text{Os}\{\kappa^2\text{-}N,C\text{-}(\text{pyC}_6\text{H}_4)\text{-}(\text{C}_6\text{H}_4\text{py})\text{-}C,N\text{-}\kappa^2\}\text{OsH}_3(\text{P}^i\text{Pr}_3)_2$  (565) and  $(\text{P}^i\text{Pr}_3)_2\text{H}_2\text{Os}\{\kappa^3\text{-}C,N,C\text{-}(\text{C}_6\text{H}_4\text{pyC}_6\text{H}_4)\text{-}(\text{C}_6\text{H}_4\text{pyC}_6\text{H}_4)\text{-}C,N,C\text{-}\kappa^3\}\text{OsH}_2(\text{P}^i\text{Pr}_3)_2$  (566). The use of 2,2'-diphenyl-4,4'-bipyridines containing an aryl, antranyl, or ethylidene spacer between the 2-phenylpyridine moieties has allowed for the preparation of related dinuclear species  $(\text{P}^i\text{Pr}_3)_2\text{H}_3\text{Os}\{\kappa^2\text{-}N,C\text{-}(\text{pyC}_6\text{H}_4)\text{-}X\text{-}(\text{pyC}_6\text{H}_4)\text{-}C,N\text{-}\kappa^2\}\text{OsH}_3(\text{P}^i\text{Pr}_3)_2$  (X = C<sub>6</sub>H<sub>4</sub>

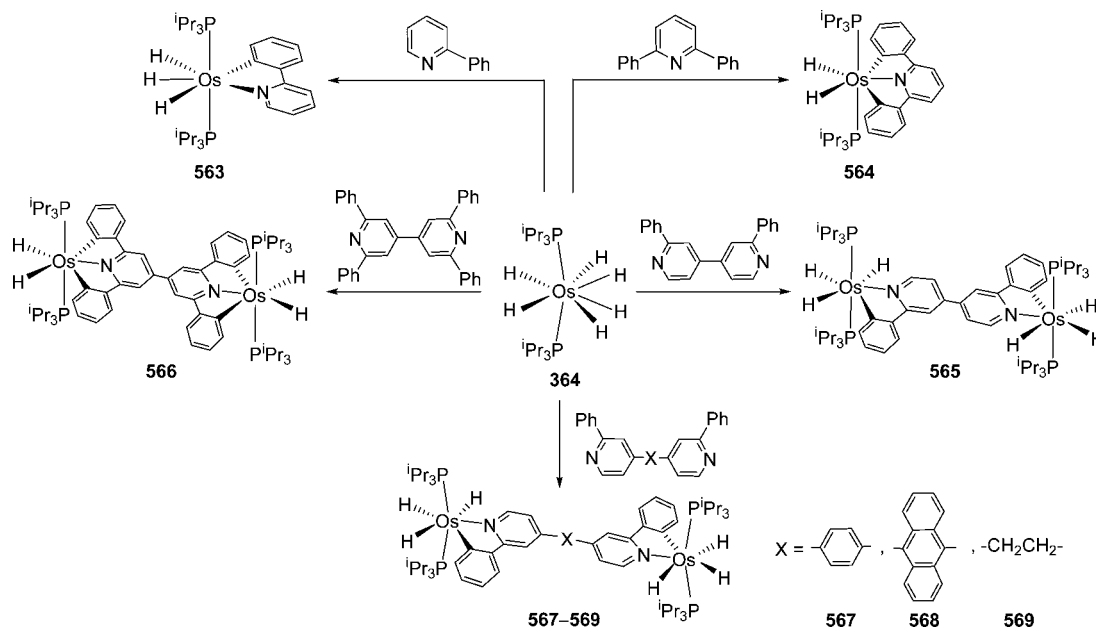
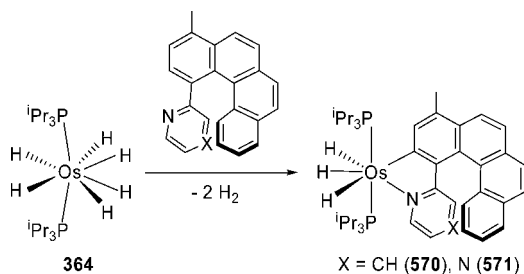
Scheme 88. Formation and C–H Bond Activation Reactions of the Hydride-Elongated Dihydrogen 557



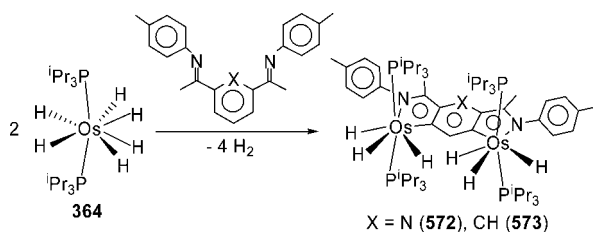
(567), C<sub>14</sub>H<sub>8</sub> (568), CH<sub>2</sub>CH<sub>2</sub> (569)). The spectroelectrochemical study of the dinuclear complexes 565, 567, and 568 has revealed significant changes in the emission spectra upon oxidation. While the transformation from Os(IV) to Os(V) produces small changes in the emission spectra of the complexes, the oxidation from Os(V) to Os(VI) produces a notable bathochromic shift of the emission band, accompanied by a moderate but significant increase in intensity.<sup>319</sup>

The interest in knowing the effect of the incorporation of the metal d electrons on the properties of helical structures has led to perform the reactions of the hexahydride 364 with 1-methyl-4-(2-pyridyl)-benzo[*g*]phenanthrene (HLpy) and 1-methyl-4-(2-pyrazinyl)-benzo[*g*]phenanthrene (HLpyz). Treatment of 364 with these substrates leads to the corresponding d<sup>4</sup>-[6]-azaosmahelicene derivatives  $\text{OsH}_3(\text{Lpy})(\text{P}^i\text{Pr}_3)_2$  (570) and  $\text{OsH}_3(\text{Lpyz})(\text{P}^i\text{Pr}_3)_2$  (571), as a result of the *ortho*-CH bond activation of the substituted ring of the starting [4]-carbohelicene (Scheme 90). The participation of the d-orbitals of the metal in the helical  $\pi$ -backbone of the resulting [6]-azaosmahelicenes produces significant perturbations in the aromaticity of the six-membered rings compared to that in the starting [4]-carbohelicenes, which gives rise to notable differences between the optical properties of the [6]-azaosmahelicene products and the [4]-carbohelicene reagents.<sup>320</sup>

The ability of the hexahydride 364 for activating C–H bonds has allowed the preparation of novel aromatic systems, formed by a central six-membered cycle fused with nitrogen-containing osma-five-membered rings, by means of the 1,3-C–H bond activation of aromatic six-membered cycles with imino substituents *meta* disposed. Treatment of 364 with 0.5 equiv of 2,6-bis{1-[(4-methylphenyl)imino]ethyl}pyridine (H<sub>2</sub>Ipy) and 1,3-bis{1-[(4-methylphenyl)imino]ethyl}benzene (H<sub>2</sub>Iph) leads to the 1,7-diosma-2,4,6-triaza-*s*-indacene complex  $(\text{P}^i\text{Pr}_3)_2\text{H}_3\text{Os}(\text{Ipy})\text{OsH}_3(\text{P}^i\text{Pr}_3)_2$  (572) and the 1,7-diosmapyrrolo[3,4-*f*]isoindole derivative  $(\text{P}^i\text{Pr}_3)_2\text{H}_3\text{Os}(\text{Iph})\text{OsH}_3(\text{P}^i\text{Pr}_3)_2$  (573), respectively (Scheme 91). The orbital situation in the tricycles is fully consistent with the aromatic character of the compounds showing interaction of  $\pi$ - and  $\delta$ -

Scheme 89. Pyridyl-Chelate-Assisted Phenyl-*ortho*-CH Bond Activation Reactions Promoted by 364Scheme 90. Formation of  $d^4$ -[6]-Azaosmahelicene Derivatives

Scheme 91. Formation of Aromatic Diosmaticryclic Nitrogen-Containing Derivatives



symmetry between the metal  $d_{xz}$  and  $d_{xy}$  orbitals and orbitals of the organic fragments.<sup>321</sup>

Polycyclic compounds of five and eight fused cycles, which have no counterpart in conventional organic chemistry, have been also formed by means of the reactions of **364** with 4,5-dimethyl-2,6-bis(4-methylphenyl)pyrimidine ( $H_2P_{Ph_2}$ ), 2,4,6-tris(4-methylphenyl)triazine ( $H_4T_{Ph_3}$ ), and 2,4,6-triphenylpyrimidine ( $H_4P_{Ph_3}$ ). The reactions of **364** with  $H_2P_{Ph_2}$  give a mixture of the metalapolycyclic derivatives  $OsH_3(HP_{Ph_2})(P^iPr_3)_2$  (**574**) and  $OsH_2(P_{Ph_2})(P^iPr_3)_2$  (**575**). The reaction of **364** with  $H_4T_{Ph_3}$  leads to a mixture of  $OsH_2(H_2T_{Ph_3})(P^iPr_3)_2$  (**576**) and  $(P^iPr_3)_2H_2Os(T_{Ph_3})OsH_2(P^iPr_3)_2$  (**577**), containing five and eight fused rings, respectively. Complex **364** reacts with  $H_4P_{Ph_3}$  to afford  $OsH_2(H_2P_{Ph_3})(P^iPr_3)_2$  (**578**) and

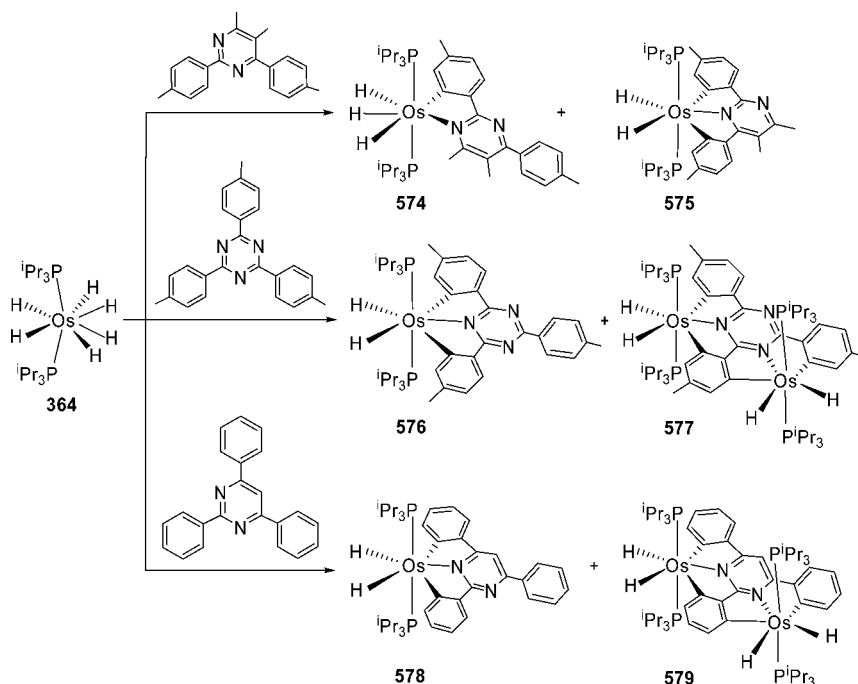
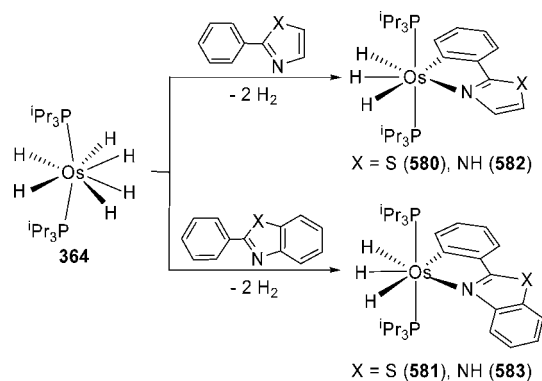
$(P^iPr_3)_2H_2Os(P_{Ph_3})OsH_2(P^iPr_3)_2$  (**579**), which are related to **576** and **577**, respectively (Scheme 92).<sup>322</sup>

Sulfur donor compounds are considered soft bases, while nitrogen donor species are viewed as hard bases. In order to investigate the capacity of **364** to discern between soft and hard assistants for the chelate-assisted C–H bond activation, the reactions of this hexahydride with 2-phenylthiazole and 2-phenylbenzothiazole have been performed. Treatment of toluene solutions of **364** with these substrates under reflux leads to the trihydride derivatives  $OsH_3\{\kappa^2-C,N-(C_6H_4\text{-thiazole})\}(P^iPr_3)_2$  (**580**) and  $OsH_3\{\kappa^2-C,N-(C_6H_4\text{-benzothiazole})\}(P^iPr_3)_2$  (**581**), containing N-coordinated thiazole and benzothiazole assistants in spite of the soft nature of the late third row transition metals. Similarly, the reactions of **364** with 2-phenylimidazole and 2-phenylbenzimidazole afford  $OsH_3\{\kappa^2-C,N-(C_6H_4\text{-imidazole})\}(P^iPr_3)_2$  (**582**) and  $OsH_3\{\kappa^2-C,N-(C_6H_4\text{-benzimidazole})\}(P^iPr_3)_2$  (**583**), respectively (Scheme 93).<sup>323</sup>

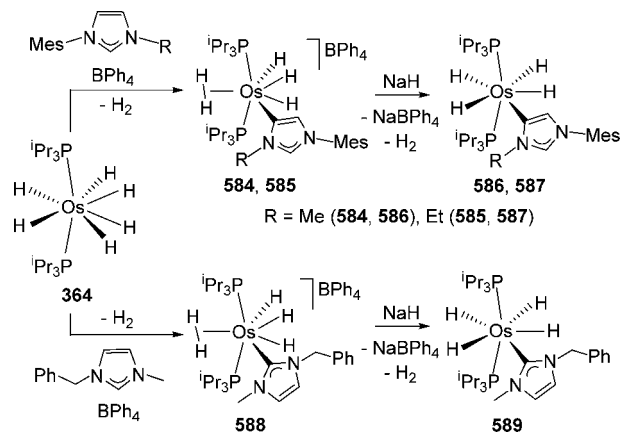
### 3.6.4. C–H Bond Activation of Imidazolium and Benzimidazolium Salts: Formation of NHC Complexes.

The hydride ligands of the hexahydride **364** are basic enough to promote the deprotonation of imidazolium salts. The treatment of tetrahydrofuran solutions of this compound with 1-mesityl-3-methylimidazolium tetraphenylborate and 1-mesityl-3-ethylimidazolium tetraphenylborate leads to the trihydride-elongated dihydrogen derivatives  $[OsH_3(\eta^2-H_2)(1\text{-mesityl-3-methylimidazol-4-ylidene})(P^iPr_3)_2]BPh_4$  (**584**) and  $[OsH_3(\eta^2-H_2)(1\text{-mesityl-3-ethylimidazol-4-ylidene})(P^iPr_3)_2]BPh_4$  (**585**), respectively, containing an abnormal NHC ligand (Scheme 94). The coordination geometry around the osmium atom of these eight-coordinate species is the expected dodecahedron, defined by two orthogonal trapezoidal planes. One of them contains the phosphorus atoms at B sites and two hydride ligands, whereas a hydride, the NHC group, and the hydrogen atoms of the elongated dihydrogen ( $d_{H-H} = 1.25(5)$  Å) lie in the other one. Although compounds **584** and **585** could be viewed as metal-imidazolium salts, the deprotonation of the  $OsH_3$ -unit is favored with regard to the  $N_2CH$ -proton. Thus, the addition of NaH to tetrahydrofuran solutions of **584** and

Scheme 92. Osmapolycyclic Compounds with Five and Eight Fused Cycles

Scheme 93. Other Chelate-Assisted Phenyl-*ortho*-CH Bond Activation Reactions Promoted by 364

Scheme 94. Direct Metalation of Imidazolium Salts Promoted by 364

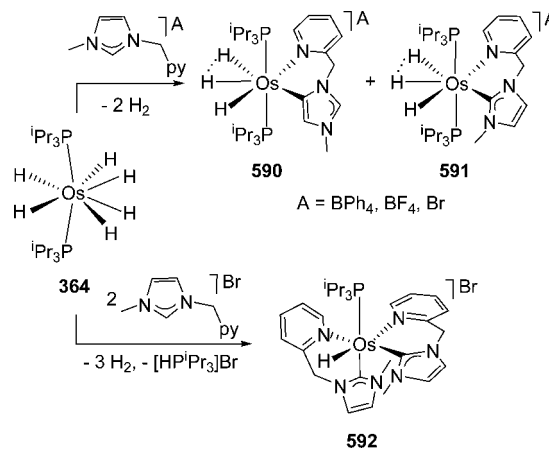


585 affords the classical tetrahydrides  $\text{OsH}_4(1\text{-mesityl-3-methylimidazol-4-ylidene})(\text{P}^i\text{Pr}_3)_2$  (586) and  $\text{OsH}_4(1\text{-mesityl-}$

3-ethylimidazol-4-ylidene) $(\text{P}^i\text{Pr}_3)_2$  (587). The replacement of the mesityl substituent by a benzyl group on the 1-mesityl-3-methylimidazolium cation diminishes the steric hindrance around the C2 carbon atom, increasing the accessibility of this atom. Thus, in contrast to 1-mesityl-3-methylimidazolium tetraphenylborate, the treatment of tetrahydrofuran solutions of 364 with 1-benzyl-3-methylimidazolium tetraphenylborate leads to the trihydride-elongated dihydrogen  $[\text{OsH}_5(1\text{-benzyl-3-methylimidazol-2-ylidene})(\text{P}^i\text{Pr}_3)_2]\text{BPh}_4$  (588), containing a normal NHC-ligand. Similarly to 584 and 585, the deprotonation of 588 affords the tetrahydride  $\text{OsH}_4(1\text{-benzyl-3-methylimidazol-2-ylidene})(\text{P}^i\text{Pr}_3)_2$  (589).<sup>324</sup>

Pyridyl-assisted C–H bond activation of imidazolium salts has been also performed (Scheme 95). The reactions of 364 with 1 equiv of  $\text{BPh}_4^-$ ,  $\text{BF}_4^-$ , and  $\text{Br}^-$  salts of 1-(2-pyridylmethyl)-3-methylimidazolium in tetrahydrofuran under reflux lead to mixtures of the abnormal  $[\text{OsH}_3\{\kappa\text{-C}^5\text{N-[1-(2-}$

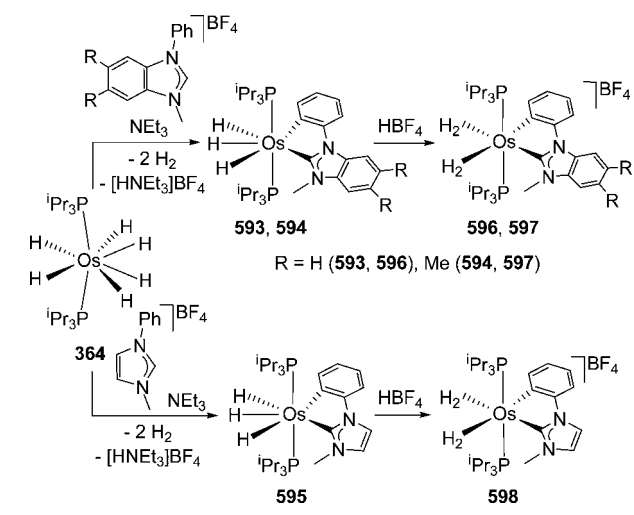
Scheme 95. Pyridyl-Chelate-Assisted Metalation of Imidazolium Salts Promoted by 364



pyridylmethyl)-3-methylimidazol-5-ylidene]](P<sup>i</sup>Pr<sub>3</sub>)<sub>2</sub>]A (A = BPh<sub>4</sub><sup>-</sup>, BF<sub>4</sub><sup>-</sup>, and Br<sup>-</sup>; **590**) and normal [OsH<sub>3</sub>{κ-C<sup>2</sup>,N-[1-(2-pyridylmethyl)-3-methylimidazol-2-ylidene]](P<sup>i</sup>Pr<sub>3</sub>)<sub>2</sub>]A (A = BPh<sub>4</sub><sup>-</sup>, BF<sub>4</sub><sup>-</sup>, and Br<sup>-</sup>; **591**) species. The amount of normal isomer increases as the basicity of the anion of the salts increases (i.e., in the sequence BPh<sub>4</sub><sup>-</sup> < BF<sub>4</sub><sup>-</sup> < Br<sup>-</sup>). The T<sub>1</sub>(min) values of the OsH<sub>3</sub>-resonances and the X-ray structure of the BPh<sub>4</sub><sup>-</sup>-salt of **590** support a hydride-compressed dihydride formulation for these compounds, with a separation between the compressed hydrides of about 1.45 Å. Reaction of **364** with 2.0 equiv of 1-(2-pyridylmethyl)-3-methylimidazolium bromide yields the bis(normal)-NHC monohydride [OsH{κ-C,N-[1-(2-pyridylmethyl)-3-methylimidazol-2-ylidene]]<sub>2</sub>(P<sup>i</sup>Pr<sub>3</sub>)<sub>2</sub>]Br (**592**).<sup>325</sup>

N-heterocyclic carbene ligands are very useful to stabilize nonclassical H–H interactions due to their significant π-accepting capacity, which is higher than those of aryl groups and alkylphosphine ligands. Hexahydride **364** reacts with the BF<sub>4</sub><sup>-</sup>-salts of 1-phenyl-3-methyl-1-*H*-benzimidazolium (H<sub>2</sub>PhbI), 1-phenyl-3-methyl-1-*H*-5,6-dimethyl-benzimidazolium (H<sub>2</sub>PhbIme<sub>2</sub>), and 1-phenyl-3-methyl-1-*H*-imidazolium (H<sub>2</sub>PhI), in the presence of NEt<sub>3</sub>, to give the respective trihydride derivatives OsH<sub>3</sub>(κ<sup>2</sup>-C<sub>aryyl</sub>C<sub>NHC</sub>)(P<sup>i</sup>Pr<sub>3</sub>)<sub>2</sub> (C<sub>aryyl</sub>C<sub>NHC</sub> = PhbI (**593**), PhbIme<sub>2</sub> (**594**), PhI (**595**)), as a result of the N<sub>2</sub>C–H bond activation of the benzimidazolium and imidazolium salts and the *ortho*-CH bond activation of the phenyl substituent (Scheme 96). The protonation of **593–595**

**Scheme 96.** Bis(dihydrogen)-Osmium(II) Complexes Stabilized by NHC Ligands

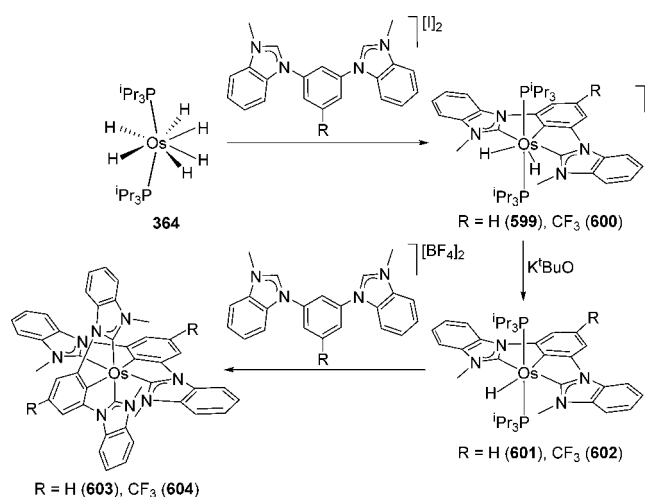


with HBF<sub>4</sub>·OEt<sub>2</sub> leads to the bis(dihydrogen) derivatives [Os(κ<sup>2</sup>-C<sub>aryyl</sub>C<sub>NHC</sub>)(η<sup>2</sup>-H<sub>2</sub>)<sub>2</sub>(P<sup>i</sup>Pr<sub>3</sub>)<sub>2</sub>]BF<sub>4</sub> (C<sub>aryyl</sub>C<sub>NHC</sub> = PhbI (**596**), PhbIme<sub>2</sub> (**597**), PhI (**598**)). In accordance with the X-ray structure of **597**, the coordinated hydrogen molecule situated trans to the aryl group disposes its hydrogen atoms almost parallel to the P–Os–P direction, separated by about 0.9 Å, whereas the other one, trans disposed to the NHC unit, lies in the plane of the C,C'-chelate ligand with the hydrogen atoms also separated by about 0.9 Å. DFT calculations using AIM and NBO methods have revealed that the Os–NHC bond of the Os–chelate link tolerates a significant π-back-donation from a doubly occupied d<sub>π</sub>(Os) atomic orbital to the p<sub>z</sub> atomic orbital of the carbene carbon atom. The π-accepting capacity of the NHC unit enhances the electrophilicity of the metal center

activating one of the coordinated hydrogen molecules toward the heterolysis. As a result, compounds **596–598** are strong Brønsted acids with pK<sub>a</sub><sup>water</sup> values between 2.5 and 2.8, which compare well with the values of phosphoric acid and organic compounds such as bromoacetic acid or chloroacetic acid.<sup>326</sup>

The direct metalation of bis-benzimidazolium salts 1,3-attached to an aromatic group along with the *ortho*-CH bond activation of the latter, have been decisive for the recent **364**-mediated preparation of novel types of blue-green emissive neutral compounds, for organic light-emitting devices (Scheme 97). Complex **364** reacts with the iodide salts of 1,3-bis(3-

**Scheme 97.** Hexahydride **364** as Precursor of Os(C<sub>NHC</sub>C<sub>aryyl</sub>C<sub>NHC</sub>)(C<sub>NHC</sub>C<sub>R-aryyl</sub>C<sub>NHC</sub>) Blue-Green Emissive Compounds

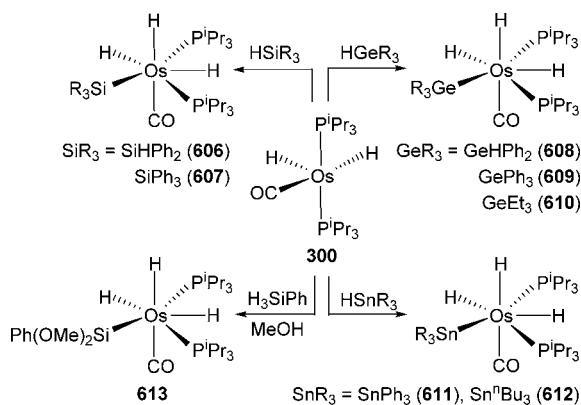


methylbenzimidazolium-1-yl)benzene and 1,3-bis(3-methylbenzimidazolium-1-yl)-5-trifluoromethylbenzene to give the respective dihydrides [OsH<sub>2</sub>(C<sub>NHC</sub>C<sub>aryyl</sub>C<sub>NHC</sub>)(P<sup>i</sup>Pr<sub>3</sub>)<sub>2</sub>]I (**599**) and [OsH<sub>2</sub>(C<sub>NHC</sub>C<sub>CF<sub>3</sub>aryyl</sub>C<sub>NHC</sub>)(P<sup>i</sup>Pr<sub>3</sub>)<sub>2</sub>]I (**600**). The subsequent deprotonation of these compounds with K<sup>t</sup>BuO yields the monohydrides OsH(C<sub>NHC</sub>C<sub>aryyl</sub>C<sub>NHC</sub>)(P<sup>i</sup>Pr<sub>3</sub>)<sub>2</sub> (**601**) and OsH(C<sub>NHC</sub>C<sub>CF<sub>3</sub>aryyl</sub>C<sub>NHC</sub>)(P<sup>i</sup>Pr<sub>3</sub>)<sub>2</sub> (**602**), which react with a second organic cation to afford the homoleptic derivatives Os(C<sub>NHC</sub>C<sub>aryyl</sub>C<sub>NHC</sub>)<sub>2</sub> (**603**) and Os(C<sub>NHC</sub>C<sub>CF<sub>3</sub>aryyl</sub>C<sub>NHC</sub>)<sub>2</sub> (**604**). The reactions of **601** with 1,3-bis(3-methylbenzimidazolium-1-yl)-5-trifluoromethylbenzene and of **602** with 1,3-bis(3-methylbenzimidazolium-1-yl)benzene lead to the heteroleptic counterpart Os(C<sub>NHC</sub>C<sub>aryyl</sub>C<sub>NHC</sub>)(C<sub>NHC</sub>C<sub>CF<sub>3</sub>aryyl</sub>C<sub>NHC</sub>) (**605**). Complexes **603–605** are emissive in the blue-green spectral region with high quantum yields in the solid state, which reach 0.62 for **604**.<sup>327</sup>

**3.6.5. Si–H, Ge–H, and Sn–H Bond Activations.** The unsaturated dihydride **300**, generated in situ from the tetrahydrideborate complex **301** or the olefin compound **475**, adds the Si–H bond of silanes, the Ge–H bond of germanes, and the Sn–H bond of stannanes to give the corresponding trihydride-silyl OsH<sub>3</sub>(SiR<sub>3</sub>)(CO)(P<sup>i</sup>Pr<sub>3</sub>)<sub>2</sub> (SiR<sub>3</sub> = SiHPh<sub>2</sub> (**606**), SiPh<sub>3</sub> (**607**)), trihydride-germyl OsH<sub>3</sub>(GeR<sub>3</sub>)(CO)(P<sup>i</sup>Pr<sub>3</sub>)<sub>2</sub> (GeR<sub>3</sub> = GeHPh<sub>2</sub> (**608**), GePh<sub>3</sub> (**609**), GeEt<sub>3</sub> (**610**)), and trihydride-stannyl OsH<sub>3</sub>(SnR<sub>3</sub>)(CO)(P<sup>i</sup>Pr<sub>3</sub>)<sub>2</sub> (SnR<sub>3</sub> = SnPh<sub>3</sub> (**611**), Sn<sup>n</sup>Bu<sub>3</sub> (**612**)) derivatives. The reaction of **300** with H<sub>3</sub>SiPh in methanol yields OsH<sub>3</sub>{Si(OMe)<sub>2</sub>Ph}(CO)(P<sup>i</sup>Pr<sub>3</sub>)<sub>2</sub> (**613**). The behavior in solution of the four types of compounds is similar, suggesting that all of them have the same

arrangement of ligands around the osmium atom. On the basis of the X-ray structure of **606** and DFT calculations on the model compound  $\text{OsH}_3(\text{SiH}_3)(\text{CO})(\text{PPh}_3)_2$ , the proposed coordination geometry around the metal center of these compounds has been described as a heavily distorted pentagonal bipyramid with a hydride ligand and the carbonyl group in the axial positions. The two other hydride ligands lie in the equatorial plane, one between the phosphines and the other between the  $\text{ER}_3$  ( $\text{E} = \text{Si, Ge, and Sn}$ ) group and a phosphine (Scheme 98).<sup>328</sup>

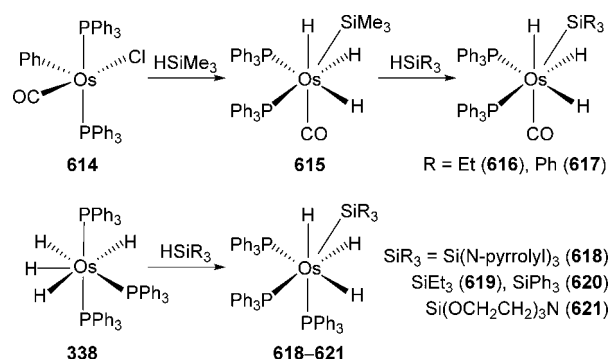
**Scheme 98. Reactions of Activation of Si–H, Ge–H, and Sn–H Bonds Promoted by 300**



Reaction of the carbonyl-bis(triphenylphosphine) complex  $\text{OsPhCl}(\text{CO})(\text{PPh}_3)_2$  (**614**) with  $\text{HSiMe}_3$  leads to  $\text{OsH}_3(\text{SiMe}_3)(\text{CO})(\text{PPh}_3)_2$  (**615**). Treatment of the latter with  $\text{HSiEt}_3$  and  $\text{HSiPh}_3$  affords  $\text{OsH}_3(\text{SiEt}_3)(\text{CO})(\text{PPh}_3)_2$  (**616**) and  $\text{OsH}_3(\text{SiPh}_3)(\text{CO})(\text{PPh}_3)_2$  (**617**), respectively. Although these compounds are  $\text{PPh}_3$ -counterparts of **606** and **607**, there are marked structural differences between them because of the cone angles of the phosphine, which have a significant influence on the coordination geometry around the osmium atom. The  $\text{P–Os–P}$  angle decreases from  $146.06(7)^\circ$  in **606** to  $98.85(2)^\circ$  in **615**. Consequently, and in contrast to the  $\text{P}^i\text{Pr}_3$ -complexes, the arrangement of ligands around the osmium atom of the  $\text{PPh}_3$ -compounds has been described as an approximately tetrahedral disposition of silyl, CO, and phosphine ligands with the three classical hydride ligands located *trans* to the CO and phosphine groups. This structure resembles that of complex **349** with the silyl in the  $\text{Sn}^n\text{Bu}_3$  position and a carbonyl group instead of a phosphine.<sup>329</sup> The reactions of the tetrahydride-tris(triphenylphosphine) complex **338** with  $\text{HSiR}_3$  lead to the corresponding trihydride-silyl-tris(triphenylphosphine) analogous  $\text{OsH}_3(\text{SiR}_3)(\text{PPh}_3)_3$  ( $\text{SiR}_3 = \text{Si}(\text{N-pyrrolyl})_3$  (**618**),  $\text{SiEt}_3$  (**619**),  $\text{SiPh}_3$  (**620**),  $\text{Si}(\text{OCH}_2\text{CH}_2)_3\text{N}$  (**621**)). These compounds have the same structure as **615–617**, with a phosphine in the position of the carbonyl group (Scheme 99). The methylation and protonation of the nitrogen atom of **621** give the salts  $[\text{OsH}_3\{\text{Si}(\text{OCH}_2\text{CH}_2)_3\text{NMe}\}(\text{PPh}_3)_3]\text{I}$  (**622**) and  $[\text{OsH}_3\{\text{Si}(\text{OCH}_2\text{CH}_2)_3\text{NH}\}(\text{PPh}_3)_3]\text{OTf}$  (**623**), respectively.<sup>330,331</sup>

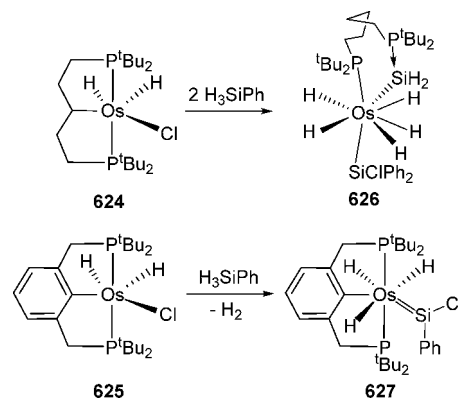
Gusev, Zargarian, and co-workers have reported novel silyl and silylene compounds resulting from reactions of  $\text{H}_3\text{SiPh}$  with the pincer complexes  $\text{OsH}_2\text{Cl}\{\text{CH}(\text{C}_6\text{H}_4\text{P}^t\text{Bu}_2)_2\}$  (**624**) and  $\text{OsH}_2\text{Cl}\{2,6-(\text{CH}_2\text{P}^t\text{Bu}_2)_2\text{C}_6\text{H}_3\}$  (**625**). Addition of 2 equiv of  $\text{H}_3\text{SiPh}$  to toluene solutions of **624** gives  $\text{OsH}_2(\text{SiPh}_2\text{Cl})\{\kappa^2\text{-Si}_i\text{P}^t\text{Bu}_2(\text{CH}_2)_5\text{P}^t\text{Bu}_2\}$  (**626**). During the process,

**Scheme 99. Si–H Bond Activation Reactions Promoted by Triphenylphosphine-Osmium Complexes**



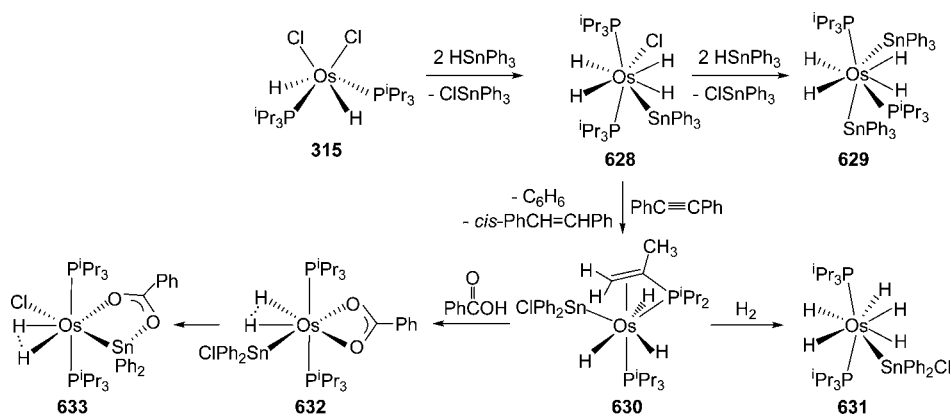
complex **624** and the two molecules of silane undergo a series of redistribution reactions culminating in the net hydrogenation of the  $\text{Os–C}(\text{sp}^3)$  bond and the generation of a silyl, one base-stabilized silylene, and five hydride ligands. The donor atoms around the metal center define a dodecahedron consisting of two orthogonal trapezoidal planes. One of them contains the Si-silyl atom and the coordinated phosphorus atom of the phosphine at B sites and two hydrides, whereas the other plane contains three hydrides and the Si atom of the base-stabilized silylene. The reaction of  $\text{H}_3\text{SiPh}$  with **625**, which has a pincer ligand with a more rigid backbone, leads to the trihydride-silylene  $\text{OsH}_3(\text{SiClPh})\{2,6-(\text{CH}_2\text{P}^t\text{Bu}_2)_2\text{C}_6\text{H}_3\}$  (**627**) and molecular hydrogen (Scheme 100).<sup>332</sup>

**Scheme 100. Si–H Bond Activation Reactions Promoted by PCP-Pincer Osmium Complexes**

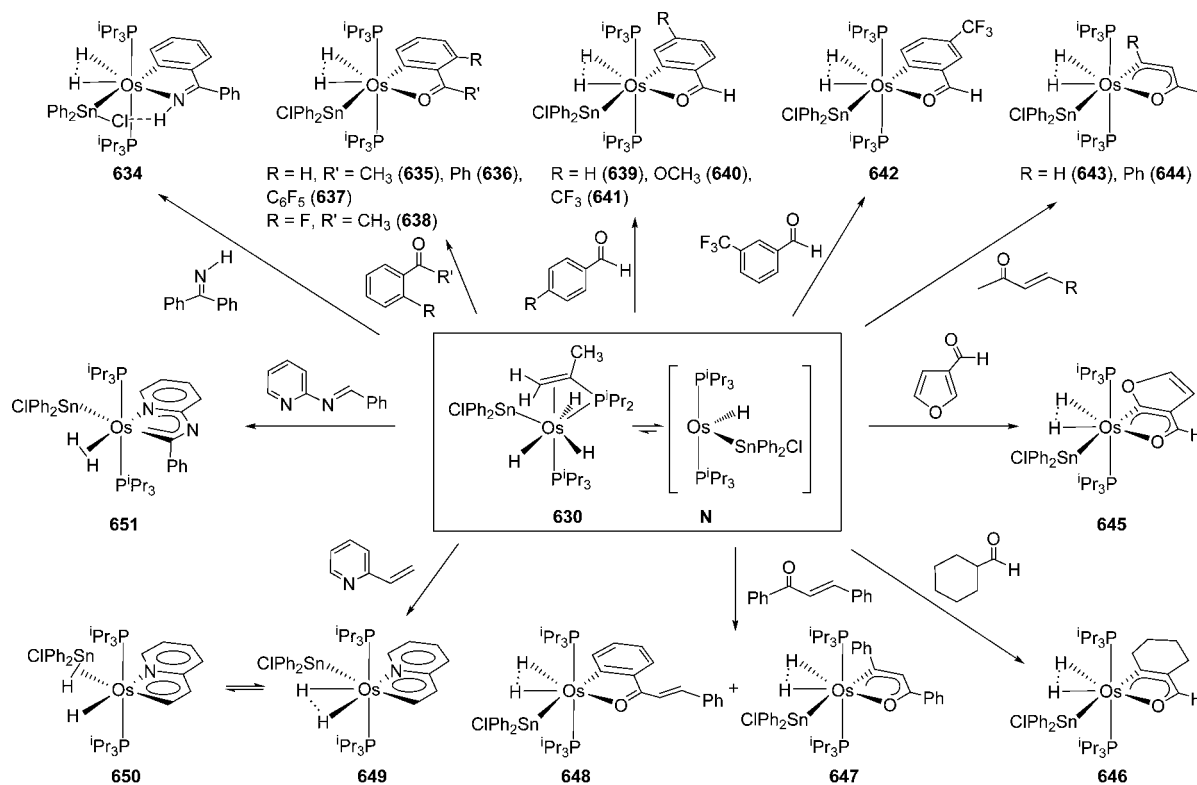


The activation of the  $\text{Sn–H}$  bond of  $\text{HSnPh}_3$  by the dichloride-dihydride complex **315** has been the starting point to the development of an interesting family of stannyl and bis(stannyl)-polyhydride compounds, including pentahydride, tetrahydride, trihydride, and compressed dihydride species (Scheme 101). Complex **315** reacts with two equiv of  $\text{HSnPh}_3$  to give the tetrahydride-stannyl  $\text{OsH}_4\text{Cl}(\text{SnPh}_3)(\text{P}^i\text{Pr}_3)_2$  (**628**) and  $\text{ClSnPh}_3$ . The structure of **628** is the expected dodecahedron with the bulky ligands at B sites of the orthogonal trapezoidal planes.<sup>333</sup> This compound reacts with other two equivalents of  $\text{HSnPh}_3$  to afford the tetrahydride-bis(stannyl) derivative  $\text{OsH}_4(\text{SnPh}_3)_2(\text{P}^i\text{Pr}_3)_2$  (**629**) and  $\text{ClSnPh}_3$ . Complex **629** is a rare example of bis(stannyl) compound with the transition metal in a high oxidation state. A distinguishing feature of the structure of this compound is the  $\text{P–Os–Sn}$  angle in both orthogonal trapezoidal planes ( $\text{B–}$

Scheme 101. Formation of Osmium-Polyhydrides via Sn–H Bond Activation Reactions



Scheme 102. C–H Bond Activation Reactions Promoted by 630



Os–B) of  $122.56(3)^\circ$ , which is significantly smaller than the related angle in other eight-coordinate osmium polyhydride complexes ( $145\text{--}156^\circ$ ). This seems to be a consequence of the steric hindrance experienced by the phosphine and stannyl ligands of different planes.<sup>334</sup> In the presence of diphenylacetylene, complex **628** gives the trihydride-stannyl  $\text{OsH}_3(\text{SnClPh}_2)\{\kappa^3\text{-P,C,C-}[\text{CH}_2=\text{C}(\text{CH}_3)]\text{P}^i\text{Pr}_2\}(\text{P}^i\text{Pr}_3)$  (**630**), *cis*-stilbene, and benzene. In the solid state, its structure has been determined by X-ray diffraction analysis and can be described as a very distorted pentagonal bipyramid, with the phosphorus atoms of the trisopropylphosphine ligand and the midpoint of the olefinic bond of the isopropenyl group of the dehydrogenated phosphine occupying axial positions. The formation of **630** is a one-pot synthesis of multiple complex reactions. Four different processes are assembled to afford this compound: (i) dehydrogenation of one isopropyl group of one phosphine, (ii) reduction of diphenylacetylene to give *cis*-

stilbene, (iii) hydrogenolysis of a phenyl group of the triphenylstannyl ligand, and (iv) migration of the chloride from the transition metal to the tin atom. The elemental steps of this synthesis appear to occur with the participation of radical-like species as intermediates. Thus, the formation of **630** is inhibited in the presence of hydroquinone. Complex **630** reacts with molecular hydrogen to form the pentahydride-stannyl  $\text{OsH}_5(\text{SnClPh}_2)(\text{P}^i\text{Pr}_3)_2$  (**631**), as a result of the hydrogenation of the coordinated olefinic bond and a  $d^4\text{--}d^2$  oxidative addition of hydrogen. The donor atoms adopt the expected dodecahedral disposition around the metal center with the bulky ligand at the B sites of the trapezoidal planes.<sup>333</sup> Complex **630** also undergoes protonation-addition of benzoic acid to initially give the compressed dihydride-stannyl derivative  $\text{OsH}_2(\text{SnClPh}_2)(\kappa^2\text{-O}_2\text{CPh})(\text{P}^i\text{Pr}_3)_2$  (**632**;  $d_{\text{H}\cdots\text{H}} = 1.50 \text{ \AA}$ ). In solution, the tin atom exchanges with the transition metal on the chloride ligand by one of the oxygen atoms of the



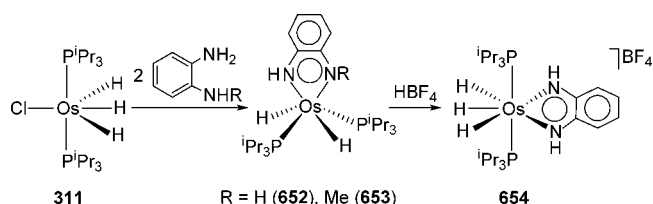
carboxylate group to afford  $\text{OsH}_2\text{Cl}\{\kappa^2\text{-O,Sn-[OC(Ph)-OSnPh}_2]\}(\text{P}^i\text{Pr}_3)_2$  (**633**;  $d_{\text{H}\cdots\text{H}} = 1.50 \text{ \AA}$ ).<sup>335</sup>

The formation of **631** and **632** is consistent with the previous transformation of **630** into the 14-valence electrons monohydride  $\text{OsH}(\text{SnClPh}_2)(\text{P}^i\text{Pr}_3)_2$  (**N**), which adds two molecules of  $\text{H}_2$  or one molecule of benzoic acid. This functionally equivalent promotes the chelate-assisted  $\text{C}(\text{sp}^2)\text{-H}$  bond activation of aromatic imines, ketones, and aldehydes;  $\alpha,\beta$ -unsaturated ketones and aldehydes; 2-vinylpyridine, and (*E*)-*N*-(phenylmethylene)-2-pyridinamine to afford compressed dihydrides (Scheme 102). The reaction with benzophenone imine leads to  $\text{OsH}_2(\text{SnClPh}_2)\{\kappa^2\text{-N,C-[NHC(Ph)C}_6\text{H}_4]\}(\text{P}^i\text{Pr}_3)_2$  (**634**), whereas acetophenone and benzophenone give  $\text{OsH}_2(\text{SnClPh}_2)\{\kappa^2\text{-O,C-[OC(R)C}_6\text{H}_4]\}(\text{P}^i\text{Pr}_3)_2$  (R = Me (**635**), Ph (**636**)). The functionally equivalent N is certainly the key species for the activation; in agreement with this, the reaction of **630** with 1 equiv of perdeuterated benzophenone affords the hydride-deuteride  $\text{Os}(\text{H})(\text{D})(\text{SnClPh}_2)\{\kappa^2\text{-O,C-[OC(C}_6\text{D}_5\text{C}_6\text{D}_4)]\}(\text{P}^i\text{Pr}_3)_2$  (**636-d**<sub>10</sub>). The *ortho*-CH bond activation is preferred over the *ortho*-CF bond activation. Thus, the reactions with 2,3,4,5,6-pentafluorobenzophenone and 2-fluoroacetophenone yield  $\text{OsH}_2(\text{SnClPh}_2)\{\kappa^2\text{-O,C-[OC(C}_6\text{F}_5\text{-C}_6\text{H}_4)]\}(\text{P}^i\text{Pr}_3)_2$  (**637**) and  $\text{OsH}_2(\text{SnClPh}_2)\{\kappa^2\text{-O,C-[OC(Me)-C}_6\text{FH}_3]\}(\text{P}^i\text{Pr}_3)_2$  (**638**), respectively.<sup>336</sup> The *ortho*-CH activation is also preferred with regard to the OC-H bond activation in benzaldehydes. Reactions of **630** with benzaldehyde and substituted benzaldehydes give the corresponding *ortho*-metalated compounds  $\text{OsH}_2(\text{SnClPh}_2)\{\kappa^2\text{-O,C-[OC(H)-C}_6\text{RH}_3]\}(\text{P}^i\text{Pr}_3)_2$  (R = H (**639**), *p*-OCH<sub>3</sub> (**640**), *p*-CF<sub>3</sub> (**641**), *m*-CF<sub>3</sub> (**642**)).<sup>337</sup>  $\alpha,\beta$ -Unsaturated ketones and aldehydes generate osmafuran derivatives, methyl vinyl ketone and benzylidenacetone give  $\text{OsH}_2(\text{SnClPh}_2)\{\kappa^2\text{-O,C-[OC(CH}_3\text{)CHCR}]\}(\text{P}^i\text{Pr}_3)_2$  (R = H (**643**), Ph (**644**)),<sup>338</sup> whereas 3-furaldehyde and 1-cyclohexene-1-carboxaldehyde form  $\text{OsH}_2(\text{SnClPh}_2)\{\kappa^2\text{-O,C-[OCHC}_4(\text{O})\text{H}_2]\}(\text{P}^i\text{Pr}_3)_2$  (**645**) and  $\text{OsH}_2(\text{SnClPh}_2)\{\kappa^2\text{-O,C-[OCHC}_6\text{H}_8]\}(\text{P}^i\text{Pr}_3)_2$  (**646**), respectively.<sup>337</sup> As expected, the functionally equivalent N activates both  $\beta$ -olefinic- and *ortho*-CH bonds of benzylidenacetophenone to give the osmafuran  $\text{OsH}_2(\text{SnClPh}_2)\{\kappa^2\text{-O,C-[OC(Ph)-CHCPh]}\}(\text{P}^i\text{Pr}_3)_2$  (**647**) and the osmaisobenzofuran  $\text{OsH}_2(\text{SnClPh}_2)\{\kappa^2\text{-O,C-[OC(CH=CHPh)C}_6\text{H}_4]\}(\text{P}^i\text{Pr}_3)_2$  (**648**). The activation of the C-H bond of the olefinic moiety is kinetically favored with regard to the *ortho*-CH bond activation of the phenyl group. However, complex **648**, resulting from the *ortho*-CH bond activation, is thermodynamically more stable than **647**. The activation of 2-vinylpyridine affords  $\text{OsH}_2(\text{SnClPh}_2)\{\kappa^2\text{-N,C-(pyCHCH)}\}(\text{P}^i\text{Pr}_3)_2$  (**649**) in equilibrium with the tautomer  $\text{OsH}\{\kappa^2\text{-N,C-(pyCHCH)}\}(\eta^2\text{-HSnClPh}_2)(\text{P}^i\text{Pr}_3)_2$  (**650**), where the stannane is bonded to the transition metal by an Os-H-Sn three-center bond ( $J_{\text{H-Sn}} = 183 \text{ Hz}$ ). The activation of (*E*)-*N*-(phenylmethylene)-2-pyridinamine leads to  $\text{Os}(\text{SnClPh}_2)\{\kappa^2\text{-N,C-(pyNCPH)}\}(\eta^2\text{-H}_2)(\text{P}^i\text{Pr}_3)_2$  (**651**). In this compound, the separation between the hydrogen atoms of the  $\text{OsH}_2$  unit of 1.32 Å is slightly shorter than in the other members of the family (1.4–1.5 Å). So, it is better described as an elongated dihydrogen species.<sup>338</sup>

**3.6.6. N-H and O-H Bond Activations.** Trihydride **311** activates one N-H bond of each NHR group of 1,2-phenylenediamine and *N*-methyl-1,2-phenylenediamine to give the six-coordinate  $d^4$ -dihydrides  $\text{OsH}_2\{\kappa\text{-N,N-(}o\text{-NH-C}_6\text{H}_4\text{-NR)}\}(\text{P}^i\text{Pr}_3)_2$  (R = H (**652**), Me (**653**)),<sup>339</sup> containing an osmabenzimidazolium core. The planarity and the length equalization of the bicycle of these compounds along with

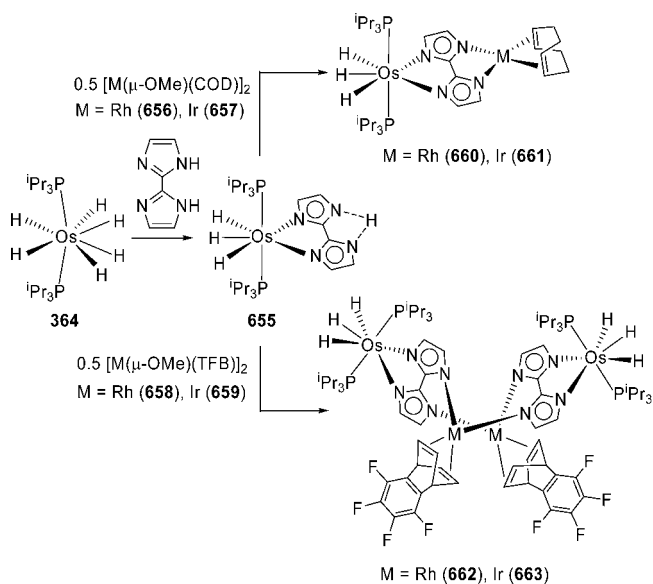
negative NICS values calculated for both rings and the aromatic MO delocalization suggest that, as the organic counterparts, the osmabenzimidazolium moiety of **652** and **653** is aromatic. The frontier HOMO-1 of the  $[\text{OsH}_2(\text{P}^i\text{Pr}_3)_2]^{2+}$  fragment remains nonbonding. In agreement with this, the addition of  $\text{HBF}_4 \cdot \text{OEt}_2$  to diethyl ether solutions of **652** produces its protonation to afford the trihydride  $[\text{OsH}_3\{\kappa\text{-N,N-(}o\text{-NH-C}_6\text{H}_4\text{-NH)}\}(\text{P}^i\text{Pr}_3)_2]\text{BF}_4$  (**654**), in high yield (Scheme 103).<sup>340</sup>

**Scheme 103.** Formation of Compounds Containing an Osmabenzimidazolium Core by Means of N-H Bond Activation of 1,2-Phenylenediamines



Abstraction of a NH-hydrogen atom of 2,2'-biimidazole ( $\text{H}_2\text{biim}$ ) by the hexahydride **364** has been the entry to heterometallic  $\text{Os}(\mu\text{-biim})\text{Rh}$  and  $\text{Os}(\mu\text{-biim})\text{Ir}$  complexes (Scheme 104). The abstraction leads to the classical trihydride

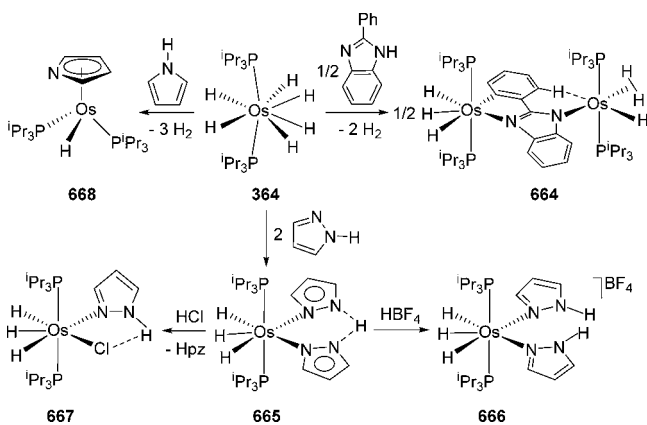
**Scheme 104.** Formation of Heterobimetallic Compounds by Means of the Double N-H Bond Activation of 2,2'-Biimidazole



derivative  $\text{OsH}_3(\text{Hbiim})(\text{P}^i\text{Pr}_3)_2$  (**655**).<sup>341</sup> Treatment of this compound with the dimers  $[\text{M}(\mu\text{-OMe})(\eta^4\text{-COD})]_2$  (M = Rh (**656**), Ir (**657**)) and  $[\text{M}(\mu\text{-OMe})(\eta^4\text{-TFB})]_2$  (M = Rh (**658**), Ir (**659**)) produces the methoxy-mediated abstraction of the second NH-hydrogen atom of the heterocycle to afford the dinuclear complexes  $(\text{P}^i\text{Pr}_3)_2\text{H}_3\text{Os}(\mu\text{-biim})\text{M}(\eta^4\text{-COD})$  (M = Rh (**660**), Ir (**661**)) and the tetranuclear compounds  $[(\text{P}^i\text{Pr}_3)_2\text{H}_3\text{Os}(\mu\text{-biim})\text{M}(\eta^4\text{-TFB})]_2$  (M = Rh (**662**), Ir (**663**)), respectively.<sup>342</sup> In solution, the hydride ligands of these species undergo quantum exchange coupling.

Hexahydride **364** also activates the N-H bond of 2-phenylbenzimidazole,<sup>323</sup> pyrazole (Hpz),<sup>341</sup> and pyrrole<sup>240</sup> (Scheme 105). Refluxing toluene solution of **364** with 0.5

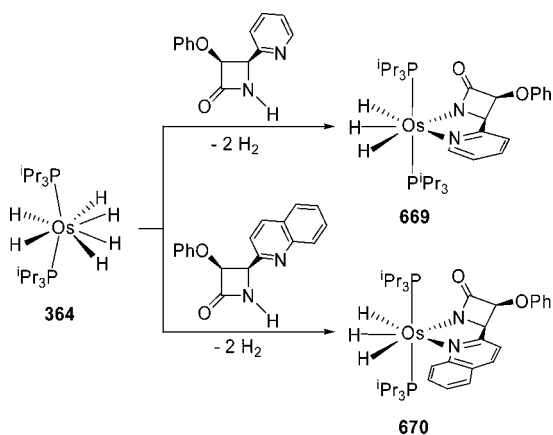
**Scheme 105. N–H Bond Activation of Heterocycles Promoted by 364**



equiv of 2-phenylbenzimidazole leads to the dinuclear compound  $(\text{P}^i\text{Pr}_3)_2\text{H}_3\text{Os}(\text{C}_6\text{H}_4\text{-benzimidazolate})\text{OsH}(\eta^2\text{-H}_2)(\text{P}^i\text{Pr}_3)_2$  (**664**). The formation of this complex can be rationalized as the hexahydride-mediated N–H bond activation of the  $\text{C}_6\text{H}_4$ -benzimidazole ligand of **583**. The N–H activation results in the release of two hydrogen molecules, which generates a coordination vacancy that is saturated by agostic coordination of the remaining *ortho*-CH bond of the metalated phenyl group of **583**. Furthermore, two classical hydrides are converted into an elongated dihydrogen ( $d_{\text{H-H}} = 1.29(1)$  Å). The spectroscopic data and electrochemical behavior of **664** indicate that the mutual influence between the metal centers is negligible.<sup>323</sup> The reaction of **364** with pyrazole gives  $\text{OsH}_3(\text{Hpz})(\text{P}^i\text{Pr}_3)_2$  (**665**), which affords  $[\text{OsH}_3(\text{Hpz})_2(\text{P}^i\text{Pr}_3)_2]\text{BF}_4$  (**666**) and  $\text{OsH}_3\text{Cl}(\text{Hpz})(\text{P}^i\text{Pr}_3)_2$  (**667**) by reaction with  $\text{HBF}_4$  and  $\text{HCl}$ , respectively.<sup>341</sup> Treatment of **364** with pyrrole yields the half-sandwich derivative  $\text{OsH}(\eta^5\text{-C}_5\text{H}_4\text{N})(\text{P}^i\text{Pr}_3)_2$  (**668**).

Chelate-assisted N–H bond activation of 2-azetidinones promoted by **364** has been investigated in the search for new inhibitors of  $\beta$ -lactamases (Scheme 106). This hexahydride reacts with 3-phenoxy-4-(pyridin-2-yl)- and 3-phenoxy-4-(quinol-2-yl)-azetidin-2-one (HAzpy and HAzquin, respectively) to give the osmatrinems  $\text{OsH}_3(\text{Azpy})(\text{P}^i\text{Pr}_3)_2$  (**669**) and  $\text{OsH}_3(\text{Azquin})(\text{P}^i\text{Pr}_3)_2$  (**670**), containing a seven-coordinate  $d^4$ -metal fragment in their skeletons. The X-ray structure

**Scheme 106. Formation of Osmatrinems via N–H Bond Activation of 2-Azetidinones<sup>a</sup>**

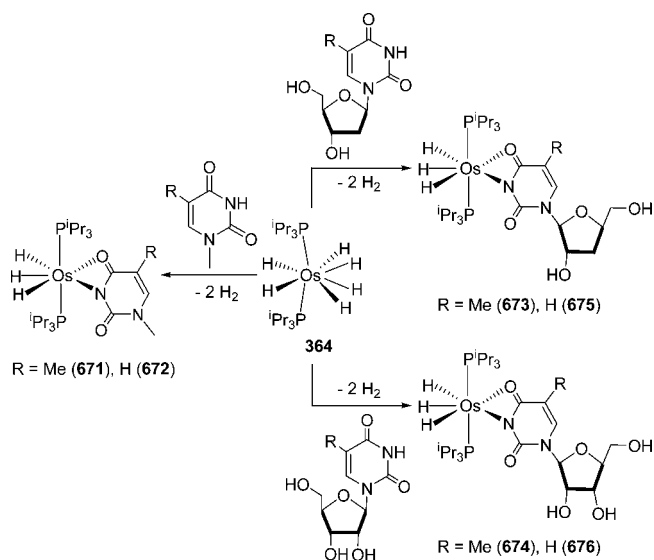


<sup>a</sup>Adapted from ref 343. Copyright 2014 American Chemical Society.

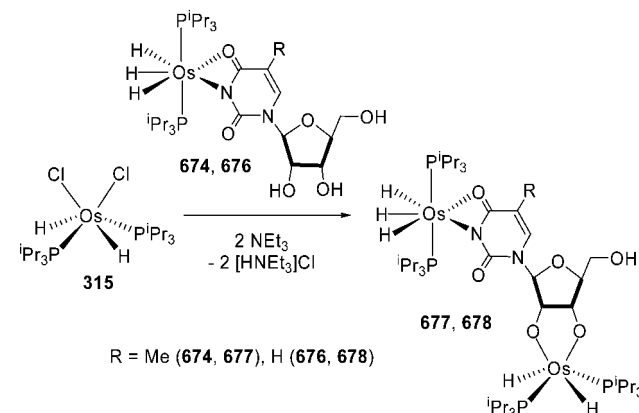
of **669** has revealed that the dihedral angle between the five-membered metalacycle and the four-membered lactamic ring is  $45.0^\circ$ .<sup>343</sup>

The N–H bond activation of pyrimidinic *N*-methyl nucleobases and nucleosides promoted by **364** has also been investigated in the search for model osmium anticancer drugs (Schemes 107 and 108).<sup>344</sup>

**Scheme 107. N–H Bond Activation Reactions of Pyrimidinic *N*-Methyl Nucleobases and Nucleosides Promoted by 364**



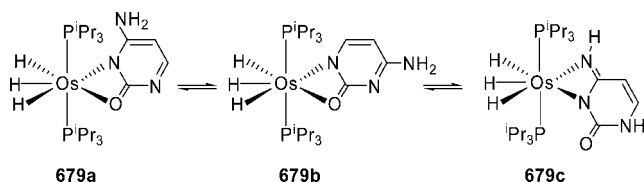
**Scheme 108. Dinuclear Compounds Containing Nucleosides Derived from Ribose**



Treatment of **364** with 1-methylthymine and 1-methyluracil leads to  $\text{OsH}_3(1\text{-methylthyminate})(\text{P}^i\text{Pr}_3)_2$  (**671**) and  $\text{OsH}_3(1\text{-methyluracilate})(\text{P}^i\text{Pr}_3)_2$  (**672**), respectively. The reactions of **364** with thymidine, 5-methyluridine, deoxyuridine, and uridine afford  $\text{OsH}_3(\text{thymidinate})(\text{P}^i\text{Pr}_3)_2$  (**673**),  $\text{OsH}_3(5\text{-methyluridinate})(\text{P}^i\text{Pr}_3)_2$  (**674**),  $\text{OsH}_3(\text{deoxyuridinate})(\text{P}^i\text{Pr}_3)_2$  (**675**), and  $\text{OsH}_3(\text{uridinate})(\text{P}^i\text{Pr}_3)_2$  (**676**), respectively (Scheme 107). Treatment of **674** and **676**, containing nucleosides derived from ribose, with **315** in the presence of  $\text{NEt}_3$  yields the dinuclear species  $\text{OsH}_3(\text{P}^i\text{Pr}_3)_2(\text{nucleobase})\text{-}(\text{ribose})\text{OsH}_2(\text{P}^i\text{Pr}_3)_2$  (**677** and **678**, respectively) formed by two different metal fragments (Scheme 108).

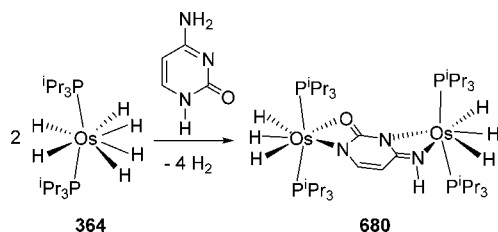
Reactions of **364** with cytosine, deoxycytosine, and cytidine have also been studied.<sup>345</sup> Complex **364** deprotonates cytosine to give the  $d^4$ -trihydride derivative  $\text{OsH}_3(\text{cytosinate})(\text{P}^i\text{Pr}_3)_2$  (**679**), which in solution exists as a mixture of isomers containing  $\kappa^2\text{-N1,O}$  (**679a**) and  $\kappa^2\text{-N3,O}$  (**679b**) amino-oxo and  $\kappa^2\text{-N3,N4}$  (**679c**) imino-oxo tautomers (Scheme 109).

Scheme 109. Coordination Modes of the Cytosinate Anion



Complex **364** is also able to perform the double deprotonation of cytosine to afford the dinuclear derivative  $(\text{P}^i\text{Pr}_3)_2\text{H}_3\text{Os}(\mu\text{-cytosinate}')\text{OsH}_3(\text{P}^i\text{Pr}_3)_2$  (**680**), where the anion is coordinated  $\kappa^2\text{-N1,O}$  and  $\kappa^2\text{-N3,N4}$  to two different  $\text{OsH}_3(\text{P}^i\text{Pr}_3)_2$  moieties (Scheme 110). Deprotonations of deoxycytidine and

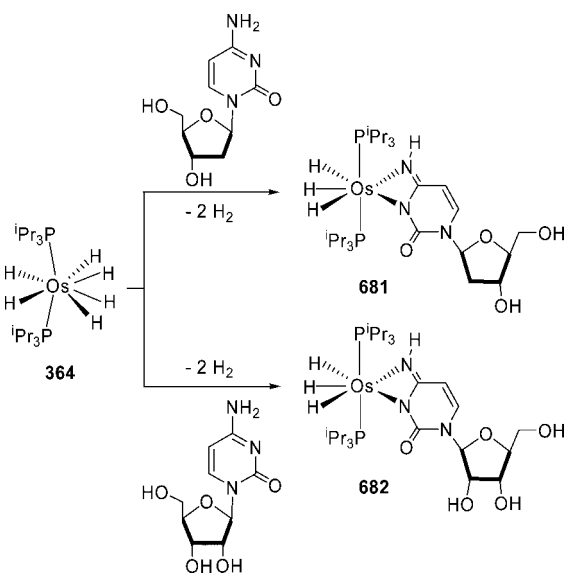
Scheme 110. Double N–H Bond Activation of Cytosine Promoted by **364**



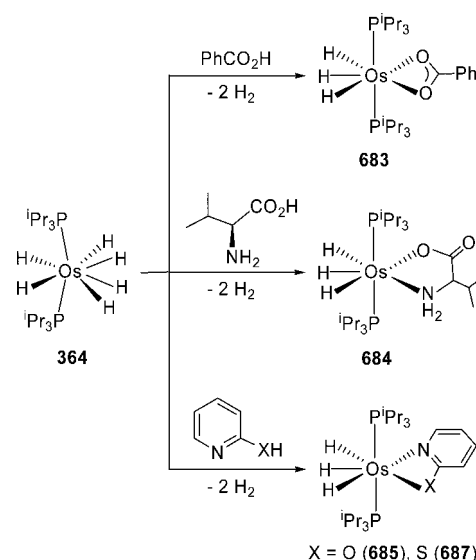
cytidine lead to  $\text{OsH}_3(\text{deoxycytidinate})(\text{P}^i\text{Pr}_3)_2$  (**681**) and  $\text{OsH}_3(\text{cytidinate})(\text{P}^i\text{Pr}_3)_2$  (**682**), respectively, containing the anion  $\kappa^2\text{-N3,N4}$  coordinated (Scheme 111).

Hexahydride **364** also promotes the cleavage of O–H bonds of a wide range of organic molecules, including benzoic acid, L-valine, and 2-hydroxypyridine (Scheme 112). The reactions

Scheme 111. Formation of Deoxycytidinate and Cytidinate Derivatives



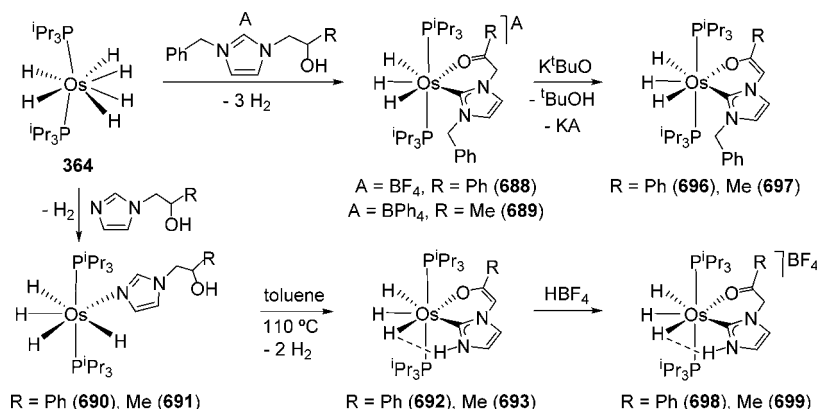
Scheme 112. O–H Bond Activation Reactions Promoted by **364**



lead to the corresponding classical trihydride derivatives  $\text{OsH}_3(\kappa^2\text{-O}_2\text{CPh})(\text{P}^i\text{Pr}_3)_2$  (**683**),<sup>307</sup>  $\text{OsH}_3\{\kappa^2\text{-N,O-}[\text{OC}(\text{O})\text{-CH}(\text{CHMe}_2)\text{NH}_2]\}(\text{P}^i\text{Pr}_3)_2$  (**684**), and  $\text{OsH}_3\{\kappa^2\text{-N,O-(py-2-O)}\}(\text{P}^i\text{Pr}_3)_2$  (**685**).<sup>342</sup> The acetate counterpart of **683**,  $\text{OsH}_3(\kappa^2\text{-O}_2\text{CMe})(\text{P}^i\text{Pr}_3)_2$  (**686**), has been prepared by reaction of the dichloride-dihydride  $\text{OsH}_2\text{Cl}_2(\text{P}^i\text{Pr}_3)_2$  (**315**) with  $\text{KO}_2\text{CMe}$  in methanol.<sup>346</sup> Similarly to 2-hydroxypyridine, 2-thiopyridine reacts with **364** to afford the pyridylthiolate derivative  $\text{OsH}_3\{\kappa^2\text{-N,S-(py-2-S)}\}(\text{P}^i\text{Pr}_3)_2$  (**687**).<sup>342</sup>

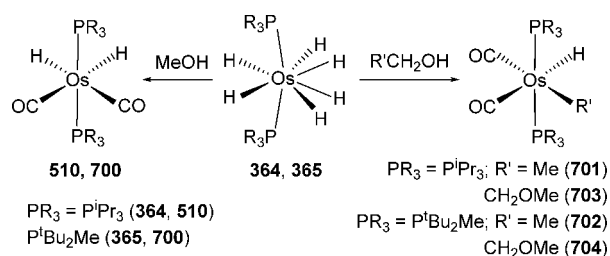
Hexahydride **364** promotes the imidazolium metalation and alcohol dehydrogenation of alcohol-functionalized imidazolium salts and the N-bound to C-bound transformation along with the alcohol deprotonation-dehydrogenation of alcohol-functionalized imidazoles. In the first case, NHC-keto-trihydride compounds are formed, whereas in the second case, NHC-enolate-trihydride derivatives bearing a N–H wingtip are obtained. The conversion between the respective NHC-keto and NHC-enolate is easily achieved by deprotonation-protonation reactions. As a proof of concept, the reactions shown in Scheme 113 have been reported.<sup>347</sup> Treatment of **364** with 3-benzyl-1-(2-hydroxy-2-phenylethyl)imidazolium tetrafluoroborate and 3-benzyl-1-(2-hydroxypropyl)imidazolium tetraphenylborate leads to the NHC-keto complexes  $[\text{OsH}_3\{\kappa^2\text{-C,O-}[\text{CN}(\text{CH}_2\text{Ph})\text{CHCHNCH}_2\text{C}(\text{R})=\text{O}]\}(\text{P}^i\text{Pr}_3)_2]\text{A}$  ( $\text{A} = \text{BF}_4$ ,  $\text{R} = \text{Ph}$  (**688**);  $\text{A} = \text{BPh}_4$ ,  $\text{R} = \text{Me}$  (**689**)), as a consequence of the direct metalation of the heterocycle and the dehydrogenation of the alcohol substituent. Similarly to pyridine, 3- and 4-methylpyridine, 1-(2-hydroxy-2-phenylethyl)imidazole, and 1-(2-hydroxypropyl)imidazole react with **364** to give the classical tetrahydrides  $\text{OsH}_4(\text{Rim})\text{-}(\text{P}^i\text{Pr}_3)_2$  ( $\text{R} = \text{CH}_2\text{CH}(\text{OH})\text{Ph}$  (**690**),  $\text{CH}_2\text{CH}(\text{OH})\text{Me}$  (**691**)), containing a N-bound imidazole ligand. In toluene under reflux, complexes **690** and **691** evolve into the C-bound imidazole derivatives  $\text{OsH}_3\{\kappa^2\text{-C,O-}[\text{CN}(\text{H})\text{CHCHNCH}=\text{C}(\text{R})\text{O}]\}(\text{P}^i\text{Pr}_3)_2$  ( $\text{R} = \text{Ph}$  (**692**),  $\text{Me}$  (**693**)). The deprotonation-dehydrogenation process of the alcohol substituent is determinant for the N-bound to C-bound transformation. In contrast to **690** and **691**, 1-mesityl and 1-methylimidazole complexes  $\text{OsH}_4(\text{MesIm})(\text{P}^i\text{Pr}_3)_2$  (**694**) and  $\text{OsH}_4(\text{MeIm})\text{-}(\text{P}^i\text{Pr}_3)_2$  (**695**) do not undergo tautomerization. An intra-

Scheme 113. Reactions of 364 with Alcohol-Functionalized-Imidazolium Salts and -Imidazoles



molecular hydrogen bond between a hydride and the NH-hydrogen atom of the C-bound heterocycle seems to contribute to the stabilization of **692** and **693**. The deprotonation of **688** and **689** with K<sup>t</sup>BuO affords the corresponding enolate compounds OsH<sub>3</sub>{κ<sup>2</sup>-C,O-[CN(CH<sub>2</sub>Ph)CHCHNCH=C(R)-O]}(P<sup>i</sup>Pr<sub>3</sub>)<sub>2</sub> (R = Ph (**696**), Me (**697**)), whereas the protonation of **692** and **693** with HBF<sub>4</sub>·OEt<sub>2</sub> yields the keto derivatives [OsH<sub>3</sub>{κ<sup>2</sup>-C,O-[CN(H)CHCHNCH<sub>2</sub>C(R)=O]}(P<sup>i</sup>Pr<sub>3</sub>)<sub>2</sub>]<sub>2</sub>BF<sub>4</sub> (R = Ph (**698**), Me (**699**)).

Hexahydride **364** and its P<sup>i</sup>Bu<sub>2</sub>Me-counterpart **365** also show a marked tendency to promote the direct O–H bond activation of primary alcohols. The reactions initially afford alkoxide species, which evolve by β-hydrogen elimination and via aldehyde intermediates into carbonyl compounds. As a consequence, these polyhydrides are unstable in solvents such as methanol, ethanol, and 2-methoxyethanol (Scheme 114).<sup>348</sup>

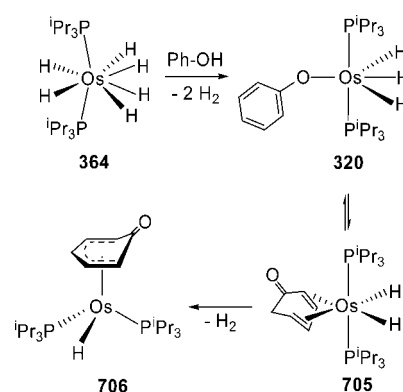
Scheme 114. O–H Bond Activation Reactions of Primary Alcohols Promoted by d<sup>2</sup>-Hexahydride-Osmium Complexes

In methanol, these compounds give the dihydride-dicarbonyl complexes OsH<sub>2</sub>(CO)<sub>2</sub>(PR<sub>3</sub>)<sub>2</sub> (PR<sub>3</sub> = P<sup>i</sup>Pr<sub>3</sub> (**510**), P<sup>i</sup>Bu<sub>2</sub>Me (**700**)). In contrast to methanol, ethanol affords the hydride-methyl-dicarbonyl derivatives OsH(CH<sub>3</sub>)(CO)<sub>2</sub>(PR<sub>3</sub>)<sub>2</sub> (PR<sub>3</sub> = P<sup>i</sup>Pr<sub>3</sub> (**701**), P<sup>i</sup>Bu<sub>2</sub>Me (**702**)). 2-Methoxyethanol behaves similarly to ethanol and yields OsH(CH<sub>2</sub>OMe)(CO)<sub>2</sub>(PR<sub>3</sub>)<sub>2</sub> (PR<sub>3</sub> = P<sup>i</sup>Pr<sub>3</sub> (**703**), P<sup>i</sup>Bu<sub>2</sub>Me (**704**)).

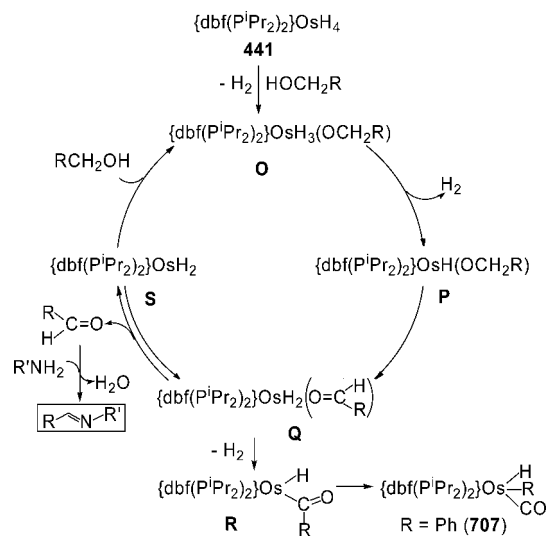
Phenol is a particularly acidic alcohol having no geminal hydrogen atoms. However, it contains a coordinating aromatic ring. The activation of its O–H bond by **364** leads to the trihydride **320**. In toluene, the latter undergoes a reductive elimination-tautomerization process to afford OsH<sub>2</sub>(η<sup>4</sup>-2,4-cyclohexadien-1-one)(P<sup>i</sup>Pr<sub>3</sub>)<sub>2</sub> (**705**). Subsequently, the equilibrium mixture of **320** and **705** evolves into OsH(η<sup>5</sup>-C<sub>6</sub>H<sub>5</sub>O)(P<sup>i</sup>Pr<sub>3</sub>)<sub>2</sub> (**706**) with loss of H<sub>2</sub> (Scheme 115).<sup>240</sup>

The POP-pincer tetrahydride **441** also shows a marked tendency to activate the O–H bond of primary alcohols. In

Scheme 115. O–H Bond Activation of Phenol Promoted by 364



agreement with **364** and **365**, complex **441** reacts with benzyl alcohol to afford the hydride-aryl-carbonyl derivative OsH(Ph)(CO){dbf(P<sup>i</sup>Pr<sub>2</sub>)<sub>2</sub>} (**707**). Its formation has been rationalized through the intermediates O–R shown in Scheme 116. The O–H bond activation of the alcohol by **441** could initially afford **O**, which should give the unsaturated species **P** by

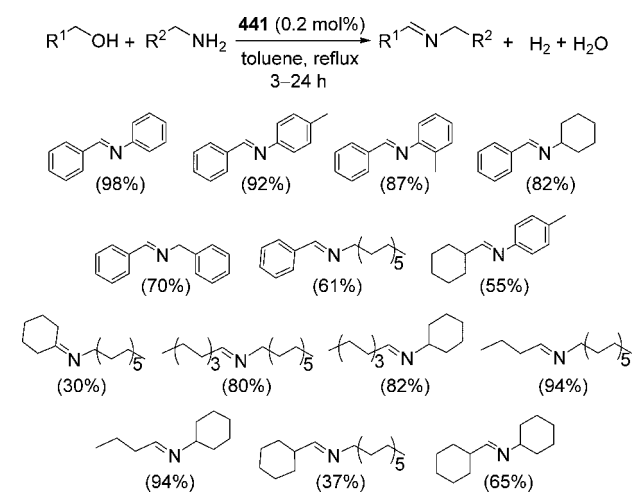
Scheme 116. Catalytic Cycle for the 441-Mediated Formation of Imines from Alcohols and Amines<sup>a</sup>

<sup>a</sup>Adapted from ref 289. Copyright 2011 American Chemical Society.

dissociation of H<sub>2</sub>. A  $\beta$ -elimination reaction in the alkoxide group could lead to the dihydride-aldehyde **Q**, which should generate the acyl intermediate **R**. Finally, the deinsertion of the phenyl group should give **707**.

Intermediate **Q** dissociates the aldehyde to afford an equilibrium mixture with the unsaturated dihydride **S**. Thus, when the reaction is carried out in the presence of a primary amine, the corresponding imine is formed. Because the addition of the O–H bond of the alcohol to **S** regenerates **O**, complex **441** catalyzes the selective formation of a variety of imines from alcohols and amines with liberation of H<sub>2</sub> under an argon atmosphere (Scheme 117). The reactions include the formation of aliphatic imines, which are inherently more challenging due to their instability.<sup>289</sup>

**Scheme 117.** Scope of the 441-Mediated Formation of Imines from Alcohols and Amines



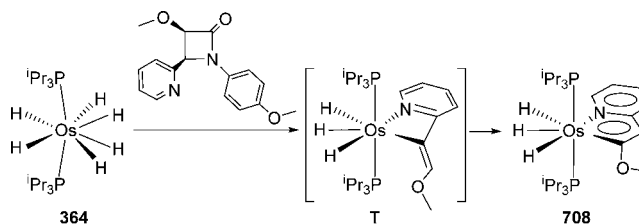
The PNP-pincer tetrahydride **452** couples primary alcohols and primary amines to afford secondary amines, in contrast to **441**. In addition, it operates as an efficient catalyst for reactions of dehydrogenative coupling of primary alcohols to symmetrical esters and for the hydrogen transfer from 2-propanol to acetophenone and cyclohexanone.<sup>291</sup> The *cis*-hydride-dihydrogen **394** is an efficient catalyst precursor for the hydrogen transfer from 2-propanol to  $\alpha,\beta$ -unsaturated ketones. In contrast to its ruthenium counterpart, complex **71**, the reduction leads to the saturated ketone via isomerization of the initially produced allylic alcohol.<sup>131</sup> The equilibrium mixture of the dihydride **300** and the dihydride-dihydrogen **345** catalyzes the hydrogen transfer from 2-propanol to  $\alpha,\beta$ -unsaturated ketones to afford the saturated alcohol via the saturated ketone.<sup>210,211</sup>

**3.6.7. Other  $\sigma$ -Bond Activations.** Hexahydride **364** is probably the transition metal-polyhydride with the highest capacity to break  $\sigma$ -bonds. As a consequence, it has been used to achieve less common ruptures, including the B-type fragmentation of the four-membered core of  $\beta$ -lactams, the cleavage of an exocyclic N–C bond of nucleobases, a C–OR bond activation, and the selective *ortho*-CF bond activation of aromatic ketones in the presence of weaker *ortho*-CH bonds.

The thermal B-type fragmentation of the four-membered ring of a  $\beta$ -lactam, involving the breakage of the N1–C4 and C2–C3 bonds is a difficult reaction with an energy barrier of more than 40 kcal mol<sup>–1</sup>. It is a concerted asynchronous [2 + 2] cycloreversion, which takes place with complete retention of

the stereochemistry to afford a C3–C4 olefin and a N1–C2–O isocyanate. The replacement of the NH-hydrogen atom of 4-(2-pyridyl)azetidin-2-ones by aryl protects the nitrogen atom against the metal center of **364**, which is directed toward the C4–H bond of the four-membered ring. The addition of this bond to the metal center allows the active participation of an osmium lone pair in the B-type  $\beta$ -lactam fragmentation process. The breakage of the N1–C4 and C2–C3 bonds is now thermally accessible through a stepwise process, which implies a much lower barrier than the concerted asynchronous mechanism of the fragmentation without metal. As a consequence, instead of osmatrinems related to **669** and **670**, the reaction of **364** with ( $\pm$ )-*cis*-1-(4-methoxyphenyl)-3-methoxy-4-(pyridine-2-yl)azetidin-2-one leads to OsH<sub>3</sub>{ $\kappa^2$ -N,C-(py-2-CHCOMe)}(P<sup>i</sup>Pr<sub>3</sub>)<sub>2</sub> (**708**) after the expansion of the four-membered heterometalating of the resulting intermediate OsH<sub>3</sub>{ $\kappa^2$ -N,C-[py-2-C=C(OMe)H]}(P<sup>i</sup>Pr<sub>3</sub>)<sub>2</sub> (**T** in Scheme 118), which involves 1,2-metal and -hydrogen shifts.<sup>349</sup>

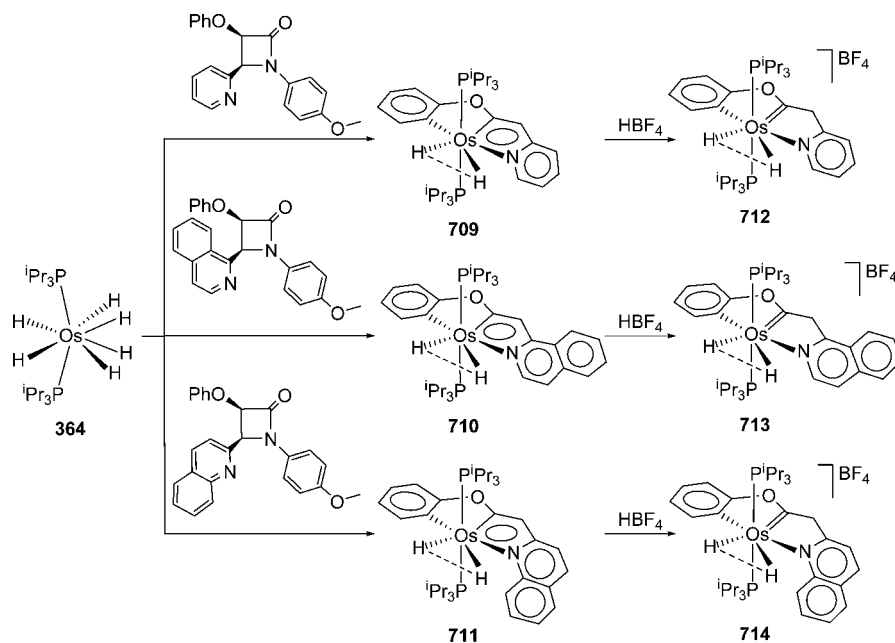
**Scheme 118.** B-Type Fragmentation of the Four-Membered Ring of ( $\pm$ )-*cis*-1-(4-methoxyphenyl)-3-methoxy-4-(pyridine-2-yl)azetidin-2-one Promoted by **364**



The arene C–H bond activation is thermodynamically and kinetically favored with regard to the alkane C–H bond activation. This fact has allowed the preparation of novel C,C',N-pincer complexes by means of the replacement of the methoxy substituent at the 3-position of the lactamic four-membered ring by a phenoxy group (Scheme 119). Reactions of **364** with ( $\pm$ )-*cis*-1-(4-methoxyphenyl)-3-phenoxy-4-(pyridine-2-yl)azetidin-2-one, ( $\pm$ )-*cis*-1-(4-methoxyphenyl)-3-phenoxy-4-(isoquinolin-2-yl)azetidin-2-one, and ( $\pm$ )-*cis*-1-(4-methoxyphenyl)-3-phenoxy-4-(quinolin-2-yl)azetidin-2-one lead to the compressed dihydrides OsH<sub>2</sub>{ $\kappa^3$ -C,C,N-(C<sub>6</sub>H<sub>4</sub>OCCH<sub>2</sub>-2-L)}(P<sup>i</sup>Pr<sub>3</sub>)<sub>2</sub> (L = py (**709**), isoquin (**710**), quin (**711**)), containing a dianionic C,C',N-pincer ligand, as a result of the degradation of the azetidinones and the additional *ortho*-CH bond activation of the phenoxy group. Complexes **709**–**711** add HBF<sub>4</sub> to yield [OsH<sub>2</sub>{ $\kappa^3$ -C,C,N-(C<sub>6</sub>H<sub>4</sub>OCCH<sub>2</sub>-2-L)}(P<sup>i</sup>Pr<sub>3</sub>)<sub>2</sub>](BF<sub>4</sub>) (L = py (**712**), isoquin (**713**), quin (**714**)) as a consequence of the protonation of the dianionic C,C',N-pincer ligand. The hydride ligands of **709**–**714** undergo quantum mechanical exchange coupling, which has been quantified according to eq 1. The comparison of the results reveals that the phenomenon is particularly intense for cations **712**–**714**. Furthermore, in these compounds the separation between the hydrides is  $\sim 0.1$  Å shorter than in the respective neutral species **709**–**711**, whereas the hydride hard sphere radius increases by  $\sim 10\%$  and the  $\nu$  value decreases by  $\sim 20\%$ .<sup>350</sup>

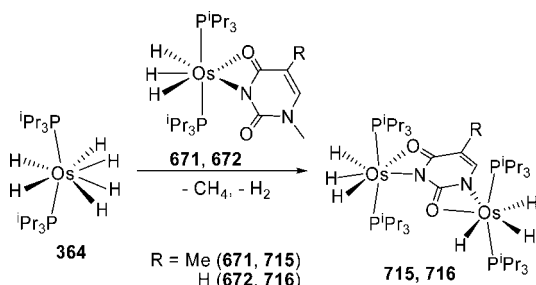
Hexahydride **364** also promotes the cleavage of the N–Me bond of the ligands 1-methylthymine and 1-methyluracil of **671** and **672** to give the dinuclear species [OsH<sub>3</sub>(P<sup>i</sup>Pr<sub>3</sub>)<sub>2</sub>]<sub>2</sub>( $\mu$ -thymine) (**715**) and [OsH<sub>3</sub>(P<sup>i</sup>Pr<sub>3</sub>)<sub>2</sub>]<sub>2</sub>( $\mu$ -uracil) (**716**)

Scheme 119. Formation of CCN-Pincer Complexes



with the nucleobase skeleton  $\kappa^2$ -N,O-coordinated to both metal fragments (Scheme 120).<sup>344</sup>

Scheme 120. Cleavage of the N–Me Bond of 1-Methyl-Thymine and 1-Methyluracil

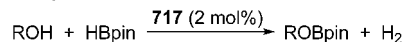


Catalysts based on cooperative ligands are having great relevance in reactions associated with conversion and storage of regenerative energy. These ligands cooperate with the metal center by participating directly in the  $\sigma$ -bond activation stage and by performing the reversible structural change in the process of product formation. A problem for the use of NHC ligands in metal–ligand cooperating catalysis is to keep the cooperation capacity between the Lewis base tethered to the imidazole moiety and the metal center, after the carbene coordination. Hexahydride **364** activates the C–OMe bond of 1-(2-methoxy-2-oxoethyl)-3-methylimidazolium chloride, in addition to promoting the direct metalation of the imidazolium group, to afford the five coordinate complex  $\text{OsCl}\{\text{C}(\text{O})\text{CH}_2\text{Im}\}(\text{P}^i\text{Pr}_3)_2$  (**717**), which is a metal ligand cooperating catalyst for the generation of molecular hydrogen by means of both the alcoholysis and the hydrolysis of HBpin (Scheme 121), via intermediates  $\text{OsHCl}\{\text{C}(\text{OBpin})\text{CH}_2\text{Im}\}(\text{P}^i\text{Pr}_3)_2$  (**718**) and  $\text{OsCl}\{\text{C}(\text{O})\text{CH}_2\text{Im}\}(\eta^2\text{-H}_2)(\text{P}^i\text{Pr}_3)_2$  (**719**).<sup>351</sup>

Hexahydride **364** activates *ortho*-CF bonds of aromatic ketones, in addition to *ortho*-CH bonds (Scheme 122). Thus, the reactions of this polyhydride with pentafluoroacetophenone, decafluorobenzophenone, and 2,6-difluoroacetophenone

Scheme 121. C–OMe Bond Activation of 1-(2-Methoxy-2-oxoethyl)-3-methylimidazolium Promoted by **364**: Formation of **717** and its Catalytic Properties

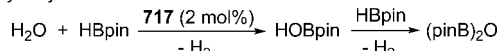
i) alcoholysis



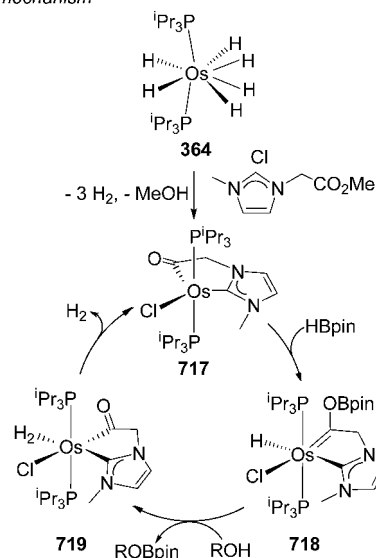
R (TOF<sub>50%</sub>, h<sup>-1</sup>) = Me (3644), Et (2108), <sup>t</sup>Bu (1395),

<sup>n</sup>Oct (1364), CH<sub>2</sub>Ph (1393), <sup>i</sup>Pr (365), <sup>t</sup>Bu (62), Ph (313)

ii) hydrolysis

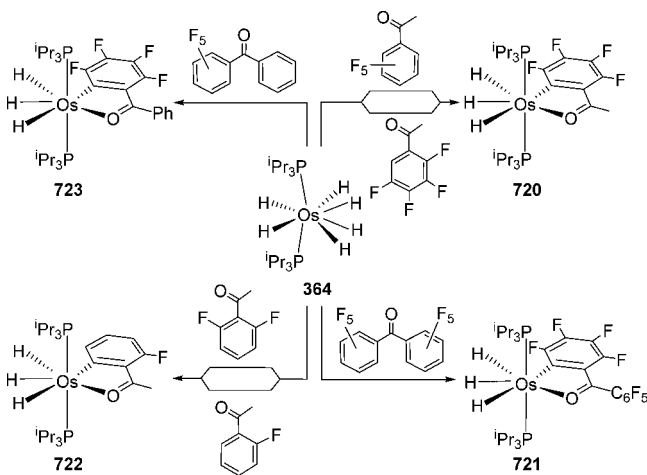


iii) mechanism



give HF and the trihydride derivatives  $\text{OsH}_3\{\kappa^2\text{-O,C-}[\text{OC}(\text{R})\text{-C}_6\text{F}_4]\}(\text{P}^i\text{Pr}_3)_2$  (R = Me (**720**), C<sub>6</sub>F<sub>5</sub> (**721**)) and  $\text{OsH}_3\{\kappa^2\text{-O,C-}[\text{OC}(\text{Me})\text{C}_6\text{H}_3\text{F}]\}(\text{P}^i\text{Pr}_3)_2$  (**722**), respectively. Complexes **720** and **722** are also obtained from the reactions of **364** with 2,3,4,5-tetrafluoroacetophenone and 2-fluoroacetophenone, respectively, indicating that for ketones with only one aromatic

**Scheme 122. Reactions of 364 with Fluorinated Aromatic Ketones: *ortho*-CF Cleavage versus *ortho*-CH Bond Activation**



ring, the *ortho*-CH bond activation is preferred over the *ortho*-CF bond activation. However, the *ortho*-CF activation is preferred over the *ortho*-CH bond activation for 2,3,4,5,6-pentafluoroacetophenone. The reaction of **364** with this ketone leads to  $\text{OsH}_3\{\kappa^2\text{-O,C-}[\text{OC}(\text{C}_6\text{H}_5)\text{C}_6\text{F}_4]\}(\text{P}^i\text{Pr}_3)_2$  (**723**). DFT calculations suggest that the hexahydride promoted C–F bond activation of aromatic ketones is thermodynamically favored over the C–H bond activation, due to the formation of HF. So, the preferred C–H activation of 2-fluoroacetophenone and 2,3,4,5-tetrafluoroacetophenone appears to have kinetic origin, which has been related with the preferred anti arrangement of the F–C–C–C=O unit of the starting ketones.<sup>312</sup>

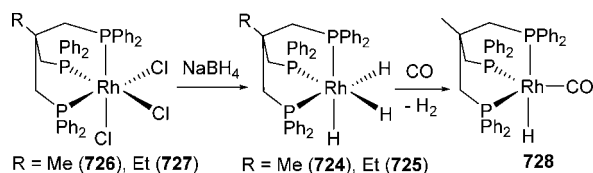
#### 4. RHODIUM

Rhodium hydride complexes have acquired great importance in homogeneous catalysis because of their hydrogenating properties. However, rhodium polyhydrides are rare as a consequence of the oxidizing character of this metal, which prevents high oxidation states. Thus, the majority of them show nonclassical interactions between the hydrogen atoms coordinated to the metal center and play a relevant role in processes associated with the storage of molecular hydrogen.

Classical trihydride complexes  $\text{RhH}_3(\text{triphos}^{\text{R}})$  ( $\text{triphos}^{\text{R}} = \text{MeC}(\text{CH}_2\text{PPh}_2)_3$ ) (**724**) and  $(\text{EtC}(\text{CH}_2\text{PPh}_2)_3)$  (**725**) have been prepared by replacement of chloride by hydride from  $\text{RhCl}_3(\text{triphos}^{\text{R}})$  ( $\text{R} = \text{Me}$  (**726**),  $\text{Et}$  (**727**)). In agreement with the trend of rhodium(III) to undergo reduction, complex **724** reacts with CO to give the carbonyl derivative  $\text{RhH}(\text{CO})(\text{triphos}^{\text{Me}})$  (**728** in Scheme 123).<sup>352</sup>

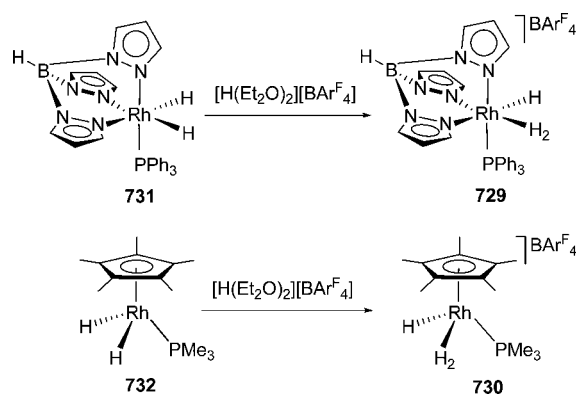
In contrast to **724** and **725**, the Tp- and Cp\*-complexes  $[\text{RhHTp}(\eta^2\text{-H}_2)(\text{PPh}_3)][\text{BAR}^{\text{F}_4}]$  (**729**)<sup>353</sup> and  $[\text{RhH}(\eta^5\text{-$

**Scheme 123. Rhodium Complexes Containing Tripodal Phosphine Ligands**



$\text{C}_5\text{Me}_5)(\eta^2\text{-H}_2)(\text{PMe}_3)][\text{BAR}^{\text{F}_4}]$  (**730**)<sup>354</sup> are hydride-dihydrogen derivatives. In both compounds the separation between the hydrogen atoms of the coordinated hydrogen molecule is about 0.9 Å, whereas the barrier ( $\Delta G^\ddagger$ ) for the exchange of hydride with dihydrogen sites is less than ca. 5 kcal mol<sup>-1</sup>. The Tp complex **729**, which is stable in solution up to 250 K, is generated by addition of 1 equiv of  $[\text{H}(\text{Et}_2\text{O})_2][\text{BAR}^{\text{F}_4}]$  to dichloromethane solutions of the dihydride  $\text{RhH}_2\text{Tp}(\text{PPh}_3)$  (**731**). The protonation of the Cp\*-dihydride  $\text{RhH}_2(\eta^5\text{-C}_5\text{Me}_5)(\text{PMe}_3)$  (**732**) gives **730** (Scheme 124), with

**Scheme 124. Hydride-Dihydrogen–Rhodium(III) Complexes with Tris(pyrazolyl)borate and Pentamethylcyclopentadienyl Ligands**

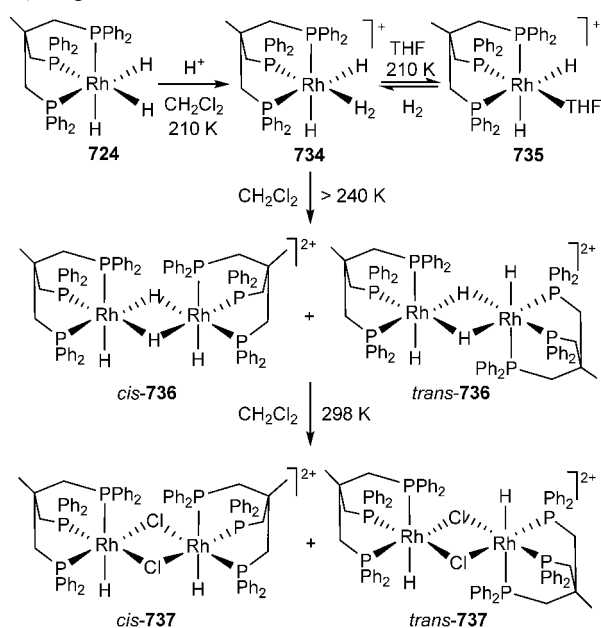
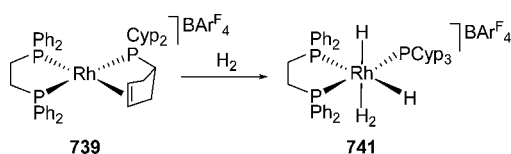


concomitant formation of the side dimer  $[\{\text{RhH}(\eta^5\text{-C}_5\text{Me}_5)(\text{PMe}_3)\}_2(\mu\text{-H})][\text{BAR}^{\text{F}_4}]$  (**733**). A free energy of activation of 9.1 kcal mol<sup>-1</sup> was measured for the exchange of terminal and bridging hydrides in this complex.

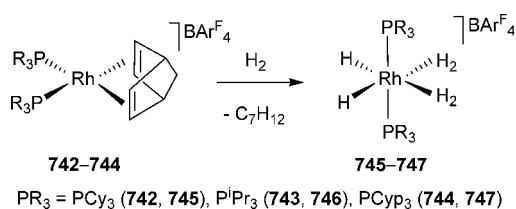
Rhodium complexes with four coordinated hydrogen atoms are dihydride-dihydrogen species. The protonation of the classical trihydride **724** at 210 K gives  $[\text{RhH}_2(\text{triphos}^{\text{Me}})(\eta^2\text{-H}_2)]^+$  (**734**;  $d_{\text{H}_2} \approx 0.9$  Å), which is thermally unstable. Above 240 K, it dissociates the coordinated hydrogen molecule. The resulting dihydride is trapped by coordinating solvents, such as THF, to afford the solvato complex  $[\text{RhH}_2(\text{triphos}^{\text{Me}})(\text{THF})]^+$  (**735**). In dichloromethane, the dimerization of the unsaturated dihydride leads to  $[\{\text{RhH}(\text{triphos}^{\text{Me}})\}(\mu\text{-H})_2]^{2+}$  (**736**), as a mixture of cis and trans isomers that are transformed into the corresponding bridging chloride dimers  $[\{\text{RhH}(\text{triphos}^{\text{Me}})\}(\mu\text{-Cl})_2]^{2+}$  (**737**) at room temperature (Scheme 125).<sup>355</sup> The Tp<sup>Me2</sup>-derivative  $\text{RhH}_2\text{Tp}^{\text{Me}_2}(\eta^2\text{-H}_2)$  (**738**) is, however, stable in the solid state.<sup>356,357</sup> DFT calculations have confirmed the dihydride-dihydrogen structure, which presents a near octahedral arrangement of the ligands around the metal center.<sup>358</sup> The barrier for the rotation of the dihydrogen ligand and the separation between the hydrogen atoms, calculated from data of inelastic neutron scattering spectroscopy, are 0.56(2) kcal mol<sup>-1</sup> and 0.94 Å, respectively.<sup>359</sup>

The salt  $[\text{Rh}\{\text{Ph}_2\text{P}(\text{CH}_2)_2\text{PPh}_2\}\{\text{PCyp}_2(\eta^2\text{-C}_5\text{H}_7)\}][\text{BAR}^{\text{F}_4}]$  (**739**), which is quantitatively formed by reaction of  $\text{NaBAR}^{\text{F}_4}$  with  $\text{RhCl}\{\text{Ph}_2\text{P}(\text{CH}_2)_2\text{PPh}_2\}(\text{PCyp}_3)$  (**740**), is easily hydrogenated under 1 atm of H<sub>2</sub> to give the dihydride-dihydrogen complex  $[\text{RhH}_2(\eta^2\text{-H}_2)\{\text{Ph}_2\text{P}(\text{CH}_2)_2\text{PPh}_2\}(\text{PCyp}_3)][\text{BAR}^{\text{F}_4}]$  (**741**;  $d_{\text{H}_2} \approx 0.9$  Å), according to Scheme 126.<sup>360</sup>

The hydrogenation of the Osborn-type complexes  $[\text{Rh}(\eta^4\text{-NBD})(\text{PR}_3)_2][\text{BAR}^{\text{F}_4}]$  ( $\text{PR}_3 = \text{PCy}_3$  (**742**),  $\text{P}^i\text{Pr}_3$  (**743**),  $\text{PCyp}_3$  (**744**)), under 4 atm of H<sub>2</sub>, at 298 K affords the dihydride-

**Scheme 125. Formation and Reactions of the Dihydride-Dihydrogen-Rhodium(III) Cation 734****Scheme 126. Formation of the Dihydride-Dihydrogen-Rhodium(III) Cation 741**

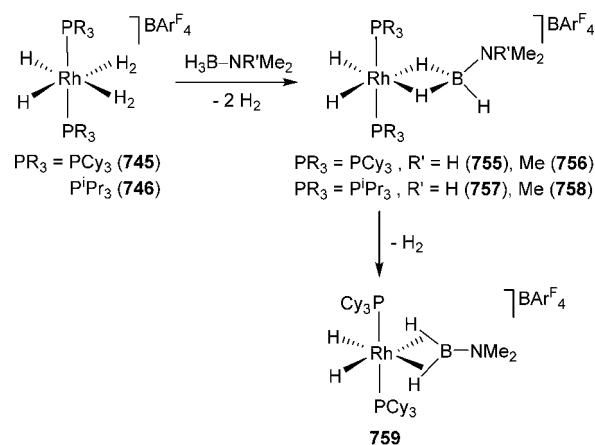
bis(dihydrogen) derivatives  $[\text{RhH}_2(\eta^2\text{-H}_2)_2(\text{PR}_3)_2][\text{BAR}^{\text{F}}_4]$  ( $\text{PR}_3 = \text{PCy}_3$  (745),  $\text{P}^i\text{Pr}_3$  (746),  $\text{PCyP}_3$  (747)).<sup>360</sup> DFT calculations support the  $d^6$ -dihydride-bis(dihydrogen) formulation, with *cis*-hydride ligands and H–H distances between the hydrogen atoms of the dihydrogen ligands of about 0.8 Å (Scheme 127). At room temperature, complexes 745 and 746

**Scheme 127. Formation of Dihydride-bis(Dihydrogen)-Rhodium(III) Complexes**

lose  $[\text{HPR}_3][\text{BAR}^{\text{F}}_4]$  and  $\text{H}_2$  to give the dicationic cluster compounds  $[\text{Rh}_6(\text{PR}_3)_6(\mu\text{-H})_{12}][\text{BAR}^{\text{F}}_4]_2$  ( $\text{PR}_3 = \text{PCy}_3$  (748),  $\text{P}^i\text{Pr}_3$  (749)), in moderate yields. The 12 hydride ligands bridge each Rh–Rh edge of a regular octahedron. Both clusters reversibly take up two molecules of hydrogen to generate  $[\text{Rh}_6(\text{PR}_3)_6\text{H}_{16}][\text{BAR}^{\text{F}}_4]_2$  ( $\text{PR}_3 = \text{PCy}_3$  (750),  $\text{P}^i\text{Pr}_3$  (751)), with 16 hydrogen atoms surrounding the metal core. The uptake of  $\text{H}_2$  is a consequence of two low-lying unoccupied molecular orbitals that readily accept two electron pairs.<sup>362</sup> The hydrogenation of 743 in the presence of  $[\text{Rh}(\eta^4\text{-NBD})_2][\text{BAR}^{\text{F}}_4]$  (752) leads to an inseparable mixture of

$[\text{Rh}_7(\text{P}^i\text{Pr}_3)_6\text{H}_{18}][\text{BAR}^{\text{F}}_4]_2$  (753) and  $[\text{Rh}_8(\text{P}^i\text{Pr}_3)_6\text{H}_{16}][\text{BAR}^{\text{F}}_4]_2$  (754).<sup>363</sup>

The dihydrogen ligands of the dihydride-bis(dihydrogen) complexes 745 and 746 can be displaced by amine-boranes to give the dihydride-(amine-borane) derivatives  $[\text{RhH}_2(\kappa^2\text{-H}_2\text{BHN}(\text{R}')\text{Me}_2)(\text{PR}_3)_2][\text{BAR}^{\text{F}}_4]$  ( $\text{PR}_3 = \text{PCy}_3$ ,  $\text{R}' = \text{H}$  (755),  $\text{Me}$  (756);  $\text{PR}_3 = \text{P}^i\text{Pr}_3$ ,  $\text{R}' = \text{H}$  (757),  $\text{Me}$  (758)), which can also be obtained by oxidative addition of  $\text{H}_2$  to the corresponding bis(phosphine)-rhodium(I)-(amine-borane) precursors. In 1,2-difluorobenzene, these compounds undergo three H/H exchange processes with activation barriers increasing in the sequence B–H bridging/terminal < Rh–H/external  $\text{H}_2$  < Rh–H/B–H.<sup>364</sup> Furthermore, they are only moderately stable. In agreement with this, it has been observed that the amine-borane ligand of 755 slowly loses  $\text{H}_2$  to afford the aminoborane derivative  $[\text{RhH}_2(\eta^2, \eta^2\text{-H}_2\text{BNMe}_2)(\text{PCy}_3)_2][\text{BAR}^{\text{F}}_4]$  (759 in Scheme 128).<sup>365</sup> Related (amine-borane)- and

**Scheme 128. Reactions of 745 and 746 with Amine-Boranes**

(aminoborane)-rhodium(III) complexes containing NHC ligands instead of  $\text{PR}_3$  groups have been prepared from the unsaturated  $\text{RhH}_2\text{Cl}(\text{IMes})_2$  starting material in the presence of  $\text{Na}[\text{BAR}^{\text{F}}_4]$ .<sup>366,367</sup>

These types of compounds have been proposed as relevant intermediates in the rhodium-promoted kinetically controlled dehydrocoupling of ammonia-borane and secondary amine-boranes.<sup>368–371</sup> The mechanism appears to be very dependent on the substrate. Lloyd-Jones, Weller, and co-workers have recently shown a remarkable diversity in mechanisms. Their study suggests a number of key processes, including dehydrogenation by catalytic cycles that can involve a change in oxidation state at rhodium or have a constant oxidation state; autocatalysis; parallel catalysis; B–N bond cleavage; and dehydrocyclization.<sup>365</sup>

## 5. Iridium

### 5.1. Phosphine Complexes

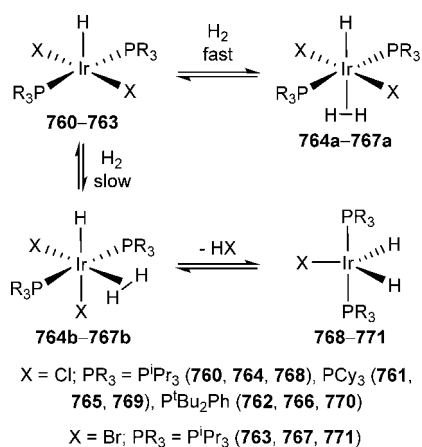
Phosphine ligands stabilize a wide range of polyhydrides, which include complexes with three, four, five, and six hydrogen atoms directly bound to the metal center.

The five-coordinate iridium(III) complexes  $\text{IrHX}_2(\text{PR}_3)_2$  ( $\text{X} = \text{Cl}$ ,  $\text{PR}_3 = \text{P}^i\text{Pr}_3$  (760),  $\text{PCy}_3$  (761),  $\text{P}^i\text{Bu}_2\text{Ph}$  (762);  $\text{X} = \text{Br}$ ,  $\text{PR}_3 = \text{P}^i\text{Pr}_3$  (763)) rapidly react with  $\text{H}_2$  to set up an equilibrium with *trans*- $\text{IrHX}_2(\eta^2\text{-H}_2)(\text{PR}_3)_2$  ( $\text{X} = \text{Cl}$ ,  $\text{PR}_3 = \text{P}^i\text{Pr}_3$  (764a),  $\text{PCy}_3$  (765a),  $\text{P}^i\text{Bu}_2\text{Ph}$  (766a);  $\text{X} = \text{Br}$ ,  $\text{PR}_3 = \text{P}^i\text{Pr}_3$  (767a)) where the elongated dihydrogen ligand binds



trans to the original hydride. A second slower reaction forms the corresponding *cis*-isomers **764b–767b**, where the *cis* disposition of the halides, and also H *cis* to H<sub>2</sub>, has been demonstrated by means of the neutron diffraction structure of **764b**. Interestingly, the iridium–hydride bond length of 1.584(3) Å is not significantly different from the separation of the iridium atom to the hydrogen atoms of the elongated dihydrogen (1.537(19) and 1.550(17) Å), indicating a strong binding of the latter. Consistently with this conclusion, the H–H distance within the dihydrogen is long, 1.11(3) Å. In contrast to the *trans* isomers, the *cis*-isomers show rapid site exchange between coordinated hydride and elongated dihydrogen. The *cis*-isomers can also be induced to lose HX to form the corresponding unsaturated iridium(III)-dihydride derivatives IrH<sub>2</sub>X(PR<sub>3</sub>)<sub>2</sub> (X = Cl, PR<sub>3</sub> = P<sup>i</sup>Pr<sub>3</sub> (**768**), PCy<sub>3</sub> (**769**), P<sup>t</sup>Bu<sub>2</sub>Ph (**770**); X = Br, PR<sub>3</sub> = P<sup>i</sup>Pr<sub>3</sub> (**771**) in Scheme 129).

Scheme 129. Formation of IrHX<sub>2</sub>(η<sup>2</sup>-H<sub>2</sub>)(PR<sub>3</sub>)<sub>2</sub> Complexes



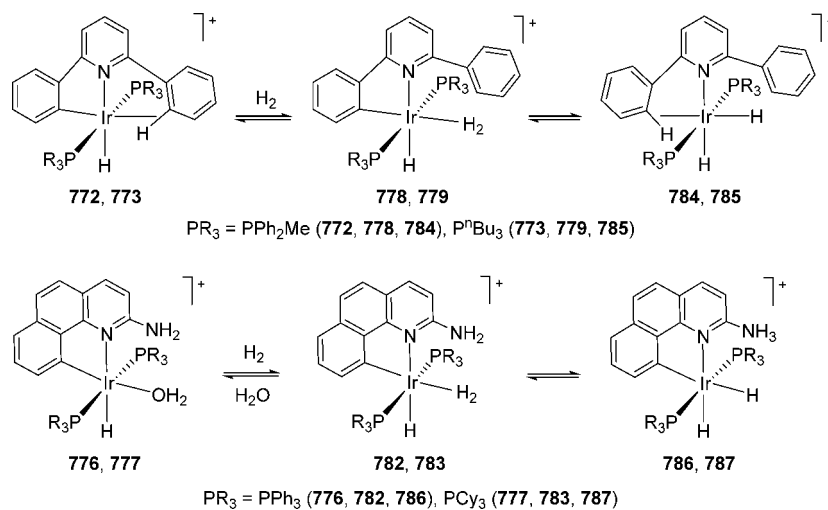
The formation of **768–771** can be rationalized as an inner-sphere process of heterolytic H–H bond activation. The outer sphere heterolytic activation of the coordinated hydrogen molecule, promoted by an external base at a cooperating ligand, has also been described (Scheme 130).<sup>375</sup> Molecular hydrogen rapidly and reversibly displaces the Ir–H–C agostic interaction between the metal center and an *ortho*-CH bond of the phenyl substituent of the orthometalated 2,6-diphenylpyridine in

[IrH{κ<sup>2</sup>-N,C-(Ph-py-C<sub>6</sub>H<sub>4</sub>)}(PR<sub>3</sub>)<sub>2</sub>]SbF<sub>6</sub> (PR<sub>3</sub> = PPh<sub>2</sub>Me (**772**), P<sup>n</sup>Bu<sub>3</sub> (**773**)) and the water molecule of [IrH(bq)-(H<sub>2</sub>O)(PR<sub>3</sub>)<sub>2</sub>]SbF<sub>6</sub> (PR<sub>3</sub> = PPh<sub>3</sub> (**774**), PCy<sub>3</sub> (**775**)) and [IrH(bq-NH<sub>2</sub>)(H<sub>2</sub>O)(PR<sub>3</sub>)<sub>2</sub>]BF<sub>4</sub> (bq-NH<sub>2</sub> = 2-amino-7,8-benzoquinolate; PR<sub>3</sub> = PPh<sub>3</sub> (**776**), PCy<sub>3</sub> (**777**)) to give the *cis*-hydride-dihydrogen derivatives [IrH{κ<sup>2</sup>-N,C-(Ph-py-C<sub>6</sub>H<sub>4</sub>)}(η<sup>2</sup>-H<sub>2</sub>)(PR<sub>3</sub>)<sub>2</sub>]SbF<sub>6</sub> (PR<sub>3</sub> = PPh<sub>2</sub>Me (**778**), P<sup>n</sup>Bu<sub>3</sub> (**779**)),<sup>376</sup> [IrH(bq)(η<sup>2</sup>-H<sub>2</sub>)(PR<sub>3</sub>)<sub>2</sub>]SbF<sub>6</sub> (PR<sub>3</sub> = PPh<sub>3</sub> (**780**), PCy<sub>3</sub> (**781**)),<sup>377</sup> and [IrH(bq-NH<sub>2</sub>)(η<sup>2</sup>-H<sub>2</sub>)(PR<sub>3</sub>)<sub>2</sub>]BF<sub>4</sub> (PR<sub>3</sub> = PPh<sub>3</sub> (**782**), PCy<sub>3</sub> (**783**)),<sup>378</sup> respectively, with a H–H distance between the hydrogen atoms of the dihydrogen ligand of about 0.9 Å. At 0 °C, complexes **778** and **779** reach an equilibrium with the hydrogenolysis dihydride products [IrH<sub>2</sub>(pyPh<sub>2</sub>)-(PR<sub>3</sub>)<sub>2</sub>]SbF<sub>6</sub> (PR<sub>3</sub> = PPh<sub>2</sub>Me (**784**), P<sup>n</sup>Bu<sub>3</sub> (**785**)) through a typical inner-sphere process. On the other hand, a free pendant 2-amino group at the benzoquinolate ligand bound to the Ir(III) center promotes the heterolytic rupture of the coordinated hydrogen molecule. Thus, complexes **782** and **783** evolve into [IrH<sub>2</sub>(bq-NH<sub>3</sub>)(PR<sub>3</sub>)<sub>2</sub>]BF<sub>4</sub> (PR<sub>3</sub> = PPh<sub>3</sub> (**786**), PCy<sub>3</sub> (**787**)).

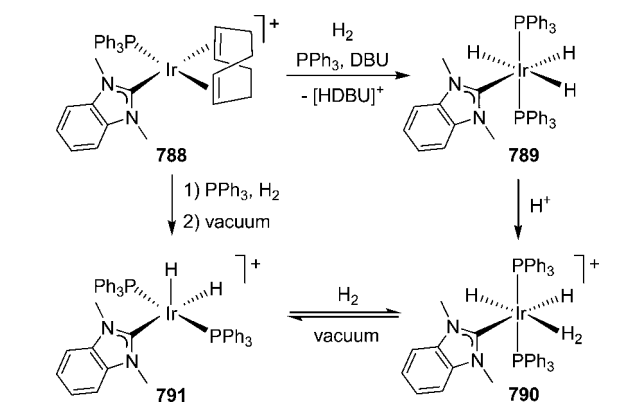
Intermolecular heterolytic H–H bond activation promoted by external N-heterocycles plays a main role in the hydrogenation of these substrates via a stepwise outer-sphere mechanism involving sequential proton and hydride transfers. The iridium(I) complex [Ir(η<sup>4</sup>-COD)(1,3-dimethylbenzimidazol-2-ylidene)(PPh<sub>3</sub>)]PF<sub>6</sub> (**788**) reacts with molecular hydrogen in the presence of 1 equiv of PPh<sub>3</sub> and 1 equiv of 1,8-diazabicyclo[5.4.0]undec-7-ene (DBU) to give the neutral meridional trihydride IrH<sub>3</sub>(1,3-dimethylbenzimidazol-2-ylidene)(PPh<sub>3</sub>)<sub>2</sub> (**789**) and [HDBU]PF<sub>6</sub>. The addition of 1 equiv of a strong acid to this compound affords the dihydride-dihydrogen derivative [IrH<sub>2</sub>(η<sup>2</sup>-H<sub>2</sub>)(1,3-dimethylbenzimidazol-2-ylidene)(PPh<sub>3</sub>)<sub>2</sub>]<sup>+</sup> (**790**; d<sub>H2</sub> ≈ 0.9 Å). Complex **790** readily converts to the unsaturated dihydride [IrH<sub>2</sub>(1,3-dimethylbenzimidazol-2-ylidene)(PPh<sub>3</sub>)<sub>2</sub>]<sup>+</sup> (**791**) on applying a vacuum. The reaction is reversible under 1 atm of H<sub>2</sub>. Complex **791** can be directly formed from the reaction of **788** with PPh<sub>3</sub> and H<sub>2</sub>, without the need for any base (Scheme 131).

Complexes **789–791** have been proposed as active intermediates in the hydrogenation of quinolines to the corresponding 1,2,3,4-tetrahydroquinolines, under mild conditions, catalyzed by the precursor **788**.<sup>379</sup> The cationic

Scheme 130. Heterolytic Activation of Hydrogen via Hydride-Dihydrogen-Iridium(III) Cations



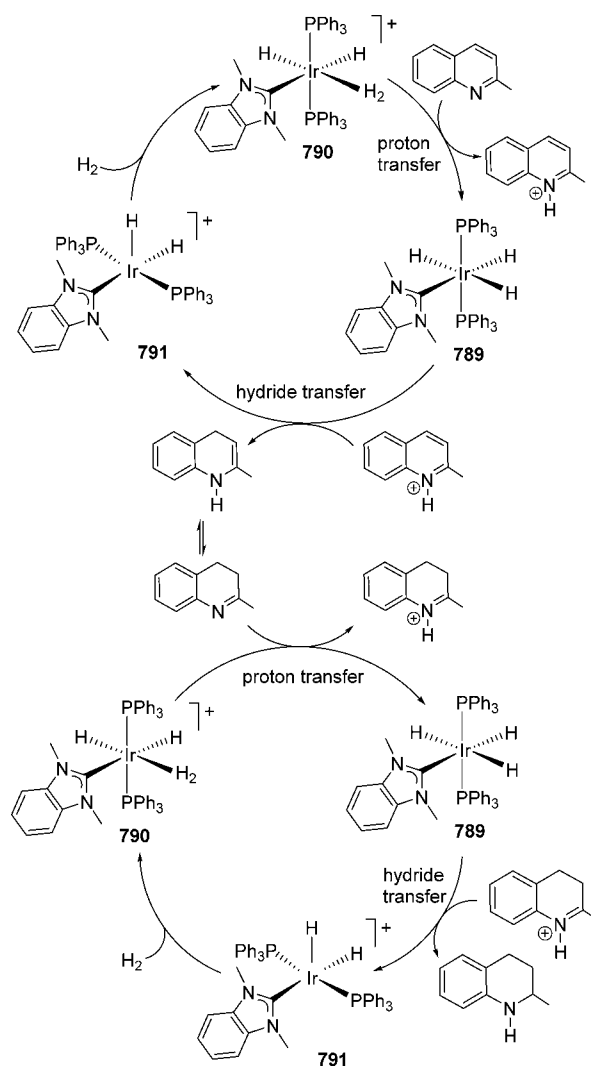
**Scheme 131. Intermolecular Heterolytic H–H Bond Activation Promoted by DBU: Formation of 789–791**



dihydride-dihydrogen complex **790** first transfers a proton to the substrate, resulting in the neutral trihydride **789** and a protonated substrate. Hydride transfer to the protonated substrate in a later step results in the formation of the unsaturated dihydride **791**, which then coordinates  $\text{H}_2$  and completes the catalytic cycle (Scheme 132). The related tris(phosphine) derivative  $[\text{IrH}_2(\eta^2\text{-H}_2)(\text{PMe}_2\text{Ph})_3]^+$  (**792**;  $T_1(\text{min}) = 20 \text{ ms}$  (360 MHz)) has been shown to be an efficient catalyst precursor for the hydrogenation of ethylene and butyne via the unsaturated dihydride  $[\text{IrH}_2(\text{PMe}_2\text{Ph})_3]^+$  (**793**).<sup>380–383</sup>

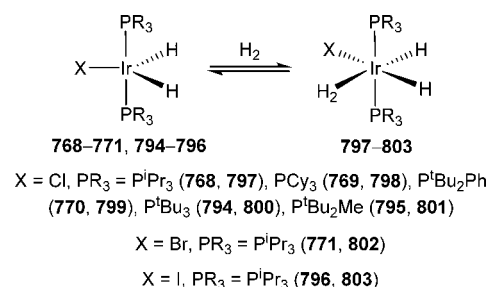
The behavior of the five-coordinate dihydride complexes  $\text{IrH}_2\text{X}(\text{PR}_3)_2$  (**768–771**;  $\text{X} = \text{Cl}$ ,  $\text{PR}_3 = \text{P}^i\text{Bu}_3$  (**794**),  $\text{P}^i\text{Bu}_2\text{Me}$  (**795**);  $\text{X} = \text{I}$ ,  $\text{PR}_3 = \text{P}^i\text{Pr}_3$  (**796**)) under hydrogen atmosphere is reminiscent of that of their monohydride counterparts (Scheme 133). Thus, the metal center coordinates the hydrogen molecule to establish an equilibrium with the corresponding dihydride-dihydrogen derivatives  $\text{IrH}_2\text{X}(\eta^2\text{-H}_2)(\text{PR}_3)_2$  ( $\text{X} = \text{Cl}$ ,  $\text{PR}_3 = \text{P}^i\text{Pr}_3$  (**797**),  $\text{PCy}_3$  (**798**),  $\text{P}^i\text{Bu}_2\text{Ph}$  (**799**),  $\text{P}^i\text{Bu}_3$  (**800**),  $\text{P}^i\text{Bu}_2\text{Me}$  (**801**);  $\text{X} = \text{Br}$ ,  $\text{PR}_3 = \text{P}^i\text{Pr}_3$  (**802**);  $\text{X} = \text{I}$ ,  $\text{PR}_3 = \text{P}^i\text{Pr}_3$  (**803**)), which undergo a rapid hydride-dihydrogen site exchange. The activation energy of this intramolecular process is similar to the barrier for the rotation motion of the dihydrogen ligand, suggesting that both phenomena are coupled to some extent.<sup>384–391</sup> The dihydrogen ligand lies trans to a hydride in the ground state. This is corroborated by the neutron diffraction structure of the iodide complex **803**.<sup>392</sup> Although the dihydrogen ligand is situated cis to the other hydride, as in the hydride-dihydrogen **764b**, a *cis*-hydride stabilization is not observed in this case. Thus, in contrast to **764b**, the iridium–hydride bond lengths of 1.579(6) and 1.589(6) Å are significantly shorter than the iridium–dihydrogen distances of 1.764(7) and 1.748(7) Å. This verifies a weaker iridium–dihydrogen interaction, which is evident in the short H–H separation of 0.856(9) Å. The thermodynamic stability of these dihydrogen complexes depends upon the halide, decreasing in the sequence  $\text{I} > \text{Br} > \text{Cl}$ .<sup>387</sup> The ordering of halides is reversed in the five (**768–771** and **794–796**) and the six-coordinate (**797–803**) sides and correlates with the fact that the X-ligand lone pairs do not simply stabilize the  $\text{H}_2$ -loss transition state, but they destabilize the  $\text{H}_2$ -adduct ground state, by filled/filled repulsions with the filled  $d_\pi$ -iridium orbitals.<sup>389</sup> In addition to dissociation, the dihydrogen ligand of these compounds is activated toward heterolytic cleavage, releasing HX. Complex **797** uses this

**Scheme 132. Proposed Mechanism for the Hydrogenation of Quinolines through 789–791<sup>a</sup>**



<sup>a</sup>Adapted from ref 379. Copyright 2011 American Chemical Society.

**Scheme 133. Formation of  $\text{IrH}_2\text{X}(\eta^2\text{-H}_2)(\text{PR}_3)_2$  Complexes**

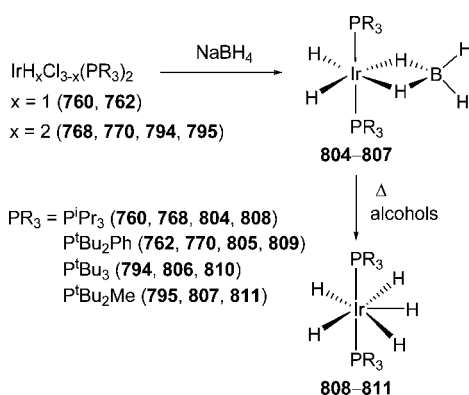


property to catalyze the hydrogenation of benzylideneacetone via the unsaturated trihydride  $\text{IrH}_3(\text{P}^i\text{Pr}_3)_2$ .<sup>393</sup>

The five-coordinate monohydrides **760** and **762** and the dihydrides **768**, **770**, **794**, and **795**, containing bulky phosphines, react with  $\text{NaBH}_4$  to give the dihydride-tetrahydrideborate derivatives  $\text{IrH}_2(\kappa^2\text{-H}_2\text{BH}_2)(\text{PR}_3)_2$  ( $\text{PR}_3 = \text{P}^i\text{Pr}_3$  (**804**),  $\text{P}^i\text{Bu}_2\text{Ph}$  (**805**),  $\text{P}^i\text{Bu}_3$  (**806**),  $\text{P}^i\text{Bu}_2\text{Me}$  (**807**)).<sup>394,395</sup> These compounds are stable in aprotic solvents but rapidly decompose on heating in alcohols to give the

pentahydride derivatives  $\text{IrH}_5(\text{PR}_3)_2$  ( $\text{PR}_3 = \text{P}^i\text{Pr}_3$  (**808**),  $\text{P}^t\text{Bu}_2\text{Ph}$  (**809**),  $\text{P}^t\text{Bu}_3$  (**810**),  $\text{P}^t\text{Bu}_2\text{Me}$  (**811**)) according to Scheme 134. Several alternative methods have been developed

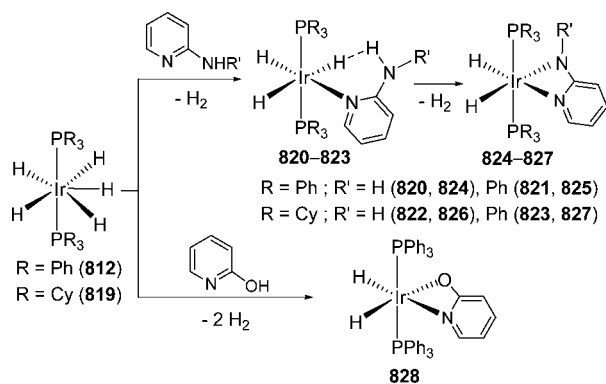
Scheme 134. Preparation of  $\text{IrH}_5(\text{PR}_3)_2$



to obtain different members of this family,<sup>98,396</sup> in particular those containing phosphines of small cone angle. Thus, complexes  $\text{IrH}_5(\text{PR}'_3)_2$  ( $\text{PR}'_3 = \text{PPh}_3$  (**812**),  $\text{P}(p\text{-F-C}_6\text{H}_4)_3$  (**813**),  $\text{PPh}_2\text{Me}$  (**814**),  $\text{PPhMe}_2$  (**815**),  $\text{PMe}_3$  (**816**),  $\text{PEt}_3$  (**817**),  $\text{PEt}_2\text{Ph}$  (**818**)) can be prepared by reaction of the corresponding square-planar precursors  $[\text{Ir}(\eta^4\text{-COD})(\text{PR}'_3)_2]^+$  with  $\text{H}_2$  in the presence of a base. Complex  $\text{IrH}_5(\text{PCy}_3)_2$  (**819**) has been similarly synthesized starting from  $[\text{Ir}(\eta^4\text{-COD})(\text{py})(\text{PCy}_3)]^+$  and  $\text{PCy}_3$ .<sup>397</sup> The neutron diffraction structure of **808** has revealed that the core of these molecules is a pentagonal bipyramid with five equatorial hydrogen atoms. The average Ir–H distance of 1.603(9) Å and the average H–H separation of 1.87(1) Å prove the classical character of these polyhydrides.<sup>398</sup> Distinctive features of these complexes include their ability to serve as hydrogen reservoirs and the accessibility of vacant coordination sites in unsaturated trihydrides, which are trapped with neutral Lewis bases to form saturated  $\text{IrH}_3\text{L}(\text{PR}_3)_2$  species.<sup>399,400</sup> These properties make such complexes particularly effective as catalysts for the hydrogenation of organic substrates<sup>396</sup> as well as for transfer hydrogenation reactions.<sup>401,402</sup>

The pentahydride complexes promote the chelated-assisted heteroatom–H bond activation to yield dihydride derivatives (Scheme 135).<sup>403–405</sup> The reactions take place via trihydride intermediates, which show moderately strong intramolecular Ir–H⋯H–X hydrogen bonds.<sup>406</sup> Treatment of the pentahy-

Scheme 135. Reactions of Pentahydrides **812** and **819** with 2-Functionalized Pyridines

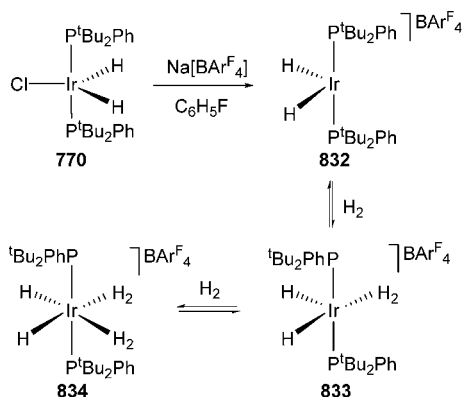


drides **812** and **819** with 2-aminopyridines in benzene at 80 °C leads to the H-bonded derivatives  $\text{IrH}_3(\text{py-2-NHR}')(\text{PR}_3)_2$  ( $\text{PR}_3 = \text{PPh}_3$ ,  $\text{R}' = \text{H}$  (**820**),  $\text{Ph}$  (**821**);  $\text{PR}_3 = \text{PCy}_3$ ,  $\text{R}' = \text{H}$  (**822**),  $\text{Ph}$  (**823**)). On warming, these species lose  $\text{H}_2$  to form the chelate amido compounds  $\text{IrH}_2\{\kappa^2\text{-N,N}(\text{py-2-NR}')\}(\text{PR}_3)_2$  ( $\text{PR}_3 = \text{PPh}_3$ ,  $\text{R}' = \text{H}$  (**824**),  $\text{Ph}$  (**825**);  $\text{PR}_3 = \text{PCy}_3$ ,  $\text{R}' = \text{H}$  (**826**),  $\text{Ph}$  (**827**)). The reaction of **812** with 2-hydroxypyridine directly gives  $\text{IrH}_2\{\kappa^2\text{-N,O}(\text{py-2-O})\}(\text{PPh}_3)_2$  (**828**).

The pentahydride complexes are weak Brønsted acids, which can be deprotonated by superbases.<sup>407,408</sup> Thus, the treatment of **808**, **812**, and **819** with KH in THF in the presence of a slight excess of the appropriate crown ether or cryptand (Q) yields the tetrahydride compounds  $[\text{K}(\text{Q})][\text{IrH}_4(\text{P}^i\text{Pr}_3)_2]$  (Q = 18-crown-6 (**829a**), 1-aza-18-crown-6 (**829b**), 1,10-diaza-18-crown-6 (**829c**), cryptand-2.2.2 (**829d**)),  $[\text{K}(\text{Q})][\text{IrH}_4(\text{PPh}_3)_2]$  (Q = 18-crown-6 (**830a**), 1,10-diaza-18-crown-6 (**830c**)), and  $[\text{K}(\text{Q})][\text{IrH}_4(\text{PCy}_3)_2]$  (Q = 18-crown-6 (**831a**), 1,10-diaza-18-crown-6 (**831c**), cryptand-2.2.2 (**831d**)), respectively. In THF solution, the stereochemistry of the anion of the salts is sensitive to the counteraction: either *trans*-phosphines as the potassium cryptand-2.2.2 salts (**829d**, **831d**) or exclusively *cis*-phosphines as the crown- and azacrown-potassium salts (**830**, **831a,c**) or a mixture of *cis* and *trans* (**829a–829c**). The contribution of four factors appears to explain these facts: (i) potassium-hydride interactions in the ion pairs that favor the *cis* isomer, (ii) protonic-hydridic bonding that could contribute to a strengthening of the cation–anion interaction, (iii) the high *trans* influence of the hydride ligand that favors the *cis* arrangement, and (iv) the interligand repulsions in the anion, expected to increase with the Tolman cone angle of the phosphine and that can explain why the stereochemistry is *trans* in the absence of potassium-hydride interaction. The potassium-hydride interactions have been confirmed by the X-ray structures of the salts **829a**, **829b**, and **830a**, which show a *cis*-disposition of the phosphine ligands, whereas three facially arranged hydrides and the potassium atom form a tetrahedron. The salts **829c** and **830c** have been also characterized by X-ray diffraction analysis. The phosphine ligands are *trans*-disposed in the first of them, whereas they lie *cis* in the second one.

The pentahydride complexes also act as Brønsted bases.<sup>377,409</sup> Thus, they react with acids to afford dihydride-bis(dihydrogen) derivatives of formula  $[\text{IrH}_2(\eta^2\text{-H}_2)_2(\text{PR}_3)_2]^+$ , which are the species involved in the catalytic hydrogenation of unsaturated organic molecules promoted by the cationic iridium precursors  $[\text{Ir}(\eta^4\text{-COD})(\text{PR}_3)_2]^+$  in noncoordinating solvents.<sup>410</sup> The protonation is reversible, the treatment of these species with a base such as  $\text{NEt}_3$  gives back the pentahydrides. In agreement with the weak binding of the dihydrogen ligand to the metal center, Lewis bases displace the hydrogen molecules.<sup>377,409,411</sup> The dihydride-bis(dihydrogen)-derivatives can also be prepared starting from the five-coordinate dihydrides  $\text{IrH}_2\text{X}(\text{PR}_3)_2$  (**768–771** and **794–796**). For instance, abstraction of the chloride ligand of **770** by  $\text{Na}[\text{BAR}^F_4]$  in fluorobenzene leads to the solvent–ligand-free cationic iridium(III) complex  $[\text{IrH}_2(\text{P}^t\text{Bu}_2\text{Ph})_2][\text{BAR}^F_4]$  (**832**). Under 1 atm of hydrogen, this compound is in equilibrium with the mono- and bis-dihydrogen derivatives  $[\text{IrH}_2(\eta^2\text{-H}_2)(\text{P}^t\text{Bu}_2\text{Ph})_2][\text{BAR}^F_4]$  (**833**) and  $[\text{IrH}_2(\eta^2\text{-H}_2)_2(\text{P}^t\text{Bu}_2\text{Ph})_2][\text{BAR}^F_4]$  (**834**) (Scheme 136). The formation of the monodihydrogen **833** is favored by decreasing temperature.<sup>412,413</sup>

Scheme 136. Formation of the Dihydride-bis(Dihydrogen)-Iridium(III) Cation 834



## 5.2. Complexes with Tripodal Phosphine Ligands

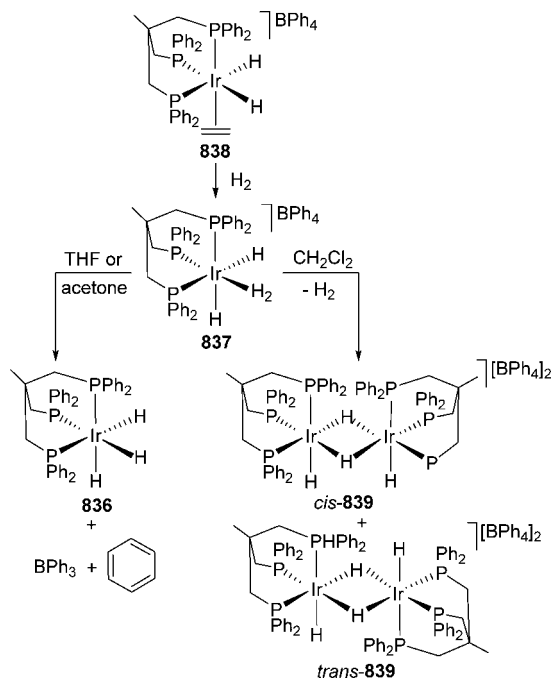
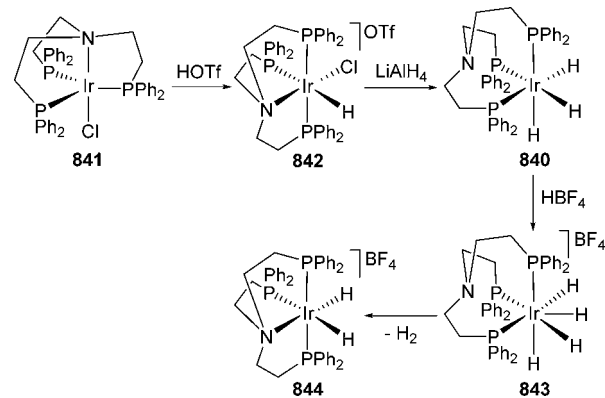
A few polyhydride–iridium complexes with the tripodal phosphines triphos<sup>Me</sup> and NP<sub>3</sub> have been reported.

Treatment of tetrahydrofuran solutions of IrCl<sub>3</sub>(triphos<sup>Me</sup>) (835) with diethyl ether solutions of LiAlH<sub>4</sub> produces the replacement of the chloride ligands by hydrides to afford the trihydride IrH<sub>3</sub>(triphos<sup>Me</sup>) (836),<sup>414</sup> which yields the cation [IrH<sub>2</sub>(η<sup>2</sup>-H<sub>2</sub>)(triphos<sup>Me</sup>)]<sup>+</sup> (837) by protonation. The [BPh<sub>4</sub>]<sup>-</sup> salt of 837 has been prepared by hydrogenation of the coordinated ethylene molecule of the dihydride complex [IrH<sub>2</sub>(η<sup>2</sup>-C<sub>2</sub>H<sub>4</sub>)(triphos<sup>Me</sup>)] [BPh<sub>4</sub>]<sup>-</sup> (838) in either the solid state (P<sub>H<sub>2</sub></sub> ≥ 1 atm) or dichloromethane (P<sub>H<sub>2</sub></sub> ≥ 3 atm). The [BPh<sub>4</sub>]<sup>-</sup> salt of 837 is unstable in solution; in dichloromethane, it loses H<sub>2</sub> converting to a mixture of the dimers *cis*- and *trans*-[IrH(triphos<sup>Me</sup>)](μ-H)<sub>2</sub> [BPh<sub>4</sub>]<sub>2</sub> (839), whereas in tetrahydrofuran and acetone it evolves into 836, BPh<sub>3</sub>, and benzene. The last process involves the formal heterolytic splitting of H<sub>2</sub> with the concomitant protonolysis of the counteranion and formation of a metal–hydride bond (Scheme 137).<sup>415–417</sup>

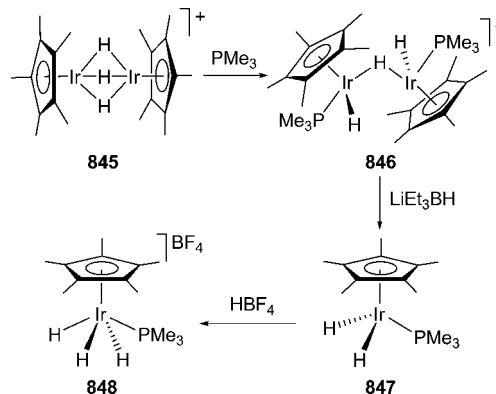
The NP<sub>3</sub>-counterpart of 836, IrH<sub>3</sub>(κ<sup>3</sup>-P,P,P-NP<sub>3</sub>) (840), has been prepared according to Scheme 138, starting from the iridium(I) precursor IrCl(κ<sup>4</sup>-NP<sub>3</sub>) (841) via the intermediate [IrHCl(κ<sup>4</sup>-NP<sub>3</sub>)]<sup>+</sup> (842). The protonation of 840 yields the expected cation [IrH<sub>4</sub>(κ<sup>3</sup>-P,P,P-NP<sub>3</sub>)]<sup>+</sup> (843). However, in contrast to 837, its structure is not clear. Discrimination between classical and nonclassical polyhydride cannot be made on the basis of DFT results of the naked cation, since both dihydride-dihydrogen and tetrahydride forms are located on an extremely low flat energy surface. On the other hand, in the presence of the [(CF<sub>3</sub>)<sub>2</sub>CHO⋯HOCH(CF<sub>3</sub>)<sub>2</sub>]<sup>-</sup> counteranion, only the dihydride-dihydrogen isomer seems to be relatively stable. The final protonation product at room temperature is the dihydride [IrH<sub>2</sub>(κ<sup>4</sup>-NP<sub>3</sub>)]<sup>+</sup> (844), resulting from the loss of a hydrogen molecule.<sup>418</sup>

## 5.3. Half Sandwich Compounds

The trihydride complex [{Ir(η<sup>5</sup>-C<sub>5</sub>Me<sub>5</sub>)<sub>2</sub>(μ-H)<sub>3</sub>]PF<sub>6</sub> (845) adds trimethylphosphine. The reaction leads to the monohydride-bridged dimer [{IrH(η<sup>5</sup>-C<sub>5</sub>Me<sub>5</sub>)(PMe<sub>3</sub>)<sub>2</sub>(μ-H)]PF<sub>6</sub> (846). Reaction of this compound with LiEt<sub>3</sub>BH affords the mononuclear dihydride IrH<sub>2</sub>(η<sup>5</sup>-C<sub>5</sub>Me<sub>5</sub>)(PMe<sub>3</sub>) (847), which gives the trihydride [IrH<sub>3</sub>(η<sup>5</sup>-C<sub>5</sub>Me<sub>5</sub>)(PMe<sub>3</sub>)]BF<sub>4</sub> (848) by protonation with HBF<sub>4</sub>·OEt<sub>2</sub> (Scheme 139).<sup>419</sup> Similarly, the protonation of the dihydrides IrH<sub>2</sub>(η<sup>5</sup>-C<sub>5</sub>Me<sub>5</sub>)(PR<sub>3</sub>) (PR<sub>3</sub> = P<sup>i</sup>Pr<sub>3</sub> (849), PCy<sub>3</sub> (850), PPh<sub>3</sub> (851), PPh<sub>2</sub>Me (852)) and IrH<sub>2</sub>(η<sup>5</sup>-C<sub>5</sub>H<sub>5</sub>)(ER<sub>3</sub>) (ER<sub>3</sub> = PMe<sub>3</sub> (853), P<sup>i</sup>Pr<sub>3</sub> (854), PCy<sub>3</sub>

Scheme 137. Iridium-Polyhydrides Containing the Triphos<sup>Me</sup> LigandScheme 138. NP<sub>3</sub>-Iridium Complexes

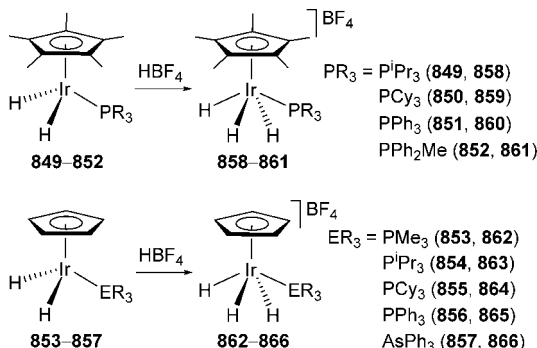
Scheme 139. Trimethylphosphine-Iridium-Pentamethylcyclopentadienyl Complexes



(855), PPh<sub>3</sub> (856), AsPh<sub>3</sub> (857)) generates the corresponding trihydrides [IrH<sub>3</sub>(η<sup>5</sup>-C<sub>5</sub>Me<sub>5</sub>)(PR<sub>3</sub>)]BF<sub>4</sub> (PR<sub>3</sub> = P<sup>i</sup>Pr<sub>3</sub> (858), PCy<sub>3</sub> (859), PPh<sub>3</sub> (860),<sup>23</sup> PPh<sub>2</sub>Me (861)<sup>420</sup>) and [IrH<sub>3</sub>(η<sup>5</sup>-

$C_5H_5(ER_3)]BF_4$  ( $ER_3 = PMe_3$  (862),  $P^iPr_3$  (863),  $PCy_3$  (864),  $PPh_3$  (865),  $AsPh_3$  (866)),<sup>421</sup> according to Scheme 140. The hydride ligands of these trihydride derivatives

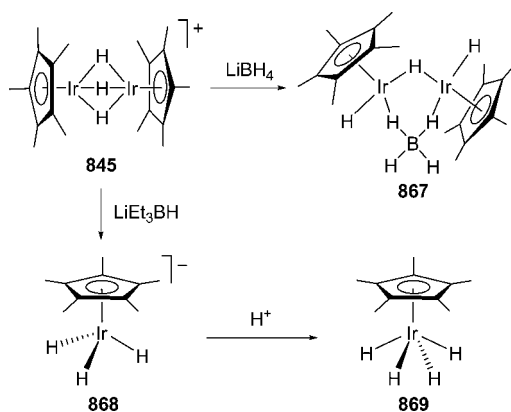
Scheme 140.  $[IrH_3(\eta^5-C_5R_5)L]BF_4$  Complexes



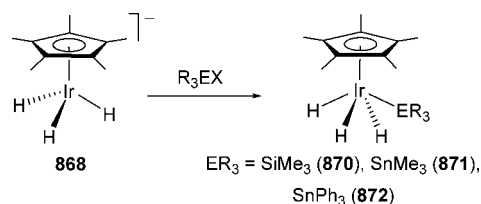
undergo thermally activated position exchange. The activation barriers for the rearrangement of the hydrides are higher for the  $Cp^*$  complexes 848 and 858–860 than for the  $Cp$  derivatives 862–866. Furthermore, they show quantum mechanical exchange coupling, which has been quantified according to eq 1. The values for  $a$  do not vary appreciably between the  $Cp^*$  and  $Cp$  systems. However, the value of  $\lambda$  for the  $Cp^*$  species (1.1 Å) is larger than for the  $Cp$  derivatives (0.9 Å), whereas the values of  $\nu$  follow an opposite trend (i.e., they are smaller for the  $Cp^*$  complexes than for the corresponding  $Cp$  counterparts). Thus, the variation in the magnitude of exchange coupling from 848 and 858–860 to 862–866 is apparently caused by differences in  $\lambda$  and  $\nu$ , which are attributed to the differences in  $Cp^*$  versus  $Cp$ .<sup>23</sup>

The cation of the salt 845 also adds the tetrahydrideborate anion. The addition gives the tetrahydrideborate-bonded dimer  $[IrH(\eta^5-C_5Me_5)]_2(\mu-H)(\mu-H_2BH_2)$  (867). In contrast to  $[BH_4]^-$ , the reaction with the more nucleophilic reducing agent  $LiEt_3BH$  leads to the anion  $[IrH_3(\eta^5-C_5Me_5)]^-$  (868), which affords the neutral tetrahydride-iridium(V) derivative  $IrH_4(\eta^5-C_5Me_5)$  (869), by hydrolysis or methanolysis (Scheme 141). Silyl- and stannylation of 868 occur with  $Me_3SiO_3SCF_3$  and  $Me_3SnCl$  and  $Ph_3SnBr$  to form the complexes  $IrH_3(\eta^5-C_5Me_5)(SiMe_3)$  (870),  $IrH_3(\eta^5-C_5Me_5)(SnMe_3)$  (871), and  $IrH_3(\eta^5-C_5Me_5)(SnPh_3)$  (872), respectively (Scheme 142).<sup>422</sup>

Scheme 141. Reactions of the Dimer 845: Iridium-Polyhydrides Stabilized by Pentamethylcyclopentadienyl



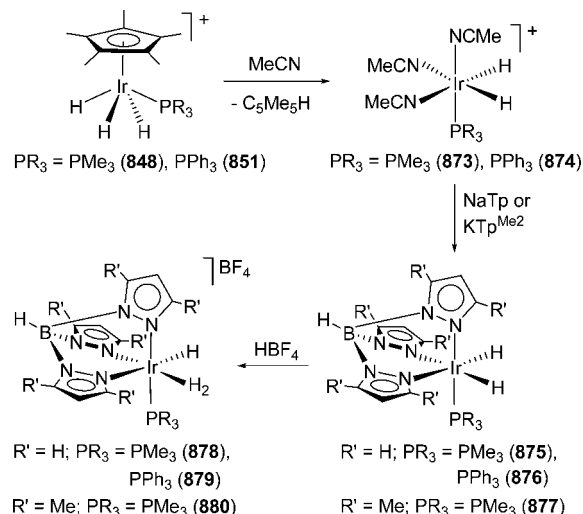
Scheme 142. Trihydride-Silyl and Trihydride-Stannyl-Iridium(V) Complexes



#### 5.4. Complexes with Tris(pyrazolyl)borate and Related Ligands

The pentamethylcyclopentadienyl complexes 848 and 851 undergo reductive elimination of pentamethylcyclopentadiene in acetonitrile.<sup>423</sup> The reduction affords the tris(solvento) species  $[IrH_2(CH_3CN)_3(PR_3)]^+$  ( $PR_3 = PMe_3$  (873),  $PPh_3$  (874)), which react with  $NaTp$  and  $KTp^{Me_2}$  to give  $IrH_2Tp(PR_3)(PR_3 = PMe_3$  (875),  $PPh_3$  (876)) and  $IrH_2Tp^{Me_2}(PMe_3)$  (877), respectively.<sup>353</sup> In contrast to their  $Cp^*$  and  $Cp$  counterparts, the protonation of these dihydrides with  $HBF_4 \cdot OEt_2$  leads to the corresponding hydride-dihydrogen derivatives  $[IrHTp(\eta^2-H_2)(PR_3)]BF_4$  ( $PR_3 = PMe_3$  (878),  $PPh_3$  (879)) and  $[IrHTp^{Me_2}(\eta^2-H_2)(PMe_3)]BF_4$  (880), in agreement with the high tendency of the  $Tp^R$ -ligands to stabilize nonclassical H–H interactions (Scheme 143).

Scheme 143. Preparation of Iridium Complexes with  $Tp^R$ -Type Ligands



substitution of the  $IrH_3$ -positions with deuterium and tritium results in large temperature-dependent isotope shift, which is consistent with the preference of the heavy isotope to occupy the hydride site. The  $J_{H-D}$  and  $T_1(\text{min})$  values are consistent with a separation between the hydrogen atoms of the coordinated hydrogen molecule of about 1 Å.<sup>353</sup>

$Tp^R$ -Counterparts of the tetrahydride 869 are also known. Complex  $IrH_4Tp^{Me_2}$  (881) has been prepared in high yield by hydrogenation of  $IrTp^{Me_2}(\eta^2-C_2H_4)_2$  (882) under forcing conditions ( $C_6H_{12}$ , 90 °C, 2 atm, 3 days), whereas  $IrH_4Tp$  (883) has been obtained only in very low yield (10%) by a similar procedure starting from  $IrTp(\eta^2-C_2H_4)_2$  (884).<sup>424</sup> On the basis of NMR spectroscopy, a ground-state  $C_{3v}$  structure in which a hydride ligand caps the face of the remaining hydrides has been proposed. However, DFT calculations suggest that

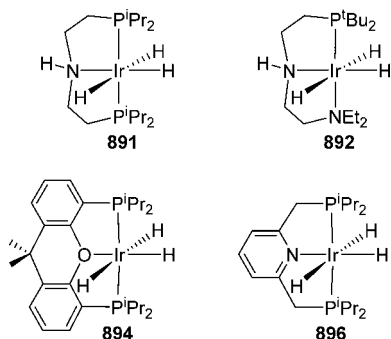
this structure is a local maximum, while a  $C_s$  edge-bridged octahedral structure (formally Ir(V)) and a  $C_1$  dihydride-dihydrogen structure (formally Ir(III)) are local minima, nearly isoenergetic, which seem to coexist in a rapid equilibrium in solution.<sup>425</sup>

The hydrogenation of the cyclooctene ligand of the  $\beta$ -diimine complex  $\text{Ir}(\text{Ir}^{\text{Pr}}\text{BDI})(\eta^2\text{-COE})(\text{N}_2)$  (**885**, BDI =  $\text{ArNC}(\text{Me})\text{CHC}(\text{Me})\text{CNAr}$ , Ar = 2,6- $\text{Pr}_2\text{C}_6\text{H}_3$ ; COE = cyclooctene) under 4 atm of  $\text{H}_2$  yields the related six-coordinate tetrahydride  $\text{IrH}_4(\text{Ir}^{\text{Pr}}\text{BDI})$  (**886**). X-ray diffraction and DFT studies have revealed a trigonal prismatic structure with close H...H contacts of about 1.25 and 1.30 Å.<sup>426</sup>

### 5.5. Complexes with Pincer Ligands

A few neutral trihydride compounds stabilized by pincer ligands have been isolated, characterized, and their catalytic potential investigated (Chart 12). Treatment of the dihydride PNP- and

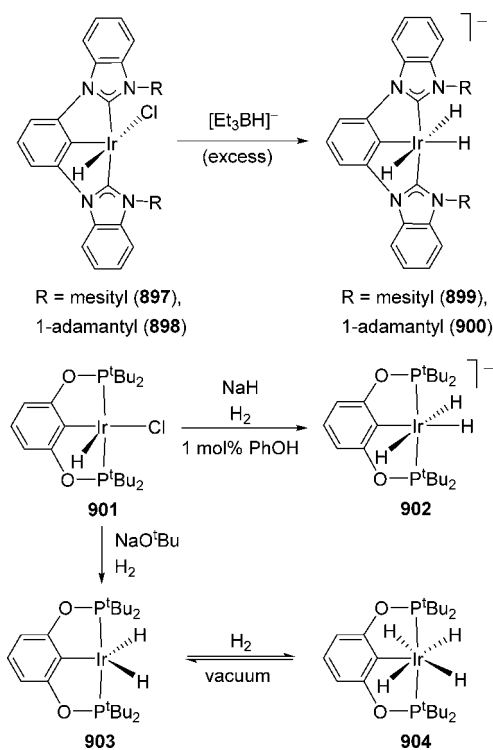
**Chart 12. Neutral Trihydride Iridium(III) Compounds with Pincer Ligands**



PNN-complexes  $\text{IrH}_2\text{Cl}\{(\text{Pr}_2\text{PCH}_2\text{CH}_2)_2\text{NH}\}$  (**887**) and  $\text{IrH}_2\text{Cl}\{\text{Bu}_2\text{PC}_2\text{H}_4\text{NHC}_2\text{H}_4\text{NET}_2\}$  (**888**) with  $\text{KO}^t\text{Bu}$  produces the deprotonation of the amine and the abstraction of the chloride ligand from the metal center to afford the amidodihydride derivatives  $\text{IrH}_2\{(\text{Pr}_2\text{PCH}_2\text{CH}_2)_2\text{N}\}$  (**889**) and  $\text{IrH}_2\{\text{Bu}_2\text{PC}_2\text{H}_4\text{NC}_2\text{H}_4\text{NET}_2\}$  (**890**), which give the trihydride derivatives  $\text{IrH}_3\{(\text{Pr}_2\text{PCH}_2\text{CH}_2)_2\text{NH}\}$  (**891**)<sup>427</sup> and  $\text{IrH}_3\{\text{Bu}_2\text{PC}_2\text{H}_4\text{NHC}_2\text{H}_4\text{NET}_2\}$  (**892**),<sup>428</sup> respectively, by hydrogen transfer from 2-propanol, the first of them, and by hydrogenation with  $\text{H}_2$ , the second one. Stirring of  $\text{IrHCl}\{\text{xant}(\text{P}^i\text{Pr}_2)[\kappa^2\text{-P,C-PrPCH}(\text{Me})\text{CH}_2]\}$  (**893**) in KOH solutions of 2-propanol leads to  $\text{IrH}_3\{\text{xant}(\text{P}^i\text{Pr}_2)_2\}$  (**894**).<sup>429</sup> The addition of an excess amount of NaH to THF solutions of  $\text{IrH}_2\text{Cl}(\text{PpyP})$  (**895**, PpyP = 2,6-bis-(diisopropylphosphinomethyl)pyridine) yields  $\text{IrH}_3(\text{PpyP})$  (**896**).<sup>430</sup> Complexes **891** and **892** are active catalysts for the hydrogen transfer from 2-propanol to ketones. Complex **891** is, furthermore, active for the reduction of ketones and aldehydes with  $\text{H}_2$  in a wide range of solvents including dichloromethane and chloroform,<sup>431</sup> as well as for the hydrogenation of carboxylic acid esters.<sup>432</sup> Trihydride **896** catalyzes the hydrogenation of  $\text{CO}_2$  to  $\text{HCOO}^-$  in aqueous base.<sup>430,433–438</sup>

Anionic trihydride complexes stabilized by pincer ligands have been generated by addition of hydrides to unsaturated chloride-hydride species (Scheme 144). For instance, it has been observed that the treatment of the  $C_{\text{benzimidazolylidene}}C_{\text{aryl}}C_{\text{benzimidazolylidene}}$  complexes  $\text{IrHCl}(\text{C}^{\text{R}}\text{CC}^{\text{R}})$  (R = mesityl (**897**), 1-adamantyl (**898**)) with an excess amount of  $\text{LiEt}_3\text{BH}$  and  $\text{NaEt}_3\text{BH}$ , respectively, affords  $[\text{IrH}_3(\text{C}^{\text{R}}\text{CC}^{\text{R}})]^-$  (R = mesityl (**899**), 1-adamantyl (**900**)).<sup>439</sup>

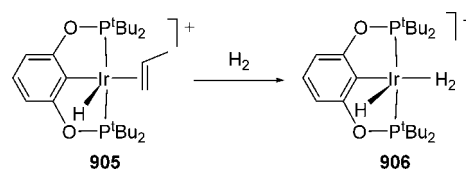
**Scheme 144. Anionic Trihydride-Iridium(III) Complexes Stabilized by Pincer Ligands**



The heterolytic cleavage of molecular hydrogen in the presence of a superbases is an alternative method. Thus, Brookhart and co-workers have reported that the treatment of  $\text{IrHCl}\{\text{C}_6\text{H}_3\text{-2,6-(OP}^t\text{Bu}_2)_2\}$  (**901**) with NaH or KH under an atmosphere of hydrogen in THF gives  $[\text{IrH}_3\{\text{C}_6\text{H}_3\text{-2,6-(OP}^t\text{Bu}_2)_2\}]^-$  (**902**). Addition of a catalytic amount of a mild Brønsted acid such as phenol or a Brønsted base such as  $\text{NaO}^t\text{Bu}$  greatly accelerates the reaction. On the other hand, the reaction of **901** with the stoichiometric amount of  $\text{NaO}^t\text{Bu}$  in aromatic solvents, under 1 atm of hydrogen, leads to the neutral dihydride  $\text{IrH}_2\{\text{C}_6\text{H}_3\text{-2,6-(OP}^t\text{Bu}_2)_2\}$  (**903**), which is in equilibrium with the tetrahydride  $\text{IrH}_4\{\text{C}_6\text{H}_3\text{-2,6-(OP}^t\text{Bu}_2)_2\}$  (**904**).<sup>440</sup>

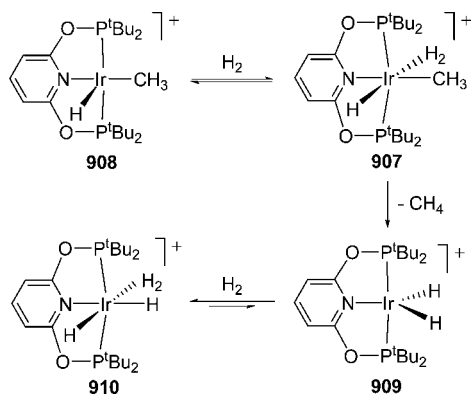
The charge of the complexes certainly determines the nature of the  $\text{IrH}_3$ -unit. The hydrogenation of the propylene complex  $[\text{IrH}\{\text{C}_6\text{H}_3\text{-2,6-(OP}^t\text{Bu}_2)_2\}(\eta^2\text{-CH}_2=\text{CHMe})][\text{BAR}^{\text{F}}_4]$  (**905**) in dichloromethane gives  $[\text{IrH}\{\text{C}_6\text{H}_3\text{-2,6-(OP}^t\text{Bu}_2)_2\}(\eta^2\text{-H}_2)]-[\text{BAR}^{\text{F}}_4]$  (**906**), which in contrast to **902** is a nonclassical hydride-dihydrogen species with a H–H separation between the hydrogen atoms of the dihydrogen ligand of about 0.9 Å (Scheme 145). This compound is quite stable in fluorobenzene, while slow decomposition occurs in chlorinated solvents.<sup>441</sup> Given the electron depletion of the metal center in these compounds, the dihydrogen ligand is activated toward its heterolytic cleavage. Thus, for instance, evidence for the key

**Scheme 145. Preparation of 906**



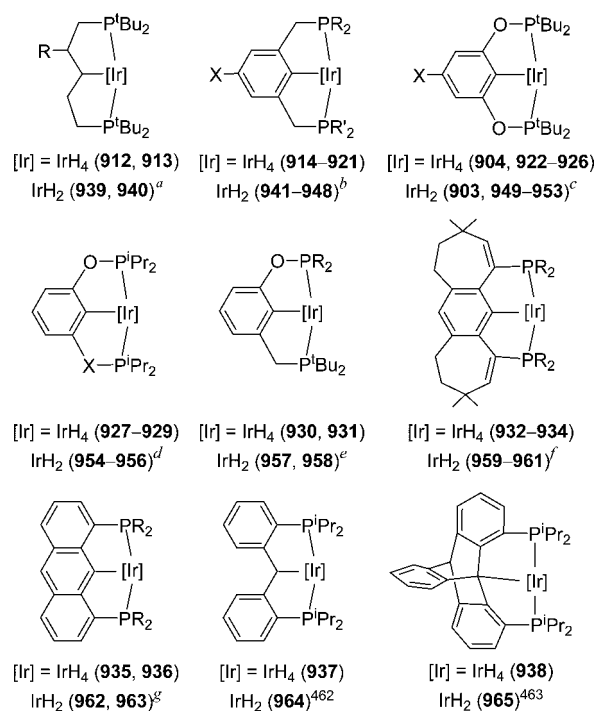
hydride-dihydrogen  $[\text{IrH}(\text{CH}_3)(\eta^2\text{-H}_2)\{\text{py-2,6-(OP}^t\text{Bu}_2)_2\}]^+$  (**907**) in the hydrogenolysis of the Ir–CH<sub>3</sub> bond of  $[\text{IrH}(\text{CH}_3)\{\text{py-2,6-(OP}^t\text{Bu}_2)_2\}]^+$  (**908**) has been obtained.<sup>442</sup> Deuterium-labeling experiments suggest the transformation of **907** into a  $\sigma\text{-CH}_4$  complex prior to the release of methane. The loss of the alkane results in the formation of the dihydride  $[\text{IrH}_2\{\text{py-2,6-(OP}^t\text{Bu}_2)_2\}]^+$  (**909**), which under H<sub>2</sub> forms the dihydride-dihydrogen  $[\text{IrH}_2(\eta^2\text{-H}_2)\{\text{py-2,6-(OP}^t\text{Bu}_2)_2\}]^+$  (**910** in Scheme 146). The hydride-dihydrogen **907** has also been proposed as a key intermediate for the *trans*-addition of H<sub>2</sub> to  $\text{Ir}(\text{CH}_3)\{\text{py-2,6-(OP}^t\text{Bu}_2)_2\}$  (**911**) catalyzed by water or alcohols.<sup>443</sup>

**Scheme 146. Formation of the Hydride-Dihydrogen 907 and the Dihydride-Dihydrogen 910**



A significant number of neutral IrH<sub>4</sub>-complexes containing anionic PCP-pincer ligands, related to **904**, are also known (Chart 13).<sup>440,444–463</sup> These IrH<sub>4</sub>(PCP) (**904** and **912–938**) compounds have been generally prepared by reduction of the corresponding IrHCl(PCP) starting complexes under an atmosphere of hydrogen. The structure of **914** in the solid state has been determined by neutron diffraction analysis. The distribution of donor atoms around the metal center can be rationalized as a distorted pentagonal bipyramid with apical phosphorus atoms and the hydrides separated by more than 1.5 Å, in agreement with a compressed tetrahydride formulation. However, the  $J_{\text{H-D}}$  obtained from spectroscopic studies ( $22 \pm 5$  Hz) is consistent with at least a H–H distance of  $1.06 \pm 0.11$  Å, which supports a dihydride-dihydrogen nature in solution. Similarly to **914**, complex **904** appears to have a dihydride-dihydrogen structure in solution with a H–H distance of  $0.97 \pm 0.09$  Å, within the coordinated hydrogen molecule. Electronic structure calculations on both **904** and **914** indicate that global minima on the potential surfaces in the gas phase are tetrahydride structures. On the other hand, the dihydride-dihydrogen forms are only slightly higher in energy (1–3 kcal mol<sup>-1</sup>) and the barriers to the interconversion between the tetrahydride and dihydride-dihydrogen species are almost negligible.<sup>464</sup> The 400 MHz  $T_1(\text{min})$  values of 104 and 105 ms for **932** and **933**, respectively, suggest tetrahydride structures in solution. The solid state structure of **932**, determined by X-ray diffraction analysis, can be regarded as a dihydride-compressed dihydride ( $d_{\text{H}\cdots\text{H}} = 1.50$  Å).<sup>460</sup> These sometimes contradictory data have been explained by arguing that the IrH<sub>4</sub>(PCP) complexes are not optimally characterized in terms of individual well-defined structures. Rather, extensive nuclear motions on exceptionally flat energy surfaces seem to offer the simplest and most appropriate description for these

**Chart 13. IrH<sub>4</sub>/IrH<sub>2</sub>-Pairs Containing Anionic PCP-Pincer Ligands<sup>a</sup>**



<sup>a</sup>*a*R = H (**912, 939**),<sup>444,445</sup> Me (**913, 940**),<sup>444</sup> <sup>b</sup>X = H; R = R' = <sup>t</sup>Bu (**914, 941**),<sup>446,447</sup> <sup>i</sup>Pr (**915, 942**),<sup>447</sup> 1-adamantyl (**916, 943**),<sup>448</sup> X = H; PR<sub>2</sub> = P<sup>t</sup>Bu<sub>2</sub>, PR'<sub>2</sub> = P<sup>t</sup>BuMe (**917, 944**),<sup>449,450</sup> PR<sub>2</sub> = PR'<sub>2</sub> = P<sup>t</sup>BuMe (**918, 945**),<sup>450</sup> X = C(O)OMe; R = R' = <sup>t</sup>Bu (**919, 946**),<sup>451</sup> X = OMe; R = R' = <sup>i</sup>Pr (**920, 947**),<sup>452</sup> R = R' = <sup>t</sup>Bu (**921, 948**),<sup>451</sup> <sup>c</sup>X = H (**904, 903**), Me (**922, 949**), OMe (**923, 950**), F (**924, 951**), C<sub>6</sub>F<sub>5</sub> (**925, 952**), 3,5-(CF<sub>3</sub>)<sub>2</sub>C<sub>6</sub>H<sub>3</sub> (**926, 953**),<sup>440,453,454</sup> <sup>d</sup>X = CH<sub>2</sub> (**927, 954**),<sup>455–457</sup> O (**928, 955**),<sup>455</sup> S (**929, 956**),<sup>458</sup> <sup>e</sup>R = <sup>t</sup>Bu (**930, 957**), <sup>i</sup>Pr (**931, 958**),<sup>459</sup> <sup>f</sup>R = <sup>i</sup>Pr (**932, 959**), Cy (**933, 960**), Ph (**934, 961**),<sup>460</sup> <sup>g</sup>R = <sup>t</sup>Bu (**935, 962**),<sup>455,461</sup> <sup>i</sup>Pr (**936, 963**).<sup>455</sup>

molecules.<sup>464</sup> This appears to be in agreement with the fact that complexes **904** and **912–938** lose H<sub>2</sub> under vacuum to afford the corresponding dihydrides IrH<sub>2</sub>(PCP) (**903** and **939–965**). The process is reversible and, interestingly, increasing electron donation by the diposphine disfavors the addition of H<sub>2</sub>, in contradiction to the idea of such addition being oxidative.<sup>451</sup> IrH<sub>4</sub>- and IrH<sub>2</sub>-species catalyze the dehydrogenation of alkanes and related reactions. The use of IrH<sub>4</sub>-species as catalyst precursors has never shown any significant difference from use of the corresponding dihydrides, other than requiring one additional mole of hydrogen acceptor in the case of transfer-dehydrogenation.<sup>56</sup>

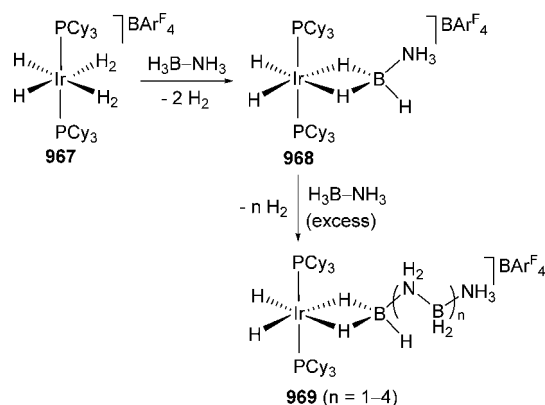
A neutral IrH<sub>4</sub>-compound containing an anionic CCC-pincer ligand has been also reported. This species, IrH<sub>2</sub>{2,6-(CH<sub>2</sub>NHC<sup>Mes</sup>)<sub>2</sub>C<sub>6</sub>H<sub>3}}( $\eta^2\text{-H}_2$ ) (**966**, NHC<sup>Mes</sup> = *N*-mesitylimidazol-2-ylidene), was described as a dihydride-dihydrogen on the basis of  $T_1(\text{min})$ ,  $J_{\text{H-D}}$  analysis, and DFT calculations, although the data do not rule out the possibility of **966** existing as a mixture of Ir(III) and Ir(V) tautomers in solution. Complex **966** activates C–H bonds of arenes at room temperature, as demonstrated by isotope exchange reactions. However, under analogous conditions, no reaction was observed with alkanes.<sup>465</sup></sub>

## 5.6. Iridium-Polyhydride Complexes Involved in $\sigma$ -Bond Activation Reactions

**5.6.1. B–H Bond Activation.** Several iridium polyhydride complexes have been employed to investigate the role of the metal center in the catalytic dehydrocoupling of amine-boranes, and some of them have been shown to play a main role in the kinetically controlled dehydrogenation of these substrates.

The dihydride-bis(dihydrogen)  $[\text{IrH}_2(\eta^2\text{-H}_2)_2(\text{PCy}_3)_2][\text{BAR}^{\text{F}}_4]$  (**967**) has allowed the characterization of multiple metal-bound oligomers which are believed to participate in the on-metal dehydrocoupling of  $\text{H}_3\text{B-NH}_3$ . The coordinated hydrogen molecules of this compound are displaced by ammonia-borane to give  $[\text{IrH}_2(\kappa^2\text{-H}_2\text{BHNH}_3)(\text{PCy}_3)_2][\text{BAR}^{\text{F}}_4]$  (**968**). The addition of further  $\text{H}_3\text{B-NH}_3$  results in the formation of higher oligomers  $[\text{IrH}_2\{\kappa^2\text{-H}_2\text{BH}(\text{NH}_2\text{BH}_2)_n\text{NH}_3\}(\text{PCy}_3)_2][\text{BAR}^{\text{F}}_4]$  ( $n = 1-4$ , **969** in Scheme 147). The identity of these species has been confirmed by the

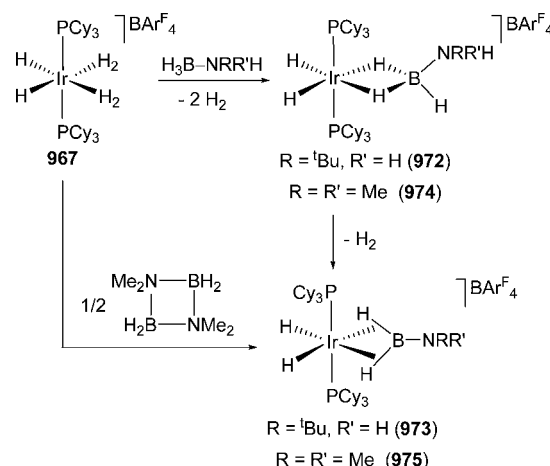
**Scheme 147. Dehydrocoupling of Ammonia-Borane Promoted by 967**



independent synthesis of some of them by means of the reaction of **967** with the preformed borazanes.<sup>466</sup> The primary amine-borane  $\text{H}_3\text{B-NMeH}_2$  forms the simplest oligomeric species. Complex **967** reacts with this amine-borane to give the amine-borane counterpart of **968**,  $[\text{IrH}_2(\kappa^2\text{-H}_2\text{BHNMeH}_2)(\text{PCy}_3)_2][\text{BAR}^{\text{F}}_4]$  (**970**), which is stable and does not undergo dehydrogenation. However, the addition of a further equivalent of amine-borane to **970** results in a relatively fast reaction to afford  $[\text{IrH}_2\{\kappa^2\text{-H}_2\text{BH}(\text{NMeHBH}_2)\text{NMeH}_2\}(\text{PCy}_3)_2][\text{BAR}^{\text{F}}_4]$  (**971**) and  $\text{H}_2$ .<sup>467</sup>

The use of bulky primary,  $\text{H}_3\text{B-N}^t\text{BuH}_2$ , or secondary,  $\text{H}_3\text{B-NMe}_2\text{H}$ , amine-boranes has also given information about the dehydrocoupling, although this suggests an on-metal dehydrogenation and an off-metal coupling. The reaction of **967** with  $\text{H}_3\text{B-N}^t\text{BuH}_2$  leads to  $[\text{IrH}_2(\kappa^2\text{-H}_2\text{BHN}^t\text{BuH}_2)(\text{PCy}_3)_2][\text{BAR}^{\text{F}}_4]$  (**972**), which eliminates  $\text{H}_2$  to afford the bis( $\sigma$ -B–H) aminoborane derivative  $[\text{IrH}_2(\eta^2, \eta^2\text{-H}_2\text{BN}^t\text{BuH})(\text{PCy}_3)_2][\text{BAR}^{\text{F}}_4]$  (**973**). The release of the aminoborane, by addition of acetonitrile to **973**, gives rise to the formation of the cyclic borazine  $[\text{HBN}^t\text{Bu}]_3$ .<sup>176,468</sup> Similarly, the addition of  $\text{H}_3\text{B-NMe}_2\text{H}$  to **967** gives  $[\text{IrH}_2(\kappa^2\text{-H}_2\text{BHNMe}_2\text{H})(\text{PCy}_3)_2][\text{BAR}^{\text{F}}_4]$  (**974**). The dehydrogenation of the amine-borane leads to  $[\text{IrH}_2(\eta^2, \eta^2\text{-H}_2\text{BNMe}_2)(\text{PCy}_3)_2][\text{BAR}^{\text{F}}_4]$  (**975**), which has also been prepared by addition of the cyclic dimer  $[\text{H}_2\text{BNMe}_2]_2$  to **967** (Scheme 148).<sup>469</sup> Related NHC-complexes  $[\text{IrH}_2(\eta^2, \eta^2\text{-H}_2\text{BNR}_2)(\text{IMes})_2][\text{BAR}^{\text{F}}_4]$  ( $\text{R} = \text{Me}$  (**976**),  $^i\text{Pr}$  (**977**),  $\text{Cy}$  (**978**)) have also been prepared by reaction of  $\text{IrH}_2\text{Cl}(\text{IMes})_2$

**Scheme 148. Dehydrogenation of Amine-Boranes Promoted by 967**

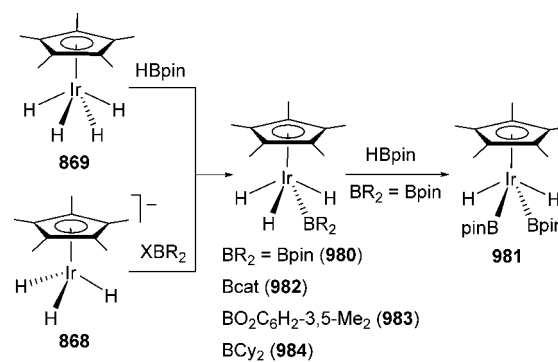


with the corresponding amine-borane in the presence of  $\text{Na}[\text{BAR}^{\text{F}}_4]$ .<sup>366,367,470</sup>

The bis(phosphinite) pincer- $\text{IrH}_2/\text{IrH}_4$ -pair **903/904** catalyzes the release of hydrogen chemically stored in ammonia-borane under mild conditions,<sup>471,472</sup> forming polyaminoborane.<sup>473,474</sup> Although a side  $\text{IrH}_2(\eta^2\text{-HBH}_2)\{\kappa^3\text{-C}_6\text{H}_3\text{-1,3-(OP}^t\text{Bu)}_2\}$  (**979**) species is formed during the reaction,<sup>39,475</sup> the active intermediate **904** is efficiently regenerated in the presence of molecular hydrogen. DFT calculations<sup>476</sup> suggest that the mechanism of the catalysis is similar to that previously described for the bis(phosphine)  $\text{OsH}_2/\text{OsH}_4$ -system **300/345**.

The B–H bond activation is also a fundamental reaction in order to perform regiospecific functionalization of hydrocarbons, since it is one of the key steps in the direct borylation of arene and alkanes.<sup>32–36</sup> Thermolysis of the  $\text{Ir(V)}$  complex **869** with a small excess of  $\text{HBpin}$  at  $80^\circ\text{C}$  for 50 h in octane forms the monoboryl trihydride  $\text{IrH}_3(\text{Bpin})(\eta^5\text{-C}_5\text{Me}_5)$  (**980**). Reaction of the latter with a large excess of  $\text{HBpin}$  for 50 h at  $100^\circ\text{C}$  produces the dihydride-bis(boryl) derivative  $\text{IrH}_2(\text{Bpin})_2(\eta^5\text{-C}_5\text{Me}_5)$  (**981**). Reaction of the anion **868** with haloboranes provides an alternative route to monoboryl species. This method is more convenient to generate **980** and allows for the synthesis of  $\text{IrH}_3(\text{BR}_2)(\eta^5\text{-C}_5\text{Me}_5)$  ( $\text{BR}_2 = \text{Bcat}$  (**982**),  $\text{BOC}_6\text{H}_2\text{-3,5-Me}_2$  (**983**),  $\text{BCy}_2$  (**984**)), according to Scheme 149. In benzene- $d_6$ , complexes **980** and **982** afford  $\text{D}_5\text{C}_6\text{BR}_2$  in 78% and 79% yield, respectively. Heating of an octane solution of **980** at  $200^\circ\text{C}$  for 2 h forms the borylated

**Scheme 149. B–H Bond Activation Reactions Promoted by Pentamethylcyclopentadienyl Complexes**



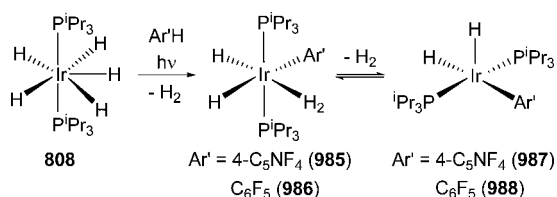


octane in 50% yield, whereas the reaction of **981** gives rise to 2 equiv of octylboronate ester in 45%.<sup>477</sup>

**5.6.2. C–H Bond Activation.** Several interesting stoichiometric and catalytic reactions involving Ir(polyhydride)-mediated activation of C–H bonds have been performed since 1985, after the revision of Hlatky and Crabtree.<sup>54</sup>

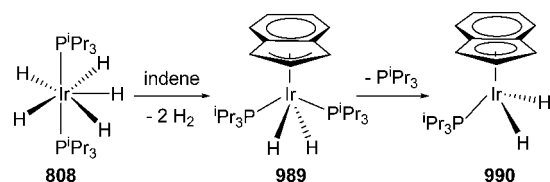
Irradiation of the pentahydride **808** with 2,3,5,6-tetrafluoropyridine and pentafluorobenzene in hexane or benzene affords the C–H bond activation products  $\text{IrH}_2(\text{Ar}')(\eta^2\text{-H}_2)(\text{P}^i\text{Pr}_3)_2$  ( $\text{Ar}' = 4\text{-C}_5\text{NF}_4$  (**985**),  $\text{C}_6\text{F}_5$  (**986**)), which lose molecular hydrogen to give the square pyramidal complexes  $\text{IrH}_2(\text{Ar}')(\text{P}^i\text{Pr}_3)_2$  ( $\text{Ar}' = 4\text{-C}_5\text{NF}_4$  (**987**),  $\text{C}_6\text{F}_5$  (**988**)), according to Scheme 150.<sup>478</sup>

**Scheme 150.** C–H Bond Activation of 2,3,5,6-Tetrafluoropyridine and Pentafluorobenzene Promoted by **808**



Complex **808** also activates indene. At 60 °C, the reaction initially leads to  $\text{IrH}_2(\eta^3\text{-C}_9\text{H}_7)(\text{P}^i\text{Pr}_3)_2$  (**989**), which dissociates triisopropylphosphine to give the  $\eta^5$ -indenyl derivative  $\text{IrH}_2(\eta^5\text{-C}_9\text{H}_7)(\text{P}^i\text{Pr}_3)_2$  (**990** in Scheme 151).<sup>479</sup>

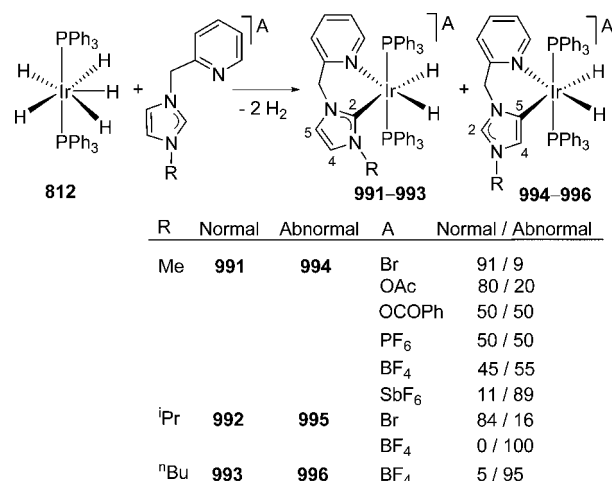
**Scheme 151.** C–H Bond Activation of Indene Promoted by **808**



The iridium-pentahydride **812** promotes the pyridyl-assisted C–H bond activation of 2-pyridylmethylimidazolium salts. The activation is kinetically controlled and takes place at both C2 and C5 to give mixtures of the normal (**991–993**) and abnormal (**994–996**) NHC products. The molar ratio between them depends upon the anion of the salt and the bulkiness of the substituent at N3 (Scheme 152). The normal product is the thermodynamically favored species. Thus, the  $\text{HBF}_4/\text{CH}_2\text{Cl}_2$  treatment of the mixtures, at room temperature, converts the abnormal products to the normal derivatives.<sup>480–482</sup>

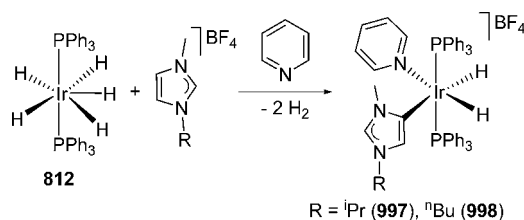
DFT calculations suggest that the formation of the abnormal products involves C–H oxidative addition to Ir(III) to give Ir(V) intermediates with little anion dependence. The formation of the normal product, in contrast, goes by heterolytic C–H activation with proton transfer to the adjacent hydride. The transferred proton is accompanied by the counteranion in an anion-coupled proton transfer, leading to an anion dependence of the normal formation pathway and, therefore, of the normal/abnormal selectivity. Steric congestion favors abnormal carbene binding ( $\text{R} = ^i\text{Pr}$ ,  $^n\text{Bu}$ ), while the less sterically demanding Me group promotes C2–H bond activation and formation of the normal carbene.<sup>482</sup> The pyridyl assistant does not play any role in the coordination mode of the

**Scheme 152.** Pyridyl-Chelate-Assisted C–H Bond Activation of 2-Pyridylmethylimidazolium Salts Promoted by **808**: Normal vs Abnormal Metalation



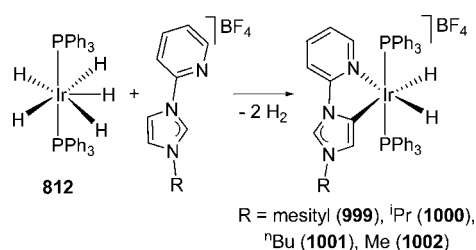
NHC group. The reactions of the tetrafluoroborate salts of 3-isopropyl- and 3-butyl-1-methylimidazolium with **812**, in the presence of free pyridine, also yield the corresponding abnormal derivatives  $[\text{IrH}_2(\text{NHC}^{\text{R}})(\text{py})(\text{PPh}_3)_2]\text{BF}_4$  ( $\text{R} = ^i\text{Pr}$  (**997**),  $^n\text{Bu}$  (**998**)), according to Scheme 153.<sup>483</sup>

**Scheme 153.** Reactions of **812** with 3-Isopropyl- and 3-Butyl-1-methylimidazolium in the Presence of Pyridine



The ligand precursors tetrafluoroborate 2-pyridylimidazolium salts, without a methylene linker between the pyridyl and imidazolium moieties, favor the abnormal coordination. Thus, the reactions with **812** lead to  $[\text{IrH}_2\{\kappa^2\text{-C}_2\text{N}(\text{py}-2\text{-abNHC}^{\text{R}})\}(\text{PPh}_3)_2]\text{BF}_4$  ( $\text{R} = \text{mesityl}$  (**999**),  $^i\text{Pr}$  (**1000**),  $^n\text{Bu}$  (**1001**), Me (**1002**)). Their formation seems to take place via an intermediate bearing a hydrogenated imidazolium ring, resulting from the hydrogen transfer from the metal to the carbene. This hydrogen transfer proves reversible on reflux, and the abnormal complexes **999–1002** are obtained as final products (Scheme 154).<sup>484</sup> If abnormal binding is blocked, the normal coordination occurs. So, this is not forbidden for small-

**Scheme 154.** Reactions of **812** with 2-Pyridylimidazolium Salts



bite angle ligands. The reactions of **812** with benzimidazolium salts give the corresponding C2 carbene complexes.

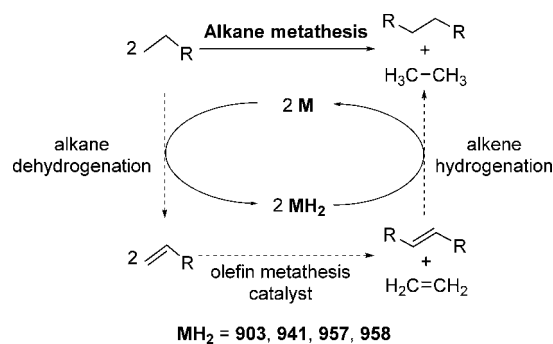
The triphenylphosphine complex **812** is insoluble in the usual organic solvents. In contrast, its triisopropylphosphine counterpart **808** is very soluble. This high solubility has greatly facilitated the use of **808** as a homogeneous catalyst precursor for a wide range of interesting organic reactions.  $\alpha,\beta$ -Ynone isomerize in the presence of **808** to give (*E,E*)- $\alpha,\beta,\gamma,\delta$ -dienones in high yield with high regioselectivity.<sup>485</sup> Deuterium–hydrogen exchange between benzene-*d*<sub>6</sub> and 3,3-dimethylbutene is also catalyzed by **808** at room temperature.<sup>486</sup> In the presence of small amounts of this olefin, after its hydrogenation, complex **808** even catalyzes the deuterium–hydrogen exchange between benzene-*d*<sub>6</sub> and methane.<sup>487</sup> By using 3,3-dimethylbutene as the hydrogen acceptor, the catalytic dehydrogenations of *n*-hexane to 1-hexene, methylcyclohexane to methylenecyclohexane,<sup>488</sup> pinane to  $\beta$ -pinene,<sup>489</sup> and cyclooctane to cyclooctene<sup>490</sup> have been performed with **808** as the catalyst precursor. The regioselective functionalization of alkanes has been achieved by dehydrogenation in the presence of **808** followed by hydrozirconation of the resulting olefin.<sup>491</sup> The formation of vinyl ethers by dehydrogenative coupling of ethers and olefins is other catalytic process promoted by **808**.<sup>492</sup>

The IrH<sub>4</sub>/IrH<sub>2</sub>-pincer pairs have also shown to be efficient catalyst precursors for organic processes involving C–H bond activation reactions. The application of this type of systems to dehydrogenation and related reactions was reviewed by MacArthur, Brookhart, and Goldman in 2011.<sup>56</sup> Since then, several findings should be highlighted. The transfer dehydrogenation of ketones by the bis(phosphine) pair **914/941** (<sup>t</sup>Bu<sub>2</sub>PCP<sup>t</sup>Bu<sub>2</sub>) has been observed. Catalytic turnover was inhibited in most cases by the formation of stable metalacycles or the O–H oxidative addition of phenolic products. Catalytic transfer dehydrogenation of 3,3-dimethylcyclohexanone was achieved, giving the corresponding  $\alpha,\beta$ -enone. The transfer dehydrogenation of cycloheptanone was found to generate a stable troponyl-iridium-hydride derivative, which catalyzes the dimerization of tropone to give a fused tricyclic dihydrodicycloheptafuranol.<sup>493</sup> Krogh-Jespersen, Goldman, and co-workers have reported the transfer-dehydrogenation of gas-phase alkanes, using ethylene or propene as hydrogen acceptor. In the solid phase, the pair **915/942** (<sup>i</sup>Pr<sub>2</sub>PCP<sup>i</sup>Pr<sub>2</sub>) is found to give extremely high rate and turnover numbers for *n*-alkane dehydrogenation and yields of  $\alpha$ -olefin that are much higher than those obtained for solution-phase experiments. Experimental mechanistic studies and DFT calculations suggest that olefin isomerization, which limits yields of  $\alpha$ -olefin, proceeds via two pathways. The more conventional pathway involves 2,1-insertion of the  $\alpha$ -olefin into an Ir–H bond of **942**, followed by 3,2- $\beta$ -H elimination. The use of ethylene as hydrogen acceptor, or high pressures of propene, precludes this pathway by rapid hydrogenation of these olefins. The other pathway proceeds via  $\alpha$ -olefin C–H addition to the iridium center to afford an allyl species. The improved understanding of the factors controlling rates and selectivity has led to solution-phase systems that afford improved yields of  $\alpha$ -olefins.<sup>457</sup> The pair **915/942** also catalyzes the conversion of *n*-alkanes to alkylaromatics using olefinic hydrogen acceptors. For instance, the reaction of *n*-octane affords up to 86% yield of aromatic products, primarily *o*-xylene and secondarily ethylbenzene. In the case of *n*-decane and *n*-dodecane, the resulting alkylarenes are exclusively unbranched, with selectivity for the corresponding *o*-(*n*-alkyl)toluene.<sup>455</sup> Huang and co-workers have reported that

the hybrid thiophosphinite-phosphinite pair **929/956** (PSCOP) catalyzes the dehydrogenation of *n*-alkanes with high regioselectivity to the  $\alpha$ -olefin and of heterocycles to heteroarenes, in the presence of 3,3-dimethylbutene.<sup>458</sup> With the same hydrogen acceptor, Yamamoto and co-workers have observed that the bis(phosphine) pincer pairs **932/959** and **934/961** bearing a 7–6–7 fused-ring skeleton are highly effective in the dehydrogenation of cyclooctane to cyclooctene. The initial rate at 230 °C is higher for **932/959** (<sup>i</sup>Pr<sub>2</sub>PCP<sup>i</sup>Pr<sub>2</sub>) than **934/961** (<sup>Ph</sup>2PCP<sup>Ph</sup>2). However, the turnover number of the overall process is higher for the latter (4600 versus 4820).<sup>460</sup>

Goldman, Brookhart, and co-workers have developed a highly productive tandem catalytic procedure for the metathesis of *n*-alkanes (Scheme 155). Each elemental reaction comprises

**Scheme 155. Tandem Catalytic Procedure for the Metathesis of *n*-Alkanes**

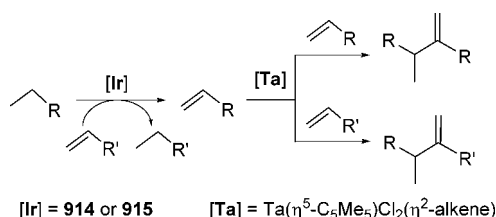


one molecular catalyst. IrH<sub>4</sub>/IrH<sub>2</sub>-pincer pairs effect alkane dehydrogenation and olefin hydrogenation whereas a Schrock-type molybdenum alkylidene derivative performs the olefin metathesis.<sup>494</sup> Both the pincer bis(phosphinite) **904/903** (<sup>t</sup>Bu<sub>2</sub>POCOP<sup>t</sup>Bu<sub>2</sub>) and bis(phosphine) **914/941** (<sup>t</sup>Bu<sub>2</sub>PCP<sup>t</sup>Bu<sub>2</sub>) cocatalyze alkane metathesis in tandem with olefin metathesis catalysts, but the two pairs have different resting states during the catalysis, suggesting that different steps are turnover-limiting in each case. In tandem with the olefin-metathesis catalyst Mo(N-2,6-<sup>i</sup>Pr<sub>2</sub>C<sub>6</sub>H<sub>3</sub>)(CHCMe<sub>2</sub>Ph)[OCMe(CF<sub>3</sub>)<sub>2</sub>]<sub>2</sub>, the hybrid phosphine-phosphinite pincer pairs **930/957** (<sup>t</sup>Bu<sub>2</sub>PCOP<sup>t</sup>Bu<sub>2</sub>) and **931/958** (<sup>t</sup>Bu<sub>2</sub>PCOP<sup>i</sup>Pr<sub>2</sub>) display significantly higher activity for the metathesis of *n*-hexane than does **904/903** and **914/941**.<sup>459</sup>

A tandem catalytic approach for the coupling of alkanes and alkenes has been recently developed by Labinger and Bercaw in order to upgrade light hydrocarbons into heavier fuel molecules. The procedure involves alkane dehydrogenation with a bis(phosphine) pincer- IrH<sub>4</sub>/IrH<sub>2</sub>-pair, for example **914/941** or **915/942**, and alkene dimerization by a Ta( $\eta^5$ -C<sub>5</sub>Me<sub>5</sub>)Cl<sub>2</sub>( $\eta^2$ -alkene) catalyst (Scheme 156). The dual homogeneous system operates with up to 60/30 cooperative turnovers (Ir/Ta) in the dimerization of 1-hexene/*n*-heptane, giving C<sub>13</sub>/C<sub>14</sub> products in 40% yield. The system can also effect the catalytic dimerization of *n*-heptane with cooperative turnover number of 22/3 (Ir/Ta), using neohexene as hydrogen acceptor.<sup>495,496</sup>

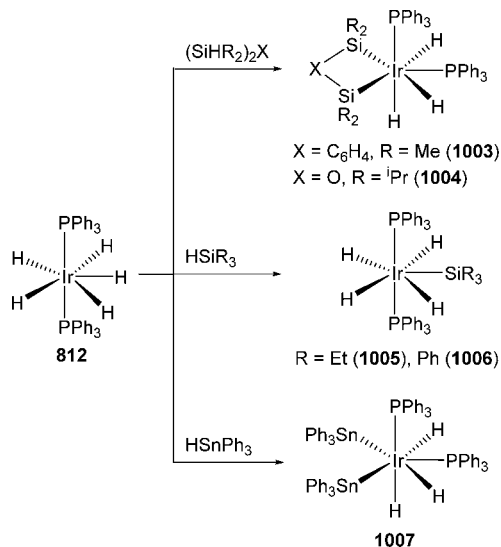
Wendt and co-workers have reported an iridium pincer promoted intramolecular coupling reaction involving three unactivated C(sp<sup>3</sup>)-H bonds to give a C–C double bond under the extrusion of dihydrogen.<sup>497</sup>

Scheme 156. Tandem Catalytic Approach for the Coupling of Alkanes and Alkenes



**5.6.3. Si–H Bond Activation.** Interesting polyhydride-iridium(V)-silyl compounds have been obtained by activation of Si–H bonds.

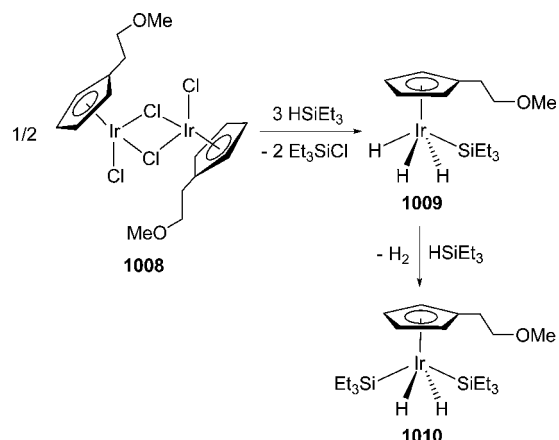
The bis(phosphine) pentahydride complex **812** reacts with disilanes with loss of molecular hydrogen to form the classical seven-coordinate distorted pentagonal bipyramidal trihydride-silyl derivatives IrH<sub>3</sub>(R<sub>2</sub>SiXSiR<sub>2</sub>)(PPh<sub>3</sub>)<sub>2</sub> (X = C<sub>6</sub>H<sub>4</sub>, R = Me (**1003**); X = O, R = <sup>i</sup>Pr (**1004**)). The reactions with monodentate silanes, HSiR<sub>3</sub>, lead to the tetrahydride compounds IrH<sub>4</sub>(SiR<sub>3</sub>)(PPh<sub>3</sub>)<sub>2</sub> (R = Et (**1005**), Ph (**1006**)), whereas with HSnPh<sub>3</sub> the trihydride-bis(stannyl) IrH<sub>3</sub>(SnPh<sub>3</sub>)<sub>2</sub>(PPh<sub>3</sub>)<sub>2</sub> (**1007**) is obtained (Scheme 157).<sup>498</sup>

Scheme 157. Si–H and Sn–H Bond Activation Reactions Promoted by **812**

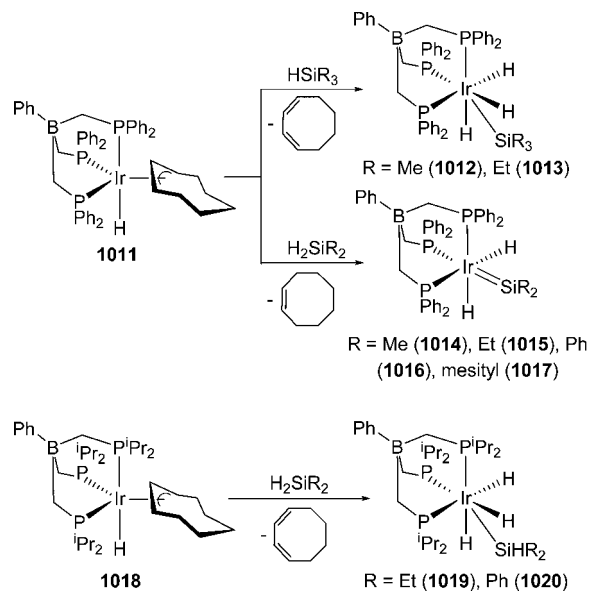
The cyclopentadienyl-dimer complex [Ir{ $\eta^5$ -C<sub>5</sub>H<sub>4</sub>(CH<sub>2</sub>)<sub>2</sub>OMe}Cl( $\mu$ -Cl)]<sub>2</sub> (**1008**) reacts with 3.0 equiv of HSiEt<sub>3</sub> per iridium to give the Ir(V) silyl-trihydride derivative IrH<sub>3</sub>(SiEt<sub>3</sub>){ $\eta^5$ -C<sub>5</sub>H<sub>4</sub>(CH<sub>2</sub>)<sub>2</sub>OMe} (**1009**), which in the presence of excess of HSiEt<sub>3</sub> is transformed into IrH<sub>2</sub>(SiEt<sub>3</sub>)<sub>2</sub>{ $\eta^5$ -C<sub>5</sub>H<sub>4</sub>(CH<sub>2</sub>)<sub>2</sub>OMe} (**1010**), according to Scheme 158. In benzene-d<sub>6</sub> at 80 °C, the selective deuteration of the hydride and cyclopentadienyl positions of **1009** takes place to afford IrD<sub>3</sub>(SiEt<sub>3</sub>){ $\eta^5$ -C<sub>5</sub>H<sub>4</sub>(CH<sub>2</sub>)<sub>2</sub>OMe} (**1009-d<sub>3</sub>**) and IrD<sub>3</sub>(SiEt<sub>3</sub>){ $\eta^5$ -C<sub>5</sub>D<sub>4</sub>(CH<sub>2</sub>)<sub>2</sub>OMe} (**1009-d<sub>7</sub>**). In benzene, the latter evolves into IrH<sub>3</sub>(SiEt<sub>3</sub>){ $\eta^5$ -C<sub>5</sub>D<sub>4</sub>(CH<sub>2</sub>)<sub>2</sub>OMe} (**1009-d<sub>4</sub>**).<sup>499</sup>

Complex IrH(PhBP<sub>3</sub><sup>Ph</sup>)( $\eta^3$ -C<sub>8</sub>H<sub>13</sub>) (**1011**, PhBP<sub>3</sub><sup>Ph</sup> = PhB-(CH<sub>2</sub>PPh<sub>2</sub>)<sub>3</sub>) reacts with tertiary silanes, HSiR<sub>3</sub>, to give the silyl-capped trihydride derivatives IrH<sub>3</sub>(PhBP<sub>3</sub><sup>Ph</sup>)(SiR<sub>3</sub>) (R = Me (**1012**), Et (**1013**)), with concomitant  $\beta$ -hydride elimination of 1,3-cyclooctadiene. However, the reactions of

Scheme 158. Si–H Bond Activation Reactions Promoted by Iridium-Cyclopentadienyl Complexes



**1011** with secondary silanes, H<sub>2</sub>SiR<sub>2</sub>, lead to the corresponding dihydride-silylene species IrH<sub>2</sub>(PhBP<sub>3</sub><sup>Ph</sup>)(=SiR<sub>2</sub>) (R = Me (**1014**), Et (**1015**), Ph (**1016**), mesityl (**1017**)) with elimination of cyclooctene. In contrast to **1011**, its <sup>i</sup>Pr-analogous IrH(PhBP<sub>3</sub><sup>iPr</sup>)( $\eta^3$ -C<sub>8</sub>H<sub>13</sub>) (**1018**, PhBP<sub>3</sub><sup>iPr</sup> = PhB-(CH<sub>2</sub>P<sup>i</sup>Pr<sub>2</sub>)<sub>3</sub>) does not induce the formation of silylene derivatives in the presence of secondary silanes. Thus, its reactions with H<sub>2</sub>SiR<sub>2</sub> lead to the corresponding trihydride complexes IrH<sub>3</sub>(PhBP<sub>3</sub><sup>iPr</sup>)(SiHR<sub>2</sub>) (R = Et (**1019**), Ph (**1020**)) and 1,3-cyclooctadiene (Scheme 159).<sup>500,501</sup> Complex **1019** has

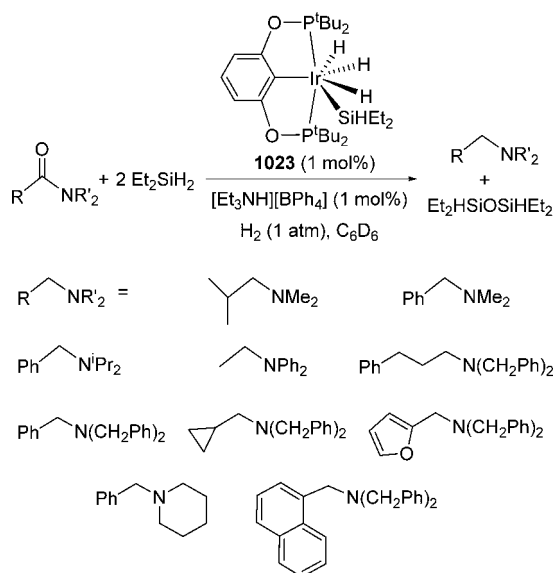
Scheme 159. Si–H Bond Activation Reactions Promoted by **1011** and **1018**

been shown to undergo H/D exchange with D<sub>2</sub> to incorporate deuterium into both the hydride and Si–H positions. A Tp<sup>Me2</sup> complex IrH<sub>3</sub>(SiEt<sub>3</sub>)Tp<sup>Me2</sup> (**1021**) with a similar structure has been isolated and characterized by X-ray diffraction analysis.<sup>424</sup>

Brookhart and co-workers have proved that a trihydride-Ir(V)-silyl complex stabilized by the pincer ligand 2,6-bis(di-*tert*-butylphosphinito)phenyl is the silylating agent in the reduction of tertiary amides to amines with secondary silanes. The iridium(III) cation [IrH(acetone){C<sub>6</sub>H<sub>3</sub>-2,6-(OP<sup>t</sup>Bu<sub>2</sub>)<sub>2</sub>}]<sup>+</sup> (**1022**) was shown to catalyze the reduction of tertiary amides

using diethylsilane as a reductant. Mechanistic studies established that complex  $\text{IrH}_3(\text{SiHEt}_2)\{\text{C}_6\text{H}_3\text{-2,6-(OP}^t\text{Bu}_2)_2\}$  (**1023**) was the active species. High concentrations of **1023** can be generated by treatment of the starting material  $\text{IrHCl}\{\text{C}_6\text{H}_3\text{-2,6-(OP}^t\text{Bu}_2)_2\}$  (**1024**) with *tert*-butoxide in the presence of  $\text{Et}_2\text{SiH}_2$  under  $\text{H}_2$ . Thus, using this mixture in the presence of a trialkylammonium salt, a wide array of tertiary amides are efficiently reduced to amines (Scheme 160). This reaction

**Scheme 160. Iridium-Mediated Reduction of Tertiary Amides to Amines with Secondary Silanes**



works as follows: complex **1023** reduces the amide to the hemiaminal silyl ether that, in the presence of a trialkylammonium salt, is ionized to the iminium ion, which is then reduced to the tertiary amine by  $\text{H}_2\text{SiEt}_2$ . Good functional group compatibility is observed, and a high stability has provided turnover numbers as high as 10000.<sup>502</sup>

**5.6.4. O–H Bond Activation.** Several catalytic processes involving the  $\text{IrH}_n$ -mediated O–H bond activation of alcohols have been described.<sup>56</sup> The bis(triisopropylphosphine)-penta-hydride complex **808** catalyzes the hydrogen transfer from 2-propanol to cyclohexanones, benzylideneacetone, styrene, and cyclohexadienes. The reduction of the carbon–carbon double bond of the  $\alpha,\beta$ -unsaturated ketone is clearly preferred, and no unsaturated alcohol is formed. With 1,4-cyclohexadiene as a substrate, different reactions are observed. Initially, the rapid isomerization of the 1,4-isomer to the thermodynamically more stable 1,3-cyclohexadiene occurs. Subsequently, the disproportionation of the latter to cyclohexene and benzene takes place.<sup>395</sup> Complex **808** also catalyzes the isomerization of allylic secondary alcohols into ketones<sup>503</sup> and the isomerization of propargylic alcohols to  $\alpha,\beta$ -enones. In toluene under reflux, the reactions proceed through the intramolecular hydrogen transfer from the alcohol function to the unsaturated carbon–carbon double bond. The significance of this type of process is demonstrated by the transformation of 3-hexyn-2,5-diol to 2,5-hexanedione.<sup>504</sup> In the absence of hydrogen acceptor, the catalyst promotes the generation of molecular hydrogen. Thus, in hexamethyldisiloxane at 100 °C, a wide range of secondary alcohols have been converted into the corresponding ketones, including allylic and homoallylic steroidal alcohols. In these cases, saturated ketones were also formed as a result of the

competition of the hydrogen transfer reaction with the dehydrogenation.<sup>505</sup> The oxidative condensation of diols promoted by **808** leads to 5- and 6-ring lactones. The regioselective dehydrogenation of unsymmetrically substituted 1,4-diols gives  $\beta$ - or  $\gamma$ -substituted  $\gamma$ -lactones in high yields.<sup>506</sup>

## 6. GROUP 10

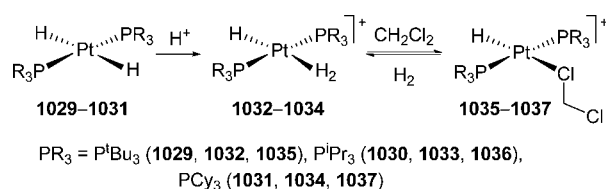
The relative stabilities of diatomic first and second row transition metal hydrides have been compared from a theoretical point of view and rationalized in terms of the electronic configuration ground state of the metal center.<sup>507</sup>

Although the calculated dissociation energies for the M–H bond in the sequence Ru, Rh, and Pd do not seem to be very different (58.9, 64.1, and 51.1 kcal mol<sup>-1</sup>, respectively),<sup>508</sup> the fact is that the chemistry of the polyhydrides of palladium is elusive in absolute terms, being confined to the salt  $\text{Na}_2[\text{PdH}_4]$  (**1025**)<sup>509</sup> and a pair of dihydrogen adducts formed at low temperature in rare-gas matrices and characterized by vibrational spectroscopy.<sup>510</sup> The dihydrogen form is favored with regard to the dihydride tautomer because the intramolecular reductive elimination of hydrogen from palladium(II) appears to be exothermic, since palladium prefers to be  $d^{10}$ , in contrast to the reductive elimination from platinum(II) which is endothermic preferring platinum to be  $s^1d^9$ .<sup>511</sup> Thus, thermally evaporated and laser-ablated palladium atoms interact with molecular hydrogen in excess argon to yield the side-bonded  $\text{Pd}(\eta^2\text{-H}_2)$  (**1026**). This species readily adds one and two more hydrogen molecules to afford  $\text{Pd}(\eta^2\text{-H}_2)_2$  (**1027**) and  $\text{Pd}(\eta^2\text{-H}_2)_3$  (**1028**), which are predicted by DFT calculations to have approximately  $D_{2d}$  and  $D_{3h}$  structures. The bonding situation in these dihydrogens has been analyzed using the electron localization function (ELF) topological method. The results suggest a predominant charge-transfer nature of the Pd–H<sub>2</sub> interaction with a minor amount of charge reorganization on the metal center in the cooperatively coupled donor–acceptor delocalization.<sup>512</sup>

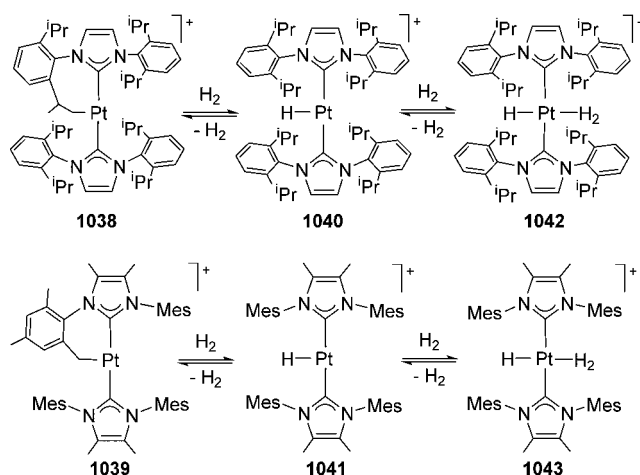
Some polyhydride complexes of platinum are known, although their chemistry is extremely poor and is limited to  $\text{PtH}_3$ -derivatives, including square-planar *trans*-hydride-dihydrogen-platinum(II) cations and a few five-coordinate and octahedral trihydride-platinum(IV) complexes.

The *trans*-dihydride-bis(phosphine) complexes  $\text{PtH}_2(\text{PR}_3)_2$  ( $\text{PR}_3 = \text{P}^t\text{Bu}_3$  (**1029**),  $\text{P}^i\text{Pr}_3$  (**1030**),  $\text{PCy}_3$  (**1031**)) undergo protonation with  $\text{CF}_3\text{SO}_3\text{H}$  (**1029**) and  $[\text{H}(\text{OEt})_2]\text{BAR}^F_4$  (**1030** and **1031**), at low temperature (183–190 K), to afford *trans*- $[\text{PtH}(\eta^2\text{-H}_2)(\text{PR}_3)_2]^+$  ( $\text{PR}_3 = \text{P}^t\text{Bu}_3$  (**1032**),  $\text{P}^i\text{Pr}_3$  (**1033**),  $\text{PCy}_3$  (**1034**)). A short separation between the hydrogen atoms of the dihydrogen ligand (0.8–0.9 Å) has been inferred from the large H–D coupling constant in the corresponding isotopomers ( $J_{\text{H-D}} = 31\text{--}35$  Hz). Complexes **1032–1034** are stable in dichloromethane at low temperature. At room temperature, they dissociate the dihydrogen ligand to afford the solvento derivatives  $[\text{PtH}(\text{ClCH}_2\text{Cl})(\text{PR}_3)_2]^+$  ( $\text{PR}_3 = \text{P}^t\text{Bu}_3$  (**1035**),  $\text{P}^i\text{Pr}_3$  (**1036**),  $\text{PCy}_3$  (**1037**)). The dissociation is reversible. Under hydrogen atmosphere, complexes **1035–1037** are in equilibrium with the hydride-dihydrogen derivatives **1032–1034** (Scheme 161).<sup>513–515</sup>

Conejero and Lledós have reported related bis(NHC) complexes. The cationic species  $[\text{Pt}(\text{NHC}')(\text{NHC})]^+$  ( $\text{NHC} = \text{IPr}$  (**1038**), 1,3-dimesityl-4,5-dimethylimidazol-2-ylidene ( $\text{IMes}^*$ ; **1039**)) containing a cyclometalated NHC ligand ( $\text{NHC}'$ ), undergo hydrogenolysis under hydrogen atmosphere, at room temperature, to give the monohydrides  $[\text{PtH}$

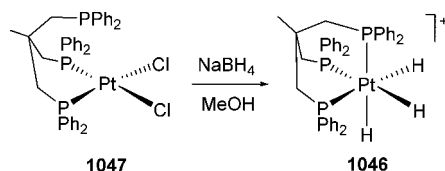
**Scheme 161. Preparation of  $trans$ -[PtH( $\eta^2$ -H<sub>2</sub>)(PR<sub>3</sub>)<sub>2</sub>]<sup>+</sup> Complexes**


(NHC)<sub>2</sub>]<sup>+</sup> (NHC = IPr (1040), IMes\* (1041)) in equilibrium with the respective *trans*-hydride-dihydrogen derivatives [PtH( $\eta^2$ -H<sub>2</sub>)(NHC)<sub>2</sub>]<sup>+</sup> (NHC = IPr (1042), IMes\* (1043)), which are the NHC counterparts of 1032–1034 (Scheme 162).<sup>516</sup> In

**Scheme 162. Preparation of [PtH( $\eta^2$ -H<sub>2</sub>)(NHC)<sub>2</sub>]<sup>+</sup> Complexes**


contrast to 1042 and 1043, the stannyl complexes PtH<sub>3</sub>(Sn<sup>t</sup>Bu<sub>3</sub>)(I<sup>t</sup>Bu) (1044)<sup>517</sup> and PtH<sub>3</sub>(Sn<sup>t</sup>Bu<sub>3</sub>)(IPr) (1045)<sup>518</sup> have been characterized as five-coordinate trihydride-platinum(IV) species.

The trihydride complex [PtH<sub>3</sub>(triphos<sup>Me</sup>)]<sup>+</sup> (1046) is quantitatively formed upon treatment of PtCl<sub>2</sub>( $\kappa^2$ -*P,P*-triphos<sup>Me</sup>) (1047) with NaBH<sub>4</sub> in methanol or methanol-dichloromethane according to Scheme 163.<sup>519</sup> The reaction is

**Scheme 163. Preparation of 1046**


proposed to occur via the platinum(II) intermediate PtH<sub>2</sub>( $\kappa^2$ -*P,P*-triphos<sup>Me</sup>) (1048), which undergoes protonation with MeOH. Treatment of [PtPh(MeOH)(PR<sub>3</sub>)<sub>2</sub>]<sup>+</sup> (PR<sub>3</sub> = PMe<sub>3</sub> (1049), PEt<sub>3</sub> (1050)) with NaBH<sub>4</sub> in methanol leads to a mixture of products containing a small amount (less than 10%) of the trihydrides *mer*-PtH<sub>3</sub>Ph(PR<sub>3</sub>)<sub>2</sub> (PR<sub>3</sub> = PMe<sub>3</sub> (1051), PEt<sub>3</sub> (1052)).<sup>520</sup>

Brookhart, Templeton, and co-workers have efficiently transformed the precursor PtH<sub>2</sub>MeTp<sup>Me2</sup> (1053) into the classical trihydride PtH<sub>3</sub>Tp<sup>Me2</sup> (1054), via the platinum(II) intermediate PtHTp<sup>Me2</sup>(CO) (1055). Under a CO atmosphere,

the protonation of 1054 with [H(OEt)<sub>2</sub>][BAR<sup>F</sup><sub>4</sub>] at 193 K, gives [PtH<sub>3</sub>( $\kappa^2$ -HTp<sup>Me2</sup>)(CO)]BAR<sup>F</sup><sub>4</sub> (1056), which loses H<sub>2</sub> to afford [PtH( $\kappa^2$ -HTp<sup>Me2</sup>)(CO)]BAR<sup>F</sup><sub>4</sub> (1057) in an almost quantitative yield (Scheme 164). The isotopic effect (2.2 ± 0.1) and the reaction entropy (24.5 ± 4 eu) are consistent with a mechanism involving reversible reductive coupling to form a dihydrogen intermediate followed by rate-limiting irreversible dissociation of H<sub>2</sub>.<sup>521,522</sup>

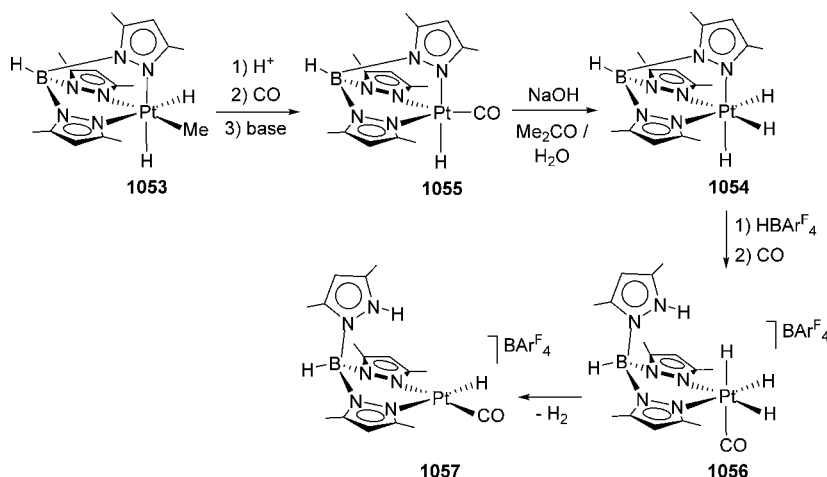
**7. CONCLUSION AND OUTLOOK**

Osmium possesses the richest chemistry among the six platinum group metals. Thus, the widest range of complexes with different stoichiometries and structures is observed. Furthermore, its polyhydrides show a highly diverse reactivity which is dominated by C–H bond activation reactions. In the opposite side, palladium polyhydrides are largely unknown. This situation is due to three general precepts in coordination chemistry: (i) the transition metals situated at the center of the periodic table exhibit the widest range of oxidation states, and in this respect, ruthenium and osmium occupy a particularly privileged position; (ii) the oxidation state of the metal center determines the coordination number and the geometry of the complexes; and (iii) the stability of the highest oxidation states increases as going down in a triade.

Ruthenium and rhodium favor the formation of dihydrogen derivatives. Osmium and iridium however prefer to stabilize elongated dihydrogen species or compressed dihydrides, of the same stoichiometry. The comparison of the ruthenium-bis(diphosphine) complexes with their osmium counterparts is an overwhelming evidence of this asseveration. The question is what are truly elongated dihydrogens and compressed dihydrides, dihydrogens, or dihydrides? Section 3.5 shows some evidence that strongly supports the dihydride character of these ligands. In this context, it should be noted that 4d metals are more oxidizing than their triade 5d analogous. However, the 5d metals are more reducing. Elongated dihydrogen and compressed dihydrides should be viewed as dihydrides undergoing some nonclassical interaction, including quantum mechanical exchange coupling. So, elongated dihydrogen and compressed dihydrides should be properly called nonclassical dihydrides.

The dihydrogen or elongated dihydrogen nature of the M( $\eta^2$ -H<sub>2</sub>) units mainly depends upon the electron richness of the metal center. However, the elongated dihydrogen or compressed dihydride character appears to be a consequence of the steric requirements of the heavy coligands, in the plane containing the coordinated hydrogen atoms. As a proof of concept, it has been observed that the hydrogen–hydrogen separation in the pincer compressed dihydrides in section 3.6.7 decreases as the steric requirements of the heterocyclic moiety of the pincers increase<sup>350</sup> (i.e., pyridine > isoquinoline > quinoline). The dihydrogen or elongated dihydrogen nature of the compounds is a consequence not only of the electron richness of the metal center but also of the geometry of the heavy coligands. The difference between half-sandwich and Tp complexes is clear evidence. Tp-type and BAEA ligands enforce dispositions allowing N–M–N angles close to 90° and in contrast to Cp and Cp\*, which favor four-legged piano stool structures, stabilize dihydrogen derivatives.

The nonclassical or classical character of the polyhydrides is decisive in the reactivity of these compounds. First because it determines the dissociation energy of a hydrogen molecule, it is the necessary step for generating the unsaturated species which initiate the  $\sigma$ -bond activation processes. Second because it

Scheme 164. Preparation of Classical Trihydride-Platinum(IV) Complexes Containing the Tp<sup>Me2</sup> Ligand

reflects the richness of the metal center, which governs the basicity of the remaining hydrides and predetermines the nature of the interaction between the metal center and the  $\sigma$ -bond which, after its coordination, will be activated. In general, nonclassical polyhydrides promote the homolysis of the  $\sigma$ -bonds, since the metal center is able to reach low oxidation states, while classical polyhydrides favor heterolytic cleavages through intermediate oxidation states of the metal center.

The improvement of quality of the characterization techniques has been certainly crucial for the development of the field. In spite of this fact, the chemistry of polyhydrides remains laborious and complex from an experimental point of view and conceptually difficult. So, it is not foreseeable that the topic will be popularized. On the contrary, it will most probably continue being restricted to specialized laboratories. However, its survival is guaranteed by the ability of the polyhydrides of platinum group metals to activate  $\sigma$ -bonds. In this context, an increased interest should be expected due to the role that this type of compound can play in understanding and developing reactions associated with conversion and storage of regenerative energy. The importance of the C–H bond activation reactions in modern organic synthetic chemistry is another relevant factor that will contribute to the reinforcement of the field, although in this case, an improvement of the experimental procedures in some organic laboratories will be necessary, in order to fully exploit the potential of the polyhydrides. The possibility of generating metalatrinems, which can be a novel type of inhibitors of  $\beta$ -lactamases, by means of the N–H bond activation of 2-azetidinones opens the door of the drugs design to the polyhydrides. Additionally, in the search for models of new anticancer drugs, the activation of N–H, O–H, and N–C bonds of nucleobases promoted by osmium hexahydrides, as well as, the ability of some hydride ligands to form hydrogen bonds<sup>523–525</sup> envisages exciting new ground. Finally, it should also be mentioned the recent use of polyhydrides for the preparation of new types of compounds with notable applications in materials science.<sup>526–528</sup> So, the chemistry of the polyhydrides of the platinum group metals is still far from their full development. Unlike other more mature areas, it offers new exciting conceptual challenges and at the same time the possibility of interacting with other fields which foresee promising advances in the near future.

## AUTHOR INFORMATION

### Corresponding Author

\*E-mail: [maester@unizar.es](mailto:maester@unizar.es).

### Notes

The authors declare no competing financial interest.

### Biographies

Miguel A. Esteruelas was born in Zaragoza and grew up in La Zaida, a small village situated on the banks of the Ebro. He attended University of Zaragoza where received his Diploma in Chemistry in 1981. He carried out his doctoral work in organometallics at University of Zaragoza under the direction of Professors Daniel Carmona and Luis A. Oro. After obtaining his Ph.D. in December 1983, he worked as a postdoctoral fellow in the laboratory of Prof. Helmut Werner at the University of Würzburg, for 18 months. In 1985, Esteruelas returned to the University of Zaragoza, where he was promoted to Professor of Inorganic Chemistry in 1988 and to Distinguished Professor in 2003. In 2007, he moved to the Spanish Research Council (CSIC), where he is currently Research Professor at the Instituto de Síntesis Química y Catálisis Homogénea (ISQCH). Esteruelas' research group focuses its interest in mechanistic, synthetic, and structural organometallic chemistry. Emphasis has been placed on the use of transition metal hydride complexes for the activation of  $\sigma$ -bonds, the generation of metal–carbon multiple bonds, and the catalytic formation of carbon–carbon and carbon–heteroatom bonds.

Ana M. López was born in Aranda de Duero, Spain, in 1962. She studied Chemistry at the University of Zaragoza where she obtained her Ph.D. in 1991 under the supervision of Professors M. Pilar García and Luis A. Oro. Then she joined the Prof. Esteruelas group. Since 2012, she has been full professor at the University of Zaragoza. Her research interests concern organometallic complexes of the platinum group metals and their applications in homogeneous catalysis.

Montserrat Oliván studied chemistry at the University of Zaragoza (Spain) and obtained her Ph.D. in 1995 working under the supervision of Profs. Miguel A. Esteruelas and Luis A. Oro. She then joined the group of Prof. Kenneth G. Caulton at Indiana University (Bloomington, IN) for a two-year postdoctoral stay. Thereafter, she returned to the University of Zaragoza. Since 2005, she has been "Científico Titular" at the Instituto de Síntesis Química y Catálisis Homogénea (Universidad de Zaragoza–CSIC). Her current research interests are mainly devoted to the study and reactivity of polyhydride and pincer derivatives of platinum group metal complexes as well as

their applications in fields ranging from homogeneous catalysis to material science.

## ACKNOWLEDGMENTS

Financial support from the MINECO of Spain (Projects CTQ2014-52799-P and CTQ2014-51912-REDC), the Diputación General de Aragón (E-35), FEDER, and the European Social Fund is acknowledged.

## DEDICATION

Dedicated to the memory of Prof. Rafael Usón (1926–2016) for his outstanding contribution to the development of organometallic chemistry.

## REFERENCES

- (1) Simões, J. A. M.; Beauchamp, J. L. Transition Metal-Hydrogen and Metal-Carbon Bond Strengths: The Keys to Catalysis. *Chem. Rev.* **1990**, *90*, 629–688.
- (2) Ortuño, M. A.; Vidossich, P.; Conejero, S.; Lledós, A. Orbital-Like Motion of Hydride Ligands around Low-Coordinate Metal Centers. *Angew. Chem., Int. Ed.* **2014**, *53*, 14158–14161.
- (3) Kubas, G. J. *Metal Dihydrogen and  $\sigma$ -Bond Complexes: Structure, Theory and Reactivity*; Kluwer: New York, 2001.
- (4) Kubas, G. J. Metal-Dihydrogen and  $\sigma$ -Bond Coordination: the Consummate Extension of the Dewar-Chett-Duncanson Model for Metal-Olefin  $\pi$  Bonding. *J. Organomet. Chem.* **2001**, *635*, 37–68.
- (5) Kubas, G. J. Fundamentals of H<sub>2</sub> Binding and Reactivity on Transition Metals Underlying Hydrogenase Function and H<sub>2</sub> Production and Storage. *Chem. Rev.* **2007**, *107*, 4152–4205.
- (6) Kubas, G. J. Activation of Dihydrogen and Coordination of Molecular H<sub>2</sub> on Transition Metals. *J. Organomet. Chem.* **2014**, *751*, 33–49.
- (7) Jia, G.; Lau, C.-P. Structural, Acidity and Chemical Properties of Some Dihydrogen/Hydride Complexes of Group 8 Metals with Cyclopentadienyls and Related Ligands. *Coord. Chem. Rev.* **1999**, *190–192*, 83–108.
- (8) Morris, R. H. Estimating the Acidity of Transition Metal Hydride and Dihydrogen Complexes by Adding Ligand Acidity Constants. *J. Am. Chem. Soc.* **2014**, *136*, 1948–1959.
- (9) Kubas, G. J. Heterolytic Splitting of H–H, Si–H, and Other Bonds on Electrophilic Metal Centers. *Adv. Inorg. Chem.* **2004**, *56*, 127–177.
- (10) Bau, R.; Drabnis, M. H. Structures of Transition Metal Hydrides Determined by Neutron Diffraction. *Inorg. Chim. Acta* **1997**, *259*, 27–50.
- (11) Jessop, P. G.; Morris, R. H. Reactions of Transition Metal Dihydrogen Complexes. *Coord. Chem. Rev.* **1992**, *121*, 155–284.
- (12) Heinekey, D. M.; Oldham, W. J., Jr. Coordination Chemistry of Dihydrogen. *Chem. Rev.* **1993**, *93*, 913–926.
- (13) Morris, R. H. Dihydrogen, Dihydride and in Between: NMR and Structural Properties of Iron Group Complexes. *Coord. Chem. Rev.* **2008**, *252*, 2381–2394.
- (14) Lin, Z.; Hall, M. B. Transition Metal Polyhydride Complexes: a Theoretical View. *Coord. Chem. Rev.* **1994**, *135–136*, 845–879.
- (15) Maseras, F.; Lledós, A.; Clot, E.; Eisenstein, O. Transition Metal Polyhydrides: From Qualitative Ideas to Reliable Computational Studies. *Chem. Rev.* **2000**, *100*, 601–636.
- (16) Heinekey, D. M.; Lledós, A.; Lluch, J. M. Elongated Dihydrogen Complexes: what Remains of the H–H Bond? *Chem. Soc. Rev.* **2004**, *33*, 175–182.
- (17) Besora, M.; Lledós, A.; Maseras, F. Protonation of Transition-Metal Hydrides: a not so Simple Process. *Chem. Soc. Rev.* **2009**, *38*, 957–966.
- (18) Devarajan, D.; Ess, D. H. Metal-Mediated Dihydrogen Activation. What Determines the Transition-State Geometry? *Inorg. Chem.* **2012**, *51*, 6367–6375.
- (19) Barea, G.; Esteruelas, M. A.; Lledós, A.; López, A. M.; Tolosa, J. I. Synthesis and Spectroscopic and Theoretical Characterization of the Elongated Dihydrogen Complex OsCl<sub>2</sub>( $\eta^2$ -H<sub>2</sub>)(NH=CPh<sub>2</sub>)(P<sup>t</sup>Pr<sub>3</sub>)<sub>2</sub>. *Inorg. Chem.* **1998**, *37*, 5033–5035.
- (20) Barrio, P.; Esteruelas, M. A.; Lledós, A.; Oñate, E.; Tomàs, J. Influence of the Cis Ligand on the H–H Separation and the Rotation Barrier of the Dihydrogen in Osmium-Elongated Dihydrogen Complexes Containing an Ortho-Metalated Ketone. *Organometallics* **2004**, *23*, 3008–3015.
- (21) Sabo-Etienne, S.; Chaudret, B. Quantum Mechanical Exchange Coupling in Polyhydride and Dihydrogen Complexes. *Chem. Rev.* **1998**, *98*, 2077–2091.
- (22) Jarid, A.; Moreno, M.; Lledós, A.; Lluch, J. M.; Bertrán, J. Quantum Mechanical Hydrogen Exchange Coupling in [(C<sub>2</sub>H<sub>5</sub>)Ir(L)H<sub>3</sub>]<sup>+</sup> Complexes (L = PH<sub>3</sub>, CO). A Combined ab Initio/Tunneling Dynamics Study. *J. Am. Chem. Soc.* **1995**, *117*, 1069–1075.
- (23) Heinekey, D. M.; Hinkle, A. S.; Close, J. D. Quantum Mechanical Exchange Coupling in Iridium Trihydride Complexes. *J. Am. Chem. Soc.* **1996**, *118*, 5353–5361.
- (24) Lin, Z. Structural and Bonding Characteristics in Transition Metal–Silane Complexes. *Chem. Soc. Rev.* **2002**, *31*, 239–245.
- (25) Lachaize, S.; Sabo-Etienne, S.  $\sigma$ -Silane Ruthenium Complexes: The Crucial Role of Secondary Interactions. *Eur. J. Inorg. Chem.* **2006**, *2006*, 2115–2127.
- (26) Alcaraz, G.; Sabo-Etienne, S. NMR: A Good Tool to Ascertain  $\sigma$ -Silane or  $\sigma$ -Borane Formulations? *Coord. Chem. Rev.* **2008**, *252*, 2395–2409.
- (27) Alcaraz, G.; Grellier, M.; Sabo-Etienne, S. Bis  $\sigma$ -Bond Dihydrogen and Borane Ruthenium Complexes: Bonding Nature, Catalytic Applications, and Reversible Hydrogen Release. *Acc. Chem. Res.* **2009**, *42*, 1640–1649.
- (28) Pandey, K. K. Transition Metal- $\sigma$ -Borane Complexes. *Coord. Chem. Rev.* **2009**, *253*, 37–55.
- (29) Young, R. D. Characterisation of Alkane  $\sigma$ -Complexes. *Chem. - Eur. J.* **2014**, *20*, 12704–12718.
- (30) Braunschweig, H.; Kollann, C.; Rais, D. Transition-Metal Complexes of Boron-New Insights and Novel Coordination Modes. *Angew. Chem., Int. Ed.* **2006**, *45*, 5254–5274.
- (31) Braunschweig, H.; Dewhurst, R. D.; Schneider, A. Electron-Precise Coordination Modes of Boron-Centered Ligands. *Chem. Rev.* **2010**, *110*, 3924–3957.
- (32) Miyaura, N. Metal-Catalyzed Reactions of Organoboronic Acids and Esters. *Bull. Chem. Soc. Jpn.* **2008**, *81*, 1535–1553.
- (33) Crudden, C. M.; Glasspoole, B. W.; Lata, C. J. Expanding the Scope of Transformations of Organoboron Species: Carbon-Carbon Bond Formation with Retention of Configuration. *Chem. Commun.* **2009**, 6704–6716.
- (34) Dang, L.; Lin, Z.; Marder, T. B. Boryl Ligands and their Roles in Metal-Catalysed Borylation Reactions. *Chem. Commun.* **2009**, 3987–3995.
- (35) Mkhaldid, I. A. I.; Barnard, J. H.; Marder, T. B.; Murphy, J. M.; Hartwig, J. F. C–H Activation for the Construction of C–B Bonds. *Chem. Rev.* **2010**, *110*, 890–931.
- (36) Ros, A.; Fernández, R.; Lassaletta, J. M. Functional Group Directed C–H Borylation. *Chem. Soc. Rev.* **2014**, *43*, 3229–3243.
- (37) Hamilton, C. W.; Baker, R. T.; Staubitz, A.; Manners, I. B–N Compounds for Chemical Hydrogen Storage. *Chem. Soc. Rev.* **2009**, *38*, 279–293.
- (38) Waterman, R. Mechanisms of Metal-Catalyzed Dehydrocoupling Reactions. *Chem. Soc. Rev.* **2013**, *42*, 5629–5641.
- (39) St. John, A.; Goldberg, K. I.; Heinekey, D. M. Pincer Complexes as Catalysts for Amine Borane Dehydrogenation. *Top. Organomet. Chem.* **2013**, *40*, 271–287.
- (40) Shilov, A. E.; Shul'pin, G. B. Activation of C–H Bonds by Metal Complexes. *Chem. Rev.* **1997**, *97*, 2879–2932.
- (41) Lersch, M.; Tilset, M. Mechanistic Aspects of C–H Activation by Pt Complexes. *Chem. Rev.* **2005**, *105*, 2471–2526.

- (42) Colby, D. A.; Bergman, R. G.; Ellman, J. A. Rhodium-Catalyzed C-C Bond Formation via Heteroatom-Directed C-H Bond Activation. *Chem. Rev.* **2010**, *110*, 624–655.
- (43) Balcells, D.; Clot, E.; Eisenstein, O. C-H Bond Activation in Transition Metal Species from a Computational Perspective. *Chem. Rev.* **2010**, *110*, 749–823.
- (44) Lyons, T. W.; Sanford, M. S. Palladium-Catalyzed Ligand-Directed C-H Functionalization Reactions. *Chem. Rev.* **2010**, *110*, 1147–1169.
- (45) Jazsar, R.; Hitce, J.; Renaudat, A.; Sofack-Kreutzer, J.; Baudoin, O. Functionalization of Organic Molecules by Transition-Metal-Catalyzed C(sp<sup>3</sup>)-H Activation. *Chem. - Eur. J.* **2010**, *16*, 2654–2672.
- (46) Ackermann, L. Carboxylate-Assisted Ruthenium-Catalyzed Alkyne Annulations by C-H/Het-H Bond Functionalizations. *Acc. Chem. Res.* **2014**, *47*, 281–295.
- (47) Hartwig, J. F. Evolution of C-H Bond Functionalizations from Methane to Methodology. *J. Am. Chem. Soc.* **2016**, *138*, 2–24.
- (48) Corey, J. Y. Reactions of Hydrosilanes with Transition Metal Complexes and Characterization of the Products. *Chem. Rev.* **2011**, *111*, 863–1071.
- (49) Huang, L.; Arndt, M.; Gooßen, K.; Heydt, H.; Gooßen, L. J. Late Transition Metal-Catalyzed Hydroamination and Hydroamidation. *Chem. Rev.* **2015**, *115*, 2596–2697.
- (50) van der Vlugt, J. I. Advances in Selective Activation and Application of Ammonia in Homogeneous Catalysis. *Chem. Soc. Rev.* **2010**, *39*, 2302–2322.
- (51) Ozerov, O. V. Oxidative Addition of Water to Transition Metal Complexes. *Chem. Soc. Rev.* **2009**, *38*, 83–88.
- (52) Piers, W. E. Future Trends in Organometallic Chemistry: Organometallic Approaches to Water Splitting. *Organometallics* **2011**, *30*, 13–16.
- (53) Perutz, R. N.; Sabo-Etienne, S. The  $\sigma$ -CAM Mechanism:  $\sigma$  Complexes as the Basis of  $\sigma$ -Bond Metathesis at Late-Transition-Metal Centers. *Angew. Chem., Int. Ed.* **2007**, *46*, 2578–2592.
- (54) Hlatky, G. G.; Crabtree, R. H. Transition-Metal Polyhydride Complexes. *Coord. Chem. Rev.* **1985**, *65*, 1–48.
- (55) Sabo-Etienne, S.; Chaudret, B. Chemistry of bis(Dihydrogen) Ruthenium Complexes and of their Derivatives. *Coord. Chem. Rev.* **1998**, *178–180*, 381–407.
- (56) Choi, J.; MacArthur, A. H. R.; Brookhart, M.; Goldman, A. S. Dehydrogenation and Related Reactions Catalyzed by Iridium Pincer Complexes. *Chem. Rev.* **2011**, *111*, 1761–1779.
- (57) Morris, R. H.; Sawyer, J. F.; Shiralian, M.; Zubkowski, J. D. Two Molecular Hydrogen Complexes: *trans*-[M( $\eta^2$ -H<sub>2</sub>)(H)(PPh<sub>2</sub>CH<sub>2</sub>CH<sub>2</sub>PPh<sub>2</sub>)<sub>2</sub>]BF<sub>4</sub> (M = Fe, Ru). The Crystal Structure Determination of the Iron Complex. *J. Am. Chem. Soc.* **1985**, *107*, 5581–5582.
- (58) Bautista, M.; Earl, K. A.; Morris, R. H.; Sella, A. NMR Properties of the Complexes *trans*-[M( $\eta^2$ -H<sub>2</sub>)(H)(PEt<sub>2</sub>CH<sub>2</sub>CH<sub>2</sub>PEt<sub>2</sub>)<sub>2</sub>]<sup>+</sup>, M = Fe, Ru, Os; Intramolecular Exchange of Atoms between  $\eta^2$ -Dihydrogen and Hydride Ligands. *J. Am. Chem. Soc.* **1987**, *109*, 3780–3782.
- (59) Bautista, M. T.; Earl, K. A.; Maltby, P. A.; Morris, R. H.; Schweitzer, C. T.; Sella, A. Estimation of the H-H Distances of  $\eta^2$ -Dihydrogen Ligands in the Complexes *trans*-[M( $\eta^2$ -H<sub>2</sub>)(H)(PR<sub>2</sub>CH<sub>2</sub>CH<sub>2</sub>PR<sub>2</sub>)<sub>2</sub>]<sup>+</sup> [M = Fe, Ru, R = Ph; M = Os, R = Et] by Solution NMR Methods. *J. Am. Chem. Soc.* **1988**, *110*, 7031–7036.
- (60) Tsukahara, T.; Kawano, H.; Ishii, Y.; Takahashi, T.; Saburi, M.; Uchida, Y.; Akutagawa, S. Preparation and Reactions of a Novel Five-Coordinate Ruthenium Complex [RuH(BINAP)<sub>2</sub>]PF<sub>6</sub> and Formation of the First Chiral Molecular Hydrogen Complex [RuH( $\eta^2$ -H<sub>2</sub>)(BINAP)<sub>2</sub>]PF<sub>6</sub> (BINAP = (R)-Bis(diphenylphosphino)-1,1'-binaphthyl). *Chem. Lett.* **1988**, 2055–2058.
- (61) Saburi, M.; Aoyagi, K.; Takahashi, T.; Uchida, Y. Chelate Site Dependence of Dihydrogen-Hydride Exchange in Ruthenium(II) Molecular Hydrogen Complexes with Diphosphines [RuH( $\eta^2$ -H<sub>2</sub>)(P-P)<sub>2</sub>]PF<sub>6</sub> (P-P = Ph<sub>2</sub>P(CH<sub>2</sub>)<sub>n</sub>PPh<sub>2</sub>; n = 2,3,4). *Chem. Lett.* **1990**, 601–604.
- (62) Saburi, M.; Aoyagi, K.; Takeuchi, H.; Takahashi, T.; Uchida, Y. Characterization of Ruthenium(II) Molecular Hydrogen Complex with (R,R)-4,5-Bis(diphenylphosphinomethyl)-2,2-dimethyl-1,3-dioxolane (diop). *Chem. Lett.* **1990**, 991–994.
- (63) Saburi, M.; Aoyagi, K.; Kodama, T.; Takahashi, T.; Uchida, Y.; Kozawa, K.; Uchida, Y. Ruthenium Hydride Complex with 1,1'-Bis(diphenylphosphino)ferrocene (dppf). Characterization and Molecular Structure of [RuH<sub>3</sub>(dppf)<sub>2</sub>]PF<sub>6</sub>. *Chem. Lett.* **1990**, 1909–1912.
- (64) Bautista, M. T.; Cappellani, E. P.; Drouin, S. D.; Morris, R. H.; Schweitzer, C. T.; Sella, A.; Zubkowski, J. D. Preparation and Spectroscopic Properties of the  $\eta^2$ -Dihydrogen Complexes [MH( $\eta^2$ -H<sub>2</sub>)(PR<sub>2</sub>CH<sub>2</sub>CH<sub>2</sub>PR<sub>2</sub>)<sub>2</sub>]<sup>+</sup> (M = Fe, Ru; R = Ph, Et) and Trends in Properties down the Iron Group Triad. *J. Am. Chem. Soc.* **1991**, *113*, 4876–4887.
- (65) Mezzetti, A.; Del Zotto, A.; Rigo, P.; Farnetti, E. Dihydrogen and Hydrido Complexes via Hydrogen Addition to d<sup>6</sup> Five-coordinate Complexes of Ruthenium and Osmium with 1,2-Bis-(dicyclohexylphosphino)ethane. *J. Chem. Soc., Dalton Trans.* **1991**, 1525–1530.
- (66) Jiménez-Tenorio, M.; Puerta, M. C.; Valerga, P. Coordination of Dioxigen at a Dihydrogen-Binding Site: Crystal Structure of [RuH( $\eta^2$ -O<sub>2</sub>)(dippe)<sub>2</sub>][BPh<sub>4</sub>] (dippe = 1,2-Bis(diisopropylphosphino)ethane). *J. Am. Chem. Soc.* **1993**, *115*, 9794–9795.
- (67) Ogasawara, M.; Saburi, M. Effects of Chelate Ring Rigidity on Intramolecular Hydrogen Exchange in Hydrido(dihydrogen) Bis-(diphosphine) Ruthenium(II) Ions [RuH( $\eta^2$ -H<sub>2</sub>)(diphosphine)<sub>2</sub>]<sup>+</sup> (diphosphine = binap and dpbp). *J. Organomet. Chem.* **1994**, *482*, 7–14.
- (68) Jiménez-Tenorio, M.; Puerta, M. C.; Valerga, P. Synthesis and Characterization of Ruthenium Hydride Complexes Containing the Bulky Diphosphine 1,2-Bis(diisopropylphosphino)ethane (dippe). Crystal Structure of [RuH( $\eta^2$ -O<sub>2</sub>)(dippe)<sub>2</sub>][BPh<sub>4</sub>]. *Inorg. Chem.* **1994**, *33*, 3515–3520.
- (69) Cappellani, E. P.; Drouin, S. D.; Jia, G.; Maltby, P. A.; Morris, R. H.; Schweitzer, C. T. Effect of the Ligand and Metal on the pK<sub>a</sub> Values of the Dihydrogen Ligand in the Series of Complexes [M(H<sub>2</sub>)H(L)<sub>2</sub>]<sup>+</sup>, M = Fe, Ru, Os, Containing Isosteric Ditertiaryphosphine Ligands, L. *J. Am. Chem. Soc.* **1994**, *116*, 3375–3388.
- (70) Chin, B.; Lough, A. J.; Morris, R. H.; Schweitzer, C. T.; D'Agostino, C. Influence of Chloride versus Hydride on H-H Bonding and Acidity of the *trans* Dihydrogen Ligand in the Complexes *trans*-[Ru(H<sub>2</sub>)X(PR<sub>2</sub>CH<sub>2</sub>CH<sub>2</sub>PR<sub>2</sub>)<sub>2</sub>]<sup>+</sup>, X = Cl, H, R = Ph, Et. Crystal Structure Determinations of [RuCl(dppe)<sub>2</sub>]PF<sub>6</sub> and *trans*-[Ru(H<sub>2</sub>-Cl)(dppe)<sub>2</sub>]PF<sub>6</sub>. *Inorg. Chem.* **1994**, *33*, 6278–6288.
- (71) Field, L. D.; Hambley, T. W.; Yau, B. C. K. Formation of Ruthenium Thiolates via Complexes of Molecular Hydrogen. *Inorg. Chem.* **1994**, *33*, 2009–2017.
- (72) Schlaf, M.; Lough, A. J.; Morris, R. H. Synthesis and Structure of the Chiral Dihydrogen Complex *trans*-[Ru( $\eta^2$ -H<sub>2</sub>)H(R,R'-Me-DuPHOS)<sub>2</sub>]PF<sub>6</sub> and the Dinitrogen Complex *trans*-[Ru(N<sub>2</sub>)H(R,R'-Me-DuPHOS)<sub>2</sub>]PF<sub>6</sub> (R,R'-Me-DuPHOS = 1,2-Bis((2R,5R)-2,5-dimethylphospholano)benzene). *Organometallics* **1997**, *16*, 1253–1259.
- (73) Ashworth, T. V.; Singleton, E. Ionic Ruthenium(IV) Trihydrides as Intermediates in the Heterolytic Fission of Dihydrogen by Five-coordinate Hydridoruthenium(II) Cations. Direct Evidence for an Oxidative Addition-Reductive Elimination Pathway. *J. Chem. Soc., Chem. Commun.* **1976**, 705–706.
- (74) Antoniutti, S.; Albertin, G.; Amendola, P.; Bordignon, E. T<sub>1</sub> Values in Hydride and New Molecular Hydrogen Phosphite Complexes of Comparable Structure. *J. Chem. Soc., J. Chem. Soc., Chem. Commun.* **1989**, 229–230.
- (75) Amendola, P.; Antoniutti, S.; Albertin, G.; Bordignon, E. Molecular Hydrogen Complexes. Preparation and Reactivity of New Ruthenium(II) and Osmium(II) Derivatives and a Comparison along the Iron Triad. *Inorg. Chem.* **1990**, *29*, 318–324.
- (76) Lough, A. J.; Morris, R. H.; Ricciuto, L.; Schleis, T. Solution and Crystal Structure of the Dihydrogen Complex [Ru(H<sub>2</sub>)(H)



(PMe<sub>2</sub>Ph)<sub>4</sub>]PF<sub>6</sub>, an Active Alkyne Hydrogenation Catalyst. *Inorg. Chim. Acta* **1998**, *270*, 238–246.

(77) Gusev, D. G.; Hübener, R.; Burger, P.; Orama, O.; Berke, H. Synthesis, Structural Diversity, Dynamics, and Acidity of the M(II) and M(IV) Complexes [MH<sub>3</sub>(PR<sub>3</sub>)<sub>4</sub>]<sup>+</sup> (M = Fe, Ru, Os; R = Me, Et). *J. Am. Chem. Soc.* **1997**, *119*, 3716–3731.

(78) Szymczak, N. K.; Zakharov, L. N.; Tyler, D. R. Solution Chemistry of a Water-Soluble η<sup>2</sup>-H<sub>2</sub> Ruthenium Complex: Evidence for Coordinated H<sub>2</sub> Acting as a Hydrogen Bond Donor. *J. Am. Chem. Soc.* **2006**, *128*, 15830–15835.

(79) Burling, S.; Hällér, L. J. L.; Mas-Marzá, E.; Moreno, A.; Macgregor, S. A.; Mahon, M. F.; Pregosin, P. S.; Whittlesey, M. K. The Influence of N-Heterocyclic Carbenes (NHC) on the Reactivity of [Ru(NHC)<sub>4</sub>H]<sup>+</sup> With H<sub>2</sub>, N<sub>2</sub>, CO and O<sub>2</sub>. *Chem. - Eur. J.* **2009**, *15*, 10912–10923.

(80) Albinati, A.; Klooster, W. T.; Koetzle, T. F.; Fortin, J. B.; Ricci, J. S.; Eckert, J.; Fong, T. P.; Lough, A. J.; Morris, R. H.; Golombek, A. P. Single-Crystal X-ray and Neutron Diffraction Structure Determination and Inelastic Neutron Scattering Study of the Dihydrogen Complex *trans*-[Ru(H<sub>2</sub>)(H)(dppe)<sub>2</sub>][BPh<sub>4</sub>]. *Inorg. Chim. Acta* **1997**, *259*, 351–357.

(81) Maseras, F.; Koga, N.; Morokuma, K. Ab Initio MO and MM Study on the Nature of [Ru(P-P)<sub>2</sub>H<sub>3</sub>]<sup>+</sup> (P-P = dpbb, diop, dpmb, dppe) Complexes. *Organometallics* **1994**, *13*, 4008–4016.

(82) Lereño, K. A.; Kranenburg, M.; Guari, Y.; Kamer, P. C. J.; van Leeuwen, P. W. N. M.; Sabo-Etienne, S.; Chaudret, B. Ruthenium Dihydrogen Complexes with Wide Bite Angle Diphosphines. *Inorg. Chem.* **2003**, *42*, 2859–2866.

(83) Heinekey, D. M.; Mellows, H.; Pratum, T. Dynamic Processes in *cis* Dihydrogen/Hydride Complexes of Ruthenium. *J. Am. Chem. Soc.* **2000**, *122*, 6498–6499.

(84) Bera, B.; Patil, Y. P.; Nethaji, M.; Jagirdar, B. R. Dynamics of H-atom Exchange in Stable *cis*-Dihydrogen/Hydride Complexes of Ruthenium(II) Bearing Phosphine and N–N Bidentate Ligands. *Dalton Trans.* **2014**, *43*, 4726–4733.

(85) Oliván, M.; Clot, E.; Eisenstein, O.; Caulton, K. G. Isomeric Hydrido/Vinylidene, MH(halide)(C=CH<sub>2</sub>)L<sub>2</sub>, and Ethylidyne, M-(halide)(C-CH<sub>3</sub>)L<sub>2</sub> (M = Os, Ru; L = Phosphine), Are Energetically Similar but Not Interconverting. *Organometallics* **1998**, *17*, 897–901.

(86) Oliván, M.; Clot, E.; Eisenstein, O.; Caulton, K. G. Hydride Is Not a Spectator Ligand in the Formation of Hydrido Vinylidene from Terminal Alkyne and Ruthenium and Osmium Hydrides: Mechanistic Differences. *Organometallics* **1998**, *17*, 3091–3100.

(87) Wilhelm, T. E.; Belderrain, T. R.; Brown, S. N.; Grubbs, R. H. Reactivity of Ru(H)(H<sub>2</sub>)Cl(PCy<sub>3</sub>)<sub>2</sub> with Propargyl and Vinyl Chlorides: New Methodology To Give Metathesis-Active Ruthenium Carbenes. *Organometallics* **1997**, *16*, 3867–3869.

(88) Oliván, M.; Eisenstein, O.; Caulton, K. G. New Access to Vinylidenes from Ruthenium Polyhydrides. *Organometallics* **1997**, *16*, 2227–2229.

(89) Werner, H.; Grünwald, C.; Laubender, M.; Gevert, O. The First Triisopropylstibane Ruthenium(II) and Ruthenium(0) Complexes Including the X-ray Crystal Structure of [Ru(η<sup>3</sup>-C<sub>3</sub>H<sub>5</sub>)<sub>2</sub>(SbPr<sub>3</sub>)<sub>2</sub>]. *Chem. Ber.* **1996**, *129*, 1191–1194.

(90) Gusev, D. G.; Vymenits, A. B.; Bakhmutov, V. I. Reactions of RuHCl(CO)[P(*i*-Pr)<sub>3</sub>]<sub>2</sub> with H<sub>2</sub> in Solution. New Molecular Hydrogen Complexes of Ruthenium: RuH(H<sub>2</sub>)Cl(CO)[P(*i*-Pr)<sub>3</sub>]<sub>2</sub> and Ru(H)<sub>2</sub>(H<sub>2</sub>)(CO)[P(*i*-Pr)<sub>3</sub>]<sub>2</sub>. *Inorg. Chem.* **1992**, *31*, 1–2.

(91) Yandulov, D. V.; Huang, D.; Huffman, J. C.; Caulton, K. G. Structural Distortions in *mer*-M(H)<sub>3</sub>(NO)L<sub>2</sub> (M = Ru, Os) and Their Influence on Intramolecular Fluxionality and Quantum Exchange Coupling. *Inorg. Chem.* **2000**, *39*, 1919–1932.

(92) Hamilton, D. G.; Crabtree, R. H. An NMR Method for Distinguishing Classical from Nonclassical Structures in Transition-Metal Polyhydrides. *J. Am. Chem. Soc.* **1988**, *110*, 4126–4133.

(93) Gusev, D. G.; Vymenits, A. B.; Bakhmutov, V. I. Is RuH<sub>4</sub>(PPh<sub>3</sub>)<sub>3</sub> in Solution Indeed a Non-classical Hydride? *Inorg. Chim. Acta* **1991**, *179*, 195–201.

(94) Li, J.; Dickson, R. M.; Ziegler, T. Dihydrogen versus Dihydride: Relativistic Effects on the Relative Stabilities of Nonclassical and Classical Isomers of M(PH<sub>3</sub>)<sub>3</sub>H<sub>4</sub> (M = Fe, Ru, Os). *J. Am. Chem. Soc.* **1995**, *117*, 11482–11487.

(95) Van Der Sluys, L. S.; Kubas, G. J.; Caulton, K. G. Reactivity of Ru(H<sub>2</sub>)(H)<sub>2</sub>(PPh<sub>3</sub>)<sub>3</sub>: Dimerization To Form (PPh<sub>3</sub>)<sub>2</sub>(H)Ru(μ-H)<sub>3</sub>Ru(PPh<sub>3</sub>)<sub>3</sub> and Decarbonylation of Ethanol under Mild Conditions. *Organometallics* **1991**, *10*, 1033–1038.

(96) Samouei, H.; Miloserdov, F. M.; Escudero-Adán, E. C.; Grushin, V. V. Solid-State Structure and Solution Reactivity of [(Ph<sub>3</sub>P)<sub>4</sub>Ru(H)<sub>2</sub>] and Related Ru(II) Complexes Used in Catalysis: A Reinvestigation. *Organometallics* **2014**, *33*, 7279–7283.

(97) Chaudret, B.; Poilblanc, R. Preparation of Polyhydride Complexes of Ruthenium by Direct Hydrogenation of Zerovalent Olefinic Derivatives. Mononuclear Complexes of the Type RuH<sub>4</sub>L<sub>2</sub> and RuH<sub>4</sub>L<sub>3</sub>. Spontaneous H-D Exchange between the Phosphine Protons and the Solvent Catalyzed by RuH<sub>4</sub>L<sub>3</sub>. *Organometallics* **1985**, *4*, 1722–1726.

(98) Grushin, V. V.; Vymenits, A. B.; Vol'pin, M. E. Synthesis of Ruthenium and Iridium Polyhydride Complexes under Conditions of Phase Transfer Catalysis. *J. Organomet. Chem.* **1990**, *382*, 185–189.

(99) Papp, G.; Horváth, H.; Laurenczy, G.; Szatmári, I.; Kathó, A.; Joó, F. Classical and Non-Classical Phosphine-Ru(II)-Hydrides in Aqueous Solutions: Many, Various, and Useful. *Dalton Trans* **2013**, *42*, 521–529.

(100) Linn, D. E., Jr.; Halpern, J. Roles of Neutral and Anionic Ruthenium Polyhydrides in the Catalytic Hydrogenation of Ketones and Arenes. *J. Am. Chem. Soc.* **1987**, *109*, 2969–2974.

(101) Wilczynski, R.; Fordyce, W. A.; Halpern, J. Coordination Chemistry and Catalytic Properties of Hydrido(phosphine)ruthenate Complexes. *J. Am. Chem. Soc.* **1983**, *105*, 2066–2068.

(102) Fordyce, W. A.; Wilczynski, R.; Halpern, J. Hydrido-(phosphine)ruthenate Complexes and their Role in the Catalytic Hydrogenation of Arenes. *J. Organomet. Chem.* **1985**, *296*, 115–125.

(103) Chan, A. S. C.; Shieh, H.-S. New Synthesis and Molecular Structure of Potassium Trihydridotris(triphenylphosphine) ruthenate. *J. Chem. Soc., Chem. Commun.* **1985**, 1379–1380.

(104) Gusev, D. G.; Lough, A. J.; Morris, R. H. New Polyhydride Anions and Proton-Hydride Hydrogen Bonding in Their Ion Pairs. X-ray Crystal Structure Determinations of Q[*mer*-Os(H)<sub>3</sub>(CO)(P<sup>*i*</sup>Pr<sub>3</sub>)<sub>2</sub>], Q = [K(18-crown-6)] and Q = [K(1-aza-18-crown-6)]. *J. Am. Chem. Soc.* **1998**, *120*, 13138–13147.

(105) Abdur-Rashid, K.; Gusev, D. G.; Lough, A. J.; Morris, R. H. Intermolecular Proton-Hydride Bonding in Ion Pairs: Synthesis and Structural Properties of [K(Q)][MH<sub>5</sub>(P<sup>*i*</sup>Pr<sub>3</sub>)<sub>2</sub>] (M = Os, Ru; Q = 18-crown-6, 1-aza-18-crown-6, 1,10-diaza-18-crown-6). *Organometallics* **2000**, *19*, 834–843.

(106) Drouin, S. D.; Amoroso, D.; Yap, G. P. A.; Fogg, D. E. Multifunctional Ruthenium Catalysts: A Novel Borohydride-Stabilized Polyhydride Complex Containing the Basic, Chelating Diphosphine 1,4-Bis(dicyclohexylphosphino)butane and Its Application to Hydrogenation and Murai Catalysis. *Organometallics* **2002**, *21*, 1042–1049.

(107) Abdur-Rashid, K.; Gusev, D. G.; Lough, A. J.; Morris, R. H. Synthesis and Characterization of RuH<sub>2</sub>(H<sub>2</sub>)<sub>2</sub>(P<sup>*i*</sup>Pr<sub>3</sub>)<sub>2</sub> and Related Chemistry. Evidence for a Bis(dihydrogen) Structure. *Organometallics* **2000**, *19*, 1652–1660.

(108) Arliguie, T.; Chaudret, B.; Morris, R. H.; Sella, A. Monomeric and Dimeric Ruthenium(II) η<sup>2</sup>-Dihydrogen Complexes with Tricyclohexylphosphine Coligands. *Inorg. Chem.* **1988**, *27*, 598–599.

(109) Burrow, T.; Sabo-Etienne, S.; Chaudret, B. RuHX(H<sub>2</sub>)(P<sup>*i*</sup>Pr<sub>3</sub>)<sub>2</sub> (X = Cl, I): 16 Electron Dihydrogen-Hydride or Trihydride Complexes? *Inorg. Chem.* **1995**, *34*, 2470–2472.

(110) Busch, S.; Leitner, W. Convenient Preparation of Mononuclear and Dinuclear Ruthenium Hydride Complexes for Catalytic Application. *Chem. Commun.* **1999**, 2305–2306.

(111) Belderrain, T. R.; Grubbs, R. H. Reaction between Ruthenium(0) Complexes and Dihalo Compounds. A New Method for the Synthesis of Ruthenium Olefin Metathesis Catalysts. *Organometallics* **1997**, *16*, 4001–4003.

- (112) Beatty, R. P.; Paciello, R. A. Process for the Preparation of Ruthenium Hydrogenation Catalysts and Products Thereof. WO Patent 96/23802, 1996.
- (113) Beatty, R. P.; Paciello, R. A. Process for the Preparation of Ruthenium Complexes and their in situ Use as Hydrogenation Catalysts. WO Patent 96/23804, 1996.
- (114) Grellier, M.; Vendier, L.; Chaudret, B.; Albinati, A.; Rizzato, S.; Mason, S.; Sabo-Etienne, S. Synthesis, Neutron Structure, and Reactivity of the Bis(dihydrogen) Complex  $\text{RuH}_2(\eta^2\text{-H}_2)_2(\text{PCy}_3)_2$  Stabilized by Two Tricyclopentylphosphines. *J. Am. Chem. Soc.* **2005**, *127*, 17592–17593.
- (115) Walaszek, B.; Adamczyk, A.; Pery, T.; Yeping, X.; Gutmann, T.; de Sousa Amadeu, N.; Ulrich, S.; Breitzke, H.; Vieth, H. M.; Sabo-Etienne, S.; Chaudret, B.; Limbach, H.-H.; Buntkowsky, G.  $^2\text{H}$  Solid-State NMR of Ruthenium Complexes. *J. Am. Chem. Soc.* **2008**, *130*, 17502–17508.
- (116) Macholl, S.; Matthes, J.; Limbach, H.-H.; Sabo-Etienne, S.; Chaudret, B.; Buntkowsky, G. High-Resolution  $^2\text{H}$  MAS NMR Applied to Deuterium Analogs of Hydrido  $\eta^2$ -Dihydrogen Complexes. *Solid State Nucl. Magn. Reson.* **2009**, *36*, 137–143.
- (117) Grellier, M.; Mason, S. A.; Albinati, A.; Capelli, S. C.; Rizzato, S.; Bijani, C.; Coppel, Y.; Sabo-Etienne, S. Probing Highly Selective H/D Exchange Processes with a Ruthenium Complex through Neutron Diffraction and Multinuclear NMR Studies. *Inorg. Chem.* **2013**, *52*, 7329–7337.
- (118) Toner, A. J.; Donnadieu, B.; Sabo-Etienne, S.; Chaudret, B.; Sava, X.; Mathy, F.; Le Floch, P. Preparation and Characterization of Ruthenium(II) Monophosphaferrocene Complexes. Reactivity, Dynamic Solution Behavior, and X-ray Structure of  $[\text{RuH}_2(\eta^2\text{-H}_2)(\text{PCy}_3)_2(2\text{-phenyl-3,4-dimethylphosphaferrocene})]$ . *Inorg. Chem.* **2001**, *40*, 3034–3038.
- (119) Giunta, D.; Hölscher, M.; Lehmann, C. W.; Mynott, R.; Wirtz, C.; Leitner, W. Room Temperature Activation of Aromatic C-H Bonds by Non-Classical Ruthenium Hydride Complexes Containing Carbene Ligands. *Adv. Synth. Catal.* **2003**, *345*, 1139–1145.
- (120) Borowski, A. F.; Sabo-Etienne, S.; Chaudret, B. Homogeneous Hydrogenation of Arenes Catalyzed by the bis(Dihydrogen) Complex  $[\text{RuH}_2(\text{H}_2)_2(\text{PCy}_3)_2]$ . *J. Mol. Catal. A: Chem.* **2001**, *174*, 69–79.
- (121) Borowski, A. F.; Vendier, L.; Sabo-Etienne, S.; Rozycka-Sokolowska, E.; Gaudyn, A. V. Catalyzed Hydrogenation of Condensed Three-ring Arenes and their N-Heteroaromatic Analogues by a bis(Dihydrogen) Ruthenium Complex. *Dalton Trans.* **2012**, *41*, 14117–14125.
- (122) Bianchini, C.; Perez, P. J.; Peruzzini, M.; Zanobini, F.; Vacca, A. Classical and Nonclassical Polyhydride Ruthenium(II) Complexes Stabilized by the Tetrakisphosphine  $\text{P}(\text{CH}_2\text{CH}_2\text{PPh}_2)_3$ . *Inorg. Chem.* **1991**, *30*, 279–287.
- (123) Bianchini, C.; Masi, D.; Peruzzini, M.; Casarin, M.; Maccato, C.; Rizzi, G. A. *Ab Initio* and Experimental Studies on the Structure and Relative Stability of the *cis*-Hydride- $\eta^2$ -Dihydrogen Complexes  $[\{\text{P}(\text{CH}_2\text{CH}_2\text{PPh}_2)_3\text{M}(\text{H})(\eta^2\text{-H}_2)\}^+]$  (M = Fe, Ru). *Inorg. Chem.* **1997**, *36*, 1061–1069.
- (124) Rossin, A.; Rossi, A.; Peruzzini, M.; Zanobini, F. Chemical Hydrogen Storage: Ammonia Borane Dehydrogenation Catalyzed by  $\text{NP}_3$  Ruthenium Hydrides ( $\text{NP}_3 = \text{N}(\text{CH}_2\text{CH}_2\text{PPh}_2)_3$ ). *ChemPlusChem* **2014**, *79*, 1316–1325.
- (125) Jia, G.; Drouin, S. D.; Jessop, P. G.; Lough, A. J.; Morris, R. H. Use of the New Ligand  $\text{P}(\text{CH}_2\text{CH}_2\text{PCy}_2)_3$  in the Synthesis of Dihydrogen Complexes of Iron(II) and Ruthenium(II). *Organometallics* **1993**, *12*, 906–916.
- (126) Bhadbhade, M. M.; Field, L. D.; Gilbert-Wilson, R.; Guest, R. W.; Jensen, P. Ruthenium Hydride Complexes of the Hindered Phosphine Ligand  $\text{Tris}(3\text{-diisopropylphosphinopropyl})\text{phosphine}$ . *Inorg. Chem.* **2011**, *50*, 6220–6228.
- (127) Eckert, J.; Albinati, A.; White, R. P.; Bianchini, C.; Peruzzini, M. The Barrier to Rotation of the Dihydrogen Ligand in the Complexes  $[\text{MH}(\eta^2\text{-H}_2)\text{PP}_3]\text{BPh}_4$  (M = Fe, Ru): Evidence for Stronger Back-Donation in the Iron Complex. *Inorg. Chem.* **1992**, *31*, 4241–4244.
- (128) Bianchini, C.; Peruzzini, M.; Zanobini, F.; Frediani, P.; Albinati, A. A Ru(II) Enynyl Complex Mediates the Catalytic Dimerization of 1-Alkynes to Z-1,4-Disubstituted Enynes. *J. Am. Chem. Soc.* **1991**, *113*, 5453–5454.
- (129) Bianchini, C.; Bohanna, C.; Esteruelas, M. A.; Frediani, P.; Meli, A.; Oro, L. A.; Peruzzini, M. A Deceptively Simple Case of Selective Hydrogenation of Phenylacetylene to Styrene Catalyzed by a *cis*-Hydrido( $\eta^2$ -dihydrogen)ruthenium(II) Complex. *Organometallics* **1992**, *11*, 3837–3844.
- (130) Bianchini, C.; Farnetti, E.; Frediani, P.; Graziani, M.; Peruzzini, M.; Polo, A. Disproportionation of Acyclic Ketones to Carboxylate Ions and Ethers: a Poisoning Reaction on the Way to the Chemoselective Reduction of  $\alpha,\beta$ -Unsaturated Ketones to Allylic Alcohols via Hydrogen-transfer Catalysed by a Nonclassical Ruthenium(II) Trihydride. *J. Chem. Soc., Chem. Commun.* **1991**, 1336–1337.
- (131) Bianchini, C.; Farnetti, E.; Graziani, M.; Peruzzini, M.; Polo, A. Chemoselective Hydrogen-Transfer Reduction of  $\alpha,\beta$ -Unsaturated Ketones Catalyzed by Isostructural Iron(II), Ruthenium(II), and Osmium(II) *cis* Hydride  $\eta^2$ -Dihydrogen Complexes. *Organometallics* **1993**, *12*, 3753–3761.
- (132) Bautista, M. T.; Earl, K. A.; Maltby, P. A.; Morris, R. H.; Schweitzer, C. T. New Dihydrogen Complexes: the Synthesis and Spectroscopic Properties of Iron(II), Ruthenium(II), and Osmium(II) Complexes Containing the *meso*-Tetraphos-1 Ligand. *Can. J. Chem.* **1994**, *72*, 547–560.
- (133) Michos, D.; Luo, X.-L.; Crabtree, R. H. Synthesis and Spectroscopic Characterization of Ruthenium(II)  $\eta^2$ -Dihydrogen Complexes of the Type  $[\text{RuH}(\eta^2\text{-H}_2)(\text{L})(\text{triphos})]^+$  (L = CO,  $\text{P}(\text{OCH}_2)_3\text{Cet}$ ,  $\text{PMe}_2\text{Ph}$ ; triphos =  $\text{PPh}(\text{CH}_2\text{CH}_2\text{PPh}_2)_2$ ). *Inorg. Chem.* **1992**, *31*, 4245–4250.
- (134) Heinekey, D. M.; Payne, N. G.; Sofield, C. D. A Revisionist View of Fluxionality in Metal Polyhydrides: The Role of Exchange Coupling. *Organometallics* **1990**, *9*, 2643–2645.
- (135) Ayllon, J. A.; Sabo-Etienne, S.; Chaudret, B.; Ulrich, S.; Limbach, H.-H. Modulation of Quantum Mechanical Exchange Couplings in Transition Metal Hydrides Through Hydrogen Bonding. *Inorg. Chim. Acta* **1997**, *259*, 1–4.
- (136) Osipov, A. L.; Gutsulyak, D. V.; Kuzmina, L. G.; Howard, J. A. K.; Lemenovskii, D. A.; Süß-Fink, G.; Nikonov, G. I. Half-Sandwich Trihydrido Ruthenium Complexes. *J. Organomet. Chem.* **2007**, *692*, 5081–5085.
- (137) Mai, V. H.; Kuzmina, L. G.; Churakov, A. V.; Korobkov, I.; Howard, J. A. K.; Nikonov, G. I. NHC Carbene Supported Half-Sandwich Hydridosilyl Complexes of Ruthenium: the Impact of Supporting Ligands on Si...H Interligand Interactions. *Dalton Trans.* **2016**, *45*, 208–215.
- (138) Arliguie, T.; Border, C.; Chaudret, B.; Devillers, J.; Poilblanc, R. Chloro- and Hydrido(pentamethylcyclopentadienyl)ruthenium Complexes: Anomalous NMR Behavior of  $\text{C}_5\text{Me}_5\text{RuH}_3\text{PR}_3$  (R =  $\text{CHMe}_2$ , Cy). *Organometallics* **1989**, *8*, 1308–1314.
- (139) Jones, A. L.; McGrady, G. S.; Sirsch, P.; Steed, J. W. Ruthenium Trihydrides with N-Heterocyclic Carbene Ligands: Effects on Quantum Mechanical Exchange Coupling. *Chem. Commun.* **2005**, 5994–5996.
- (140) Suzuki, H.; Lee, D. H.; Oshima, M.; Moro-oka, Y. Hydride and Borohydride Derivatives of (Pentamethylcyclopentadienyl) (tertiary phosphine)ruthenium. *Organometallics* **1987**, *6*, 1569–1575.
- (141) Gründemann, S.; Limbach, H.-H.; Rodriguez, V.; Donnadieu, B.; Sabo-Etienne, S.; Chaudret, B. Coherent and Incoherent Dihydrogen Dynamics in a Ruthenium Trihydride Complex with the  $\text{Tris}(\text{pyrrolyl})\text{phosphine}$  Ligand. *Ber. Bunsenges. Phys. Chem.* **1998**, *102*, 344–353.
- (142) Aneetha, H.; Jiménez-Tenorio, M.; Puerta, M. C.; Valerga, P. Ruthenium Hydrides Bearing  $\text{SbPh}_3$  and  $\text{AsPh}_3$  Ligands: Characterization of the bis(Dihydrogen) Complexes  $[\text{Cp}^*\text{Ru}(\text{H}_2)_2(\text{EPh}_3)]^+$  ( $\text{Cp}^* = \text{C}_5\text{Me}_5$ ; E = Sb, As). *J. Organomet. Chem.* **2002**, *663*, 151–157.
- (143) Jiménez-Tenorio, M.; Puerta, M. C.; Valerga, P.; Moncho, S.; Ujaque, G.; Lledós, A. Proton-Transfer Reactions to Half-Sandwich

Ruthenium Trihydride Complexes Bearing Hemilabile P,N Ligands: Experimental and Density Functional Theory Studies. *Inorg. Chem.* **2010**, *49*, 6035–6057.

(144) Johnson, T. J.; Coan, P. S.; Caulton, K. G. Spectroscopic Investigation of the Reactivity of Cp\*Ru(PiPr<sub>2</sub>Ph)X toward H<sub>2</sub> and Silanes: Formation in Solution of Cp\*Ru(PiPr<sub>2</sub>Ph)(H)<sub>3</sub> and Cp\*Ru(PiPr<sub>2</sub>Ph)(H)<sub>2</sub>Y (Y = Halide, OR, and SiR'<sub>3</sub>). *Inorg. Chem.* **1993**, *32*, 4594–4599.

(145) Manzano, B.; Jalon, F.; Matthes, J.; Sabo-Etienne, S.; Chaudret, B.; Ulrich, S.; Limbach, H.-H. Exchange Couplings and Hydrogen Dynamics in Ruthenium Trihydride Adducts with Coinage-Metal Cations. *J. Chem. Soc., Dalton Trans.* **1997**, 3153–3160.

(146) Arliguie, T.; Chaudret, B.; Jalon, F. A.; Otero, A.; Lopez, J. A.; Lahoz, F. J. Reactivity of Ruthenium Trihydrides with Brønsted and Lewis Acids. X-ray Crystal Structures of {Cp\* Ru[C<sub>6</sub>H<sub>5</sub>P(C<sub>6</sub>H<sub>11</sub>)<sub>2</sub>]}BF<sub>4</sub> and {Cp\* RuH[P(C<sub>6</sub>H<sub>11</sub>)<sub>3</sub>]}(μ-H)<sub>2</sub>Cu(μ-Cl)<sub>2</sub>. Evidence for Exchange Coupling between Two Hydrogen Atoms. *Organometallics* **1991**, *10*, 1888–1896.

(147) Pavlik, S.; Puchberger, M.; Mereiter, K.; Kirchner, K. Synthesis and Reactivity of the Ru<sup>III</sup> Complexes [RuTp(PR<sub>3</sub>)Cl<sub>2</sub>] – Precursors for RuTp Dihydrogen Complexes. *Eur. J. Inorg. Chem.* **2006**, *2006*, 4137–4142.

(148) Moreno, B.; Sabo-Etienne, S.; Chaudret, B.; Rodriguez-Fernandez, A.; Jalon, F.; Trofimenko, S. Synthesis and Reactivity of a Stable Hydrido Bis(dihydrogen) Derivative in a Nitrogen Donor Environment LRuH(H<sub>2</sub>)<sub>2</sub> (L = HB(3,5-Me<sub>2</sub>-pz), HB(3-*i*Pr<sub>4</sub>-B-*pz*)). *J. Am. Chem. Soc.* **1994**, *116*, 2635–2636.

(149) Moreno, B.; Sabo-Etienne, S.; Chaudret, B.; Rodriguez, A.; Jalon, F.; Trofimenko, S. Synthesis and Reactivity of Hydridotris(pyrazolyl) Borate Dihydrogen Ruthenium Complexes. *J. Am. Chem. Soc.* **1995**, *117*, 7441–7451.

(150) Esteruelas, M. A.; Fernández, I.; Fuertes, S.; López, A. M.; Oñate, E.; Sierra, M. A. Aromatization of a Dihydro-3-ruthenaindolizine Complex. *Organometallics* **2009**, *28*, 4876–4879.

(151) Halcrow, M.; Chaudret, B.; Trofimenko, S. Tris-pyrazolylborate Dihydrogen Complexes of Ruthenium. *J. Chem. Soc., Chem. Commun.* **1993**, 465–467.

(152) Chen, Y.-Z.; Chan, W. C.; Lau, C. P.; Chu, H. S.; Lee, H. L.; Jia, G. Synthesis of Alkyl- and Aryl[hydrotris(pyrazolyl)borato]-carbonylruthenium Complexes by Decarbonylation of Alcohols. Synthesis of TpRuH(H<sub>2</sub>)(PPh<sub>3</sub>) [Tp = Hydrotris(pyrazolyl)borate], an Observable Intermediate in the Decarbonylation Reaction. *Organometallics* **1997**, *16*, 1241–1246.

(153) Jiménez Tenorio, M. A.; Jiménez Tenorio, M.; Puerta, M. C.; Valerga, P. Neutral and Cationic Ruthenium Hydrotris(pyrazolyl)borate Derivatives Containing Bulky Monodentate Phosphines. Crystal Structures of [RuTp(H<sub>2</sub>O)(PPr<sup>*i*</sup><sub>2</sub>Me)<sub>2</sub>][CF<sub>3</sub>SO<sub>3</sub>].EtOH and [RuTp(N<sub>2</sub>)(PEt<sub>3</sub>)<sub>2</sub>][BPh<sub>4</sub>]. *J. Chem. Soc., Dalton Trans.* **1998**, 3601–3608.

(154) Shima, T.; Namura, K.; Kameo, H.; Kakuta, S.; Suzuki, H. Synthesis and Structure of a Novel Ruthenium Hydrido Bis(dihydrogen) Complex with 1,4,7-Trimethyl-1,4,7-triazacyclononane Ligand: A Useful Precursor for Synthesis of Heterometallic Complexes. *Organometallics* **2010**, *29*, 337–346.

(155) Namura, K.; Kakuta, S.; Suzuki, H. Synthesis of Ruthenium Polyhydride Clusters with 1,4,7-Triazacyclononane-Type Ligands: Stereo and Electronic Effects of Ancillary Ligands. *Organometallics* **2010**, *29*, 4305–4311.

(156) Ledger, A. E. W.; Moreno, A.; Ellul, C. E.; Mahon, M. F.; Pregosin, P. S.; Whittlesey, M. K.; Williams, J. M. J. Pincer Phosphine Complexes of Ruthenium: Formation of Ru(P-O-P)(PPh<sub>3</sub>)HCl (P-O-P = xantphos, DPEphos, (Ph<sub>2</sub>PCH<sub>2</sub>CH<sub>2</sub>)<sub>2</sub>O) and Ru(dppf)(PPh<sub>3</sub>)HCl and Characterization of Cationic Dioxigen, Dihydrogen, Dinitrogen, and Arene Coordinated Phosphine Products. *Inorg. Chem.* **2010**, *49*, 7244–7256.

(157) Alós, J.; Bolaño, T.; Esteruelas, M. A.; Oliván, M.; Oñate, E.; Valencia, M. POP-Pincer Ruthenium Complexes: d<sup>6</sup> Counterparts of Osmium d<sup>4</sup> Species. *Inorg. Chem.* **2014**, *53*, 1195–1209.

(158) Watson, L. A.; Coalter, J. N., III; Ozerov, O.; Pink, M.; Huffman, J. C.; Caulton, K. G. Amido/Phosphine Pincer Hydrides of Ruthenium. *New J. Chem.* **2003**, *27*, 263–273.

(159) Choi, J.-H.; Schloerer, N. E.; Berger, J.; Precht, M. H. G. Synthesis and Characterisation of Ruthenium Dihydrogen Complexes and their Reactivity towards B–H Bonds. *Dalton Trans.* **2014**, *43*, 290–299.

(160) Choi, J.-H.; Precht, M. H. G. Tuneable Hydrogenation of Nitriles into Imines or Amines with a Ruthenium Pincer Complex under Mild Conditions. *ChemCatChem* **2015**, *7*, 1023–1028.

(161) Gunanathan, C.; Hölscher, M.; Leitner, W. Reduction of Nitriles to Amines with H<sub>2</sub> Catalyzed by Nonclassical Ruthenium Hydrides – Water-Promoted Selectivity for Primary Amines and Mechanistic Investigations. *Eur. J. Inorg. Chem.* **2011**, *2011*, 3381–3386.

(162) Precht, M. H. G.; Hölscher, M.; Ben-David, Y.; Theyssen, N.; Loschen, R.; Milstein, D.; Leitner, W. H/D Exchange at Aromatic and Heteroaromatic Hydrocarbons Using D<sub>2</sub>O as the Deuterium Source and Ruthenium Dihydrogen Complexes as the Catalyst. *Angew. Chem., Int. Ed.* **2007**, *46*, 2269–2272.

(163) Jia, G.; Meek, D. W. Syntheses and Reactivity of Ruthenium Hydride Complexes Containing Chelating Triphosphines. I. Characterization of the Molecular Dihydrogen Complex RuH<sub>2</sub>(H<sub>2</sub>)(Cytpp)(Cytpp = PhP(CH<sub>2</sub>CH<sub>2</sub>CH<sub>2</sub>P(c-C<sub>6</sub>H<sub>11</sub>)<sub>2</sub>)<sub>2</sub>). *J. Am. Chem. Soc.* **1989**, *111*, 757–758.

(164) Precht, M. H. G.; Ben-David, Y.; Giunta, D.; Busch, S.; Taniguchi, Y.; Wisniewski, W.; Görls, H.; Mynott, R. J.; Theyssen, N.; Milstein, D.; Leitner, W. Synthesis and Characterisation of Non-classical Ruthenium Hydride Complexes Containing Chelating Bidentate and Tridentate Phosphine Ligands. *Chem. - Eur. J.* **2007**, *13*, 1539–1546.

(165) Gunanathan, C.; Capelli, S. C.; Englert, U.; Hölscher, M.; Leitner, W. Structures and Dynamics of the Mixed Dihydrogen/Hydride Complexes [Ru(PCP)(H)(H<sub>2</sub>)<sub>n</sub>] (n = 1, 2) and [Ru(PNP)(H)<sub>2</sub>(H<sub>2</sub>)]. *Eur. J. Inorg. Chem.* **2013**, *2013*, 5075–5080.

(166) Lachaize, S.; Essalah, K.; Montiel-Palma, V.; Vendier, L.; Chaudret, B.; Barthelat, J. C.; Sabo-Etienne, S. Coordination Modes of Boranes in Polyhydride Ruthenium Complexes: σ-Borane versus Dihydridoborate. *Organometallics* **2005**, *24*, 2935–2943.

(167) Montiel-Palma, V.; Lumbierres, M.; Donnadiou, B.; Sabo-Etienne, S.; Chaudret, B. σ-Borane and Dihydroborate Complexes of Ruthenium. *J. Am. Chem. Soc.* **2002**, *124*, 5624–5625.

(168) Essalah, K.; Barthelat, J.-C.; Montiel, V.; Lachaize, S.; Donnadiou, B.; Chaudret, B.; Sabo-Etienne, S. 9-BBN Activation. Synthesis, Crystal Structure and Theoretical Characterization of the Ruthenium Complex Ru[(μ-H)<sub>2</sub>BC<sub>8</sub>H<sub>14</sub>]<sub>2</sub>(PCy<sub>3</sub>). *J. Organomet. Chem.* **2003**, *680*, 182–187.

(169) Caballero, A.; Sabo-Etienne, S. Ruthenium-Catalyzed Hydroboration and Dehydrogenative Borylation of Linear and Cyclic Alkenes with Pinacolborane. *Organometallics* **2007**, *26*, 1191–1195.

(170) Gloaguen, Y.; Alcaraz, G.; Vendier, L.; Sabo-Etienne, S. *Tert*-butylborane: A bis(σ-B–H) Ligand in Ruthenium Hydride Chemistry. *J. Organomet. Chem.* **2009**, *694*, 2839–2841.

(171) Alcaraz, G.; Clot, E.; Helmstedt, U.; Vendier, L.; Sabo-Etienne, S. Mesitylborane as a Bis(σ-B–H) Ligand: An Unprecedented Bonding Mode to a Metal Center. *J. Am. Chem. Soc.* **2007**, *129*, 8704–8705.

(172) Gloaguen, Y.; Bénac-Lestrelle, G.; Vendier, L.; Helmstedt, U.; Clot, E.; Alcaraz, G.; Sabo-Etienne, S. Monosubstituted Borane Ruthenium Complexes RuH<sub>2</sub>(η<sup>2</sup>:η<sup>2</sup>-H<sub>2</sub>BR)(PR'<sub>3</sub>)<sub>2</sub>: A General Approach to the Geminal Bis(σ-B–H) Coordination Mode. *Organometallics* **2013**, *32*, 4868–4877.

(173) Alcaraz, G.; Helmstedt, U.; Clot, E.; Vendier, L.; Sabo-Etienne, S. A Terminal Borylene Ruthenium Complex: From B–H Activation to Reversible Hydrogen Release. *J. Am. Chem. Soc.* **2008**, *130*, 12878–12879.

(174) Alcaraz, G.; Vendier, L.; Clot, E.; Sabo-Etienne, S. Ruthenium Bis(σ-B–H) Aminoborane Complexes from Dehydrogenation of

Amine-Boranes: Trapping of  $\text{H}_2\text{B}-\text{NH}_2$ . *Angew. Chem., Int. Ed.* **2010**, *49*, 918–920.

(175) Alcaraz, G.; Sabo-Etienne, S. Coordination and Dehydrogenation of Amine-Boranes at Metal Centers. *Angew. Chem., Int. Ed.* **2010**, *49*, 7170–7179.

(176) Alcaraz, G.; Chaplin, A. B.; Stevens, C. J.; Clot, E.; Vendier, L.; Weller, A. S.; Sabo-Etienne, S. Ruthenium, Rhodium, and Iridium Bis( $\sigma\text{-B}-\text{H}$ ) Diisopropylaminoborane Complexes. *Organometallics* **2010**, *29*, 5591–5595.

(177) Bénac-Lestrelle, G.; Helmstedt, U.; Vendier, L.; Alcaraz, G.; Clot, E.; Sabo-Etienne, S. Dimethylaminoborane ( $\text{H}_2\text{BNMe}_2$ ) Coordination to Late Transition Metal Centers: Snapshots of the B-H Oxidative Addition Process. *Inorg. Chem.* **2011**, *50*, 11039–11045.

(178) Wallis, C. J.; Dyer, H.; Vendier, L.; Alcaraz, G.; Sabo-Etienne, S. Dehydrogenation of Diamine-Monoboranes to Cyclic Diaminoboranes: Efficient Ruthenium-Catalyzed Dehydrogenative Cyclization. *Angew. Chem., Int. Ed.* **2012**, *51*, 3646–3648.

(179) Wallis, C. J.; Alcaraz, G.; Petit, A. S.; Poblador-Bahamonde, A. I.; Clot, E.; Bijani, C.; Vendier, L.; Sabo-Etienne, S. A Highly Effective Ruthenium System for the Catalyzed Dehydrogenative Cyclization of Amine-Boranes to Cyclic Boranes under Mild Conditions. *Chem. - Eur. J.* **2015**, *21*, 13080–13090.

(180) Gloaguen, Y.; Alcaraz, G.; Petit, A. S.; Clot, E.; Coppel, Y.; Vendier, L.; Sabo-Etienne, S. Ruthenium Agostic (Phosphinoaryl)-borane Complexes: Multinuclear Solid-State and Solution NMR, X-ray, and DFT Studies. *J. Am. Chem. Soc.* **2011**, *133*, 17232–17238.

(181) Cassen, A.; Vendier, L.; Daran, J.-C.; Poblador-Bahamonde, A. I.; Clot, E.; Alcaraz, G.; Sabo-Etienne, S. B–C Bond Cleavage and Ru–C Bond Formation from a Phosphinoborane: Synthesis of a Bis- $\sigma$  Borane Aryl-Ruthenium Complex. *Organometallics* **2014**, *33*, 7157–7163.

(182) Cassen, A.; Gloaguen, Y.; Vendier, L.; Duhayon, C.; Poblador-Bahamonde, A.; Raynaud, C.; Clot, E.; Alcaraz, G.; Sabo-Etienne, S. B–H, C–H, and B–C Bond Activation: The Role of Two Adjacent Agostic Interactions. *Angew. Chem., Int. Ed.* **2014**, *53*, 7569–7573.

(183) Bontemps, S.; Vendier, L.; Sabo-Etienne, S. Borane-Mediated Carbon Dioxide Reduction at Ruthenium: Formation of  $\text{C}_1$  and  $\text{C}_2$  Compounds. *Angew. Chem., Int. Ed.* **2012**, *51*, 1671–1674.

(184) Bontemps, S.; Sabo-Etienne, S. Trapping Formaldehyde in the Homogeneous Catalytic Reduction of Carbon Dioxide. *Angew. Chem., Int. Ed.* **2013**, *52*, 10253–10255.

(185) Bontemps, S.; Vendier, L.; Sabo-Etienne, S. Ruthenium-Catalyzed Reduction of Carbon Dioxide to Formaldehyde. *J. Am. Chem. Soc.* **2014**, *136*, 4419–4425.

(186) Gunanathan, C.; Hölscher, M.; Pan, F.; Leitner, W. Ruthenium Catalyzed Hydroboration of Terminal Alkynes to Z-Vinylboronates. *J. Am. Chem. Soc.* **2012**, *134*, 14349–14352.

(187) Reguillo, R.; Grellier, M.; Vautravers, N.; Vendier, L.; Sabo-Etienne, S. Ruthenium-Catalyzed Hydrogenation of Nitriles: Insights into the Mechanism. *J. Am. Chem. Soc.* **2010**, *132*, 7854–7855.

(188) Guari, Y.; Sabo-Etienne, S.; Chaudret, B. Exchange Couplings between a Hydride and a Stretched Dihydrogen Ligand in Ruthenium Complexes. *J. Am. Chem. Soc.* **1998**, *120*, 4228–4229.

(189) Matthes, J.; Gründemann, S.; Toner, A.; Guari, Y.; Donnadieu, B.; Spandl, J.; Sabo-Etienne, S.; Clot, E.; Limbach, H.-H.; Chaudret, B. Ortho-Metalated Ruthenium Hydrido Dihydrogen Complexes: Dynamics, Exchange Couplings, and Reactivity. *Organometallics* **2004**, *23*, 1424–1433.

(190) Busch, S.; Leitner, W. Ruthenium-Catalyzed Murai-Type Couplings at Room Temperature. *Adv. Synth. Catal.* **2001**, *343*, 192–195.

(191) Buskens, P.; Giunta, D.; Leitner, W. Activation and Deactivation of a Carbene Containing non-Classical Ruthenium Hydride Complex in Catalytic Processes Involving C–H Bond Cleavage. *Inorg. Chim. Acta* **2004**, *357*, 1969–1974.

(192) Guari, Y.; Castellanos, A.; Sabo-Etienne, S.; Chaudret, B.  $\text{RuH}_2(\text{H}_2)_2(\text{PCy}_3)_2$ : a Room Temperature Catalyst for the Murai Reaction. *J. Mol. Catal. A: Chem.* **2004**, *212*, 77–82.

(193) Toner, A. J.; Gründemann, S.; Clot, E.; Limbach, H.-H.; Donnadieu, B.; Sabo-Etienne, S.; Chaudret, B. Ruthenium Assisted Reversible Proton Transfer from an Aromatic Carbon to a Hydride. *J. Am. Chem. Soc.* **2000**, *122*, 6777–6778.

(194) Toner, A.; Matthes, J.; Gründemann, S.; Limbach, H.-H.; Chaudret, B.; Clot, E.; Sabo-Etienne, S. Agostic Interaction and Intramolecular Proton Transfer from the Protonation of Dihydrogen ortho Metalated Ruthenium Complexes. *Proc. Natl. Acad. Sci. U. S. A.* **2007**, *104*, 6945–6950.

(195) Zhang, X.; Kanzelberger, M.; Emge, T. J.; Goldman, A. S. Selective Addition to Iridium of Aryl C–H Bonds Ortho Coordinating Groups. Not Chelation-Assisted. *J. Am. Chem. Soc.* **2004**, *126*, 13192–13193.

(196) Alós, J.; Esteruelas, M. A.; Oliván, M.; Oñate, E.; Puylaert, P. C–H Bond Activation Reactions in Ketones and Aldehydes Promoted by POP-Pincer Osmium and Ruthenium Complexes. *Organometallics* **2015**, *34*, 4908–4921.

(197) Precht, M. H. G.; Hölscher, M.; Ben-David, Y.; Theyssen, N.; Milstein, D.; Leitner, W. Ruthenium Dihydrogen Complex for C–H Activation: Catalytic H/D Exchange under Mild Conditions. *Eur. J. Inorg. Chem.* **2008**, *2008*, 3493–3500.

(198) Lachaize, S.; Caballero, A.; Vendier, L.; Sabo-Etienne, S. Activation of Chlorosilanes at Ruthenium: A Route to Silyl  $\sigma$ -Dihydrogen Complexes. *Organometallics* **2007**, *26*, 3713–3721.

(199) Lachaize, S.; Vendier, L.; Sabo-Etienne, S. Silyl and  $\sigma$ -Silane Ruthenium Complexes: Chloride Substituent Effects on the Catalyzed Silylation of Ethylene. *Dalton Trans.* **2010**, *39*, 8492–8500.

(200) Gutsulyak, D. V.; Osipov, A. L.; Kuzmina, L. G.; Howard, J. A. K.; Nikonov, G. I. Unexpected Effect of the Ring on the Extent of Si–H Interligand Interactions in Half-Sandwich Silyl Hydrides of Ruthenium. *Dalton Trans.* **2008**, 6843–6850.

(201) Grellier, M.; Ayed, T.; Barthelat, J.-C.; Albinati, A.; Mason, S.; Vendier, L.; Coppel, Y.; Sabo-Etienne, S. Versatile Coordination of 2-Pyridinetetramethylsilylazine at Ruthenium: Ru(II) vs Ru(IV) As Evidenced by NMR, X-ray, Neutron, and DFT Studies. *J. Am. Chem. Soc.* **2009**, *131*, 7633–7640.

(202) Montiel-Palma, V.; Muñoz-Hernández, M. A.; Cuevas-Chávez, C. A.; Vendier, L.; Grellier, M.; Sabo-Etienne, S. Phosphinodi-(benzylsilane)  $\text{PhP}\{(\text{o}-\text{C}_6\text{H}_4\text{CH}_2)\text{SiMe}_2\text{H}\}_2$ : A Versatile “ $\text{PSi}_2\text{H}_x$ ” Pincer-Type Ligand at Ruthenium. *Inorg. Chem.* **2013**, *52*, 9798–9806.

(203) Montiel-Palma, V.; Muñoz-Hernández, M. A.; Ayed, T.; Barthelat, J.-C.; Grellier, M.; Vendier, L.; Sabo-Etienne, S. Agostic Si–H Bond Coordination Assists C–H Bond Activation at Ruthenium in Bis(phosphinobenzylsilane) Complexes. *Chem. Commun.* **2007**, 3963–3965.

(204) Smart, K. A.; Mothes-Martin, E.; Annaka, T.; Grellier, M.; Sabo-Etienne, S. Silane Deuteration Catalyzed by Ruthenium Bis(dihydrogen) Complexes or Simple Metal Salts. *Adv. Synth. Catal.* **2014**, *356*, 759–764.

(205) Borowski, A. F.; Sabo-Etienne, S.; Donnadieu, B.; Chaudret, B. Reactivity of the Bis(dihydrogen) Complex  $[\text{RuH}_2(\eta^2\text{-H}_2)_2(\text{PCy}_3)_2]$  toward N-Heteroaromatic Compounds. Regioselective Hydrogenation of Acridine to 1,2,3,4,5,6,7,8-Octahydroacridine. *Organometallics* **2003**, *22*, 1630–1637.

(206) Guari, Y.; Sabo-Etienne, S.; Chaudret, B. Synthesis and Reactivity of Stretched-Dihydrogen-Ruthenium Complexes. Unexpected Formation of a Vinylidene Ligand. *Organometallics* **1996**, *15*, 3471–3473.

(207) Guari, Y.; Ayllon, J. A.; Sabo-Etienne, S.; Chaudret, B.; Hessen, B. Influence of Hydrogen Bonding on the Spectroscopic Properties and on the Reactivity of Ruthenium Hydrido Dihydrogen Complexes. *Inorg. Chem.* **1998**, *37*, 640–644.

(208) Bolton, P. D.; Grellier, M.; Vautravers, N.; Vendier, L.; Sabo-Etienne, S. Access to Ruthenium(0) Carbonyl Complexes via Dehydrogenation of a Tricyclopentylphosphine Ligand and Decarbonylation of Alcohols. *Organometallics* **2008**, *27*, 5088–5093.

(209) Choi, J.-H.; Heim, L. E.; Ahrens, M.; Precht, M. H. G. Selective Conversion of Alcohols in Water to Carboxylic Acids by *in*

*situ* Generated Ruthenium *trans* Dihydrido Carbonyl PNP Complexes. *Dalton Trans* **2014**, 43, 17248–17254.

(210) Esteruelas, M. A.; Sola, E.; Oro, L. A.; Werner, H.; Meyer, U. MHCl(CO)(P<sup>i</sup>Pr<sub>3</sub>)<sub>2</sub> (M = Ru, Os) Complexes as Catalyst Precursors for the Reduction of Unsaturated Substrates. *J. Mol. Catal.* **1988**, 45, 1–5.

(211) Esteruelas, M. A.; Sola, E.; Oro, L. A.; Werner, H.; Meyer, U. The Reduction of  $\alpha,\beta$ -Unsaturated Ketones and Cyclohexadienes Catalyzed by MHCl(CO)(P<sup>i</sup>Pr<sub>3</sub>)<sub>2</sub> (M = Ru, Os) Complexes. *J. Mol. Catal.* **1989**, 53, 43–52.

(212) Vicente, C.; Shul'pin, G. B.; Moreno, B.; Sabo-Etienne, S.; Chaudret, B. Reduction of Ketones by Dihydrogen or Hydrogen Transfer Catalysed by a Ruthenium Complex of the Hydridotris(3,5-dimethyl) Pyrazolyl Borate Ligand. *J. Mol. Catal. A: Chem.* **1995**, 98, L5–L8.

(213) Oliván, M.; Caulton, K. G. The First Double Oxidative Addition of CH<sub>2</sub>Cl<sub>2</sub> to a Metal Complex: Facile Synthesis of [Ru(CH<sub>2</sub>)Cl<sub>2</sub>{P(C<sub>6</sub>H<sub>11</sub>)<sub>3</sub>}<sub>2</sub>]. *Chem. Commun.* **1997**, 1733–1734.

(214) Oliván, M.; Caulton, K. G. C-(Halide) Oxidative Addition Routes to Ruthenium Carbenes. *Inorg. Chem.* **1999**, 38, 566–570.

(215) Chaudret, B.; Chung, G.; Eisenstein, O.; Jackson, S. A.; Lahoz, F. J.; Lopez, J. A. Preparation, X-ray Molecular Structure, and Electronic Structure of the First 16-Electron Dihydrogen Complexes RuH(H<sub>2</sub>)X(PCy<sub>3</sub>)<sub>2</sub>. *J. Am. Chem. Soc.* **1991**, 113, 2314–2316.

(216) Miloserdov, F. M.; McKay, D.; Muñoz, B. K.; Samouei, H.; Macgregor, S. A.; Grushin, V. V. Exceedingly Facile Ph-X Activation (X = Cl, Br, I) with Ruthenium(II): Arresting Kinetics, Autocatalysis, and Mechanisms. *Angew. Chem., Int. Ed.* **2015**, 54, 8466–8470.

(217) Christ, M. L.; Sabo-Etienne, S.; Chaudret, B. Synthesis, Characterization, and Chemistry of 16-Electron Dihydrogen Complexes of Ruthenium. *Organometallics* **1994**, 13, 3800–3804.

(218) Smart, K. A.; Mothes-Martin, E.; Vendier, L.; Perutz, R. N.; Grellier, M.; Sabo-Etienne, S. A Ruthenium Dihydrogen Germylene Complex and the Catalytic Synthesis of Digerimoxane. *Organometallics* **2015**, 34, 4158–4163.

(219) Borowski, A. F.; Sabo-Etienne, S.; Donnadiou, B.; Chaudret, B. Reactivity of the Bis(dihydrogen) Complex [RuH<sub>2</sub>( $\eta^2$ -H<sub>2</sub>)<sub>2</sub>(PCy<sub>3</sub>)<sub>2</sub>] toward S-Heteroaromatic Compounds. Catalytic Hydrogenation of Thiophene. *Organometallics* **2003**, 22, 4803–4809.

(220) Bautista, M. T.; Earl, K. A.; Morris, R. H. NMR Studies of the Complexes *trans*-[M( $\eta^2$ -H<sub>2</sub>)(H)(Ph<sub>2</sub>PCH<sub>2</sub>CH<sub>2</sub>PEt<sub>2</sub>)<sub>2</sub>]X (M = Fe, X = BPh<sub>4</sub>; M = Os, X = BF<sub>4</sub>): Evidence for Unexpected Shortening of the H-H Bond. *Inorg. Chem.* **1988**, 27, 1124–1126.

(221) Earl, K. A.; Jia, G.; Maltby, P. A.; Morris, R. H.  $\eta^2$ -Dihydrogen on the Brink of Homolytic Cleavage: *trans*-[Os(H $\cdots$ H)H-(PEt<sub>2</sub>CH<sub>2</sub>CH<sub>2</sub>PEt<sub>2</sub>)<sub>2</sub>]<sup>+</sup> Has Spectroscopic and Chemical Properties between Those of the Isoelectronic Complexes *trans*-[OsH-(PPh<sub>2</sub>CH<sub>2</sub>CH<sub>2</sub>PPh<sub>2</sub>)<sub>2</sub>( $\eta^2$ -H<sub>2</sub>)<sup>+</sup> and ReH<sub>3</sub>(PPh<sub>2</sub>CH<sub>2</sub>CH<sub>2</sub>PPh<sub>2</sub>)<sub>2</sub>. *J. Am. Chem. Soc.* **1991**, 113, 3027–3039.

(222) Schlünken, C.; Esteruelas, M. A.; Lahoz, F. J.; Oro, L. A.; Werner, H. Synthesis, Molecular Structure and Catalytic Activity of Six-Coordinate Chloro(hydrido)- and Dihydridoruthenium(II) and -osmium(II) Complexes with the Chiral Ligands P<sup>i</sup>Pr<sub>2</sub>NH(Me)Ph, (S,S)-Chiraphos and (S,S)-Diop. *Eur. J. Inorg. Chem.* **2004**, 2004, 2477–2487.

(223) Rocchini, E.; Mezzetti, A.; Rüegger, H.; Burckhardt, U.; Gramlich, V.; Del Zotto, A.; Martinuzzi, P.; Rigo, P. Heterolytic H<sub>2</sub> Activation by Dihydrogen Complexes. Effects of the Ligand X in [M(X)H<sub>2</sub>{Ph<sub>2</sub>P(CH<sub>2</sub>)<sub>2</sub>PPh<sub>2</sub>}<sub>2</sub>]<sup>++</sup> (M = Ru, Os; X = CO, Cl, H). *Inorg. Chem.* **1997**, 36, 711–720.

(224) Albertin, G.; Antoniutti, S.; Baldan, D.; Bordignon, E. Preparation and Properties of New Dinitrogen Osmium(II) Complexes. *Inorg. Chem.* **1995**, 34, 6205–6210.

(225) Werner, H.; Gotzig, J. Synthesis and Reactivity of OsH( $\eta^2$ -CH<sub>2</sub>PMe<sub>2</sub>)<sub>2</sub>(PMe<sub>3</sub>)<sub>2</sub> and of the Basic Dihydridoosmium Complex *cis*-OsH<sub>2</sub>(PMe<sub>3</sub>)<sub>4</sub>. *Organometallics* **1983**, 2, 547–549.

(226) Desrosiers, P. J.; Shinomoto, R. S.; Deming, M. A.; Flood, T. C. Acid-Catalyzed Hydrogenolysis of Osmium-Alkyl Bonds. *Organometallics* **1989**, 8, 2861–2865.

(227) Siedle, A. R.; Newmark, R. A.; Pignolet, L. H. Protonation of Iron, Ruthenium, and Osmium Hydrides with Fluorocarbon Acids. Stereochemical Rigidity in Seven-Coordinate [(Ph<sub>3</sub>P)<sub>4</sub>OsH<sub>3</sub>]<sup>+</sup>[HC(SO<sub>2</sub>CF<sub>3</sub>)<sub>2</sub>]<sup>-</sup>. *Inorg. Chem.* **1986**, 25, 3412–3418.

(228) Castillo, A.; Esteruelas, M. A.; Oñate, E.; Ruiz, N. Dihydrido and Trihydrido Diolefin Complexes Stabilized by the Os(PiPr<sub>3</sub>)<sub>2</sub> Unit: New Examples of Quantum Mechanical Exchange Coupling in Trihydrido Osmium Compounds. *J. Am. Chem. Soc.* **1997**, 119, 9691–9698.

(229) Esteruelas, M. A.; García, M. P.; López, A. M.; Oro, L. A.; Ruiz, N.; Schlünken, C.; Valero, C.; Werner, H. Reactivity of MH( $\eta^2$ -H<sub>2</sub>BH<sub>2</sub>)(CO)(PiPr<sub>3</sub>)<sub>2</sub> (M = Os, Ru) toward Electrophiles: Synthesis of New Hydridocarbonylosmium(II) and -ruthenium(II) Complexes Containing Triisopropylphosphine as Ligand. *Inorg. Chem.* **1992**, 31, 5580–5587.

(230) Bohanna, C.; Callejas, B.; Edwards, A. J.; Esteruelas, M. A.; Lahoz, F. J.; Oro, L. A.; Ruiz, N.; Valero, C. The Five-Coordinate Hydrido-Dihydrogen Complex [OsH( $\eta^2$ -H<sub>2</sub>)(CO)(P<sup>i</sup>Pr<sub>3</sub>)<sub>2</sub>]BF<sub>4</sub> Acting as a Template for the Carbon-Carbon Coupling between Methyl Propiolate and 1,1-Diphenyl-2-propyn-1-ol. *Organometallics* **1998**, 17, 373–381.

(231) Esteruelas, M. A.; Sola, E.; Oro, L. A.; Meyer, U.; Werner, H. Coordination of H<sub>2</sub> and O<sub>2</sub> to [OsHCl(CO)(PiPr<sub>3</sub>)<sub>2</sub>]: A Catalytically Active M( $\eta^2$ -H<sub>2</sub>) Complex. *Angew. Chem., Int. Ed. Engl.* **1988**, 27, 1563–1564.

(232) Andriollo, A.; Esteruelas, M. A.; Meyer, U.; Oro, L. A.; Sánchez-Delgado, R. A.; Sola, E.; Valero, C.; Werner, H. Kinetic and Mechanistic Investigation of the Sequential Hydrogenation of Phenylacetylene Catalyzed by OsHCl(CO)(PR<sub>3</sub>)<sub>2</sub> [PR<sub>3</sub> = *PMe-t-Bu*<sub>2</sub> and *P-i-Pr*<sub>3</sub>]. *J. Am. Chem. Soc.* **1989**, 111, 7431–7437.

(233) Bakhmutov, V. I.; Bertrán, J.; Esteruelas, M. A.; Lledós, A.; Maseras, F.; Modrego, J.; Oro, L. A.; Sola, E. Dynamic Behavior in Solution of the *trans*-Hydridodihydrogen Complex [OsHCl( $\eta^2$ -H<sub>2</sub>)(CO)(PiPr<sub>3</sub>)<sub>2</sub>]: Ab Initio and NMR Studies. *Chem. - Eur. J.* **1996**, 2, 815–825.

(234) Esteruelas, M. A.; Oro, L. A.; Valero, C. Hydrogenation of Benzylideneacetone Catalyzed by OsHCl(CO)(PR<sub>3</sub>)<sub>2</sub> (PR<sub>3</sub> = *P-i-Pr*<sub>3</sub>, *PMe-t-Bu*<sub>2</sub>): New Roles of Dihydrogen Complexes in Homogeneous Catalytic Hydrogenation. *Organometallics* **1992**, 11, 3362–3369.

(235) Ferrando, G.; Caulton, K. G. Dehydrohalogenation as a Source of OsH<sub>n</sub>Cl(PPh<sub>3</sub>)<sub>3</sub> (n = 1, 3). *Inorg. Chem.* **1999**, 38, 4168–4170.

(236) Yousufuddin, M.; Wen, T. B.; Mason, S. A.; McIntyre, G. J.; Jia, G.; Bau, R. A Neutron Diffraction Study of [OsClH<sub>3</sub>(PPh<sub>3</sub>)<sub>3</sub>]: A Complex Containing a Highly “Stretched” Dihydrogen Ligand. *Angew. Chem., Int. Ed.* **2005**, 44, 7227–7230.

(237) Kuhlman, R.; Clot, E.; Leforestier, C.; Streib, W. E.; Eisenstein, O.; Caulton, K. G. Quantum Exchange Coupling: A Hypersensitive Indicator of Weak Interactions. *J. Am. Chem. Soc.* **1997**, 119, 10153–10169.

(238) Gusev, D. G.; Kuhlman, R.; Sini, G.; Eisenstein, O.; Caulton, K. G. Distinct Structures for Ruthenium and Osmium Hydrido Halides: Os(H)<sub>3</sub>(P<sup>i</sup>Pr<sub>3</sub>)<sub>2</sub> (X = Cl, Br, I) Are Nonoctahedral Classical Trihydrides with Exchange Coupling. *J. Am. Chem. Soc.* **1994**, 116, 2685–2686.

(239) Clot, E.; Leforestier, C.; Eisenstein, O.; Pélessier, M. Dynamics on an *ab Initio* Surface for Calculating J<sub>HH</sub> NMR Exchange Coupling. The Case of OsH<sub>3</sub>X(PH<sub>3</sub>)<sub>2</sub>. *J. Am. Chem. Soc.* **1995**, 117, 1797–1799.

(240) Esteruelas, M. A.; García-Raboso, J.; Oliván, M. Preparation of Half-Sandwich Osmium Complexes by Deprotonation of Aromatic and Pro-aromatic Acids with a Hexahydride Bronsted Base. *Organometallics* **2011**, 30, 3844–3852.

(241) Esteruelas, M. A.; Larramona, C.; Oñate, E. Hydroosmiation of Allenes and Reductive Elimination of Olefin in Unsaturated Osmium(IV) Polyhydrides: Hydride versus Chloride. *Organometallics* **2013**, 32, 2567–2575.

(242) Huang, D.; Oliván, M.; Huffman, J. C.; Eisenstein, O.; Caulton, K. G. CO-Induced C(sp<sup>2</sup>)/C(sp) Coupling on Ru and Os: A Comparative Study. *Organometallics* **1998**, 17, 4700–4706.

- (243) Esteruelas, M. A.; López, A. M.; Oñate, E.; Royo, E. A Useful Access to the Chemistry of the Indenyl-Osmium-Triisopropylphosphine Moiety. *Organometallics* **2005**, *24*, 5780–5783.
- (244) Crabtree, R. H.; Hamilton, D. G. Classical (M = Os) and Nonclassical (M = Fe, Ru) Polyhydride Structures for the Complexes  $MH_4(PR_3)_3$ . *J. Am. Chem. Soc.* **1986**, *108*, 3124–3125.
- (245) Desrosiers, P. J.; Cai, L.; Lin, Z.; Richards, R.; Halpern, J. Assessment of the “ $T_1$  Criterion” for Distinguishing between Classical and Nonclassical Transition-Metal Hydrides: Hydride Relaxation Rates in Tris(triarylphosphine)osmium Tetrahydrides and Related Polyhydrides. *J. Am. Chem. Soc.* **1991**, *113*, 4173–4184.
- (246) Leigh, G. J.; Levison, J. J.; Robinson, S. D. Osmium Tetrahydrides and their High-field  $^1H$  Nuclear Magnetic Resonance Spectra. *J. Chem. Soc. D* **1969**, 705.
- (247) Levison, J. J.; Robinson, S. D. Transition-metal Complexes containing Phosphorus Ligands. Part III. Convenient Syntheses of Some Triphenylphosphine Complexes of the Platinum Metals. *J. Chem. Soc. A* **1970**, 2947–2954.
- (248) Douglas, P. G.; Shaw, B. L. Multihydrido-complexes of Osmium and Related Complexes. *J. Chem. Soc. A* **1970**, 334–338.
- (249) Bell, B.; Chatt, J.; Leigh, G. J. Hydrido-complexes of Osmium(II) and Osmium(IV). *J. Chem. Soc., Dalton Trans.* **1973**, 997–1104.
- (250) Hart, D. W.; Bau, R.; Koetzle, T. F. Neutron and X-Ray Diffraction Studies on Tris(dimethylphenylphosphine)osmium Tetrahydride. *J. Am. Chem. Soc.* **1977**, *99*, 7557–7564.
- (251) Werner, H.; Esteruelas, M. A.; Meyer, U.; Wrackmeyer, B. ( $\eta^2$ -Tetrahydroborato)ruthenium(II)- und osmium(II)-Komplexe mit fluktuierender Struktur. *Chem. Ber.* **1987**, *120*, 11–15.
- (252) Gusev, D. G.; Kuhlman, R. L.; Renkema, K. G.; Eisenstein, O.; Caulton, K. G. Structure and  $H_2$ -Loss Energies of  $OsHX(H_2)(CO)L_2$  Complexes (L = P(*t*-Bu) $_2$ Me, P(*i*-Pr) $_3$ ; X = Cl, I, H): Attempted Correlation of  $^1J(H-D)$ ,  $T_{1min}$ , and  $\Delta G^\ddagger$ . *Inorg. Chem.* **1996**, *35*, 6775–6783.
- (253) Guilera, G.; McGrady, G. S.; Steed, J. W.; Jones, A. L. Complex Formation and Rearrangement Reactions of the Phosphine Hydride Anions  $[OsH_3(PPh_3)_3]^-$  and  $[IrH_2(PPh_3)_3]^-$ . *Organometallics* **2006**, *25*, 122–127.
- (254) Huffman, J. C.; Green, M. A.; Kaiser, S. L.; Caulton, K. G. A Lipophilic Salt of a Transition-Metal Polyhydride:  $KOsH_3(PMe_2Ph)_3$ . *J. Am. Chem. Soc.* **1985**, *107*, 5111–5115.
- (255) Bruno, J. W.; Huffman, J. C.; Green, M. A.; Caulton, K. G. Hydride-Rich Zirconium-Osmium and Zirconium-Rhenium Dimers. *J. Am. Chem. Soc.* **1984**, *106*, 8310–8312.
- (256) Desrosiers, P. J.; Cai, L.; Halpern, J. Ortho-Vinylation and Alkylation of Coordinated Triarylphosphines by Reaction of Olefins with Osmium Polyhydrides. *J. Am. Chem. Soc.* **1989**, *111*, 8513–8514.
- (257) Johnson, T. J.; Huffman, J. C.; Caulton, K. G.; Jackson, S. A.; Eisenstein, O. Facile Olefin Hydrogenation with an Osmium Dihydrogen Complex. *Organometallics* **1989**, *8*, 2073–2074.
- (258) Johnson, T. J.; Albinati, A.; Koetzle, T. F.; Ricci, J.; Eisenstein, O.; Huffman, J. C.; Caulton, K. G.  $OsH_3(PMe_2Ph)_3^+$ : Structure, Reactivity, and Its Use as a Catalyst Precursor for Olefin Hydrogenation and Hydroformylation. *Inorg. Chem.* **1994**, *33*, 4966–4976.
- (259) Bruno, J. W.; Huffman, J. C.; Caulton, K. G. Stepwise Reductive Acidolysis of  $OsH_4(PMe_2Ph)_3$ . Mechanism of Hydrogen Elimination/Ligand Addition. *J. Am. Chem. Soc.* **1984**, *106*, 1663–1669.
- (260) Connelly, N. G.; Howard, J. A. K.; Spencer, J. L.; Woodley, P. K. Complexes of Rhenium and Osmium Polyhydrides with Metallic Lewis Acids: X-Ray Crystal Structure of  $[Ag\{ReH_7(PPhPr^i)_2\}_2][PF_6]$ . *J. Chem. Soc., Dalton Trans.* **1984**, 2003–2009.
- (261) Howard, J. A.; Johnson, O.; Koetzle, T. F.; Spencer, J. L. Crystal and Molecular Structure of Bis(diisopropylphenylphosphine)-hexahydroosmium,  $[OsH_6(PC_{12}H_{19})_2]$ : Single-Crystal Neutron Diffraction Study at 20 K. *Inorg. Chem.* **1987**, *26*, 2930–2933.
- (262) Esteruelas, M. A.; Jean, Y.; Lledós, A.; Oro, L. A.; Ruiz, N.; Volatron, F. Preparation and Spectroscopic and Theoretical Characterization of the Tetrahydroborate Complex  $OsH_3(\eta^2-H_2BH_2)(P-i-Pr)_2$ . *Inorg. Chem.* **1994**, *33*, 3609–3611.
- (263) Aracama, M.; Esteruelas, M. A.; Lahoz, F. J.; Lopez, J. A.; Meyer, U.; Oro, L. A.; Werner, H. Synthesis, Reactivity, Molecular Structure, and Catalytic Activity of the Novel Dichlorodihydroosmium(IV) Complexes  $OsH_2Cl_2(PR_3)_2$  ( $PR_3 = P-i-Pr_3, PMe-t-Bu_3$ ). *Inorg. Chem.* **1991**, *30*, 288–293.
- (264) Richter, B.; Werner, H. Hydrido-Osmium(II), -Osmium(IV) and -Osmium(VI) Complexes with Functionalized Phosphanes as Ligands. *Eur. J. Inorg. Chem.* **2009**, 2009, 5433–5438.
- (265) Demachy, I.; Esteruelas, M. A.; Jean, Y.; Lledós, A.; Maseras, F.; Oro, L. A.; Valero, C.; Volatron, F. Hydride Exchange Processes in the Coordination Sphere of Transition Metal Complexes: The  $OsH_3(BH_4)(PR_3)_2$  System. *J. Am. Chem. Soc.* **1996**, *118*, 8388–8394.
- (266) Frost, P. W.; Howard, J. A. K.; Spencer, J. L. An Osmium Tetrahydroborate Complex with Unusual Dynamic Behaviour: X-Ray Crystal Structure of  $[Os(BH_4)H_3\{P(c-C_5H_9)_3\}_2]$  ( $c-C_5H_9 = cyclo-C_5H_9$ ). *J. Chem. Soc., Chem. Commun.* **1984**, 1362–1363.
- (267) Esteruelas, M. A.; Lledós, A.; Martín, M.; Maseras, F.; Osés, R.; Ruiz, N.; Tomàs, J. Synthesis and Characterization of Mixed-Phosphine Osmium Polyhydrides: Hydrogen Delocalization in  $[OsH_5P_3]^+$  Systems. *Organometallics* **2001**, *20*, 5297–5309.
- (268) Smith, K.-T.; Tilst, M.; Kuhlman, R.; Caulton, K. G. Reactions of  $(P^iPr_3)_2OsH_6$  Involving Addition of Protons and Removal of Electrons. Characterization of  $(P^iPr_3)_2Os(NCMe)_xH_y^{z+}$  ( $x = 0, 2, 3; y = 1, 2, 3, 4, 7; z = 1, 2$ ), Including Dicationic  $\eta^2-H_2$  Complexes. *J. Am. Chem. Soc.* **1995**, *117*, 9473–9480.
- (269) Buil, M. L.; Esteruelas, M. A.; Garcés, K.; García-Raboso, J.; Oliván, M. Trapping of a 12-Valence-Electron Osmium Intermediate. *Organometallics* **2009**, *28*, 4606–4609.
- (270) Anderson, B. G.; Hoyte, S. A.; Spencer, J. L. Synthesis and Characterization of the Dinuclear Polyhydrides  $[Os_2H_7(PPhPr_2)_4]^+$  and  $[Os_2H_6(PPhPr_2)_4]$ . *Inorg. Chem.* **2009**, *48*, 7977–7983.
- (271) Bautista, M. T.; Earl, K. A.; Maltby, P. A.; Morris, R. H. Stereochemical Control of the Exchange of Hydrogen Atoms between Hydride and Dihydrogen Ligands in the Complexes  $[M(\eta^2-H_2)(H)(meso- or rac-tetraphos-1)]^+$ , M = Fe, Os. *J. Am. Chem. Soc.* **1988**, *110*, 4056–4057.
- (272) Bianchini, C.; Linn, K.; Masi, D.; Peruzzini, M.; Polo, A.; Vacca, A.; Zanobini, F. Classical, Nonclassical, and Mixed-Metal Osmium(II) Polyhydrides Stabilized by the Tetrakisphosphine  $P(CH_2CH_2PPh_2)_3$ . H/D Isotope Exchange Reactions Promoted by a Strongly Bound Dihydrogen Ligand. *Inorg. Chem.* **1993**, *32*, 2366–2376.
- (273) Heinekey, D. M.; Harper, T. G. P. (Arene)osmium Trihydride Complexes: Synthesis and Studies of Proton-Proton Exchange Coupling. *Organometallics* **1991**, *10*, 2891–2895.
- (274) Castarlenas, R.; Esteruelas, M. A.; Oñate, E. Preparation, X-ray Structure, and Reactivity of an Osmium-Hydroxo Complex Stabilized by an N-Heterocyclic Carbene Ligand: A Base-Free Catalytic Precursor for Hydrogen Transfer from 2-Propanol to Aldehydes. *Organometallics* **2008**, *27*, 3240–3247.
- (275) Baya, M.; Crochet, P.; Esteruelas, M. A.; Gutiérrez-Puebla, E.; Ruiz, N. Oxidative Addition of HX (X = H, SiR $_3$ , GeR $_3$ , SnR $_3$ , Cl) Molecules to the Complex  $Os(\eta^5-C_5H_5)Cl(P^iPr_3)_2$ . *Organometallics* **1999**, *18*, 5034–5043.
- (276) Esteruelas, M. A.; Hernández, Y. A.; López, A. M.; Oliván, M.; Oñate, E. Reduction and C(sp $^2$ )-H Bond Activation of Ketones Promoted by a Cyclopentadienyl-Osmium-Dihydride-Dihydrogen Complex. *Organometallics* **2005**, *24*, 5989–6000.
- (277) Gross, C. L.; Wilson, S. R.; Girolami, G. S. Synthesis and Characterization of  $(C_5Me_5)_2Os_2Br_4$  and the Osmium Polyhydride  $(C_5Me_5)OsH_5$ : A New Synthetic Entry into Mono-(pentamethylcyclopentadienyl)osmium Chemistry. *J. Am. Chem. Soc.* **1994**, *116*, 10294–10295.
- (278) Shima, T.; Suzuki, H. Heterobimetallic Polyhydride Complex,  $Cp^*Ru(\mu-H)_4OsCp^*$  ( $Cp^* = \eta^5-C_5Me_5$ ). Synthesis and Reaction with Ethylene. *Organometallics* **2005**, *24*, 3939–3945.

- (279) Bayse, C. A.; Couty, M.; Hall, M. B. Transition Metal Polyhydride Complexes. 8. Pentahydrido(cyclopentadienyl)osmium(VI). *J. Am. Chem. Soc.* **1996**, *118*, 8916–8919.
- (280) Bayse, C. A.; Hall, M. B. Pseudo Second-order Jahn-Teller Effects and Symmetry Considerations in Transition Metal Polyhydride Complexes. *Inorg. Chim. Acta* **1997**, *259*, 179–184.
- (281) Gross, C. L.; Girolami, G. S. Synthesis and Characterization of Osmium Polyhydrides. X-ray Crystal Structures of  $(C_5Me_5)OsH_5$  and  $(C_5Me_5)_2Os_2H_4$ . *Organometallics* **2007**, *26*, 160–166.
- (282) Gross, C. L.; Girolami, G. S. Synthesis and Characterization of Osmium(IV) Polyhydride Complexes of Stoichiometry  $(C_5Me_5)_nOsH_3(L)$ . Crystal Structures of  $(C_5Me_5)_2OsH_3(AsPh_3)$  and  $(C_5Me_5)_2OsH_3(PPh_3)$ . *Organometallics* **2006**, *25*, 4792–4798.
- (283) Gross, C. L.; Young, D. M.; Schultz, A. J.; Girolami, G. S. Neutron Diffraction Study of the 'Elongated' Molecular Dihydrogen Complex  $[(C_5Me_5)_2Os(H_2)_2(PPh_3)]^+$ . *J. Chem. Soc., Dalton Trans.* **1997**, 3081–3082.
- (284) Gross, C. L.; Girolami, G. S. Synthesis and NMR Studies of  $[(C_5Me_5)_2Os(L)H_2(H_2)]^+$  Complexes. Evidence of the Adoption of Different Structures by a Dihydrogen Complex in Solution and the Solid State. *Organometallics* **2007**, *26*, 1658–1664.
- (285) Webster, C. E.; Gross, C. L.; Young, D. M.; Girolami, G. S.; Schultz, A. J.; Hall, M. B.; Eckert, J. Electronic and Steric Effects on Molecular Dihydrogen Activation in  $[Cp^*OsH_4(L)]^+$  ( $L = PPh_3, AsPh_3, and PCy_3$ ). *J. Am. Chem. Soc.* **2005**, *127*, 15091–15101.
- (286) Castro-Rodrigo, R.; Esteruelas, M. A.; López, A. M.; Oliván, M.; Oñate, E. Preparation, Spectroscopic Characterization, X-ray Structure, and Theoretical Investigation of Hydride-, Dihydrogen-, and Acetone-OsTp Complexes: A Hydridotris(pyrazolyl)borate-Cyclopentadienyl Comparison. *Organometallics* **2007**, *26*, 4498–4509.
- (287) Bajo, S.; Esteruelas, M. A.; López, A. M.; Oñate, E. Reactions of an Osmium Bis(dihydrogen) Complex under Ethylene: Phosphine Addition to a C–C Double Bond and C–H Bond Activation of Fluoroarenes. *Organometallics* **2011**, *30*, 5710–5715.
- (288) Baya, M.; Esteruelas, M. A.; Oliván, M.; Oñate, E. Monocationic Trihydride and Dicationic Dihydride-Dihydrogen and Bis(dihydrogen) Osmium Complexes Containing Cyclic and Acyclic Triamine Ligands: Influence of the N–Os–N Angles on the Hydrogen-Hydrogen Interactions. *Inorg. Chem.* **2009**, *48*, 2677–2686.
- (289) Esteruelas, M. A.; Honeczek, N.; Oliván, M.; Oñate, E.; Valencia, M. Direct Access to POP-Type Osmium(II) and Osmium(IV) Complexes: Osmium a Promising Alternative to Ruthenium for the Synthesis of Imines from Alcohols and Amines. *Organometallics* **2011**, *30*, 2468–2471.
- (290) Alós, J.; Bolaño, T.; Esteruelas, M. A.; Oliván, M.; Oñate, E.; Valencia, M. POP-Pincer Osmium-Polyhydrides: Head-to-Head (Z)-Dimerization of Terminal Alkynes. *Inorg. Chem.* **2013**, *52*, 6199–6213.
- (291) Bertoli, M.; Choualeb, A.; Gusev, D. G.; Lough, A. J.; Major, Q.; Moore, B. PNP Pincer Osmium Polyhydrides for Catalytic Dehydrogenation of Primary Alcohols. *Dalton Trans.* **2011**, *40*, 8941–8949.
- (292) Liu, S. H.; Huang, X.; Lin, Z.; Lau, C. P.; Jia, G. Synthesis and Characterization of Dihydrogen(olefin)osmium Complexes with  $(E)-Ph_2P(CH_2)_2CH=CH(CH_2)_2PPh_2$ . *Eur. J. Inorg. Chem.* **2002**, *2002*, 1697–1702.
- (293) Kuznetsov, V. F.; Gusev, D. G. Chiral Hydride and Dihydrogen Pincer-Type Complexes of Osmium. *Organometallics* **2007**, *26*, 5661–5666.
- (294) Esteruelas, M. A.; Fernández-Alvarez, F. J.; López, A. M.; Mora, M.; Oñate, E. Borinium Cations as  $\sigma$ -B–H Ligands in Osmium Complexes. *J. Am. Chem. Soc.* **2010**, *132*, 5600–5601.
- (295) Esteruelas, M. A.; Fernández, I.; López, A. M.; Mora, M.; Oñate, E. Preparation, Structure, Bonding, and Preliminary Reactivity of a Six-Coordinate  $d^4$  Osmium–Boryl Complex. *Organometallics* **2012**, *31*, 4646–4649.
- (296) Buil, M. L.; Cardo, J. J. F.; Esteruelas, M. A.; Fernández, I.; Oñate, E. Unprecedented Addition of Tetrahydroborate to an Osmium–Carbon Triple Bond. *Organometallics* **2014**, *33*, 2689–2692.
- (297) Esteruelas, M. A.; López, A. M.; Mora, M.; Oñate, E. B–H Activation and H–H Formation: Two Consecutive Heterolytic Processes on an Osmium–Hydrogensulfide Bond. *Chem. Commun.* **2013**, *49*, 7543–7545.
- (298) Esteruelas, M. A.; Fernández, I.; López, A. M.; Mora, M.; Oñate, E. Osmium-Promoted Dehydrogenation of Amine–Boranes and B–H Bond Activation of the Resulting Amino–Boranes. *Organometallics* **2014**, *33*, 1104–1107.
- (299) Esteruelas, M. A.; López, A. M.; Mora, M.; Oñate, E. Boryl-Dihydrideborate Osmium Complexes: Preparation, Structure, and Dynamic Behavior in Solution. *Organometallics* **2015**, *34*, 941–946.
- (300) Esteruelas, M. A.; López, A. M.; Mora, M.; Oñate, E. Ammonia-Borane Dehydrogenation Promoted by an Osmium Dihydride Complex: Kinetics and Mechanism. *ACS Catal.* **2015**, *5*, 187–191.
- (301) Buil, M. L.; Esteruelas, M. A.; Fernández, I.; Izquierdo, S.; Oñate, E. Cationic Dihydride Boryl and Dihydride Silyl Osmium(IV) NHC Complexes: A Marked Diagonal Relationship. *Organometallics* **2013**, *32*, 2744–2752.
- (302) Ferrando, G.; Gérard, H.; Spivak, G. J.; Coalter, J. N., III; Huffman, J. C.; Eisenstein, O.; Caulton, K. G. Facile  $C(sp^2)/OR$  Bond Cleavage by Ru or Os. *Inorg. Chem.* **2001**, *40*, 6610–6621.
- (303) Coalter, J. N., III; Ferrando, G.; Caulton, K. G. Geminal Dehydrogenation of a  $C(sp^3)CH_2$  Group by Unsaturated Ru(II) or Os(II). *New J. Chem.* **2000**, *24*, 835–836.
- (304) Espuelas, J.; Esteruelas, M. A.; Lahoz, F. J.; Oro, L. A.; Valero, C. Reactivity of  $OsH_4(CO)(PiPr_3)_2$  toward Terminal Alkynes: Synthesis and Reactions of the Alkynyl-Dihydrogen Complexes  $OsH(C_2R)(\eta^2-H_2)(CO)(PiPr_3)_2$  ( $R = Ph, SiMe_3$ ). *Organometallics* **1993**, *12*, 663–670.
- (305) Werner, H.; Meyer, U.; Esteruelas, M. A.; Sola, E.; Oro, L. A. Bis-alkynyl and Hydrido-Alkynyl-Osmium(II) and Ruthenium(II) Complexes Containing Triisopropylphosphine as Ligand. *J. Organomet. Chem.* **1989**, *366*, 187–196.
- (306) Tse, S. K. S.; Bai, W.; Sung, H. H.-Y.; Williams, I. D.; Jia, G. Substituted Cyclopentadienyl Osmium Complexes from the Reactions of  $OsH_3Cl(PPh_3)_3$  with Fulvenes and Cyclopentadienes. *Organometallics* **2010**, *29*, 3571–3581.
- (307) Barrio, P.; Esteruelas, M. A.; Oñate, E. Reactions of a Hexahydride-Osmium Complex with Aldehydes: Double C–H $_{\alpha}$  Activation-Decarbonylation and Single C–H $_{\alpha}$  Activation-Hydroxylation Tandem Processes and Catalytic Tishchenko Reactions. *Organometallics* **2004**, *23*, 1340–1348.
- (308) Eguillor, B.; Esteruelas, M. A.; García-Raboso, J.; Oliván, M.; Oñate, E. Stoichiometric and Catalytic Deuteration of Pyridine and Methylpyridines by H/D Exchange with Benzene- $d_6$  Promoted by an Unsaturated Osmium Tetrahydride Species. *Organometallics* **2009**, *28*, 3700–3709.
- (309) Esteruelas, M. A.; Forcén, E.; Oliván, M.; Oñate, E. Aromatic C–H Bond Activation of 2-Methylpyridine Promoted by an Osmium(VI) Complex: Formation of an  $\eta^2(N,C)$ -Pyridyl Derivative. *Organometallics* **2008**, *27*, 6188–6192.
- (310) Barea, G.; Esteruelas, M. A.; Lledós, A.; López, A. M.; Oñate, E.; Tolosa, J. I. Synthesis and Characterization of  $OsX\{NH=C(Ph)C_6H_4\}H_2(PiPr_3)_2$  ( $X = H, Cl, Br, I$ ): Nature of the  $H_2$  Unit and Its Behavior in Solution. *Organometallics* **1998**, *17*, 4065–4076.
- (311) Barrio, P.; Castarlenas, R.; Esteruelas, M. A.; Oñate, E. Triple C–H Activation of a Cycloalkyl Ketone Using an Osmium-Hexahydride Complex. *Organometallics* **2001**, *20*, 2635–2638.
- (312) Barrio, P.; Castarlenas, R.; Esteruelas, M. A.; Lledós, A.; Maseras, F.; Oñate, E.; Tomás, J. Reactions of a Hexahydride-Osmium Complex with Aromatic Ketones: C–H Activation versus C–F Activation. *Organometallics* **2001**, *20*, 442–452.
- (313) Esteruelas, M. A.; Hernández, Y. A.; López, A. M.; Oliván, M.; Oñate, E. One-Pot Dehydrogenative Addition of Isopropyl to Alkynes Promoted by Osmium: Formation of  $\gamma$ -( $\eta^3$ -Allyl)- $\alpha$ -Alkenylphosphine Derivatives Starting from a Dihydride-Dihydrogen-Triisopropylphosphine Complex. *Organometallics* **2007**, *26*, 2193–2202.

- (314) Esteruelas, M. A.; Hernández, Y. A.; López, A. M.; Oñate, E. Preparation and Characterization of a Monocyclopentadienyl Osmium-Allenylcarbene Complex. *Organometallics* **2007**, *26*, 6009–6013.
- (315) Baya, M.; Eguillor, B.; Esteruelas, M. A.; Lledós, A.; Oliván, M.; Oñate, E. Coordination and Rupture of Methyl C(sp<sup>3</sup>)-H Bonds in Osmium-Polyhydride Complexes with  $\delta$  Agostic Interaction. *Organometallics* **2007**, *26*, 5140–5152.
- (316) Barrio, P.; Esteruelas, M. A.; Oñate, E. Activation of C(sp<sup>2</sup>)-H and Reduction of C=E (E = CH, N) Bonds with an Osmium-Hexahydride Complex: Influence of E on the Behavior of RCH=E-py Substrates. *Organometallics* **2004**, *23*, 3627–3639.
- (317) Buil, M. L.; Esteruelas, M. A.; Garcés, K.; Oliván, M.; Oñate, E. Understanding the Formation of N-H Tautomers from  $\alpha$ -Substituted Pyridines: Tautomerization of 2-Ethylpyridine Promoted by Osmium. *J. Am. Chem. Soc.* **2007**, *129*, 10998–10999.
- (318) Buil, M. L.; Esteruelas, M. A.; Garcés, K.; Oliván, M.; Oñate, E. C <sub>$\beta$</sub> (sp<sup>2</sup>)-H Bond Activation of  $\alpha,\beta$ -Unsaturated Ketones Promoted by a Hydride-Elongated Dihydrogen Complex: Formation of Osmafuran Derivatives with Carbene, Carbyne, and NH-Tautomerized  $\alpha$ -Substituted Pyridine Ligands. *Organometallics* **2008**, *27*, 4680–4690.
- (319) Esteruelas, M. A.; Fernández, I.; Gómez-Gallego, M.; Martín-Ortiz, M.; Molina, P.; Oliván, M.; Otón, F.; Sierra, M. A.; Valencia, M. Mono- and Dinuclear Osmium N,N'-di- and Tetraphenylbipyridyls and Extended Bipyridyls. Synthesis, Structure and Electrochemistry. *Dalton Trans.* **2013**, *42*, 3597–3608.
- (320) Crespo, O.; Eguillor, B.; Esteruelas, M. A.; Fernández, I.; García-Raboso, J.; Gómez-Gallego, M.; Martín-Ortiz, M.; Oliván, M.; Sierra, M. A. Synthesis and Characterisation of [6]-Azaosmahelicenes: the First d<sup>4</sup>-Heterometalhelices. *Chem. Commun.* **2012**, *48*, 5328–5330.
- (321) Esteruelas, M. A.; Masamunt, A. B.; Oliván, M.; Oñate, E.; Valencia, M. Aromatic Diosmatricyclic Nitrogen-Containing Compounds. *J. Am. Chem. Soc.* **2008**, *130*, 11612–11613.
- (322) Esteruelas, M. A.; Fernández, I.; Herrera, A.; Martín-Ortiz, M.; Martínez-Álvarez, R.; Oliván, M.; Oñate, E.; Sierra, M. A.; Valencia, M. Multiple C-H Bond Activation of Phenyl-Substituted Pyrimidines and Triazines Promoted by an Osmium Polyhydride: Formation of Osmapolycycles with Three, Five, and Eight Fused Rings. *Organometallics* **2010**, *29*, 976–986.
- (323) Eguillor, B.; Esteruelas, M. A.; Fernández, I.; Gómez-Gallego, M.; Lledós, A.; Martín-Ortiz, M.; Oliván, M.; Sierra, M. A.; Oñate, E. Azole Assisted C-H Bond Activation Promoted by an Osmium-Polyhydride: Discerning between N and NH. *Organometallics* **2015**, *34*, 1898–1910.
- (324) Eguillor, B.; Esteruelas, M. A.; Oliván, M.; Puerta, M. Abnormal and Normal N-Heterocyclic Carbene Osmium Polyhydride Complexes Obtained by Direct Metalation of Imidazolium Salts. *Organometallics* **2008**, *27*, 445–450.
- (325) Baya, M.; Eguillor, B.; Esteruelas, M. A.; Oliván, M.; Oñate, E. Influence of the Anion of the Salt Used on the Coordination Mode of an N-Heterocyclic Carbene Ligand to Osmium. *Organometallics* **2007**, *26*, 6556–6563.
- (326) Bolaño, T.; Esteruelas, M. A.; Fernández, I.; Oñate, E.; Palacios, A.; Tsai, J.-Y.; Xia, C. Osmium(II)-Bis(dihydrogen) Complexes Containing C<sub>aryl</sub>C<sub>NHC</sub>-Chelate Ligands: Preparation, Bonding Situation, and Acidity. *Organometallics* **2015**, *34*, 778–789.
- (327) Alabau, R. G.; Eguillor, B.; Esler, J.; Esteruelas, M. A.; Oliván, M.; Oñate, E.; Tsai, J.-Y.; Xia, C. CCC-Pincer-NHC Osmium Complexes: New Types of Blue-Green Emissive Neutral Compounds for Organic Light-Emitting Devices (OLEDs). *Organometallics* **2014**, *33*, 5582–5596.
- (328) Buil, M. L.; Espinet, P.; Esteruelas, M. A.; Lahoz, F. J.; Lledós, A.; Martínez-Illarduya, J. M.; Maseras, F.; Modrego, J.; Oñate, E.; Oro, L. A.; et al. Oxidative Addition of Group 14 Element Hydrido Compounds to OsH<sub>2</sub>( $\eta^2$ -CH<sub>2</sub>=CHEt) (CO)(P<sup>t</sup>Pr<sub>3</sub>)<sub>2</sub>: Synthesis and Characterization of the First Trihydrido-Silyl, Trihydrido-Germyl, and Trihydrido-Stannyl Derivatives of Osmium(IV). *Inorg. Chem.* **1996**, *35*, 1250–1256.
- (329) Möhlen, M.; Rickard, C. E. F.; Roper, W. R.; Salter, D. M.; Wright, L. J. The Synthesis, Structure, and Reactivity of the Osmium(IV) Trihydrido Silyl Complex, OsH<sub>3</sub>(SiMe<sub>3</sub>) (CO) (PPh<sub>3</sub>)<sub>2</sub>. *J. Organomet. Chem.* **2000**, *593–594*, 458–464.
- (330) Hübler, K.; Hübler, U.; Roper, W. R.; Schwerdtfeger, P.; Wright, L. J. The Nature of the Metal-Silicon Bond In [M(SiR<sub>3</sub>-H<sub>3</sub>(PPh<sub>3</sub>)<sub>3</sub>] (M = Ru, Os) and the Crystal Structure of [Os{Si(N-pyrrolyl)<sub>3</sub>}H<sub>3</sub>(PPh<sub>3</sub>)<sub>3</sub>]. *Chem. - Eur. J.* **1997**, *3*, 1608–1616.
- (331) Rickard, C. E. F.; Roper, W. R.; Woodgate, S. D.; Wright, L. J. Silatranyl, Hydride Complexes of Osmium(II) and Osmium(IV): Crystal Structure of Os(Si{OCH<sub>2</sub>CH<sub>2</sub>}<sub>3</sub>N)H<sub>3</sub>(PPh<sub>3</sub>)<sub>3</sub>. *J. Organomet. Chem.* **2000**, *609*, 177–183.
- (332) Gusev, D. G.; Fontaine, F.-G.; Lough, A. J.; Zargarian, D. Polyhydrido(silylene)osmium and Silyl(dinitrogen)ruthenium Products Through Redistribution of Phenylsilane with Osmium and Ruthenium Pincer Complexes. *Angew. Chem., Int. Ed.* **2003**, *42*, 216–219.
- (333) Esteruelas, M. A.; Lledós, A.; Maseras, F.; Oliván, M.; Oñate, E.; Tajada, M. A.; Tomás, J. Preparation and Characterization of Osmium-Stannyl Polyhydrides: d<sup>4</sup>-d<sup>2</sup> Oxidative Addition of Neutral Molecules in a Late Transition Metal. *Organometallics* **2003**, *22*, 2087–2096.
- (334) Esteruelas, M. A.; Lledós, A.; Maresca, O.; Oliván, M.; Oñate, E.; Tajada, M. A. Preparation and Full Characterization of a Tetrahydride-bis(stannyl)-osmium(VI) Derivative. *Organometallics* **2004**, *23*, 1453–1456.
- (335) Eguillor, B.; Esteruelas, M. A.; Oliván, M. Preparation, X-ray Structures, and NMR Spectra of Elongated Dihydrogen Complexes with Four- and Five-Coordinate Tin Centers. *Organometallics* **2006**, *25*, 4691–4694.
- (336) Esteruelas, M. A.; Lledós, A.; Oliván, M.; Oñate, E.; Tajada, M. A.; Ujaque, G. *Ortho*-CH Activation of Aromatic Ketones, Partially Fluorinated Aromatic Ketones, and Aromatic Imines by a Trihydride-Stannyl-Osmium(IV) Complex. *Organometallics* **2003**, *22*, 3753–3765.
- (337) Eguillor, B.; Esteruelas, M. A.; Oliván, M.; Oñate, E. C <sub>$\beta$</sub> -H Activation of Aldehydes Promoted by an Osmium Complex. *Organometallics* **2004**, *23*, 6015–6024.
- (338) Eguillor, B.; Esteruelas, M. A.; Oliván, M.; Oñate, E. C(sp<sup>2</sup>)-H Activation of RCH=E-py (E = CH, N) and RCH=CHC(O)R' Substrates Promoted by a Highly Unsaturated Osmium-Monohydride Complex. *Organometallics* **2005**, *24*, 1428–1438.
- (339) Ferrando-Miguel, G.; Wu, P.; Huffman, J. C.; Caulton, K. G. New d<sup>4</sup> Dihydrides of Ru(IV) and Os(IV) with  $\pi$ -Donor Ligands: M(H)<sub>2</sub>(chelate)(P<sup>i</sup>Pr<sub>3</sub>)<sub>2</sub> with Chelate = *ortho*-XYC<sub>6</sub>H<sub>4</sub> with X, Y = O, NR; R = H or CH<sub>3</sub>. *New J. Chem.* **2005**, *29*, 193–204.
- (340) Baya, M.; Esteruelas, M. A.; Oñate, E. Analysis of the Aromaticity of Osmabicycles Analogous to the Benzimidazolium Cation. *Organometallics* **2011**, *30*, 4404–4408.
- (341) Esteruelas, M. A.; Lahoz, F. J.; López, A. M.; Oñate, E.; Oro, L. A.; Ruiz, N.; Sola, E.; Tolosa, J. I. Quantum Mechanical Exchange Coupling in Trihydridoosmium Complexes Containing Azole Ligands. *Inorg. Chem.* **1996**, *35*, 7811–7817.
- (342) Castillo, A.; Barea, G.; Esteruelas, M. A.; Lahoz, F. J.; Lledós, A.; Maseras, F.; Modrego, J.; Oñate, E.; Oro, L. A.; Ruiz, N.; Sola, E. Thermally Activated Site Exchange and Quantum Exchange Coupling Processes in Unsymmetrical Trihydride Osmium Compounds. *Inorg. Chem.* **1999**, *38*, 1814–1824.
- (343) Casarrubios, L.; Esteruelas, M. A.; Larramona, C.; Muntaner, J. G.; Oliván, M.; Oñate, E.; Sierra, M. A. Chelated Assisted Metal-Mediated N-H Bond Activation of  $\beta$ -Lactams: Preparation of Irida-, Rhoda-, Osmia-, and Ruthenatrinems. *Organometallics* **2014**, *33*, 1820–1833.
- (344) Esteruelas, M. A.; García-Raboso, J.; Oliván, M.; Oñate, E. N-H and N-C Bond Activation of Pyrimidinic Nucleobases and Nucleosides Promoted by an Osmium Polyhydride. *Inorg. Chem.* **2012**, *51*, 5975–5984.
- (345) Esteruelas, M. A.; García-Raboso, J.; Oliván, M. Reactions of an Osmium-Hexahydride Complex with Cytosine, Deoxycytidine, and



Cytidine: The Importance of the Minor Tautomers. *Inorg. Chem.* **2012**, *51*, 9522–9528.

(346) Esteruelas, M. A.; Oro, L. A.; Ruiz, N. Reactions of Osmium Hydride Complexes with Terminal Alkynes: Synthesis and Catalytic Activity of  $\text{OsH}(\eta^2\text{-O}_2\text{CCH}_3)(\text{C}\equiv\text{CHPh})(\text{P}i\text{Pr}_3)_2$ . *Organometallics* **1994**, *13*, 1507–1509.

(347) Eguillor, B.; Esteruelas, M. A.; García-Raboso, J.; Oliván, M.; Oñate, E.; Pastor, I. M.; Peñafiel, L.; Yus, M. Osmium NHC Complexes from Alcohol-Functionalized Imidazoles and Imidazolium Salts. *Organometallics* **2011**, *30*, 1658–1667.

(348) Esteruelas, M. A.; Lahoz, F. J.; Lopez, J. A.; Oro, L. A.; Schlünken, C.; Valero, C.; Werner, H. Synthesis, Molecular Structure, and Reactivity of Octahedral Alkylhydridoosmium(II) Complexes  $[\text{OsH}(\text{R})(\text{CO})_2(\text{PR}'_3)_2]$ . *Organometallics* **1992**, *11*, 2034–2043.

(349) Casarrubios, L.; Esteruelas, M. A.; Larramona, C.; Lledós, A.; Muntaner, J. G.; Oñate, E.; Ortuño, M. A.; Sierra, M. A. Mechanistic Insight into the Facilitation of  $\beta$ -Lactam Fragmentation through Metal Assistance. *Chem. - Eur. J.* **2015**, *21*, 16781–16785.

(350) Casarrubios, L.; Esteruelas, M. A.; Larramona, C.; Muntaner, J. G.; Oñate, E.; Sierra, M. A. 2-Azetidinones as Precursors of Pincer Ligands: Preparation, Structure, and Spectroscopic Properties of CC'N-Osmium Complexes. *Inorg. Chem.* **2015**, *54*, 10998–11006.

(351) Bolaño, T.; Esteruelas, M. A.; Gay, M. P.; Oñate, E.; Pastor, I. M.; Yus, M. An Acyl-NHC Osmium Cooperative System: Coordination of Small Molecules and Heterolytic B–H and O–H Bond Activation. *Organometallics* **2015**, *34*, 3902–3908.

(352) Ott, J.; Venanzi, L. M.; Ghilardi, C. A.; Midollini, S.; Orlandini, A. Some Rhodium(I) and Rhodium(III) Complexes with the Tripod-like Ligands  $\text{RC}(\text{CH}_2\text{PPh}_2)_3$  (R = Me: triphos; R = Et: triphos-I) and the X-ray Crystal Structure of  $[\text{RhH}_3(\text{triphos-I})]$ . *J. Organomet. Chem.* **1985**, *291*, 89–100.

(353) Oldham, W. J., Jr.; Hinkle, A. S.; Heinekey, D. M. Synthesis and Characterization of Hydrotris(pyrazolyl)borate Dihydrogen/Hydride Complexes of Rhodium and Iridium. *J. Am. Chem. Soc.* **1997**, *119*, 11028–11036.

(354) Taw, F. L.; Mellows, H.; White, P. S.; Hollander, F. J.; Bergman, R. G.; Brookhart, M.; Heinekey, D. M. Synthesis and Investigation of  $[\text{Cp}^*(\text{PMe}_3)\text{Rh}(\text{H})(\text{H}_2)]^+$  and Its Partially Deuterated and Tritiated Isotopomers: Evidence for a Hydride/Dihydrogen Structure. *J. Am. Chem. Soc.* **2002**, *124*, 5100–5108.

(355) Bakhmutov, V. I.; Bianchini, C.; Peruzzini, M.; Vizza, F.; Vorontsov, E. V.  $^1\text{H}$ - and  $^2\text{H}$ - $T_1$  Relaxation Behavior of the Rhodium Dihydrogen Complex  $[(\text{Triphos})\text{Rh}(\eta^2\text{-H}_2)\text{H}_2]^+$ . *Inorg. Chem.* **2000**, *39*, 1655–1660.

(356) Bucher, U. E.; Lengweiler, T.; Nanz, D.; von Philipsborn, W.; Venanzi, L. M. Synthesis and 2D- $(^1\text{H},^{103}\text{Rh})$ -NMR Study of the First “Non-Classical” Polyhydrido Complex Stabilized by a Nitrogen Donor Ligand. *Angew. Chem., Int. Ed. Engl.* **1990**, *29*, 548–549.

(357) Nanz, D.; von Philipsborn, W.; Bucher, U. E.; Venanzi, L. M. Characterization of Partially Deuterated Transition Metal Polyhydrido Complexes by Heteronuclear 2D NMR Techniques. *Magn. Reson. Chem.* **1991**, *29*, S38–S44.

(358) Gelabert, R.; Moreno, M.; Lluch, J. M.; Lledós, A. Structure and Dynamics of  $\text{LRh“H}_4$ ” (L = Cp, Tp) Systems. A Theoretical Study. *Organometallics* **1997**, *16*, 3805–3814.

(359) Eckert, J.; Albinati, A.; Bucher, U. E.; Venanzi, L. M. Nature of the Rh–H<sub>2</sub> Bond in a Dihydrogen Complex Stabilized Only by Nitrogen Donors. Inelastic Neutron Scattering Study of  $\text{Tp}^{\text{Me}_2}\text{RhH}_2(\eta^2\text{-H}_2)$  ( $\text{Tp}^{\text{Me}_2}$  = Hydrotris(3,5-dimethylpyrazolyl)-borate). *Inorg. Chem.* **1996**, *35*, 1292–1294.

(360) Douglas, T. M.; Brayshaw, S. K.; Dallanegra, R.; Kociok-Köhn, G.; Macgregor, S. A.; Moxham, G. L.; Weller, A. S.; Wondimagegn, T.; Vadivelu, P. Intramolecular Alkyl Phosphine Dehydrogenation in Cationic Rhodium Complexes of Tris(cyclopentylphosphine). *Chem. - Eur. J.* **2008**, *14*, 1004–1022.

(361) Ingleson, M. J.; Brayshaw, S. K.; Mahon, M. F.; Ruggiero, G. D.; Weller, A. S. Dihydrogen Complexes of Rhodium:  $[\text{RhH}_2(\text{H}_2)_x(\text{PR}_3)_2]^+$  (R = Cy,  $i\text{Pr}$ ; x = 1, 2). *Inorg. Chem.* **2005**, *44*, 3162–3171.

(362) Brayshaw, S. K.; Ingleson, M. J.; Green, J. C.; McIndoe, J. S.; Raithby, P. J.; Kociok-Köhn, G.; Weller, A. S. High Hydride Count Rhodium Octahedra,  $[\text{Rh}_6(\text{PR}_3)_6\text{H}_{12}][\text{BArF}_4]_2$ : Synthesis, Structures, and Reversible Hydrogen Uptake under Mild Conditions. *J. Am. Chem. Soc.* **2006**, *128*, 6247–6263.

(363) Brayshaw, S. K.; Green, J. C.; Edge, R.; McInnes, E. J. L.; Raithby, P. J.; Warren, J. E.; Weller, A. S.  $[\text{Rh}_7(\text{P}i\text{Pr}_3)_6\text{H}_{18}][\text{BArF}_4]_2$ : A Molecular Rh(111) Surface Decorated with 18 Hydrogen Atoms. *Angew. Chem., Int. Ed.* **2007**, *46*, 7844–7848.

(364) Algarra, A. G.; Sewell, L. J.; Johnson, H. C.; Macgregor, S. A.; Weller, A. S. A Combined Experimental and Computational Study of Fluxional Processes in Sigma Amine–Borane Complexes of Rhodium and Iridium. *Dalton Trans.* **2014**, *43*, 11118–11128.

(365) Sewell, L. J.; Lloyd-Jones, G. C.; Weller, A. S. Development of a Generic Mechanism for the Dehydrocoupling of Amine–Boranes: A Stoichiometric, Catalytic, and Kinetic Study of  $\text{H}_3\text{B}\cdot\text{NMe}_2\text{H}$  Using the  $[\text{Rh}(\text{PCy}_3)_2]^+$  Fragment. *J. Am. Chem. Soc.* **2012**, *134*, 3598–3610.

(366) Tang, C. Y.; Thompson, A. L.; Aldridge, S. Rhodium and Iridium Aminoborane Complexes: Coordination Chemistry of BN Alkene Analogues. *Angew. Chem., Int. Ed.* **2010**, *49*, 921–925.

(367) Tang, C. Y.; Thompson, A. L.; Aldridge, S. Dehydrogenation of Saturated CC and BN Bonds at Cationic N-Heterocyclic Carbene Stabilized M(III) Centers (M = Rh, Ir). *J. Am. Chem. Soc.* **2010**, *132*, 10578–10591.

(368) Douglas, T. M.; Chaplin, A. B.; Weller, A. S. Amine–Borane  $\sigma$ -Complexes of Rhodium. Relevance to the Catalytic Dehydrogenation of Amine–Boranes. *J. Am. Chem. Soc.* **2008**, *130*, 14432–14433.

(369) Douglas, T. M.; Chaplin, A. B.; Weller, A. S.; Yang, X.; Hall, M. B. Monomeric and Oligomeric Amine–Borane  $\sigma$ -Complexes of Rhodium. Intermediates in the Catalytic Dehydrogenation of Amine–Boranes. *J. Am. Chem. Soc.* **2009**, *131*, 15440–15456.

(370) Chaplin, A. B.; Weller, A. S. B–H Activation at a Rhodium(I) Center: Isolation of a Bimetallic Complex Relevant to the Transition-Metal-Catalyzed Dehydrocoupling of Amine–Boranes. *Angew. Chem., Int. Ed.* **2010**, *49*, 581–584.

(371) Butera, V.; Russo, N.; Sicilia, E. Do Rhodium Bis( $\sigma$ -amine–borane) Complexes Play a Role as Intermediates in Dehydrocoupling Reactions of Amine–boranes? *Chem. - Eur. J.* **2011**, *17*, 14586–14592.

(372) Gusev, D. G.; Bakhmutov, V. I.; Grushin, V. V.; Vol'pin, M. E. NMR Spectra and the Products of Interaction of Iridium Monohydrides  $\text{IrHCl}_2\text{L}_2$  (L =  $\text{P}(\text{CH}(\text{CH}_3)_2)_3$  and  $\text{P}(\text{c-C}_6\text{H}_{11})_3$ ) with Molecular Hydrogen. *Inorg. Chim. Acta* **1990**, *177*, 115–120.

(373) Albinati, A.; Bakhmutov, V. I.; Caulton, K. G.; Clot, E.; Eckert, J.; Eisenstein, O.; Gusev, D. G.; Grushin, V. V.; Hauger, B. E.; Klooster, W. T.; et al. Reaction of  $\text{H}_2$  with  $\text{IrHCl}_2\text{P}_2$  (P =  $\text{P}i\text{Pr}_3$  or  $\text{P}^t\text{Bu}_2\text{Ph}$ ): Stereoelectronic Control of the Stability of Molecular  $\text{H}_2$  Transition Metal Complexes. *J. Am. Chem. Soc.* **1993**, *115*, 7300–7312.

(374) Bakhmutov, V. I.; Vymenits, A. B.; Grushin, V. V.  $\text{H}_2$  Binding to  $[(i\text{-Pr}_3\text{P})_2\text{Ir}(\text{H})\text{Br}_2]$  in Solution. Evidence for the Formation of *cis*- and *trans*- $[(i\text{-Pr}_3\text{P})_2\text{Ir}(\text{H})(\text{H}_2)\text{Br}_2]$ . *Inorg. Chem.* **1994**, *33*, 4413–4414.

(375) Crabtree, R. H. Multifunctional Ligands in Transition Metal Catalysis. *New J. Chem.* **2011**, *35*, 18–23.

(376) Albéniz, A. C.; Schulte, G.; Crabtree, R. H. Facile Reversible Metalation in an Agostic Complex and Hydrogenolysis of a Metal Aryl Complex via a Dihydrogen Complex. *Organometallics* **1992**, *11*, 242–249.

(377) Crabtree, R. H.; Lavin, M.; Bonneviot, L. Some Molecular Hydrogen Complexes of Iridium. *J. Am. Chem. Soc.* **1986**, *108*, 4032–4037.

(378) Gruet, K.; Clot, E.; Eisenstein, O.; Lee, D. H.; Patel, B.; Macchioni, A.; Crabtree, R. H. Ion Pairing Effects in Intramolecular Heterolytic  $\text{H}_2$  Activation in an Ir(III) Complex: a Combined Theoretical/Experimental Study. *New J. Chem.* **2003**, *27*, 80–87.

(379) Dobereiner, G. E.; Nova, A.; Schley, N. D.; Hazari, N.; Miller, S. J.; Eisenstein, O.; Crabtree, R. H. Iridium-Catalyzed Hydrogenation of N-Heterocyclic Compounds under Mild Conditions by an Outer-Sphere Pathway. *J. Am. Chem. Soc.* **2011**, *133*, 7547–7562.

- (380) Rhodes, L. F.; Caulton, K. G.  $\text{IrH}_4(\text{PMe}_2\text{Ph})_3^+$ : Its Characteristic Reactivity and Use as a Catalyst for Isomerization of  $\text{IrH}_3(\text{PMe}_2\text{Ph})_3$ . *J. Am. Chem. Soc.* **1985**, *107*, 259–260.
- (381) Lundquist, E. G.; Huffman, J. C.; Foltling, K.; Caulton, K. G. Mechanism of Ethylene Hydrogenation by the Molecular Hydrogen Complex  $[\text{Ir}(\text{H})_2(\text{H}_2)(\text{PMe}_2\text{Ph})_3]^+$ -Characterization of Intermediates. *Angew. Chem., Int. Ed. Engl.* **1988**, *27*, 1165–1167.
- (382) Marinelli, G.; Rachidi, I. E.-I.; Streib, W. E.; Eisenstein, O.; Caulton, K. G. Alkyne Hydrogenation by a Dihydrogen Complex: Synthesis and Structure of an Unusual Iridium/Butyne Complex. *J. Am. Chem. Soc.* **1989**, *111*, 2346–2347.
- (383) Lundquist, E. G.; Foltling, K.; Streib, W. E.; Huffman, J. C.; Eisenstein, O.; Caulton, K. G. Reactivity of the Molecular Hydrogen Complex  $[\text{IrH}_4(\text{PMe}_2\text{Ph})_3]\text{BF}_4$  toward Olefins. The Origin of Stereochemical Rigidity of  $\text{M}(\text{PR}_3)_3(\text{olefin})_2$  Species. *J. Am. Chem. Soc.* **1990**, *112*, 855–863.
- (384) Mediat, M.; Tachibana, G. N.; Jensen, C. M. Isolation and Characterization of  $\text{IrH}_2\text{Cl}(\eta^2\text{-H}_2)[\text{P}(i\text{-Pr})_3]_2$ : A Neutral Dihydrogen Complex of Iridium. *Inorg. Chem.* **1990**, *29*, 3–5.
- (385) Mediat, M.; Tachibana, G. N.; Jensen, C. Solid-State and Solution Dynamics of the Reversible Loss of Hydrogen from the Iridium Nonclassical Polyhydride Complexes  $\text{IrClH}_2(\text{PR}_3)_2(\text{H}_2)$  ( $\text{R} = \text{Pr}^i, \text{Cy}, \text{Bu}^t$ ). *M. Inorg. Chem.* **1992**, *31*, 1827–1832.
- (386) Eckert, J.; Jensen, C. M.; Jones, G.; Clot, E.; Eisenstein, O. An Extremely Low Barrier to Rotation of Dihydrogen in the Complex  $\text{IrClH}_2(\eta^2\text{-H}_2)(\text{P}^i\text{Pr}_3)_2$ . *J. Am. Chem. Soc.* **1993**, *115*, 11056–11057.
- (387) Le-Husebo, T.; Jensen, C. M. Influence of Halide Ligands on the Energetics of the Reversible Loss of Hydrogen from the Iridium Nonclassical Polyhydride Complexes  $\text{IrXH}_2(\text{H}_2)(\text{PPr}^i)_2$  ( $\text{X} = \text{Cl}, \text{Br}, \text{I}$ ). *Inorg. Chem.* **1993**, *32*, 3797–3798.
- (388) Wisniewski, L. L.; Mediat, M.; Jensen, C. M.; Zilm, K. W. Mechanism of Hydride Scrambling in a Transition-Metal Dihydrogen Dihydride As Studied by Solid-State Proton NMR. *J. Am. Chem. Soc.* **1993**, *115*, 7533–7534.
- (389) Hauger, B. E.; Gusev, D.; Caulton, K. G.  $\text{H}_2$  Binding to and Fluxional Behavior of  $\text{Ir}(\text{H})_2\text{X}(\text{P}^i\text{Bu}_2\text{R})_2$  ( $\text{X} = \text{Cl}, \text{Br}, \text{I}$ ;  $\text{R} = \text{Me}, \text{Ph}$ ). *J. Am. Chem. Soc.* **1994**, *116*, 208–214.
- (390) Lee, D. W.; Jensen, C. M. Substitution of  $\eta^2$ -Dihydrogen by Toluene and Alkanes in  $\text{IrXH}_2(\text{H}_2)(\text{PPr}^i)_2$  Complexes. *J. Am. Chem. Soc.* **1996**, *118*, 8749–8750.
- (391) Li, S.; Hall, M. B.; Eckert, J.; Jensen, C. M.; Albinati, A. Transition Metal Polyhydride Complexes. 10. Intramolecular Hydrogen Exchange in the Octahedral Iridium(III) Dihydrogen Dihydride Complexes  $\text{IrXH}_2(\eta^2\text{-H}_2)(\text{PR}_3)_2$  ( $\text{X} = \text{Cl}, \text{Br}, \text{I}$ ). *J. Am. Chem. Soc.* **2000**, *122*, 2903–2910.
- (392) Eckert, J.; Jensen, C. M.; Koetzle, T. F.; Husebo, T. L.; Nicol, J.; Wu, P. Inelastic Neutron Scattering Studies of  $\text{IrH}_2(\text{H}_2)(\text{PPr}^i)_2$  and Neutron Diffraction Structure Determination of  $\text{IrH}_2(\text{H}_2)(\text{PPr}^i)_2\text{-C}_{10}\text{H}_8$ : Implications on the Mechanism of the Interconversion of Dihydrogen and Hydride Ligands. *J. Am. Chem. Soc.* **1995**, *117*, 7271–7272.
- (393) Esteruelas, M. A.; Herrero, J.; López, A. M.; Oro, L. A.; Schulz, M.; Werner, H. Hydrogenation of Benzylideneacetone Catalyzed by  $\text{IrClH}_2(\text{P}^i\text{Pr}_3)_2$ : Kinetic Evidence for the Participation of an  $\text{Ir}(\eta^2\text{-H}_2)$  Complex in the Activation of Molecular Hydrogen. *Inorg. Chem.* **1992**, *31*, 4013–4014.
- (394) Empsall, H. D.; Hyde, E. M.; Mentzer, E.; Shaw, B. L.; Uttely, M. F. Some Iridium Hydride and Tetrahydroborate Complexes with Bulky Tertiary Phosphine Ligands. *J. Chem. Soc., Dalton Trans.* **1976**, 2069–2074.
- (395) Werner, H.; Schulz, M.; Esteruelas, M. A.; Oro, L. A.  $\text{IrCl}_2\text{H}(\text{P}^i\text{Pr}_3)_2$  as Catalyst Precursor for the Reduction of Unsaturated Substrates. *J. Organomet. Chem.* **1993**, *445*, 261–265.
- (396) Werner, H.; Höhn, A.; Schulz, M. Vinylidene Transition-metal Complexes. Part 13. The Reactivity of  $[\text{IrH}_5(\text{PPr}^i)_2]$  and  $[\text{IrH}_2\text{Cl}(\text{PPr}^i)_2]$  toward Alk-1-yne: Synthesis of Four-, Five- and Six-Coordinate Iridium Complexes containing Alkynyl, Vinyl and Vinylidene Ligands. *J. Chem. Soc., Dalton Trans.* **1991**, 777–781.
- (397) Crabtree, R. H.; Felkin, H.; Morris, G. E. Cationic Iridium Complexes as Alkene Hydrogenation Catalysts and the Isolation of Some Related Hydrido Complexes. *J. Organomet. Chem.* **1977**, *141*, 205–215.
- (398) Garlaschelli, L.; Khan, S. I.; Bau, R.; Longoni, G.; Koetzle, T. F. X-ray and Neutron Diffraction Study of  $\text{H}_3\text{Ir}[\text{P}(i\text{-Pr})_3]_2$ . *J. Am. Chem. Soc.* **1985**, *107*, 7212–7213.
- (399) Mann, B. E.; Masters, C.; Shaw, B. L. Formation and Properties of Complexes of Type  $\text{IrH}_3(\text{PR}_3)_2\text{L}$ . *J. Chem. Soc. D* **1970**, 846–847.
- (400) Bau, R.; Schwerdtfeger, C. J.; Garlaschelli, L.; Koetzle, T. F. Neutron Diffraction Study of  $\text{fac-}[\text{IrH}_3(\text{PPh}_2\text{Me})_3]\text{-MeOH}$ . *J. Chem. Soc., Dalton Trans.* **1993**, 3359–3362.
- (401) Goldman, A. S.; Halpern, J. Novel Catalytic Chemistry of Iridium Polyhydride Complexes. *J. Am. Chem. Soc.* **1987**, *109*, 7537–7539.
- (402) Goldman, A. S.; Halpern, J. Reactivity Patterns and Catalytic Chemistry of Iridium Polyhydride Complexes. *J. Organomet. Chem.* **1990**, *382*, 237–253.
- (403) Lee, J. C., Jr.; Peris, E.; Rheingold, A. L.; Crabtree, R. H. An Unusual Type of  $\text{H}\cdots\text{H}$  Interaction:  $\text{Ir-H}\cdots\text{H-O}$  and  $\text{Ir-H}\cdots\text{H-N}$  Hydrogen Bonding and Its Involvement in  $\sigma$ -Bond Metathesis. *J. Am. Chem. Soc.* **1994**, *116*, 11014–11019.
- (404) Peris, E.; Lee, J. C., Jr.; Rambo, J. R.; Eisenstein, O.; Crabtree, R. H. Factors Affecting the Strength of  $\text{X-H}\cdots\text{H-M}$  Hydrogen Bonds. *J. Am. Chem. Soc.* **1995**, *117*, 3485–3491.
- (405) Dobereiner, G. E.; Wu, J.; Manas, M. G.; Schley, N. D.; Takase, M. K.; Crabtree, R. H.; Hazari, N.; Maseras, F.; Nova, A. Mild, Reversible Reaction of Iridium(III) Amido Complexes with Carbon Dioxide. *Inorg. Chem.* **2012**, *51*, 9683–9693.
- (406) Crabtree, R. H. Recent Advances in Hydrogen Bonding Studies Involving Metal Hydrides. *J. Organomet. Chem.* **1998**, *557*, 111–115.
- (407) Abdur-Rashid, K.; Gusev, D. G.; Landau, S. E.; Lough, A. J.; Morris, R. H. Organizing Chain Structures by Use of Proton-Hydride Bonding. The Single-Crystal X-ray Diffraction Structures of  $[\text{K}(\text{Q})]\text{-}[\text{Os}(\text{H})_5(\text{P}^i\text{Pr}_3)_2]$  and  $[\text{K}(\text{Q})][\text{Ir}(\text{H})_4(\text{P}^i\text{Pr}_3)_2]$ ,  $\text{Q} = 18\text{-Crown-6}$  and  $1,10\text{-Diaza-18-crown-6}$ . *J. Am. Chem. Soc.* **1998**, *120*, 11826–11827.
- (408) Landau, S. E.; Groh, K. E.; Lough, A. J.; Morris, R. H. Large Effects of Ion Pairing and Protonic-Hydridic Bonding on the Stereochemistry and Basicity of Crown-, Azacrown-, and Cryptand-222-potassium Salts of Anionic Tetrahydride Complexes of Iridium(III). *Inorg. Chem.* **2002**, *41*, 2995–3007.
- (409) Crabtree, R. H.; Lavin, M. J.  $[\text{IrH}_2(\text{H}_2)_2\text{L}_2]^+[\text{L} = \text{P}(\text{C}_6\text{H}_{11})_3]$ : A Non-classical Polyhydride Complex. *J. Chem. Soc., Chem. Commun.* **1985**, 1661–1662.
- (410) Esteruelas, M. A.; Oro, L. A. Dihydrogen Complexes as Homogeneous Reduction Catalysts. *Chem. Rev.* **1998**, *98*, 577–588.
- (411) Dahlenburg, L.; Menzel, R.; Heinemann, F. W. Synthesis and Catalytic Applications of Chiral Hydrido-iridium(III) Complexes with Diamine/Bis(monophosphane) and Diamine/Diphosphane Coordination. *Eur. J. Inorg. Chem.* **2007**, *2007*, 4364–4374.
- (412) Cooper, A. C.; Streib, W. E.; Eisenstein, O.; Caulton, K. G. *tert*-Butyl Is Superior to Phenyl as an Agostic Donor to 14-Electron  $\text{Ir}(\text{III})$ . *J. Am. Chem. Soc.* **1997**, *119*, 9069–9070.
- (413) Cooper, A. C.; Eisenstein, O.; Caulton, K. G. 16-Electron, non- $\pi$ -Stabilized  $\text{Ir}(\text{H})_2(\text{H}_2)(\text{PBu}^t_2\text{Ph})_2^+$  and 18-Electron  $\text{Ir}(\text{H})_2(\text{H}_2)_2(\text{PBu}^t_2\text{Ph})_2^+$ : Fluxionality and H/D Exchange as Independent Processes. *New J. Chem.* **1998**, *22*, 307–309.
- (414) Janser, P.; Venanzi, L. M.; Bachechi, F. Some Iridium(I) and Iridium(III) Complexes with the Tripod-like Ligand  $\text{CH}_3\text{C}(\text{CH}_2\text{PPh}_2)_3$  (triphos) and the X-Ray Crystal Structure of  $[\text{IrCl}(\text{CO})\text{(triphos)}]$ . *J. Organomet. Chem.* **1985**, *296*, 229–242.
- (415) Barbaro, P.; Bianchini, C.; Meli, A.; Peruzzini, M.; Vacca, A.; Vizza, F. Assembling Ethylene, Alkyl, Hydride, and CO Ligands at Iridium. *Organometallics* **1991**, *10*, 2227–2238.
- (416) Bianchini, C.; Farnetti, E.; Graziani, M.; Kaspar, J.; Vizza, F. Molecular Solid-State Organometallic Chemistry of Tripodal

(Polyphosphine)metal Complexes. Catalytic Hydrogenation of Ethylene at Iridium. *J. Am. Chem. Soc.* **1993**, *115*, 1753–1759.

(417) Bianchini, C.; Moneti, S.; Peruzzini, M.; Vizza, F. Synthesis and Reactivity of the Labile Dihydrogen Complex  $[\{\text{MeC}(\text{CH}_2\text{PPh}_2)_3\}\text{Ir}(\text{H}_2)(\text{H})_2\text{BPh}_4]$ . *Inorg. Chem.* **1997**, *36*, 5818–5825.

(418) Rossin, A.; Gutsul, E. I.; Belkova, N. V.; Epstein, L. M.; Gonsalvi, L.; Lledós, A.; Lyssenko, K. A.; Peruzzini, M.; Shubina, E. S.; Zanobini, F. Mechanistic Studies on the Interaction of  $[(\kappa^3\text{-}P,P,P\text{-}NP_3)\text{IrH}_3][\text{NP}_3 = \text{N}(\text{CH}_2\text{CH}_2\text{PPh}_2)_3]$  with  $\text{HBF}_4$  and Fluorinated Alcohols by Combined NMR, IR, and DFT Techniques. *Inorg. Chem.* **2010**, *49*, 4343–4354.

(419) Gilbert, T. M.; Bergman, R. G. Synthesis of Trimethylphosphine-Substituted Pentamethylcyclopentadienyliridium Hydride Complexes; Protonation and Deprotonation of  $(\text{C}_5(\text{CH}_3)_3)\text{Ir}(\text{P}(\text{CH}_3)_3)_2\text{H}_2$ . *J. Am. Chem. Soc.* **1985**, *107*, 3502–3507.

(420) Talavera, M.; Bolaño, S.; Bravo, J.; Castro, J.; García-Fontán, S. Synthesis and Characterization of New Pentamethylcyclopentadienyl Iridium Hydride Complexes. *J. Organomet. Chem.* **2012**, *715*, 113–118.

(421) Heinekey, D. M.; Millar, J. M.; Koetzle, T. F.; Payne, N. G.; Zilm, K. W. Structural and Spectroscopic Characterization of Iridium Trihydride Complexes: Evidence for Proton–Proton Exchange Coupling. *J. Am. Chem. Soc.* **1990**, *112*, 909–919.

(422) Gilbert, T. M.; Hollander, F. J.; Bergman, R. G. Pentamethylcyclopentadienyliridium Polyhydride Complexes: Synthesis of Intermediates in the Mechanism of Formation of  $(\text{C}_5(\text{CH}_3)_3)\text{IrH}_4$  and the Preparation of Several Iridium(V) Compounds. *J. Am. Chem. Soc.* **1985**, *107*, 3508–3516.

(423) Pedersen, A.; Tilst, M. Solvent-Induced Reductive Elimination of Pentamethylcyclopentadiene from a (Pentamethylcyclopentadienyl)metal Hydride. *Organometallics* **1993**, *12*, 3064–3068.

(424) Gutiérrez-Puebla, E.; Monge, A.; Paneque, M.; Poveda, M. L.; Taboada, S.; Trujillo, M.; Carmona, E. Synthesis and Properties of  $\text{Tp}^{\text{Me}_2}\text{IrH}_4$  and  $\text{Tp}^{\text{Me}_2}\text{IrH}_3(\text{SiEt}_3)$ : Ir(V) Polyhydride Species with  $\text{C}_3v$  Geometry. *J. Am. Chem. Soc.* **1999**, *121*, 346–354.

(425) Webster, C. E.; Singleton, D. A.; Szymanski, M. J.; Hall, M. B.; Zhao, C.; Jia, G.; Lin, Z. Minimum Energy Structure of Hydridotris-(pyrazolyl)borato Iridium(V) Tetrahydride Is Not a  $\text{C}_{3v}$  Capped Octahedron. *J. Am. Chem. Soc.* **2001**, *123*, 9822–9829.

(426) Bernskoetter, W. H.; Lobkovsky, E.; Chirik, P. J. Synthesis of a  $\beta$ -Diiminate Iridium Tetrahydride for Arene C–H Bond Activation. *Chem. Commun.* **2004**, 764–765.

(427) Clarke, Z. E.; Maragh, P. T.; Dasgupta, T. P.; Gusev, D. G.; Lough, A. J.; Abdur-Rashid, K. A Family of Active Iridium Catalysts for Transfer Hydrogenation of Ketones. *Organometallics* **2006**, *25*, 4113–4117.

(428) Choualeb, A.; Lough, A. J.; Gusev, D. G. Hemilabile Pincer-Type Hydride Complexes of Iridium. *Organometallics* **2007**, *26*, 5224–5229.

(429) Esteruelas, M. A.; Oliván, M.; Vélez, A. Xantphos-Type Complexes of Group 9: Rhodium versus Iridium. *Inorg. Chem.* **2013**, *52*, 5339–5349.

(430) Tanaka, R.; Yamashita, M.; Nozaki, K. Catalytic Hydrogenation of Carbon Dioxide Using Ir(III)-Pincer Complexes. *J. Am. Chem. Soc.* **2009**, *131*, 14168–14169.

(431) Chen, X.; Jia, W.; Guo, R.; Graham, T. W.; Gullons, M. A.; Abdur-Rashid, K. Highly Active Iridium Catalysts for the Hydrogenation of Ketones and Aldehydes. *Dalton Trans.* **2009**, 1407–1410.

(432) Junge, K.; Wendt, B.; Jiao, H.; Beller, M. Iridium-Catalyzed Hydrogenation of Carboxylic Acid Esters. *ChemCatChem* **2014**, *6*, 2810–2814.

(433) Ahlquist, M. S. G. Iridium Catalyzed Hydrogenation of  $\text{CO}_2$  under Basic Conditions-Mechanistic Insight from Theory. *J. Mol. Catal. A: Chem.* **2010**, *324*, 3–8.

(434) Tanaka, R.; Yamashita, M.; Chung, L. W.; Morokuma, K.; Nozaki, K. Mechanistic Studies on the Reversible Hydrogenation of Carbon Dioxide Catalyzed by and Ir-PNP Complex. *Organometallics* **2011**, *30*, 6742–6750.

(435) Yang, X. Hydrogenation of Carbon Dioxide Catalyzed by PNP Pincer Iridium, Iron, and Cobalt Complexes: A Computational Design of Base Metal Catalysts. *ACS Catal.* **2011**, *1*, 849–854.

(436) Schmeier, T. J.; Dobereiner, G. E.; Crabtree, R. H.; Hazari, N. Secondary Coordination Sphere Interactions Facilitate the Insertion Step in an Iridium(III)  $\text{CO}_2$  Reduction Catalyst. *J. Am. Chem. Soc.* **2011**, *133*, 9274–9277.

(437) Wang, W.-H.; Himeda, Y.; Muckerman, J. T.; Manbeck, G. F.; Fujita, E.  $\text{CO}_2$  Hydrogenation of Formate and Methanol as an Alternative to Photo- and Electrochemical  $\text{CO}_2$  Reduction. *Chem. Rev.* **2015**, *115*, 12936–12973.

(438) Osadchuk, I.; Tamm, T.; Ahlquist, M. S. G. Theoretical Investigation of a Parallel Catalytic Cycle in  $\text{CO}_2$  Hydrogenation by (PNP)IrH<sub>3</sub>. *Organometallics* **2015**, *34*, 4932–4940.

(439) Chianese, A. R.; Drance, M. J.; Jensen, K. H.; McCollom, S. P.; Yusufova, N.; Shaner, S. E.; Shopov, D. Y.; Tendler, J. A. Acceptorless Alkane Dehydrogenation Catalyzed by Iridium CCC-Pincer Complexes. *Organometallics* **2014**, *33*, 457–464.

(440) Göttker-Schnetmann, I.; White, P. S.; Brookhart, M. Synthesis and Properties of Iridium Bis(phosphinite) Pincer Complexes (*p*-XPCP)IrH<sub>2</sub>, (*p*-PCP)Ir(CO), (*p*-XPCP)Ir(H) (aryl), and  $\{(p\text{-XPCP})\text{Ir}\}_2\{\mu\text{-N}_2\}$  and Their Relevance in Alkane Transfer Dehydrogenation. *Organometallics* **2004**, *23*, 1766–1776.

(441) Findlater, M.; Schultz, K. M.; Bernskoetter, W. H.; Cartwright-Sykes, A.; Heinekey, D. M.; Brookhart, M. Dihydrogen Complexes of Rhodium and Iridium. *Inorg. Chem.* **2012**, *51*, 4672–4678.

(442) Campos, J.; Kundu, S.; Pahls, D. R.; Brookhart, M.; Carmona, E.; Cundari, T. R. Mechanism of Hydrogenolysis of an Iridium-Methyl Bond: Evidence for a Methane Complex Intermediate. *J. Am. Chem. Soc.* **2013**, *135*, 1217–1220.

(443) Findlater, M.; Bernskoetter, W. H.; Brookhart, M. Proton-Catalyzed Hydrogenation of a  $d^8$  Ir(I) Complex Yields a *trans* Ir(III) Dihydride. *J. Am. Chem. Soc.* **2010**, *132*, 4534–4535.

(444) Errington, R. J.; Shaw, B. L. The Preparation of Fluxional Tetrahydrides,  $[\text{IrH}_4\{\text{Bu}^t\text{PCH}_2\text{CH}_2\text{CHCHRCH}_2\text{P}^t\text{Bu}^t\}_2]$  (R = H or Me) and their Reactions with CO,  $\text{Bu}^t\text{NC}$  or  $\text{HBr}$ . *J. Organomet. Chem.* **1982**, *238*, 319–325.

(445) McLoughlin, M. A.; Flesher, R. J.; Kaska, W. C.; Mayer, H. A. Synthesis and Reactivity of  $[\text{IrH}_2(\text{Bu}_2\text{P})\text{CH}_2\text{CH}_2\text{CHCH}_2\text{CH}_2\text{P}(\text{Bu}_2)]$ , a Dynamic Iridium Polyhydride Complex. *Organometallics* **1994**, *13*, 3816–3822.

(446) Gupta, M.; Hagen, C.; Kaska, W. C.; Cramer, R. E.; Jensen, C. M. Catalytic Dehydrogenation of Cycloalkanes to Arenes by a Dihydrido Iridium P-C-P Pincer Complex. *J. Am. Chem. Soc.* **1997**, *119*, 840–841.

(447) Liu, F.; Pak, E. B.; Singh, B.; Jensen, C. M.; Goldman, A. S. Dehydrogenation of *n*-Alkanes Catalyzed by Iridium “Pincer” Complexes: Regioselective Formation of  $\alpha$ -Olefins. *J. Am. Chem. Soc.* **1999**, *121*, 4086–4087.

(448) Punji, B.; Emge, T. J.; Goldman, A. S. A Highly Stable Adamantyl-Substituted Pincer-Ligated Iridium Catalyst for Alkane Dehydrogenation. *Organometallics* **2010**, *29*, 2702–2709.

(449) Ahuja, R.; Kundu, S.; Goldman, A. S.; Brookhart, M.; Vicente, B. C.; Scott, S. L. Catalytic Ring Expansion, Contraction, and Metathesis-polymerization of Cycloalkanes. *Chem. Commun.* **2008**, 253–255.

(450) Kundu, S.; Choliy, Y.; Zhuo, G.; Ahuja, R.; Emge, T. J.; Warmuth, R.; Brookhart, M.; Krogh-Jespersen, K.; Goldman, A. S. Rational Design and Synthesis of Highly Active Pincer-Iridium Catalysts for Alkane Dehydrogenation. *Organometallics* **2009**, *28*, 5432–5444.

(451) Krogh-Jespersen, K.; Czerw, M.; Zhu, K.; Singh, B.; Kanzelberger, M.; Darji, N.; Achord, P. D.; Renkema, K. B.; Goldman, A. S. Combined Computational and Experimental Study of Substituent Effects on the Thermodynamics of  $\text{H}_2$ , CO, Arene, and Alkane Addition to Iridium. *J. Am. Chem. Soc.* **2002**, *124*, 10797–10809.

(452) Zhu, K.; Achord, P. D.; Zhang, X.; Krogh-Jespersen, K.; Goldman, A. S. Highly Effective Pincer-Ligated Iridium Catalysts for

Alkane Dehydrogenation. DFT Calculation of Relevant Thermodynamic, Kinetic, and Spectroscopic Properties. *J. Am. Chem. Soc.* **2004**, *126*, 13044–13053.

(453) Göttker-Schnetmann, I.; White, P.; Brookhart, M. Iridium Bis(phosphinite) *p*-XPCP Pincer Complexes: Highly Active Catalysts for the Transfer Dehydrogenation of Alkanes. *J. Am. Chem. Soc.* **2004**, *126*, 1804–1811.

(454) Göttker-Schnetmann, I.; Brookhart, M. Mechanistic Studies of the Transfer Dehydrogenation of Cyclooctane Catalyzed by Iridium Bis(phosphinite) *p*-XPCP Pincer Complexes. *J. Am. Chem. Soc.* **2004**, *126*, 9330–9338.

(455) Ahuja, R.; Punji, B.; Findlater, M.; Supplee, C.; Schinski, W.; Brookhart, M.; Goldman, A. S. Catalytic Dehydroaromatization of *n*-Alkanes by Pincer-Ligated Iridium Complexes. *Nat. Chem.* **2011**, *3*, 167–171.

(456) Lyons, T. W.; Guironnet, D.; Findlater, M.; Brookhart, M. Synthesis of *p*-Xylene from Ethylene. *J. Am. Chem. Soc.* **2012**, *134*, 15708–15711.

(457) Kumar, A.; Zhou, T.; Emge, T. J.; Mironov, O.; Saxton, R. J.; Krogh-Jespersen, K.; Goldman, A. S. Dehydrogenation of *n*-Alkanes by Solid-Phase Molecular Pincer-Iridium Catalysts. High Yields of  $\alpha$ -Olefin Product. *J. Am. Chem. Soc.* **2015**, *137*, 9894–9911.

(458) Yao, W.; Zhang, Y.; Jia, X.; Huang, Z. Selective Catalytic Transfer Dehydrogenation of Alkanes and Heterocycles by an Iridium Pincer Complex. *Angew. Chem., Int. Ed.* **2014**, *53*, 1390–1394.

(459) Nawara-Hultsch, A. J.; Hackenberg, J. D.; Punji, B.; Supplee, C.; Emge, T. J.; Bailey, B. C.; Schrock, R. R.; Brookhart, M.; Goldman, A. S. Rational Design of Highly Active “Hybrid” Phosphine-Phosphinite Pincer Iridium Catalysts for Alkane Metathesis. *ACS Catal.* **2013**, *3*, 2505–2514.

(460) Shi, Y.; Suguri, T.; Dohi, C.; Yamada, H.; Kojima, S.; Yamamoto, Y. Highly Active Catalysts for the Transfer Dehydrogenation of Alkanes: Synthesis and Application of Novel 7–6–7 Ring-Based Pincer Iridium Complexes. *Chem. - Eur. J.* **2013**, *19*, 10672–10689.

(461) Haenel, M. W.; Oevers, S.; Angermund, K.; Kaska, W. C.; Fan, H.-J.; Hall, M. B. Thermally Stable Homogeneous Catalysts for Alkane Dehydrogenation. *Angew. Chem., Int. Ed.* **2001**, *40*, 3596–3600.

(462) Burford, R. J.; Piers, W. E.; Parvez, M.  $\beta$ -Elimination-Immune PC<sub>carbene</sub>P Iridium Complexes via Double C–H Activation: Ligand-Metal Cooperation in Hydrogen Activation. *Organometallics* **2012**, *31*, 2949–2952.

(463) Bézier, D.; Brookhart, M. Applications of PC(sp<sup>3</sup>)P Iridium Complexes in Transfer Dehydrogenation of Alkanes. *ACS Catal.* **2014**, *4*, 3411–3420.

(464) Hebden, T. J.; Goldberg, K. I.; Heinekey, D. M.; Zhang, X.; Emge, T. J.; Goldman, A. S.; Krogh-Jespersen, K. Dihydrogen/Dihydride or Tetrahydride? An Experimental and Computational Investigation of Pincer Iridium Polyhydrides. *Inorg. Chem.* **2010**, *49*, 1733–1742.

(465) Schultz, K. M.; Goldberg, K. I.; Gusev, D. G.; Heinekey, D. M. Synthesis, Structure, and Reactivity of Iridium NHC Pincer Complexes. *Organometallics* **2011**, *30*, 1429–1437.

(466) Kumar, A.; Johnson, H. C.; Hooper, T. N.; Weller, A. S.; Algarrá, A. G.; Macgregor, S. A. Multiple Metal-Bound Oligomers from Ir-Catalysed Dehydropolymerisation of H<sub>3</sub>B–NH<sub>3</sub> as Probed by Experiment and Computation. *Chem. Sci.* **2014**, *5*, 2546–2553.

(467) Johnson, H. C.; Robertson, A. P. M.; Chaplin, A. B.; Sewell, L. J.; Thompson, A. L.; Haddow, M. F.; Manners, I.; Weller, A. S. Catching the First Oligomerization Event in the Catalytic Formation of Polyaminoboranes: H<sub>3</sub>B–NMeHBH<sub>2</sub>–NMeH<sub>2</sub> Bound to Iridium. *J. Am. Chem. Soc.* **2011**, *133*, 11076–11079.

(468) Johnson, H. C.; Weller, A. S. A *tert*-Butyl-Substituted Aminoborane Bound to an Iridium Fragment: A Latent Source of Free H<sub>2</sub>B = N<sup>t</sup>BuH. *J. Organomet. Chem.* **2012**, *721–722*, 17–22.

(469) Stevens, C. J.; Dallanegra, R.; Chaplin, A. B.; Weller, A. S.; Macgregor, S. A.; Ward, B.; McKay, D.; Alcaraz, G.; Sabo-Etienne, S. [Ir(PCy<sub>3</sub>)<sub>2</sub>(H)<sub>2</sub>(H<sub>2</sub>B–NMe<sub>2</sub>)<sup>+</sup>] as a Latent Source of Aminoborane: Probing the Role of Metal in the Dehydrocoupling of H<sub>3</sub>B–NMe<sub>2</sub>H

and Retrodimerisation of [H<sub>2</sub>BNMe<sub>2</sub>]<sub>2</sub>. *Chem. - Eur. J.* **2011**, *17*, 3011–3020.

(470) Tang, C. Y.; Phillips, N.; Bates, J. I.; Thompson, A. L.; Gutmann, M. J.; Aldridge, S. Dimethylamine Borane Dehydrogenation Chemistry: Syntheses, X-ray and Neutron Diffraction Studies of 18-Electron Aminoborane and 14-Electron Aminoboryl Complexes. *Chem. Commun.* **2012**, *48*, 8096–8098.

(471) Denney, M. C.; Pons, V.; Hebden, T. J.; Heinekey, D. M.; Goldberg, K. I. Efficient Catalysis of Ammonia Borane Dehydrogenation. *J. Am. Chem. Soc.* **2006**, *128*, 12048–12049.

(472) Dietrich, B. L.; Goldberg, K. I.; Heinekey, D. M.; Autrey, T.; Linehan, J. C. Iridium-Catalyzed Dehydrogenation of Substituted Amine Boranes: Kinetics, Thermodynamics, and Implications for Hydrogen Storage. *Inorg. Chem.* **2008**, *47*, 8583–8585.

(473) Staubitz, A.; Presa-Soto, A.; Manners, I. Iridium-Catalyzed Dehydrocoupling of Primary Amine-Borane Adducts: A Route to High Molecular Weight Polyaminoboranes, Boron–Nitrogen Analogues of Polyolefins. *Angew. Chem., Int. Ed.* **2008**, *47*, 6212–6215.

(474) Staubitz, A.; Sloan, M. E.; Robertson, A. P. M.; Friedrich, A.; Schneider, S.; Gates, P. J.; Schmedt auf der Günne, J.; Manners, I. Catalytic Dehydrocoupling/Dehydrogenation of *N*-Methylamine-Borane and Ammonia-Borane: Synthesis and Characterization of High Molecular Weight Polyaminoboranes. *J. Am. Chem. Soc.* **2010**, *132*, 13332–13345.

(475) Hebden, T. J.; Denney, M. C.; Pons, V.; Piccoli, P. M. B.; Koetzle, T. F.; Schultz, A. J.; Kaminsky, W.; Goldberg, K. I.; Heinekey, D. M.  $\sigma$ -Borane Complexes of Iridium: Synthesis and Structural Characterization. *J. Am. Chem. Soc.* **2008**, *130*, 10812–10820.

(476) Paul, A.; Musgrave, C. B. Catalyzed Dehydrogenation of Ammonia-Borane by Iridium Dihydrogen Pincer Complexes Differs from Ethane Dehydrogenation. *Angew. Chem., Int. Ed.* **2007**, *46*, 8153–8156.

(477) Kawamura, K.; Hartwig, J. F. Isolated Iridium(V) Boryl Complexes and Their Reactions with Hydrocarbons. *J. Am. Chem. Soc.* **2001**, *123*, 8422–8423.

(478) Salomon, M. A.; Braun, T.; Krossing, I. Iridium Derivatives of Fluorinated Aromatics by C–H Activation: Isolation of Classical and non-Classical Hydrides. *Dalton Trans.* **2008**, 5197–5206.

(479) Husebo, T. L.; Jensen, C. M. Formation of Indenyl Dihydride Complexes from an Iridium Polyhydride Complex: Molecular Structures of ( $\eta^5$ -C<sub>9</sub>H<sub>7</sub>)IrH<sub>2</sub>(PPR<sub>3</sub>)<sub>3</sub> and the  $\eta^3$ -Indenyl Intermediate ( $\eta^3$ -C<sub>9</sub>H<sub>7</sub>)IrH<sub>2</sub>(PPR<sub>3</sub>)<sub>2</sub>. *Organometallics* **1995**, *14*, 1087–1088.

(480) Gründemann, S.; Kovacevic, A.; Albrecht, M.; Faller Robert, J. W.; Crabtree, R. H. Abnormal Binding in a Carbene Complex Formed from an Imidazolium Salt and a Metal Hydride Complex. *Chem. Commun.* **2001**, 2274–2275.

(481) Kovacevic, A.; Gründemann, S.; Miecznikowski, J. R.; Clot, E.; Eisenstein, O.; Crabtree, R. H. Counter-Ion Effects Switch Ligand Binding from C-2 to C-5 in Kinetic Carbenes Formed from and Imidazolium Salt and IrH<sub>3</sub>(PPh<sub>3</sub>)<sub>2</sub>. *Chem. Commun.* **2002**, 2580–2581.

(482) Appelhans, L. N.; Zuccaccia, D.; Kovacevic, A.; Chianese, A. R.; Miecznikowski, J. R.; Macchioni, A.; Clot, E.; Eisenstein, O.; Crabtree, R. H. An Anion-Dependent Switch in Selectivity Results from a Change of C–H Activation Mechanism in the Reaction of an Imidazolium Salt with IrH<sub>3</sub>(PPh<sub>3</sub>)<sub>2</sub>. *J. Am. Chem. Soc.* **2005**, *127*, 16299–16311.

(483) Chianese, A. R.; Kovacevic, A.; Zeglis, B. M.; Faller, J. W.; Crabtree, R. H. Abnormal C5-Bound N-Heterocyclic Carbenes: Extremely Strong Electron Donor Ligands and Their Iridium(I) and Iridium(III) Complexes. *Organometallics* **2004**, *23*, 2461–2468.

(484) Gründemann, S.; Kovacevic, A.; Albrecht, M.; Faller, J. W.; Crabtree, R. H. Abnormal Ligand Binding and Reversible Ring Hydrogenation in the Reaction of Imidazolium Salts with IrH<sub>3</sub>(PPh<sub>3</sub>)<sub>2</sub>. *J. Am. Chem. Soc.* **2002**, *124*, 10473–10481.

(485) Ma, D.; Yu, Y.; Lu, X. Highly Stereoselective Isomerization of Ynones to Conjugated Dienones. *J. Org. Chem.* **1989**, *54*, 1105–1109.

(486) Faller, J. W.; Felkin, H. Homogeneous Catalytic Activation of Vinylic C–H Bonds. Stereoselective H–D Exchange in Neohexene. *Organometallics* **1985**, *4*, 1488–1490.

- (487) Cameron, C. J.; Felkin, H.; Fillebeen-Khan, T.; Forrow, N. J.; Guittet, E. Activation of C–H Bonds in Saturated Hydrocarbons. H–D Exchange between Methane and Benzene Catalysed by a Soluble Iridium Polyhydride System. *J. Chem. Soc., Chem. Commun.* **1986**, 801–802.
- (488) Felkin, H.; Fillebeen-Khan, T.; Holmes-Smith, R.; Yingrui, L. Activation of C–H Bonds in Saturated Hydrocarbons. The selective, Catalytic Functionalisation of Methyl Groups by Means of a Soluble Iridium Polyhydride System. *Tetrahedron Lett.* **1985**, 26, 1999–2000.
- (489) Lin, Y.; Ma, D.; Lu, X. Selective Conversion of Pinane into  $\beta$ -Pinene Catalyzed by an Iridium Pentahydride Complex. *J. Organomet. Chem.* **1987**, 323, 407–409.
- (490) Felkin, H.; Fillebeen-Khan, T.; Gault, Y.; Holmes-Smith, R.; Zakrzewski, J. Activation of C–H Bonds in Saturated Hydrocarbons. The Catalytic Functionalisation of Cyclooctane by Means of Some Soluble Iridium and Ruthenium Polyhydride Systems. *Tetrahedron Lett.* **1984**, 25, 1279–1282.
- (491) Kuninobu, Y.; Ureshino, T.; Yamamoto, S.; Takai, K. Regioselective Functionalization of Alkanes by Sequential Dehydrogenation-Hydrozirconation. *Chem. Commun.* **2010**, 46, 5310–5312.
- (492) Yingrui, L.; Dawei, M.; Xiyuan, L. Iridium Pentahydride Complex Catalyzed Formation of C–C Bond by C–H Bond Activation Followed by Olefin Insertion. *Tetrahedron Lett.* **1987**, 28, 3249–3252.
- (493) Zhang, X.; Wang, D. Y.; Emge, T. J.; Goldman, A. S. Dehydrogenation of Ketones by Pincer-Ligated Iridium: Formation and Reactivity of Novel Enone Complexes. *Inorg. Chim. Acta* **2011**, 369, 253–259.
- (494) Haibach, M. C.; Kundu, S.; Brookhart, M.; Goldman, A. S. Alkane Metathesis by Tandem Alkane-Dehydrogenation–Olefin-Metathesis Catalysis and Related Chemistry. *Acc. Chem. Res.* **2012**, 45, 947–958.
- (495) Leitch, D. C.; Lam, Y. C.; Labinger, J. A.; Bercaw, J. E. Upgrading Light Hydrocarbons via Tandem Catalysis: A Dual Homogeneous Ta/Ir System for Alkane/Alkene Coupling. *J. Am. Chem. Soc.* **2013**, 135, 10302–10305.
- (496) Leitch, D. C.; Labinger, J. A.; Bercaw, J. E. Scope and Mechanism of Homogeneous Tantalum/Iridium Tandem Catalytic Alkane/Alkene Upgrading using Sacrificial Hydrogen Acceptors. *Organometallics* **2014**, 33, 3353–3365.
- (497) Polukeev, A. V.; Marcos, R.; Ahlquist, M. S. G.; Wendt, O. F. Formation of a C–C Double Bond from two Aliphatic Carbons. Multiple C–H Activations in an Iridium Pincer Complex. *Chem. Sci.* **2015**, 6, 2060–2067.
- (498) Loza, M.; Faller, J. W.; Crabtree, R. H. Seven-Coordinate Iridium(V) Polyhydrides with Chelating Bis(silyl) Ligands. *Inorg. Chem.* **1995**, 34, 2937–2941.
- (499) Esteruelas, M. A.; Fernández-Alvarez, F. J.; López, A. M.; Oñate, E.; Ruiz-Sánchez, P. Iridium(I), Iridium(III), and Iridium(V) Complexes Containing the (2-Methoxyethyl)cyclopentadienyl Ligand. *Organometallics* **2006**, 25, 5131–5138.
- (500) Feldman, J. D.; Peters, J. C.; Tilley, T. D. Activations of Silanes with  $[\text{PhB}(\text{CH}_2\text{PPh}_2)_3\text{Ir}(\text{H})(\eta^3\text{-C}_8\text{H}_{13})]$ . Formation of Iridium Silylene Complexes via the Extrusion of Silylenes from Secondary Silanes  $\text{R}_2\text{SiH}_2$ . *Organometallics* **2002**, 21, 4065–4075.
- (501) Turculet, L.; Feldman, J. D.; Tilley, T. D. Coordination Chemistry and Reactivity of New Zwitterionic Rhodium and Iridium Complexes Featuring the Tripodal Phosphine Ligand  $[\text{PhB}(\text{CH}_2\text{PPh}_2)_3]^-$ . Activation of H–H, Si–H, and Ligand B–C Bonds. *Organometallics* **2004**, 23, 2488–2502.
- (502) Park, S.; Brookhart, M. Development and Mechanistic Investigation of a Highly Efficient Iridium(V) Silyl Complex for the Reduction of Tertiary Amides to Amines. *J. Am. Chem. Soc.* **2012**, 134, 640–653.
- (503) Lu, X. Y.; Lin, Y. Q. G.; Ma, D. W. Novel Reactions Catalyzed by Iridium Pentahydride Complex. *Pure Appl. Chem.* **1988**, 60, 1299–1306.
- (504) Ma, D.; Lu, X. Isomerization of Propargylic Alcohols Catalyzed by an Iridium Complex. *Tetrahedron Lett.* **1989**, 30, 2109–2112.
- (505) Lin, Y.; Ma, D.; Lu, X. Iridium Pentahydride Complex Catalyzed Dehydrogenation of Alcohols in the Absence of a Hydrogen Acceptor. *Tetrahedron Lett.* **1987**, 28, 3115–3118.
- (506) Lin, Y.; Zhu, X.; Zhou, Y. A Convenient Lactonization of Diols to  $\gamma$ - and  $\delta$ -Lactones Catalyzed by Transition Metal Polyhydrides. *J. Organomet. Chem.* **1992**, 429, 269–274.
- (507) Langhoff, S. R.; Pettersson, L. G. M.; Bauschlicher, C. W., Jr.; Partridge, H. Theoretical Spectroscopic Parameters for the Low-Lying States of the Second-Row Transition Metal Hydrides. *J. Chem. Phys.* **1987**, 86, 268–278.
- (508) Siegbahn, P. E. M. A Comparative Study of the Bond Strengths of the Second Row Transition Metal Hydrides, Fluorides, and Chlorides. *Theor. Chim. Acta* **1993**, 86, 219–228.
- (509) Bronger, W.; Auffermann, G. High Pressure Synthesis and Structure of  $\text{Na}_2\text{PdH}_4$ . *J. Alloys Compd.* **1995**, 228, 119–121.
- (510) Dedieu, A. Theoretical Studies in Palladium and Platinum Molecular Chemistry. *Chem. Rev.* **2000**, 100, 543–600.
- (511) Low, J. J.; Goddard, W. A., III. Theoretical Studies of Oxidative Addition and Reductive Elimination. 2. Reductive Coupling of H–H, H–C, and C–C Bonds from Palladium and Platinum Complexes. *Organometallics* **1986**, 5, 609–622.
- (512) Andrews, L.; Wang, X.; Alikhani, M. E.; Manceron, L. Observed and Calculated Infrared Spectra of  $\text{Pd}(\text{H}_2)_{1,2,3}$  Complexes and Palladium Hydrides in Solid Argon and Neon. *J. Phys. Chem. A* **2001**, 105, 3052–3063.
- (513) Gusev, D. G.; Notheis, J. U.; Rambo, J. R.; Hauger, B. E.; Eisenstein, O.; Caulton, K. G. Characterization of  $\text{PtH}_3(\text{PtBu}_3)_2^+$  as the First Dihydrogen Complex of  $d^8$ , Pt(II). *J. Am. Chem. Soc.* **1994**, 116, 7409–7410.
- (514) Butts, M. D.; Scott, B. L.; Kubas, G. J. Syntheses and Structures of Alkyl and Aryl Halide Complexes of the Type  $[(\text{P}i\text{Pr}_3)_2\text{PtH}(\eta^1\text{-XR})]\text{BAR}_f$  and Analogues with  $\text{Et}_2\text{O}$ , THF, and  $\text{H}_2$  Ligands. Halide-to-metal  $\pi$  Bonding in Halocarbon Complexes. *J. Am. Chem. Soc.* **1996**, 118, 11831–11843.
- (515) Stahl, S. S.; Labinger, J. A.; Bercaw, J. E. Investigations of the Factors Affecting the Stability of Dihydrogen Adducts of Platinum(II). *Inorg. Chem.* **1998**, 37, 2422–2431.
- (516) Rivada-Wheleghan, O.; Roselló-Merino, M.; Ortuño, M. A.; Vidossich, P.; Gutiérrez-Puebla, E.; Lledós, A.; Conejero, S. Reactivity of Coordinatively Unsaturated Bis(N-heterocyclic carbene) Pt(II) Complexes toward  $\text{H}_2$ . Crystal Structure of a 14-Electron Pt(II) Hydride Complex. *Inorg. Chem.* **2014**, 53, 4257–4268.
- (517) Koppaka, A.; Yempally, V.; Zhu, L.; Fortman, G. C.; Temprado, M.; Hoff, C. D.; Captain, B. Synthesis of  $[\text{Pt}(\text{SnBu}_3)(\text{IBu}^t)(\mu\text{-H})_2]$ , a Coordinatively Unsaturated Dinuclear Compound which Fragments upon Addition of Small Molecules to Form Mononuclear Pt–Sn Complexes. *Inorg. Chem.* **2016**, 55, 307–321.
- (518) Koppaka, A.; Captain, B. Reversible Inter- and Intramolecular Carbon–Hydrogen Activation, Hydrogen Addition, and Catalysis by the Unsaturated Complex  $\text{Pt}(\text{IPr})(\text{SnBu}_3)(\text{H})$ . *Inorg. Chem.* **2016**, 55, 2679–2681.
- (519) Peter, M.; Wachtler, H.; Ellmerer-Müller, E.; Ongania, K.-H.; Wurst, K.; Peringer, P. Synthesis and NMR Spectroscopy of  $[\text{PtH}_3(\text{triphos})]^+$  and  $[\text{Pt}(\text{AuPPh}_3)_3(\text{triphos})]^+$  Crystal Structure of  $[\text{Pt}(\text{AuPPh}_3)_3(\text{triphos})]^+$  (triphos =  $\text{CH}_3\text{C}(\text{CH}_2\text{PPh}_2)_3$ ). *J. Organomet. Chem.* **1997**, 542, 227–233.
- (520) Arnold, D. P.; Bennett, M. A. Preparation, Spectroscopic Properties, and Reactivity of *trans*-Hydridoaryl and *trans*-Hydrido-methyl Complexes of Platinum(II). *Inorg. Chem.* **1984**, 23, 2110–2116.
- (521) Reinartz, S.; White, P. S.; Brookhart, M.; Templeton, J. L.  $\text{Tp}'\text{PtH}_3$ : A Stable Platinum(IV) Trihydride. *Organometallics* **2000**, 19, 3748–3750.
- (522) West, N. M.; Reinartz, S.; White, P. S.; Templeton, J. L. Carbon Monoxide Promoted Reductive Elimination of Hydrogen from  $\text{Tp}'$  Platinum Complexes. *J. Am. Chem. Soc.* **2006**, 128, 2059–2066.
- (523) Custelcean, R.; Jackson, J. E. Dihydrogen Bonding: Structures, Energetics, and Dynamics. *Chem. Rev.* **2001**, 101, 1963–1980.

(524) Epstein, L. M.; Shubina, E. S. New Types of Hydrogen Bonding in Organometallic Chemistry. *Coord. Chem. Rev.* **2002**, *231*, 165–181.

(525) Belkova, N. V.; Shubina, E. S.; Epstein, L. M. Diverse World of Unconventional Hydrogen Bonds. *Acc. Chem. Res.* **2005**, *38*, 624–634.

(526) Xia, C.; Tsai, J.-Y.; Eguillor, B.; Esteruelas, M. A.; Gómez, R.; Oliván, M.; Oñate, E. Heteroleptic Osmium Complex and Method of Making the Same. Patent Appl. U.S. 201313950591, 2013.

(527) Tsai, J.-Y.; Xia, C.; Esteruelas, M. A.; Oñate, E.; Bolaño, T.; Palacios, A. U. Osmium Complexes Comprising Three Different Bidentate Ligands and Method of Making the Same. Patent Appl. U.S. 201314075527, 2013.

(528) Tsai, J.-Y.; Xia, C.; Esteruelas, M. A. Osmium(IV) Complexes for OLED Material. Patent Appl. U.S. 201314075653, 2013.